Fixational eye movements - keeping the eyes on target

Anna-Katharina Hauperich

A thesis submitted for the degree of

Doctor of Philosophy



Pembroke College

Department of Experimental Psychology

University of Oxford

Trinity 2019

Fixational eye movements - keeping the eyes on target

Anna-Katharina Hauperich

Abstract

This thesis presents three different strands of research into fixational eye movements: the detection of microsaccades, the interaction between fixational eye movements and the visual stimulus, and the interplay of microsaccades and drift. Fixational eye movements actively sample the visual stimulus, generating spatial and temporal information about its structure while also preventing fading of the percept.

Two new microsaccade detection methods are presented: the binocular correlation method most suited to data from video-based eye trackers and the monocular microsaccade detection method suited to microsaccade detection from high resolution adaptive optics eye tracking. These methods are systematically compared to the established standard method in the field by (Engbert & Kliegl, 2003) using the F1 score of the precision-recall metric. Manually labelled eye movement data will be made available online to be used as training and testing data for future microsaccade detection methods.

The active responses of fixational eye movements to visual stimuli of different eccentricities, grating orientations, and levels of blur were also investigated. It was found that fixational eye movements exhibit systematic changes in response to stimulus eccentricity and orientation, but not to the different levels of blur tested. To explore possible underlying mechanisms data are presented on correlations of unreferenced motion thresholds and centre estimations with measures of fixational stability. Both were good predictors of fixational stability, suggesting that these or mutual underlying processes contribute to fixational eye movement control.

Microsaccades and drifts are compared for their relative contribution to fixational stability. Traditionally microsaccades were considered to be correcting for the random error introduced by drift, but the data examined in this thesis suggest a complimentary role between microsaccades and drift in stabilising gaze.

Acknowledgements

This thesis would never have been possible without the kind and enduring support from my lab and my family. First of all I would like to thank my supervisor Hannah Smithson for her patience, insight, kind and motivating words, and the time she has taken to support me. Throughout the four years this project has taken she has always known the right thing to say to help me get back on track when I was feeling stuck or lost and the friendly lab she has created has been a wonderful place to work.

I would also like to thank Laura Young, for her help with everything AOSLO-related. A special thank you goes to Sarah - we've been in it together from the start and I'm so glad I got to do this with you. Thank you also to all past and present lab members who have helped this project progress by enlightening or distracting tea and lunch breaks - (in the order of seating in the lab from close to Hannah's door to further away) Mital, Joshua, Manuel, Mira, Takuma, Alix, Rebekah, Biswajit, Allie, Dan, and Rob.

My most steady support has come from my family. Guy - you've been there for the good days and the bad, the sickness and the health and I'm looking forward to everything to come with you. My parents, Sabine and Heinz, also deserve a special thank you. Nie hätte ich es ohne eure andauernde Unterstützung, Motivation und Geduld schaffen können. Juliet and Peter, my parents-in-law have also supported me throughout this thesis adventure and I'm so thankful that they have made me feel at home. Dante the black cat also deserves an honourable mention for being the cat in my life.

I also thank my funding body the Biotechnology and Biological Sciences Research Council for providing me with the freedom to undertake this research with a roof over my head and a warm meal in my belly.

Glossary

2AFC Two Alternative Forced Choice task. Paradigm in which two opposing perceptual events occur one in each interval (temporal or spatial) and the participant has to make a judgement in which interval one of the two events occurred

AOSLO Adaptive Optics Scanning Laser Ophthalmoscope

BC Binocular Correlation. Novel method for detecting microsaccades in eye movement data.

BCEA Bivariate Contour Ellipse Area. Measure of how dispersed a movement is in 2-dimensional space. Calculated by fitting an ellipse to the movement which captures 68% of the area which the movement covers. An assumption of this method is that the underlying movement follows a Gaussian distribution.

DPI Dual Purkinje Image eye tracker. Eye tracker tracking the first and fourth Purkinje reflections to deduce eye position.

Drift Slow, meandering movement during fixation

EOG Electrooculogram. Type of eye tracker

EK Engbert and Kliegel (2003) microsaccade detection method based on an adaptive velocity threshold.

FEF Frontal Eye Fields

Fixation Period during which the eye's gaze is stabilised on a stationary object

FWHM Full Width at Half Maximum. Measure to estimate the extent of a blurry stimulus by finding the point at which its intensity value reaches the mid point between the minimum and maximum displayed value

IQR Interquartile Range

LGN Lateral Geniculate Nucleus. Structure in the thalamus involved in visual processing and eye movements.

Lund Dataset Manually classified eye movement traces from four observers collected by Nyström, Andersson, Niehorster and Hooge (2017) at the University of Lund. The data were collected at 1000 Hz binocularly using an Eyelink1000 Plus and the dataset is available online at https://osf.io/ayjs9/

.

Microsaccade Small jump-like movement that occurs during fixation

MPE Maximum permissible exposure. Published guideline specifying the amount of light to which the eye can be safely exposed.

Optic Flow Changes in the visual image due to relative movement between the observer and the scene. These can be used to judge motion.

Oxford Dataset Manually classified eye movement traces from five observers. The data were collected at 1000 Hz binocularly using an Eyelink1000 and was collected as part of Experiment One in Chapter 7

P-R Precision-Recall. Used to evaluate performance of classification method.

RMS Root mean square error. Used to evaluate stability of fixation by comparing fixation positions to a reference point.

SC Superior Colliculus. Midbrain structure involved in eye movements.

Saccade Large, jump-like eye movement used to relocate gaze to an object of interest

Slow Control A slow type of fixational eye movement, described as position-correcting drift.

Smooth Pursuit Following movement of the eye in response to moving target

Tremor Very small oscillatory movement during fixation

Useful Numbers

Measures of Visual Angle

Degree [°] Customarily the sizes of visual stimuli and eye gaze position are given in degrees of visual angle. One degree of visual angle is approximately the same size as the width of a thumb at arms length.

Minute of Arc/arcmin [’] Sixty minutes of arc form one degree of visual angle.

Second of Arc/arcsec [”] Sixty seconds of arc form one minute of arc.

Retinal Structure

Note: all values in this section are approximations.

Diameter of Macula Lutea 18°

Diameter of Fovea 5°

Diameter of Foveola 1°

Cone width in fovea 13-15”

Number of Cones in Retina 6.4 million

Number of Rods in Retina 110 million

Size of one degree of visual angle on the retina 288μ

List of Figures

1.1 Minimum and maximum values of peak velocity and distance as extracted from the reviewed literature. . . . 25

1.2 Maximum microsaccade size by year of publication. . . . 29

1.3 Approximate comparison of the ranges of movement that can be recorded using the different types of eye tracker. . . . 46

1.4 Comparison of accuracy, precision and resolution. . . . 46

1.5 Photo of an observer wearing a contact lens for eye movement recording and image stabilisation. . . . 48

1.6 Photo of scleral coil contact lenses. . . . 49

1.7 Photo of EOG used for interacting with a computer interface. . . . 49

1.8 Photo of DPI eye tracker. . . . 50

1.9 Example of the video-based eye tracker EyeLink 1000. . . . 51

1.10 Numbers of papers that contain either the search term 'microsaccades' or 'microsaccades AND attention' in abstract, title or keyword searches in Scopus, from 1948 to 2018. . . . 51

1.11 Photo of piezoelectric strain gauge method for eye tracking. . . . 53

2.1 Montaged image of the author's retina captured as part of the data for Experiment Two, Chapter 7. . . . 59

2.2 Participant during eye tracking with the AOSLO. . . . 60

2.3 Schematic description of motion extraction from AOSLO recordings. . . . 61

2.4 Schematic description of the work flow for AOSLO eye tracking. . . . 61

2.5 Example of a raw frame and the corresponding averaged and motion-reduced frame. 65

2.6 Schematic description of the work flow for Eyelink1000 eye tracking. . . . 66

2.7 Following-responses recorded using the Eyelink1000 (top panel) and the AOSLO (bottom panel). . . . 71

2.8 Example of eye movements recorded by the Eyelink1000 and the AOSLO during one trial for participant P3. 73
2.9 Example of eye movements recorded by the Eyelink1000 and the AOSLO during one trial for participant P3.The assumed fixation position in green was calculated based on the median of positions in black. The blue cross indicates where the target moved to relative to that assumed initial fixation position. 73
2.10 Example of the raw eye movement trace, compared to the trace when the residual in-frame motion has been removed. 74
2.11 Example of manually classified microsaccades in AOSLO data for participant P3. . . 76

3.1 Example of eye movement trace containing microsaccades. 82
3.2 Example of microsaccade detection using the EK method. 85
3.3 Example of the stimuli used during the experiment. 89
3.4 The effect of ω on microsaccade detection. 92
3.5 Example of eye trace and microsaccade detection. 93
3.6 Plots showing the interaction between the different microsaccade detection parameters and the F1 score. 96
3.7 Comparison of the EK and the BC methods using the F1 score. 96
3.8 Microsaccade main sequences for the Oxford dataset using Savitzky-Golay smoothing. 97
3.9 Transferability of the different detection methods between datasets. 97
3.10 Best parameter values and corresponding F1 scores. 98
3.11 Best parameter values and corresponding merged and split events. 99

4.1 Examples of different sample-to-sample angles and how local and consistent-curve angle criteria are applied. 106
4.2 Box plots of highest recorded F1 scores for a given detection method and smoothing type. 108
4.3 Influence of the different parameters on the F1 score. 108
4.4 Microsaccade main sequences for participant P3. 109
4.5 Example of microsaccade detection on AOSLO data for participant P3. 110

5.1 This figure shows examples of 7 pixels of horizontal/vertical movement across a horizontally aligned grating. 117
5.2 Information based on which the deviation of the Gaussian target was chosen. 122

5.3 This figure shows the trial sequence of events schematically on the left side. 123
5.4 Figure showing the exclusion of participants based on missing data. 124
5.5 Box plot of number of missing data for each experimental condition. 125
5.6 This plot shows the temporal progression of the local RMS error. 126
5.7 This plot shows the temporal progression of the global RMS error. 127
5.8 Box plots of RMS error to the median of fixation for all ANOVA conditions. 128
5.9 Box plot of microsaccade distances for the different experimental conditions. 129
5.10 Box plot of microsaccade frequencies for the different experimental conditions. . . . 130
5.11 Box plots of the difference between the median fixation position when the fixation helper is present and when it is absent by eccentricity. 130
5.12 Example of the grating stimulus in our study, compared to a Gabor. 134
5.13 This figure shows the trial sequence of events schematically on the left side. 134
5.14 Figure showing the exclusion of participants based on missing data. 135
5.15 Box plot of the amount of data missing from all trials that were included in the analysis.136
5.16 This plot shows the temporal progression of the local RMS error. 137
5.17 This plot shows the temporal progression of the global RMS error. 138
5.18 This plot shows the temporal progression of the local RMS error ratio. 139
5.19 This plot shows the temporal progression of the global RMS error ratio. 140
5.20 Box plot of RMS error ratios for the different experimental conditions. 140
5.21 Box plot of RMS error for the different experimental conditions. 141

6.1 Comparison plots of actual step size in pixels compared to requested step size in pixels.148
6.2 Graphical representation of the trial sequence during the 2afc task. 150
6.3 Box plots of the proportion of trials which were successfully triggered during the experiment for all participants. 151
6.4 Comparing raw psychometric functions with eye movement adjusted ones under two different methods of performing the adjustment. 152
6.5 Comparison of the correlation between the RMS error, unreferenced motion thresholds and centre estimations. 153

7.1 Example of a possible local summation of luminance signals for the three stimuli used in the experiment. 156
7.2 The stimuli used in this experiment and their corresponding luminance profiles. . . 160
7.3 Timing of stimulus presentation during the experiment. 160

7.4 Box plots of the RMS error within trials of five participants in response to the blurry stimuli. . . . 161
7.5 Local RMS error over time across five participants. . . . 162
7.6 Global RMS error over time across 5 participants. . . . 162
7.7 Figure showing which participants were automatically excluded due to too much missing data. . . . 165
7.8 RMS error within trials of 11 participants in response to the blurry stimuli. . . . 165
7.9 RMS error across trials of 11 participants in response to the blurry stimuli. . . . 166
7.10 Local RMS error over time across 11 participants. . . . 166
7.11 Global RMS error over time across 11 participants. . . . 167
7.12 Box plots of the stimulus centre estimates using mouse clicks. . . . 167

8.1 Graphical explanation of the Start-To-End-Error measure. . . . 175
8.2 Graphical explanation of the Movement-Towards-Median measure. . . . 176
8.3 The four possible outcomes of calculating the Optimal-Achievable-Movement. . . . 178
8.4 Box plots of drift and microsaccade Start-To-End-Errors. . . . 181
8.5 Cumulative probabilities of the the Start-End-Error. . . . 181
8.6 Movement-Toward-Median measure for all participants and edge removal factors. . . . 183
8.7 Box plot of the Optimal-Achievable-Movement for drift and microsaccades with different edge removal factors. . . . 184
8.8 Cumulative probabilities of the the Optimal-Achievable-Movement. . . . 184
8.9 Heat maps of the distribution of actual and optimal movement directions for microsaccades (left) and drifts (right). A diagonal line though 0,0 with a gradient of 1 would represent the ideal movement. . . . 185
8.10 Heat map of the distribution of actual and optimal movement distances for microsaccades (left) and drifts (right). . . . 186

List of Tables

1.1 Selected data from the literature review on microsaccades. 31

Contents

1 Fixational Eye Movements - An Overview **21**

1.1 Introduction to fixational eye movements 21

1.2 Types of fixational eye movements 23

1.2.1 Microsaccades [1] 23

1.2.2 Drift 34

1.2.3 Tremor 36

1.3 Neural systems involved in fixational eye movements 37

1.3.1 A brief overview of visual processing 37

1.3.2 Eye movements: Motor Control 39

1.3.3 Microsaccade Generation 39

1.3.4 Neural control of drift and tremor 41

1.3.5 Consequences for research 41

1.4 Fixational Eye Movements and Task Performance 42

1.4.1 Theoretical Improvements Due to Motion 42

1.4.2 Prevention of fading 43

1.4.3 Grating Orientation Discrimination 44

1.5 Eye trackers 45

1.5.1 Contact lens mirror methods 47

1.5.2 Scleral coil 48

1.5.3 Electrooculograms 49

1.5.4 Dual Purkinje Image trackers 50

1.5.5 Limbus trackers 50

1.5.6 Video-based trackers 51

1.5.7 Other eye trackers 52

[1] Part of this work is under review as a publication in the Journal of Eye Movement Research. Sections taken from the paper are included in section 1.2.1: Properties of Microsaccades This chapter expands on the paper. I have only reproduced work here that is my own.

1.5.8 AOSLO . . . 52
1.6 Thesis Overview . . . 54

2 Manual Microsaccade Detection and Eye Tracker Differences 57

Abstract . . . 57
2.1 Comparing Data . . . 57
2.2 Description of Eye Trackers . . . 58
2.2.1 AOSLO . . . 58
2.2.2 Eyelink1000 . . . 65
2.3 Aims . . . 67
2.4 Direct Comparison of AOSLO and Eyelink1000 . . . 68
2.4.1 Methods . . . 69
2.4.2 Qualitative Interpretation of the Data . . . 69
2.5 Manually Labelled Datasets . . . 74
2.5.1 Methods . . . 74
2.6 Discussion . . . 76

3 Binocular Microsaccade Detection 79

Abstract . . . 79
3.1 Why microsaccade detection is difficult . . . 80
3.1.1 Detecting large saccades . . . 80
3.1.2 Established microsaccade detection methods . . . 81
3.1.3 Formally comparing detection methods . . . 86
3.1.4 Possible features of microsaccade detection mechanisms . . . 87
3.2 The binocular correlation method for microsaccade detection [2] . . . 88
3.3 Methods: Optimising the binocular correlation method . . . 88
3.3.1 Participants . . . 88
3.3.2 Materials . . . 88
3.3.3 Procedure . . . 89
3.4 Microsaccade detection . . . 89
3.5 Comparison of Detection Methods . . . 92
3.6 Results . . . 95
3.7 Discussion . . . 98

[2] Part of this work is currently under review in the Journal of Eye Movement Research. This chapter expands on the paper. I have only reproduced work here that is my own.

4 Monocular Microsaccade Detection **101**

Abstract . . . 101

4.1 Why monocular microsaccade detection is important . . . 101

4.2 Related problems in other fields . . . 102

4.3 The monocular microsaccade detection method . . . 103

4.4 Methods . . . 106

4.4.1 Data Preparation . . . 107

4.4.2 Refinement of Detection Methods . . . 107

4.5 Results . . . 108

4.6 Discussion . . . 109

5 Fixational Eye Movements and Stimulus Structure **113**

Abstract . . . 113

5.1 The structure of the visual field . . . 113

5.2 The periphery and fixation . . . 115

5.3 Factors influencing fixational stability . . . 116

5.4 Assessing fixational stability . . . 117

5.5 Experiment One: Eccentricity . . . 119

5.5.1 Methods . . . 120

5.5.2 Results . . . 124

5.5.3 Discussion . . . 130

5.5.4 Potential Underlying Mechanisms . . . 132

5.6 Experiment Two: Orientation . . . 132

5.6.1 Methods . . . 133

5.6.2 Results . . . 135

5.6.3 Discussion . . . 138

5.7 Overall Discussion . . . 141

6 How Does Fixational Stability Correlate With Unreferenced Motion Thresholds and Centre Estimation Abilities? **143**

Abstract . . . 143

6.1 Potential factors in fixational stability . . . 143

6.1.1 Motion Perception . . . 144

6.1.2 Unreferenced Motion . . . 145

6.1.3 Centre Estimation . . . 146

6.1.4 Complexity of determining the underlying mechanisms of fixational stability 146
6.2 Methods . . . 147
6.2.1 Participants . . . 147
6.2.2 Set Up . . . 147
6.2.3 Stimuli . . . 147
6.2.4 Procedure . . . 148
6.2.5 Analysis . . . 149
6.3 Results . . . 151
6.3.1 Automatic Triggering Success . . . 151
6.3.2 Comparison of Stability Measures . . . 151
6.4 Discussion . . . 153

7 Fixational Eye Movements and Gaussian Blur 155

Abstract . . . 155
7.1 Does Gaussian blur interact with fixational stability? . . . 156
7.2 Choice of eye tracker . . . 158
7.3 Experiment One . . . 158
7.3.1 Methods . . . 159
7.3.2 Results . . . 161
7.3.3 Discussion . . . 161
7.4 Experiment Two . . . 163
7.4.1 Methods . . . 163
7.4.2 Results . . . 164
7.5 Follow Up: Experiment Three . . . 166
7.6 Overall Discussion . . . 168
7.6.1 Natural occurrence of blur during fixation . . . 168

8 Position Correction due to Microsaccades and Drift 171

Abstract . . . 171
8.1 Historical Debate . . . 171
8.2 Defining Drifts and Microsaccades . . . 172
8.3 Measures of Corrective Power . . . 173
8.3.1 Measures used in previous research . . . 174
8.3.2 Measures used in this Chapter . . . 175
8.3.3 Missing Information . . . 177

8.4 Methods . . . 179
8.4.1 Data . . . 179
8.4.2 Data Analysis . . . 179
8.5 Results . . . 180
8.5.1 Start-End-Error . . . 180
8.5.2 Movement-Towards-Median . . . 182
8.6 Discussion . . . 184

9 Discussion **189**
9.1 Improvements in microsaccade detection and data analysis . . . 189
9.2 Progress in understanding the interaction between the stimulus and fixational eye movements . . . 190
9.3 Keeping the eyes on target using microsaccades and drifts . . . 191
9.4 Future avenues for research . . . 191

References **193**

10 Appendix **213**
10.1 Table of Microsaccade Features . . . 213

Chapter 1

Fixational Eye Movements - An Overview

1.1 Introduction to fixational eye movements

Fixational eye movements are small eye movements that occur during visual fixation. They are typically divided into three different types: tremor (small, < 0.01° but high-frequency, up to 90 Hz), drift (slow, with amplitudes of 0.04 - 0.13°) and microsaccades (small jump-like movements, up to 1°) (Moshel et al., 2008). When a stimulus is stabilised on the retina by counteracting eye movements perceptual fading of the stimulus is reported within seconds (e.g. Martinez-Conde, Macknik, Troncoso & Dyar, 2006; Riggs, Ratliff, Cornsweet & Cornsweet, 1953; Troxler, 1804). Therefore fixational eye movements are necessary to maintain the visibility of static scenes. Thus, counterintuitively, movement is required to fixate on and see stimuli, as without these movements the perceptual world would continually fade to a featureless grey.

Initially, it was thought that these movements occurred because of a central 'insensitive region' (Boyce, 1967), as a lack of sensitivity would explain why these movements were not bothersome to observers. Now we know that the opposite is true and that even vision using the region of highest sensitivity, our foveola, is dependent on constant motion in the form of fixational eye movements. The most obvious explanation for this phenomenon is that to counteract adaptation, continual change in the visual stimulus is necessary to help us see the world.

Despite these movements being central to our ability to complete visual tasks that require a relatively stable gaze, little is known about fixational eye movements. One reason for this is that eye tracking techniques have been limiting our ability to study fixational eye movements, which are typically very small. Some, mainly historic, eye trackers have a high tracking resolution, but require complex experimental set-ups and limit participant comfort, and sometimes even eye safety. This lead to those techniques only being applied to very few participants and eventually most of them fell out of use. Video-based eye trackers are the most common way to record eye movements today.

They offer more participant comfort and ease of use, but do so at the expense of tracking accuracy. They readily provide large amounts of digitised data, which can be challenging to analyse.

There are several reasons to believe that the study of fixational eye movements is an important and under-explored topic. One reason is that all healthy, large-scale oculomotor activity is valuable to our perception of the world around us: smooth pursuit helps us follow objects of interest with our gaze (e.g. Bahill & McDonald, 1983; Madelain & Krauzlis, 2003; Pola & Wyatt, 1980), whilst larger saccades help us in exploring the visual scene (Otero-Millan, Troncoso, Macknik, Serrano-Pedraza & Martinez-Conde, 2008). There is no reason to believe the same is not true for smaller eye movements, leaving their contribution to perception a field for exploration. After all, the visual system is very good at incorporating the features of our visual realities into its processing: we develop use of our foveola for high acuity vision (Curcio, Sloan, Kalina & Hendrickson, 1990; Curcio et al., 1991; Curcio, Sloan, Packer, Hendrickson & Kalina, 1987), whilst it has famously been shown in animals that there are systematic changes in the the neural tuning of the visual system depending on the available stimuli (Blakemore & Cooper, 1970; Hubel & Wiesel, 1970). Thus, we are interested in learning if fixational eye movements, like larger eye movements, are tuned to an individual's retinal mosaic, optimise the sampling of a given stimulus, and improve the associated extraction of information from the visual image.

Another reason to study fixational eye movements is that, especially microsaccades, exhibit systematic changes in a number of diseases (e.g. Fried et al., 2014; Otero-Millan, Macknik, Langston & Martinez-Conde, 2013; McInnis, 2014). It would therefore be of interest to better understand the underlying mechanisms of action, to further our knowledge of these diseases, and perhaps to be able to develop visually adapted stimuli to alleviate some of the visual symptoms.

The recurring questions in the field of fixational eye movements are:

1. Which properties of a stimulus support stable fixation?

2. Which changes occur in fixational eye movements in response to changes in the visual stimulus?

3. Which component of the eye movement trace allows the eyes to stay on target for prolonged periods of time?

Despite many researchers attempting to answer those questions, no consensus has been reached for these questions. It is important to strive to find answers to these questions as they may shed light on how our visual systems interpret low level visual information and act on it.

A re-examination of these questions is timely because of (i) advances in understanding the visual system; and (ii) the availability of an adaptive optics scanning laser ophthalmoscope (AOSLO) to track eye movements in high spatial and temporal resolution and high participant comfort, providing a direct reference to the photoreceptor mosaic.

1.2 Types of fixational eye movements

The most important issue when trying to analyse specific sub-types of fixational eye movements is to accurately identify them in the eye-movement trace. This is a complex problem which has not been solved completely, although methods are constantly improving. The following section will give an overview of what is known about the different types of fixational eye movements with a view to identifying their distinguishing features. It should be noted, however, that evaluation of a type of eye movement in any particular paper is inherently biased by the identification method for, e.g. microsaccades, as well as the recording method, and that it is through repetition and changes in methods that we can assume the average consensus represents the true nature of these movements adequately.

1.2.1 Microsaccades [1]

Microsaccades have been the object of systematic study for over 70 years. Over time the focus of research on microsaccades has shifted, from trying to learn more about their properties and purpose, to using them as a measure of cognitive processes such as covert attention (e.g. Engbert & Kliegl, 2003; Hafed & Clark, 2002; Laubrock, Engbert & Kliegl, 2005). With the increase in microsaccade research (see Fig. 1.10) the central problem facing the field is reaching consensus on features and characteristics of microsaccades, as well as improving automated detection methods.

Properties of Microsaccades

To be able to compare findings on microsaccades between different bodies of research it is important that the same type of movement is consistently identified and characterised and that a common vocabulary and conventions are established. For microsaccades this agreement has grown over time, but still has a way to come before a satisfying level of consistency is achieved. This spans many different aspects of microsaccade research ranging from the terminology used (microsaccades vs. jerks, vs. flicks vs. saccades) to data-segmentation methods (manual, automated) to which

[1] Part of this work is under review as a publication in the Journal of Eye Movement Research. Sections taken from the paper are included in section 1.2.1: Properties of Microsaccades This chapter expands on the paper. I have only reproduced work here that is my own.

features of microsaccades are described and with which parameters. Research articles from the past 70 years have been reviewed to identify which features of microsaccades have been reported consistently across time, which microsaccade parameter estimates have remained stable, and which have changed or remained under-explored over this reporting period. Understanding the defining features of microsaccades and being explicit about the parameters that define them can be a part of providing new avenues for microsaccade detection and contribute towards unifying the vocabulary used when describing microsaccades.

Over the last 70 years some features of microsaccades have been consistently reported in different set-ups and tasks. It has been established that microsaccades follow the same so-called main sequence relationship between their peak velocity and displacement as larger saccades (Zuber & Stark, 1965; Bahill, Clark & Stark, 1975). However, there appears to be some inconsistency in whether this relationship is plotted in linear or logarithmic space. A linear relationship on logarithmic coordinates implies a power law relationship between the underlying linear variables (peak velocity and distance), with the gradient of the line representing the exponent. Therefore, a linear main sequence on logarithmic coordinates only represents a linear relationship between peak velocity and distance when the gradient of the line is equal to one.

Early papers consistently plot the relationship on log-log coordinates for both microsaccades (Zuber & Stark, 1965) and large saccades (Westheimer, 1954). It is only in some more recent publications that the relationship is sometimes plotted in linear space (McCamy et al., 2012; Valsecchi, Betta & Turatto, 2007), with some even plotting it in both (Fang, Gill, Poletti & Rucci, 2018; Martinez-Conde, 2006). Over the distance and velocity ranges that can be measured with current eye trackers, the main sequence does appear to be linear for most reported data. However, plotting the data consistently on log-log coordinates may be more informative, particularly as tracking methods and algorithms develop. The main sequence for all data points collected from the review appears to be reasonably consistent across participants and set-ups (see Fig. 1.1), supporting the notion that the main sequence is a stable feature of microsaccades.

Another consistent finding is the variability of microsaccade rate with task instructions. First reported by Steinman and colleagues, it is a well-replicated effect that microsaccade rate declines with instructions to 'hold' the eye in place (Steinman, Cunitz, Timberlake & Herman, 1967), with increased mental load (Barlow, 1952) or in high acuity tasks (Armington & Bloom, 1974), whilst under free viewing, 'fixate' instructions, or a low mental load microsaccades occur more frequently. Microsaccade frequency is also reliably influenced by target onsets, which lead to a reduction in microsaccade frequency (Engbert & Kliegl, 2003; Rolfs, Kliegl & Engbert, 2008; White & Rolfs, 2016).

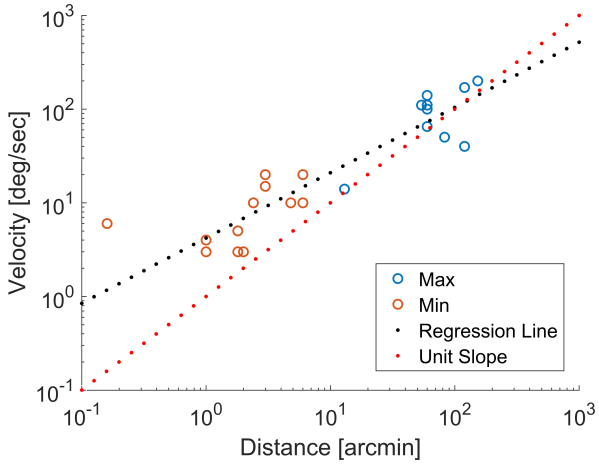


Figure 1.1: Minimum and maximum values of peak velocity and distance as extracted from the reviewed literature. To ensure that distance and velocity samples correspond to the same saccade only values read from graphs are included.

Modifying microsaccade rate using these methods will not be able to provide improvements in microsaccade detection methods. However, using data that should display a change in microsaccade frequency could be a useful tool for evaluating microsaccade detection methods: if a detection method fails to reveal the expected patterns in the data, it is unlikely to be a robust method.

A predominantly horizontal orientation of microsaccades has also been reported. Whilst microsaccades can occur in any direction (e.g. Haddad & Steinman, 1973), the vast majority of microsaccades fall predominantly on the horizontal axis (e.g. Moshel et al., 2008). Some eye tracking set-ups have exploited this feature and only recorded horizontal eye position (e.g. Armington & Bloom, 1974; de Weese Puckett & Steinman, 1969; Cunitz & Steinman, 1969; Deaner & Platt, 2003; Rattle & Foley-Fisher, 1968; Schor & Hallmark, 1978). It is not recommended to ignore eye movements in the vertical direction though, as important information may be missed. When the visual stimulus is not balanced in space, microsaccades have been shown to be biased towards the visual target (Cui, Wilke, Logothetis, Leopold & Liang, 2009; Laubrock et al., 2005), or, when social cues of direction, even spurious ones, are available microsaccades are also biased in that direction (Deaner & Platt, 2003). Microsaccades may also be biased to irrelevant, but salient stimuli (Galfano, Betta & Turatto, 2004). Analogous to the dependence of microsaccade frequency on task instruction, the fact that most microsaccades occur in the horizontal direction or are target-directed can be used as a sanity check when analysing microsaccade data.

Microsaccades are also frequently described as ballistic in nature. This term has led to some confusion about the expected trajectories of microsaccades. When an object is moving ballistically it is subject to an initial force that sets it in motion until this motion is stopped by forces acting against it, such as friction or gravity. Similarly, microsaccades are hypothesised to be ballistic; they are set in motion by the eye muscles (Riggs, Armington & Ratliff, 1954) following an initial

cortical signal, after which their trajectory cannot be altered, as shown by double-step tasks for large saccades (Becker & Jürgens, 1979). However, this does not necessarily mean that their actual trajectories are linear in space. Ballistic motion can still result in complex curved paths (e.g. a ball being thrown follows a parabolic trajectory). Another source of uncertainty is the eye tracker, which may also have non-linearities distorting recorded eye positions and potentially leading to distorted path recordings. Despite this many researchers have described microsaccade paths as linear (Engbert & Kliegl, 2003; Martinez-Conde & Macknik, 2007; Moshel et al., 2008) or imposed linearity criteria on their microsaccade detection (Thaler, Schütz, Goodale & Gegenfurtner, 2013). As shown by examples of real recorded microsaccade paths, there are many different recorded trajectories ranging from linear paths (Rucci & Poletti, 2015) to paths with "significant curvature" (Nyström et al., 2017). Whilst microsaccade paths are smoother than the zigzagging of tremor superimposed on drift, it would be wrong to assume that microsaccade trajectories are strictly linear. Given the complex, potentially curved nature of microsaccade trajectories it is difficult to use the ballistic property of microsaccade mechanics in detection methods, since an accurate model of the trajectory can only be achieved if we know all of the forces acting on the eye.

The emerging consensus is that binocularity (resulting in simultaneous, though not necessarily conjugate, or directionally correlated motions in the two eyes) is another defining feature of microsaccades. Conversely, drift and tremor have been shown not to contain any significant temporally co-ordinated components in humans (e.g. Krauskopf, Cornsweet & Riggs, 1960). The earliest recordings of binocular fixation data already showed a clear correlation between microsaccade occurrences in each eye (Krauskopf et al., 1960). Significant correlations between the direction and magnitude of microsaccades in the two eyes have also been reported (St. Cyr & Fender, 1969), as the majority of microsaccades are made in the same direction, with a subset being convergent, or even rarer, divergent (Van Horn & Cullen, 2012). This property is not matched by large saccades, which are nearly always conjugate, i.e. move both eyes in the same direction by the same amount. A special case in which saccades usually are not conjugate is when the gaze is not just redirected to a different target, but also to a different depth. In these cases one eye needs to move by more than the other. A reason this is not frequently discussed in the literature is that as a proportion of the total movement, this difference is negligible for large saccades, whilst it is much more noticeable for microsaccades. Additionally these differences may often lie close to the measurement error of the eye tracker. However, this may be evidence that for any saccadic motion (micro- or otherwise) it is the landing position which is programmed. During fixation, drift may have converged or diverged the eyes by larger proportionate amounts compared to microsaccade size, which may be why some

fixational saccades result in convergent or divergent movement, or with movements of different sizes in both eyes.

More recently monocular microsaccades have been reported to exist, which has lead to studies investigating that claim (Gautier, Bedell, Siderov & Waugh, 2016). However, it is very likely that any reported monocular microsaccades are artefacts of the recording and automated detection methods used (Nyström et al., 2017). In particular, it would appear that some tracker and algorithm combinations result in more frequent classifications of microsaccades as monocular. For example head-free viewing (Fang et al., 2018) is a challenge to microsaccade classification, as eye tracking is harder and less accurate, with head motion often leading to false spikes in eye velocity, which may then be falsely detected as saccadic motion. As binocularity appears a fundamental feature of microsaccades, it is a promising avenue for an automated detection method, whenever binocular eye tracking is available.

Microsaccades have also been identified as the trigger for some illusions of motion. Microsaccade rate is correlated with the amount of motion perceived in the Enigma illusion (Troncoso, Macknik, Otero-Millan & Martinez-Conde, 2008), with periods of high perceived motion being preceded by an increase in microsaccade rate and periods of low illusory motion being preceeded by fewer microsaccades. Otero-Millan, Macknik and Martinez-Conde (2012) also identified that microsaccades are one of the triggers for illusory motion in the "rotating snakes" illusion (Kitaoka & Ashida, 2003), along with blinks and saccades, i.e. events that produce large ocular transients. Yet it would appear that any fixational eye movements, perhaps proportionally to the amount of retinal image shift, can contribute to the perception of illusory motion (Murakami, 2003; Murakami, Kitaoka & Ashida, 2006).

Some diseases also lead to characteristic changes in microsaccades. In Parkinson's Disease microsaccades occur more frequently and are often larger (McInnis, 2014). This increased occurrence of larger microsaccades is hypothesised to, in turn, lead to an increased number of square-wave jerks, which are two microsaccades occurring one after the other, the first one triggering a positional error signal which is then corrected by the second microsaccade (Otero-Millan et al., 2013). In the attention deficit hyperactivity disorder (ADHD) population microsaccade rates are also elevated, but return to control baseline when medicated (Fried et al., 2014). From these disease profiles we can also learn more about microsaccades: the change in microsaccade behaviour in Parkinson's Disease, for example, suggests that microsaccades are at least partially controlled by the motor-control pathways or neurotransmitters affected in Parkinson's Disease. Therefore understanding both microsaccades and the diseases leading to changes in microsaccade behaviour can help us

understand more about the underlying systems of both.

Other reported aspects of microsaccades have changed considerably over time. The size of microsaccades has increased (Nyström, Hansen, Andersson & Hooge, 2016) from some reports as small as 10' (Winterson & Collewijn, 1976) and 15' (Bridgeman & Palca, 1980), to some reports of microsaccades as big as 60-120' (Cherici, Kuang, Poletti & Rucci, 2012; Fried et al., 2014; Hipp & Siegel, 2013; Ko, Poletti & Rucci, 2010; Laubrock et al., 2005; Møller, Laursen, Tygesen & Sjølie, 2002; Pastukhov & Braun, 2010; Siegenthaler et al., 2014). Fig. 1.2 illustrates this change in the largest reported microsaccade sizes, although it should be noted that the large spread of maximum distances reported since 2000 is in part caused by a change in the convention by which microsaccades are separated from larger saccades. Some studies set a hard upper limit, which results in a cluster of papers with a maximum size of 1° whilst others reported all saccades (micro- and large) that happened during a fixation task. In cases where both an upper limit and all saccades during fixation were reported, we decided to plot the largest value, so as not to be influenced by the adequacy of a cut-off point.

It is suggested that there is no hard boundary between fixational saccades and large saccades, as they appear to be supported by the same neural systems (Otero-Millan et al., 2013) and display many similar properties (Abadi & Gowen, 2004). Therefore, any saccades made during fixation should be treated as microsaccades. However, in some circumstances it may be questioned if some of the larger saccades in datasets could be target-directed. For example, the edge of a monitor or other features in the visual scene, not controlled within the experiment, might attract the participant's gaze and therefore an exclusion threshold might be warranted. Even with a fixation task, the size of the fixation target may need to be considered as saccades might be made to different parts of the visual stimulus. There are several possible ways to define the maximum size of a microsaccade based on experimental data: Bridgeman and Palca (1980) decided on "the maximum size of stimulus displacement which does not normally induce a subject to perform a saccadic re-targeting of the eye" (15', according to Rashbass (1961)), although the smallest voluntary saccades in the absence of a new fixational target can be as small as 5.6' (Haddad & Steinman, 1973). Other candidates could be the maximum size of saccades participants fail to self-report (Haddad & Steinman, 1973, ca. 10'), or a direct reference to the size of relevant retinal anatomy, e.g. the foveola

The theory that microsaccades are predominantly correcting for errors in eye position has enjoyed popularity for the last 70 years (for a detailed discussion see Collewijn & Kowler, 2008). Steinman, Haddad, Skavenski and Wyman (1973), however, showed that instead of microsaccades, a component of the motion trace named *slow control*, a type of drift, is mainly responsible for

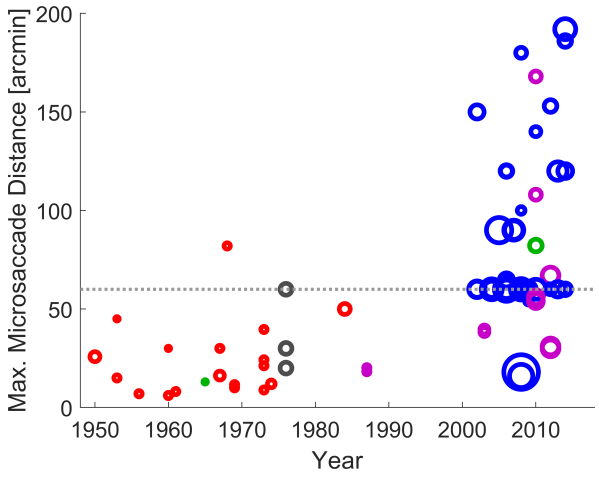


Figure 1.2: Maximum microsaccade size by year of publication. The area of each circle is scaled in relation to the number of participants. The circle colour represents type of eye tracker: red – contact lens mirror; blue – video-based; grey – search coil; green – limbus, purple – DPI. The dashed grey line indicates a microsaccade size of 1° .

keeping the eyes on target with others reporting similar results (Deubel & Elsner, 1986; Møller, Laursen & Sjølie, 2006). Although some microsaccades, perhaps most, return the eyes closer to target position (Engbert & Kliegl, 2004), this is not true for a large proportion of them (Ratliff & Riggs, 1950), and the return to target is marked by significant overshoot (Cornsweet, 1956). Despite slow control being an interesting target for research on the neural control of eye position, little has been reported on slow control since the advent of video-based eye trackers.

To establish an overview of the typical features of microsaccades a table was compiled listing information on a set of central criteria that were taken from the literature. Rolfs (2009) review of microsaccades was used to identify a set of papers to review between 1948 and 2009. Of those papers a list of papers with experimental data from human participants that include at least one piece of information from the central criteria was compiled. This resulted in a list of 53 articles (for the full table see appendix). For papers published between 2009 and 2018 the Scopus database was searched using the term *microsaccades* for "Article title, Abstract, Keywords". The results were narrowed by using the Scopus inbuilt tool to select only documents listed under *Articles* written in English. This resulted in a list of 204 documents. Any papers without experimental data that had been included, mainly those focused on modelling, as well as any papers without human participants were excluded manually. The remaining articles were studied in order of most cited to least cited, stopping after having found 20 articles containing details featured in our central criteria. The literature research was limited to 20 articles, to avoid over-representing the most recent research in the analyses. In total 73 articles contributed to the data presented in Figure 1.2 and 1.1. A subsection of articles is presented in Table 1.1, with a full version featuring all 73 articles available in the appendix.

It should be noted that the physical properties in the list of central criteria vary between papers (see Table 1.1). For example, in the column 'Minimum Speed' some papers report the smallest peak speed of all detected microsaccades, whilst others report the smallest speed of a sample considered to be part of a microsaccade. Similarly, there are three different ways in which microsaccade distances may have been reported: (i) the Euclidean distance from the first to the last sample; (ii) the sum of the Euclidean distances between all consecutive samples (the integrated path length); or (iii) the maximum Euclidean distance between any two samples in a microsaccade. If microsaccade paths are completely linear, all these would be the same, but if microsaccades exhibit any form of curvature or overshoot, or if the recording method introduces systematic errors that cause these paths to deviate from being linear there may be significant differences between the three possible metrics.

Some physical properties of microsaccades appear to be consistently under-reported. Most prominently microsaccade duration is hardly discussed (7 out of 73 papers: Beeler, 1967; Dimigen, Valsecchi, Sommer & Kliegl, 2009; McCamy et al., 2012; Otero-Millan et al., 2012, 2008; Schulz, 1984; Troncoso, Macknik & Martinez-Conde, 2008), although a lot of automated detection methods set minimum duration criteria (e.g. Dimigen et al., 2009). Information about acceleration profiles of microsaccades is also reported on rarely (3 out of 73 papers: Ditchburn & Ginsborg, 1953; Møller et al., 2006, 2002). Some trackers might not provide sufficient temporal and spatial resolution for a meaningful calculation of acceleration; however, acceleration profiles might provide a useful metric for microsaccade detection. It would be advantageous to the field if more authors shared these details, so that microsaccades across experiments, trackers and external conditions can be more extensively quantified.

The purpose of microsaccades

Given the size, frequency, and saccadic suppression caused by microsaccades (Hafed & Krauzlis, 2010; Zuber & Stark, 1966), researchers have long hunted for their purpose. Saccadic suppression is a term used for the elevated perceptual thresholds during a saccade, which goes beyond a degradation of the stimulus due to the speed of the eye movement. Rather it is assumed that saccadic suppression is used to manage the large amount of visual information that becomes available during a saccade. Bridgeman and Palca (1980) said that "a phenomenon which triples visual thresholds in normal humans for over an hour each day requires explanation.". This is probably an overestimation, as even assuming an average microsaccade duration of 25 ms, at a rate of 2 Hz for a 16 h day would only lead to a total of about 48 min of microsaccading. Especially

Paper	Analysis Method	Eye Tracker	Number of Participants	Min Distance [′]	Mean Distance [′]	Max Distance [′]	Min Speed [°/s]	Mean Speed[°/s]	Max Speed[°/s]	Mean Acceleration [°/s²]	Max Acceleration [°/s²]	Min Duration [ms]	Mean Duration [ms]	Max Duration [ms]	Min Frequency [1/s]	Mean Frequency [1/s]	Max Frequency [1/s]
Dimigen et al., 2009	EK	VB	12	**1.8**	13.8	**60**	**3**	/	**65**	/	/	/	/	/	**0.2**	1.46834	**6.5**
Ditchburn & Ginsborg, 1953	M	CLM	2	5	6.1/5.8	15	/	10	/	/	1000	/	/	/	0.2	.9-1.4	33.33
Martinez-Conde, Macknik, Troncoso, & Dyar, 2006	MC	VB	8	**1**	**14.4**	**120**	**3**	/	**40**	/	/	/	/	/	**3.2**	ng	**4.5**
McCamy et al., 2012	EK	VB	6	**1.8**	/	**60**	**5**	/	**140**	/	/	/	20	/	**0.5**	1.07	**2.6**
Møller et al., 2002	TH	VB	10	**6**	13-66	**150**	/	19-40	28-98	2321-6439	/	/	/	/	0.23†	0.61	0.93†
Otero-Millan et al., 2008	EK	VB	8	**2.4**	24.6	**60**	**10**	/	42	/	/	**4**	13	**34**	/	0.8	/
Otero-Millan et al., 2012	EK	VB	8	**3**	30	**153**	**15**	28 (peak)	**200**	/	/	4.3†	8	12†	0.48†	0.8	1.3†
Schulz, 1984	/	CLM	6	3	/	50	8.3	/	35	/	/	16	/	25	1	/	3
Siegenthaler et al., 2014	EK	VB	11	**6**	27	**120**	**10**	/	**170**	/	/	/	/	/	/	1.35	/
Troncoso, Macknik, & Martinez-Conde, 2008	EK	VB	6	**1.8**	24.6	180	/	41 (peak)	**100**	/	/	**2**	13	**101**	**0.2**	0.7	**2**
Valsecchi et al., 2007	EK	VB	17	**2**	/	90	**3**	/	**290**	/	/	/	/	/	0.733	1.544-1.797	**3.1**
Winterson & Collewijn, 1976	/	SC	7	**1**	7	**60**	/	/	/	/	/	/	/	/	0.079	1.25	1.78
Zuber & Stark, 1965	/	L	1	**2**	/	**13**	**3**	/	**14**	/	/	/	/	/	/	/	/
Hauperich, Young & Smithson	BCρ	VB	5	0.1	34	352	6.3	15.2	43.3	2800	5700	2	30	239	0.8	1.1	1.4
Hauperich, Young & Smithson	EK	VB	5	0.2	25	1218	10.2	28.8	62.5	3600	9200	3	25	92	1.4	2.4	3.4
Hauperich, Young & Smithson	M	VB	5	2.6	28	633	2.6	22.9	441	3300	6800	11	34	165	0.55	0.85	1.12

Table 1.1: Selected data from the literature review on microsaccades. For the full table please refer to the appendix. Note: The articles selected to appear in this table were chosen for completeness of criteria, as well as to represent a spread of papers through time. Data in bold represent values read off graphs, daggers indicate that the value given represents a median. In the column *Analysis method*, EK refers to variants of the Engbert and Kliegl (2003) method; MC refers to the criteria used by Martinez-Conde et al (2000); M indicates manual coding and TH refers to other threshold methods. In the column *Eye Tracker*, VB indicates video-based eye tracking; CLM refers to contact lens mirror systems; SC refers to scleral coil systems and L refers to limbus trackers. The shaded values in grey represent results obtained as part of Chapter 3.

considering that during free viewing we probably perform far fewer microsaccades in favour of larger exploratory saccades, which serve a clear purpose. Because of the obvious reason to make large saccades no one has questioned how many minutes of saccadic suppression we accept in return for being able to explore the scene - clearly intermittent saccadic suppression is not detrimental to our visual perception of the world. Yet over the years many researchers have hunted for the reason humans make microsaccades.

The research consensus at this point in time is that microsaccades lie on a continuum with larger saccades: they display the same features (binocularity, main sequence relationship), exhibit the same saccadic suppression (Hafed & Krauzlis, 2010; Zuber & Stark, 1966) and are served, as far as we know today, by the same underlying neural pathways (Martinez-Conde, Otero-Millan & Macknik, 2013) as larger saccades. Therefore we also have to assume that their functions are related. One obvious explanation would be that microsaccades are used for the exploration of the area immediately surrounding the fixation point. However, it may be argued that due to the high resolution available at the fovea, visual exploration of the area immediately surrounding the preferred retinal locus is not necessary and that, on the contrary, the saccadic suppression resulting from microsaccades would be more counter-productive than simply relying on drift and the foveal resolution for exploration.

An alternative explanation for how microsaccades resemble larger saccades might be that there is some advantage to making large and small saccades at regular intervals, e.g. to prevent fatigue of the eye muscles or strain of the eye. In that way, microsaccades may simply have been evolutionarily speaking unimportant to deselect. It should be noted that there is another type of eye movement, which serves no purpose, apart from to prevent adverse consequences from stillness, which can be suppressed voluntarily up to a certain point, which changes in frequency depending on task instruction (Bentivoglio et al., 1997) and has a similar baseline frequency (0.4 per second; Karson, Burns, LeWitt, Foster & Newman, 1984), is always binocular and which, just like microsaccades, interrupts visual perception: blinks. Of course it would be wrong to say that microsaccades and blinks therefore must serve similar functions. The blink comparison is intended to facilitate a shift in thinking about microsaccades: they do not necessarily have to provide a visual benefit to exist, they may simply be a consequence of a different and useful motor system.

A different way of thinking about microsaccades may be necessary as many groups have worked hard to find a *purpose* for microsaccades and failed. The most prominent example was borne out in a letter exchange between Ditchburn, and Kowler and Steinman, which brought the issue to a head, and the field of research to a standstill. Kowler and Steinman argued that they 'have now shown

that microsaccades serve no useful purpose in a cognitive task' (Kowler & Steinman, 1979, p. 108). Despite modern research attempting to offer more varied ways of thinking about microsaccades, I do not believe that anyone has conclusively shown that microsaccades serve any useful purpose in visual and cognitive tasks as the following have emerged as scientific consensus:

- Fixational eye movements in general prevent fading and not microsaccades in particular, as no foveal fading occurs even during long phases without microsaccades (e.g. Deubel & Elsner, 1986). Further evidence for this is that even very small shifts in the retinal image during stabilisation tasks, much smaller than microsaccades, caused by slippage of the stabilising lens disrupted fading (Barlow, 1963).

- Microsaccades are not necessary to keep the eyes on target. Many microsaccades overshoot significantly, even if they move in the correct direction for keeping the eyes on target and slow control appears to be an effective tool at maintaining a stable line of sight (Møller et al., 2006).

- Microsaccades are suppressed during high acuity tasks, such as threading a needle (Winterson & Collewijn, 1976). This suggests that they do not benefit us in such tasks and that perhaps the corresponding saccadic suppression would be an obstacle to task completion (Hafed & Krauzlis, 2010; Zuber & Stark, 1966).

- Microsaccades may be markers for some processes, like covert attention (Laubrock, Engbert, Rolfs & Kliegl, 2007), but are not necessarily a sufficient indicator of covert attention to be used as a reliable predictor or proxy (Horowitz, Fine, Fencsik, Yurgenson & Wolfe, 2007).

Finally, even if microsaccades can be shown to offer some benefit to human perception, it does not solve the issue of exactly how to define them. Researchers were initially intrigued by microsaccades, as they appear to go unnoticed by observers and can not be fully suppressed. However, empirically these involuntary and unnoticed fixational saccades are indistinguishable from target-directed microsaccades (such as to a different part of a fixation cross). Similarly, some microsaccades are used to keep the eyes on target, e.g. correcting for drift in amblyopia (Schor & Hallmark, 1978), however that does not necessarily extend to the majority of microsaccades. Microsaccades are divided into those that *deliberately* correct for positional error and those that do not and it is hard to experimentally distinguish between them. It has to be accepted that it may be the same system acting in different ways and that, as of yet, we have no way to differentially study *voluntary* saccades which are as small as microsaccades and *involuntary* microsaccades, whose

rate of occurrence may be lowered by task instructions or stimulus changes, but which cannot be predicted or entirely eliminated by the observer.

Conclusion

Microsaccades are small jerk-like movements that occur approximately 1-2 times each second. They are the fastest and largest of the fixational eye movements and have therefore been investigated most with regards to their potential visual benefits. We know that microsaccades occur simultaneously in both eyes, however this does not mean that they always display the same direction or magnitude of movement binocularly. Initially it was thought that microsaccades represent their own type of eye movement, however, now it is believed that they lie on the same spectrum as large, target-directed saccades. One feature that is sometimes used to distinguish microsaccades from larger saccades is that they occur involuntarily and that, especially for the smallest ones, observers cannot accurately report they made them.

1.2.2 Drift

Drift is a slow, meandering part of the fixational eye movement trace. During a phase of drifting, tremor is superimposed on the drift component. Comparatively little research is focussed on drift compared microsaccades, despite drift having a potentially substantial role in the visual information acquisition process (Ko, Snodderly & Poletti, 2016). There is evidence that drift is independent between the two eyes (Krauskopf et al., 1960), which has lead to the suggestion that drift is unimportant in keeping the eyes on a visual target, as it suggests that no higher processing areas are involved in generating it. However, there is mounting evidence, that drift plays a central role in keeping the eyes on target, or at the very least, that drift is influenced by the fixational stimulus. St. Cyr and Fender (1969) demonstrated that drift direction directly depends on the interaction between the observer and the target and that overall, for vertical or horizontal lines, drift occurred almost exclusively in the direction of the target. This is also the same direction, in which least neural information about a change in position is available. Therefore, drift may be influenced by the target's spatial pattern.

Drift has a speed of around 1°/sec (Ko et al., 2016; Cherici et al., 2012) on average and does not present as linear motion in space, but rather a curving, meandering one (Cherici et al., 2012). Poletti, Listorti and Rucci (2013) suggest that the interplay between drift and microsaccades is important: microsaccades relocate the preferred retinal locus precisely onto the desired target, while drifts are then necessary to extract the visual information. Ultimately at this point in time

it is unknown exactly what visual purpose microsaccades and drifts serve, however, we do know that motion at varying spatial and temporal scales is necessary for normal visual function. Thus, better quantifying drifts is an important aspect of progressing our understanding of fixational eye movements.

Slow Control

Slow control is a special type of drift movement, which is used to keep the eyes on target. Not much is known about slow control, as modern research has largely ignored its existence. It is not clear if drift and slow control are the same type of movement, or if slow control represents either a subset of drifts or is a separate type of movement. Several theories for how slow control comes about have been postulated. One early hypothesis for how slow control could be achieved was that it is part of the smooth pursuit system, effectively 'tracking' a target at zero velocity. If drift could act to keep the eyes on target it would suggest that both drift and saccades are responsible for maintaining a stable line of sight. More analogous to smooth pursuit, the eyes would continuously track the target smoothly, thereby countering their own positional variations, rather than the target's. However, it seems unlikely that smooth pursuit could be responsible for slow control, as the neural circuitry in charge of smooth pursuit is not suitable to it (Thier & Ilg, 2005). Moreover, Murphy, Kowler and Steinman (1975) showed that observers can dynamically change whether to smooth pursuit a moving pattern or to stay fixated on a target in front of the moving pattern. Additionally, they were also able to show that when instructed to use slow control to maintain their gaze in the centre of the moving grating without a fixation point, observers could do so, albeit with a slight bias in the direction of movement of the grating. This they suggested is evidence that slow control is not part of the smooth pursuit system, as we can use it in the absence of a moving target to maintain a line of sight.

Therefore the question of the existence and nature of slow control remains. The most important questions to answer would be (i) whether or not slow control is a binocularly synchronised phenomenon and (ii) if it is different from drift. Previous research suggests that drift is independent between the two eyes (Krauskopf, 1960), yet there are claims that slow control and/or drift are yoked between both eyes (Steinman et al., 1973). Thus, the following options are possible:

1. Drift and slow control are the same type of movement. They are both correlated between the two eyes and help control eye position.

2. Drift and slow control are the same type of movement. They are not correlated between the two eyes, but local mechanisms help control gaze position.

3. Drift and slow control are not the same type of movement. Drift is not correlated between the two eyes, but slow control is and helps to actively maintain a line of sight.

4. Drift and slow control are not the same type of movement, but both are, or are not, correlated between the two eyes. This would make it very difficult to distinguish between the two concepts based on non-invasive psychophysical methods.

1.2.3 Tremor

Tremor is a high frequency oscillatory movement superimposed on the drift component of fixation. It is considered independent between the two eyes (Krauskopf et al., 1960), but measuring it has been difficult due to its very small size (estimated as 6" (Eizenman, Hallet & Frecker, 1985)) and high temporal frequency (approximately 80 Hz (Bolger, Bojanic, Sheahan, Coakley & Malone, 1999)). A thorough review and study of tremor was undertaken by Bolger et al. (1999). They used a piezoelectric strain gauge technique to record eye movements and found that across 105 participants the tremor frequency ranged from 70 - 103 Hz with a mean frequency of 83.68 Hz, which is in good agreement with previous studies (e.g. Eizenman et al. (1985) who placed tremor in the range of 40 - 100 Hz).

The central problem to studying tremor and putting weight on findings relating to tremor is the accuracy of tremor recordings. The majority of eye trackers in use today, such as video-based or limbus trackers, are unable to record it. It cannot be said with certainty that eye trackers used in the past to study tremor, such as the piezoelectric technique (Bolger et al., 1999; Bengi & Thomas, 1968), or the corneal reflex method used by Eizenman et al. (1985) (for details of the technique see: Eizenman, Frecker & Hallett, 1984) are indeed sufficiently accurate. In fact Eizenman et al. (1985) report tremor of the order of 6", whilst acknowledging that 'system noise is less than 30 arc sec' for their version of the corneal reflex method. The piezoelectric technique is reported to have a higher resolution of 'a few seconds of arc' (Bengi & Thomas, 1968) and may be more suitable for accurate recordings of tremor.

Modern adaptive-optics eye trackers should be able to record tremor and provide exact information on how many cone distances tremor shifts the retinal image. However, as it has not been in the spotlight of research recently, only very few studies have examined it, some with diverging results. Stevenson, Roorda and Kumar (2010) claim that in their recording of fixational eye movements they were not able to identify a clear tremor trace. However, the same lab, eight years later self-deposited an article (not peer-reviewed) studying tremor and reported a tremor component in the same frequency range as previous reports (50 - 100 Hz) but much smaller (about 1") (Bowers, Boehm &

Roorda, 2018).

Further evidence comes from DPI eye trackers. Ko et al. (2016) characterised scleral coil and DPI systems and found their DPI tracker resolution to be sufficient to study tremor. They are the first to report on the imbalance on tremor of horizontal and vertical components, finding that tremor is more pronounced horizontally.

Assuming that the larger 6” amplitude estimation for tremor is correct, it is unlikely to have any visual consequences, as even in the centre of the fovea the cone-to-cone distance is about 20” (Nachmias, 1959) and the smallest cones no smaller than 13-15” (Riggs & Ratliff, 1951). This would mean that the average shift in fixation position due to tremor would be only about a third to a half a cone, which is very unlikely to have a large influence on day-to-day perception. However it may be able to sharpen our vision (Pääkkönen & Morgan, 2001; Patrick, Roach & McGraw, 2017) in a process that may be regarded as analogous to dithering in display technologies. Dithering is a technique designed to improve the spatial resolution of a display by rapidly changing the displayed value of a pixel so that the resulting percept is changed to a smoother one. However, it may be possible to design tasks that require minute shifts of the retinal image to identify targets adequately and tremor may play a role in completing such tasks. However, it is hard to imagine how tremor could play a large role in perception, given the much greater retinal shifts induced by drift.

1.3 Neural systems involved in fixational eye movements

1.3.1 A brief overview of visual processing

The first visual processing area is the retina. There, retinal photoreceptors detect the visual stimulus and provide initial processing, collecting information on the intensity of light with regards to the sensitivity of the photopigment. The retinal mosaic, which changes with eccentricity, imposes limits on the information our eyes can collect: foveal cones are smaller and packed tightly, whereas in the periphery rods are interspersed and cones become larger (Curcio et al., 1990). Signals from several photoreceptors are collected in interneurons (horizontal, amacrine and bipolar) and compared by ganglion cells, whose receptive fields change in size and structure depending on type and retinal location (Dacey & Lee, 1994; Dacey, Peterson, Robinson & Gamlin, 2003; Lee, 1996). Most ganglion-cell receptive fields display a centre-surround antagonistic organisation, which exhibits spatial selectivity based on the size of the receptive field and colour selectivity based on the cone inputs to the centre vs. the surround. This pre-processed signal is passed to sub-cortical and cortical areas for further information extraction and also the generation of signals to control eye movements. The further along the visual pathway information travels, the more complex the operations on

the information are, and the less scientific consensus there is about exactly how and where this processing occurs or how this data is combined into actionable or conscious information.

After the initial retinal processing the information from both eyes is separated into the left and right hemifield by the passing of the nerve fibres relating to each nasal side through the optic chiasm to the contralateral side of the brain. Then the information is relayed to the subcortical processing areas: the superior colliculus (SC), the lateral geniculate nucleaus (LGN) and the pretectal region. These nuclei in the midbrain further process the information from the contralateral visual hemifield (Kandel, Schwartz & Jessell, 2000). The SC receives direct projections from the retina and represents mulitsensory events and saccadic behaviour in a retinotopic map (Hafed, 2018). The LGN is the main subcortical processing area, receiving 90% of the axonal inputs from the retina. Information about colour, luminance, spatial and temporal frequency is processed and relayed to the cortex via the parvo- (Merigan, Katz & Maunsell, 1991), magno- (Merigan, Byrne & Maunsell, 1991) and koniocellular layers of the LGN (Casagrande, 1994). The pretectum controls the direct and consensual pupillary reflexes (Magoun, Atlas, Hare & Ranson, 1936). After subcortical processing the visual information travels via the optic radiations to the cortex.

In the cortex the first processing area is V1, which is retinotopically organised, dedicating most area to the high acuity region of the fovea and then progressively less to more peripheral retinal areas, a feature called cortical magnification with a psychophysical counterpart called M-scaling (Cowey & Rolls, 1974). Damage to V1 may result in a condition called blindsight in which the affected observer cannot report the shape of visual inputs, but can successfully determine the direction of movement of objects and avoid collisions with objects when walking. After V1 and V2 it is generally thought that the visual stream separates into a dorsal ('where') and a ventral ('what') pathway. The types of information represented by neurons in higher processing areas become more elaborate, featuring for example more complex motion detection (MT/V5) (Newsome & Pare, 1988) or colour perception (V4) (Lueck et al., 1989).

The combined result of our visual system is that we can successfully interact with the visual world around us. Each step in the processing contributes to this goal. Movement of the eyes is an active contributor to how we collect the visual information available to us and as such plays a large role in our visual perception, as evidenced by the rare patients who can not make any eye movements (Gilchrist, Brown & Findlay, 1997; Gilchrist, Brown, Findlay & Clarke, 1998).

1.3.2 Eye movements: Motor Control

The eyes are moved by six muscles, comprising three pairs: the superior and inferior rectus muscles, which allow the eye to move up and down; the medial and lateral rectus muscles, which allow the eye to move left and right; and the superior and inferior obliques which allow for torsional eye movements. There are considered to be six systems for keeping the eyes on target: the *vestibulo-ocular* and *optokinetic* movements help counteract abrupt and sustained movements of the head; the *saccadic* and *smooth pursuit systems* allow us to shift our gaze to and follow targets. These four systems are all characterised by their conjugate nature: i.e. both eyes move in the same direction by the same amounts. The exception to this rule is the *vergence system*, which allows us to focus our gaze on objects at differing distances to us: converging for objects very close to us and diverging again when we focus on targets further away. Lastly, the sixth system is the *fixation system*, which suppresses large eye movements, but allows fixational eye movements, which enable us to see during sustained fixations (Kandel et al., 2000).

Saccades are programmed cortically, with the frontal eye fields (FEF) encoding specific saccade information, and integrating cognitive signals related to saccades from the supplementary eye fields and the dorsolateral prefrontal cortex. These signals are then directly passed to the SC where the saccade is triggered, as well as to the caudate nucleus which inhibits the substantia nigra, which otherwise would inhibit saccadic movements (Gaymard, Ploner, Rivaud, Vermersch & Pierrot-Deseilligny, 1998).

Smooth pursuit requires the accurate estimation and matching of the target's velocity. Information about the velocity of the target comes from the medial temporal and medial superior temporal areas. The frontal eye fields also contribute to the smooth pursuit system. Sub-cortical areas necessary for smooth pursuit as are the cerebellum and pons (Thier & Ilg, 2005).

As fixational eye movements are much smaller and less well studied than other eye movements, our understanding of their neural origins is more limited. It remains debated if fixational eye movements, especially microsaccades have any cortical origins. Similarly, it is not entirely understood if drift and tremor are binocular or monocular phenomena and where their neural origins lie.

1.3.3 Microsaccade Generation

Current understanding of the origin of microsaccades is limited to brain stem structures (Hafed, 2011), with regions involved in microsaccadic generation also generally linked to the generation of larger saccades (Martinez-Conde et al., 2013). Among these are the pontomedullary reticular formation, the abducens nucleus (Van Gisbergen & Robinson, 1977; Van Gisbergen, Robinson &

Gielen, 1981), and the rostral pole of the SC (Munoz & Wurtz, 1993). However, the exact mechanisms and pathways remain unclear. For example it is not known whether they are subject to external or internal triggers, what the exact role of neural noise is (Otero-Millan et al., 2011) and whether or not cortical structures are involved (Hafed, 2011).

One of the few brain regions involved in microsaccade generation of which we have reached a somewhat deeper understanding is the superior colliculus. The SC is a midbrain structure receiving direct input from the retina and cortex and has been known to be instrumental in coordinating large saccades for a long time (Krauzlis, 2013). It should be noted that the SC in mammals is homologous to the tectum in other animals (Krauzlis, 2013) underlining the necessity of picking suitable model organisms for the study of the neural origins of fixational eye movements. In mammals the SC consists of seven distinct layers, each organised retinotopically. The superficial layers of the SC receive inputs from the retina and visual cortex, while the intermediate and deep layers receive information form a variety of sources, including sensory and motor areas of the cortex. There is now evidence that the SC encodes and combines features of the stimulus into retinotopic maps (Hafed, 2018).

The SC has been studied for its contribution for microsaccade generation and encoding. Hafed and Krauzlis (2012) have been able to show that single cells in the SC display selectivity for saccade direction and size, including some whose size preferences stretched the gap between larger and microsaccades. This strongly suggests that microsaccades and larger saccades are indeed part of the same type of eye movement. The same group was also able to show that microsaccade generation is impaired following lesions to the SC (Hafed, Goffart & Krauzlis, 2009). They argue that the SC is not, as previously thought, formed of a peripheral 'motor' and a central 'fixation' zone, which inhibits saccades, but rather that it encodes the location of objects of interest in space and that by lesioning parts of the SC, these estimates become biased and less accurate, leading to visuo-motor errors.

A further obstacle to understanding the neural origins of microsaccades is the fact that non-human primates have to be trained to make fixational eye movements, including microsaccades (Bair & O'Keefe, 1998). Even monkeys trained to make fixational eye movements may still exhibit different fixational behaviours to humans. Snodderly (1987) showed that the direction of microsaccades in macaques changed depending on whether they were detecting the dimming of a dot in the light or the dark, whilst in humans the lighting condition had no effect on microsaccade direction. Ultimately, we lack a good model organism and many conclusions drawn from non-human primate studies are more limited than for neural systems in which our behaviours are more similar.

1.3.4 Neural control of drift and tremor

Our understanding of how drift and tremor are generated is even poorer. There is evidence that these types of movement are not conjugate between the two eyes (Krauskopf et al., 1960), suggesting there is not a central control system for them. Supporting this is research that showed the frequency of tremor is correlated with the random firing of clock-like motor units, which drive eye muscles, resulting in the conclusion that tremor is likely caused by physiological noise (Eizenman et al., 1985). But not all studies agree on this, some have found correlation between the drifts of the two eyes, which led them to conclude that they are at least in part centrally generated (Spauschus, Marsden, Halliday, Rosenberg & Brown, 1999). Riggs and Ratliff (1951) also described dirfts and microsaccades as "*in general rather closely synchronized*" which is in agreement with the findings of Ditchburn and Ginsborg (1953), who reported a significant relationship between the vertical drift components between the two eyes. The extent to which drifts are related between both eyes is as of yet unclear as the evidence is weak, conflicting, and often eye tracking idiosyncrasies, such as changes in accommodation (Ditchburn & Ginsborg, 1953) or pupil size (for video-based eye trackers) interfere with the accurate measurement of drift. More research is needed to reconcile the different findings on drift and tremor generation.

1.3.5 Consequences for research

Based on our knowledge of the visual system, we can make certain assumptions about the neural origins of fixational eye movements. For movements to always be binocular in nature, the visual information has to have at least been processed in the subcortical areas: the LGN, SC or pretectum, as these are the first areas where information from both eyes is combined. To study the binocular nature of eye movements it is necessary to record eye movements binocularly, and careful selection of techniques, such as haploscopic viewing, may help to uncover more information about fixational eye movements. Another consideration in the psychophysical study of eye movements is the time course of events. Any region involved in generating fixational eye movements is limited by the information available to it. Therefore, changes in fixational eye movements in response to different stimulus parameters can indicate how much processing the visual stimulus has undergone, before a movement response. The longer after an initial stimulus before an eye movement response, the further up the visual processing stream the information can assumed to have travelled (although there is some conflicting evidence about this assumption in monkeys (Fabre-Thorpe, Richard & Thorpe, 1998)). Similarly, the more complex the features fixational eye movements respond to, the higher the processing areas involved are likely to be . If the assumption holds then psychophysical

experiments in humans can contribute to the debate on external vs. internal triggers for fixational eye movements and the question of cortical involvement.

A limitation of studies on the neural origin of fixational eye movements is that they are mainly done in non-human animals, mainly primates, but also turtles (Greschner, Bongard, Rujan & Ammermüller, 2002) and other animals (e.g. cats Winterson & Robinson, 1975). Any conclusions for human eye movements are limited by how different the visual systems are to the human one, both physiologically and in the functions that they have developed to support. In particular, not all animals display even a similar retinal structure to humans. The human visual system is foveating, meaning that the highest acuity vision is only possible in the centre of the fovea, which we have to move to be able to extract fine details. This feature of our retinas has direct consequences for eye movements and animals which do not exhibit it, are very unlikely to be adequate model organisms. Turtles, for example have a "topographic organizations centered on a linear visual streak" (Ammermüller & Kolb, 1996), which does not suggest them to have a strong need to move their eyes in similar ways to humans.

1.4 Fixational Eye Movements and Task Performance

One recurring question about fixational eye movements is if they actively improve visual task performance. This question has two aspects: firstly, if the eye movements confer a benefit in task performance and, secondly, if they actively do so. These two concepts are linked but not identical, as an epiphenomenon of, for example microsaccades may prevent the fading of peripheral stimuli, yet if they are not actively triggered by peripheral fading, it may be argued that microsaccades are not actively conferring that benefit.

Research into fixational eye movements and microsaccades in particular was dampened by an exchange between Kowler and Steinman (1980, 1979) and Ditchburn (1980) discussing the *purpose of microsaccades* (Rolfs, 2009). Their exchange highlighted the fact that no convincing improvements in task performance by microsaccades had been described, despite many attempts to find such a task. Only in the 2000s was interest in fixational eye movements and task performance revived.

1.4.1 Theoretical Improvements Due to Motion

Theoretically it is known that movement can improve the sampling of an object. As such, a number of papers modelling this effect have been published. Desbordes and Rucci (2007) modelled the responses of parvocellular and magnocellular ganglion cells in the macaque retina in response

to natural images moving across the photoreceptors based on prior recordings of fixational eye movements. They found that the small fixational eye movements, combined with the statistics of retinal images and the properties of parvo-and magnocellular ganglion cells, lead to a dynamic spatial decorrelation of retinal activity. They argue that fixational eye movements influence retinal activity in systematic ways that are integral to the representation of the visual stimulus at this early stage of processing. This hypothesis is supported by electrophyiological recordings in visual cortical areas 17 and 18 in aneasthetised cats and subsequent simulations of cat retinas up to ganglion cell level by Hennig, Kerscher, Funke and Wörgötter (2002). They report that moving gratings lead to greater cortical responses if small amounts of jitter were added to the movement and that, based on the findings from the simulation, this may be due to spatiotemporal integration of information.

Donner and Hemilä (2007) presented a model in which microsaccades could lead to a sharpening of borders and the better resolution of two closely-spaced lines. A similar finding was reported by Poletti and Rucci (2008), who attempted to model the responses of parvocellular ganglion cells in response to the stimuli and recorded eye movements of a previous study (Rucci, Iovin, Poletti & Santini, 2007). They also found that there was significant synchronisation in responses during the viewing of high spatial frequency gratings, but not low spatial frequency ones, replicating the previous behavioural result.

That small amounts of movement can improve perception when the receptor field under-samples the stimulus is an intuitive concept. A small shift in the stimulus can lead different stimulus features to be sampled, which were previously not detected, due to the under-sampling of the receptor field. If the visual system has a way of combining the features sampled at different time points, small amounts of movement have the potential to meaningfully improve the amount of information and therefore decision-making based on the stimulus. That this is theoretically possible, either in the peripheral retina, or in cases of retinal disease was shown by Patrick et al. (2017). Similar enhancements of natural images due to fixational eye movements were also reported by Olmedo-Payá, Martínez-Álvarez, Cuenca-Asensi, Ferrández and Fernández (2015).

1.4.2 Prevention of fading

From stabilisation studies we know the importance of fixational eye movements in maintained visibility of visual targets (Barlow, 1963). When an image is kept stationary relative to the retinal photoreceptor mosaic the visual target will fade in a matter of seconds. If stabilisation is achieved in only one cardinal direction, image components disappear in the same direction of stabilisation (Bradley & Schor, 1988; Ditchburn & Ginsborg, 1952). The underlying assumption for this is that

moving vertically across a horizontal border will generate a clear neural signal that the underlying stimulus has changed, whilst moving horizontally along a horizontal border, no change occurs at a photoreceptor level and therefore the percept fades.

Riggs et al. (1953) were able to show that under stabilised conditions the stimulus is initially clearly visible, next the high spatial frequency components fade whilst lastly, and intermittently, probably due to imperfect stabilisation, the low spatial frequency components fade. This can be explained by non-sustained firing of neurons. Initially, as the stimulus appears neurons fire in response to it. As the stimulus is present for longer, the stimulus fades, however, high spatial frequencies and low spatial frequencies may be differently affected by the presence of residual motion from imperfect image stabilisation. Under perfect conditions we would assume that all components fade equally fast.

During the viewing of equal luminance chromatic boundaries under varying degrees of image stabilisation, greater amounts of movement improve visibility of the chromatic boundary (Clowes, 1961, 1962). This suggests that movement is beneficial at the point where chromatic information is processed.

The exact amount of movement needed to prevent a stimulus from fading depends both on the stimulus and the retinal eccentricity that it falls on. Generally speaking, stimuli with higher contrasts and sharper borders are less likely to fade than those without. Stimuli presented a greater retinal eccentricities also fade more easily than those displayed close to the centre of fixation. The easier a stimulus fades, the larger the retinal movement required to restore visibility. Martinez-Conde et al. (2006) found that microsaccades correlate with periods of restored visibility of peripheral Troxler targets. This suggests that microsaccades can have the correct amplitude and velocity of movement to restore visibility for these stimuli. They present no evidence that microsaccades are actively generated to restore visibility, as periods of fading of variable lengths occur in their behavioural recordings.

1.4.3 Grating Orientation Discrimination

Once a stimulus is above its detection threshold, discriminating features of the stimulus becomes possible. As small shifts of the image on the retina should theoretically improve sampling and neural responses, it is to be expected that this may confer benefits in the discrimination of grating orientation. Fixational eye movements were shown to improve the orientation discrimination for high spatial frequency gratings (Rucci et al., 2007) but not low spatial frequency ones. A later study found that microsaccades in particular would be more beneficial to the perception of low

spatial frequency gratings (Mostofi, Boi & Rucci, 2016). Thus, the exact nature of the influence of eye movements on the discriminability of grating direction depending on spatial frequency needs further work.

1.5 Eye trackers

For a long time, eye-tracking equipment was not well suited to investigating the influence of the visual scene on small scale eye movements, nor to how the retinal structure may influence eye movements. In the past, eye tracking was always a compromise between accuracy and comfort. Most eye trackers measure the position of the eye in the head, like techniques based on pupil or iris position (e.g. video-based trackers (e.g. EyeLink, Tobii, pupillabs), limbus trackers (Zuber & Stark, 1965)), the reflections of plane mirrors (Adler & Fliegelman, 1934; Ditchburn & Ginsborg, 1953), Dual-Purkinje-Imaging (DPI) (Crane & Steele, 1985), scleral coils (Fuchs & Robinson, 1966; Remmel, 1984) or electrooculograms (Kolder & Brecher, 1966), to name the most common ones. Measuring the position of the eye in the head is useful for studying the control of eye movement, however to draw stronger conclusions about the consequences of these movements it is most useful to know how the photoreceptors are shifted over the image. This can now be done with modern adaptive-optics eye trackers, which will be discussed in more detail later. These eye trackers take high resolution images of the retina at single cell resolution and can resolve eye movements that move the retina by fractions of a cone.

Some eye trackers have, generally speaking, higher resolution than others. Based on the literature review of microsaccade features the following approximate ranking based on recording resolutions becomes apparent: AOSLOs and contact lens mirror methods offer the highest resolutions, followed by DPI trackers. Next there are video-based methods and scleral search coils, while limbus trackers and electrooculograms offer lower resolution data.

Yet resolution is not the only thing to consider when deciding which type of eye tracker to use. Whilst DPI trackers are the current gold standard for non-invasive high-resolution eye tracking, they require specialist knowledge to use and maintain. Therefore the most commonly used eye trackers are video-based. However, in many cases it is hard to adequately compare eye tracker performance, as often not all necessary variables are given. To fully quantify eye trackers we need to know the accuracy, resolution and precision of the instrument. The accuracy tells us about how large the systematic errors associated with an instrument are. Precision gives us the statistical variability of sampling the same *true* value whilst resolution tells us about the size of the measurable steps (see Fig 1.4). Ideally all these values should be as small as possible. For tracking fixational

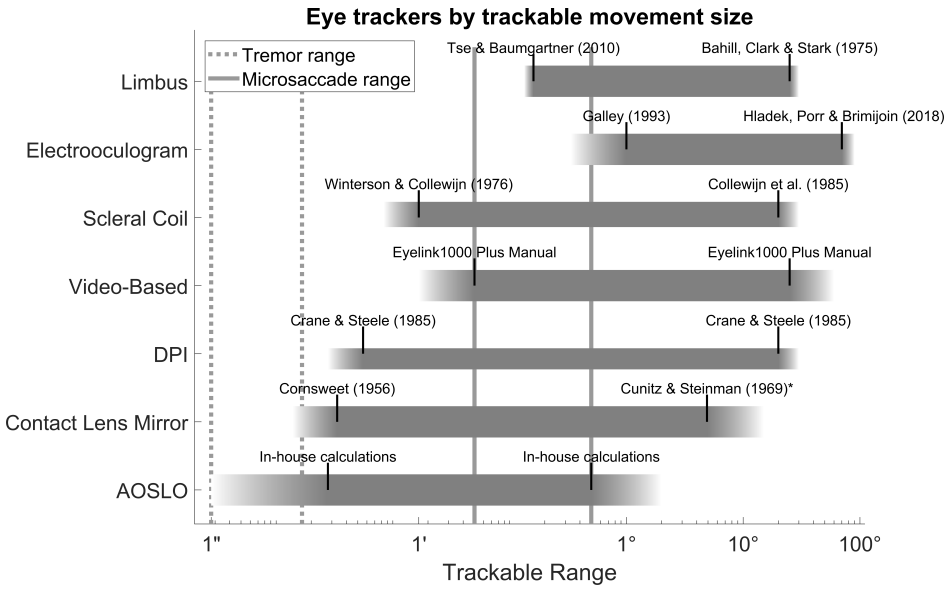


Figure 1.3: Approximate comparison of the ranges of movement that can be recorded using the different types of eye tracker. Citations marked with a * indicate that this is the largest movement recorded in the citation, not necessarily the largest possible trackable movement.

eye movements accuracy may often not be as important as precision, as it is less important to ascertain exactly where the line of sight fell, than it is to establish how much motion occurred between adjacent temporal samples. A high resolution is still very much desirable for fixational eye movements, as the tracker needs to be able to resolve very small changes in eye position to be useful. Only then can tremor be resolved, or the small changes in position caused by drift be studied extensively.

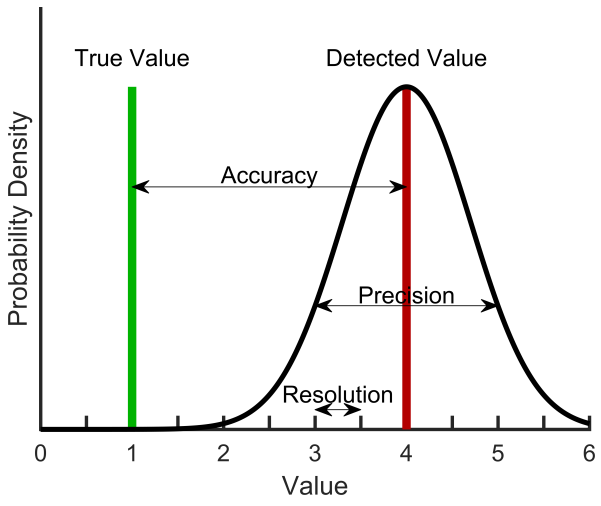


Figure 1.4: Comparison of accuracy, precision and resolution.

However, eye movements translate the visual image on the observer's retina, the structure of which is unique to each individual (Hofer, Carroll, Neitz, Neitz & Williams, 2005). Therefore it is important to consider the structure of the retina when studying eye movements, which is a feature automatically part of the AOSLO eye tracking process, during which high resolution images of the

retina are captured. It allows us to answer questions like: What effect does the interaction between an observer's retinal mosaic, their eye movements and the visual stimulus have on the processing of visual information?

1.5.1 Contact lens mirror methods

The earliest eye trackers used in research predominantly employed variants of the contact lens mirror method (e.g. Armington & Bloom, 1974; Ditchburn & Ginsborg, 1953; Nachmias, 1961; Riggs et al., 1954), which requires custom-made tight-fitting hard contact lenses to be worn by participants (see Figure 1.5). These provide high temporal and spatial resolution eye tracking when the angle of reflection of a beam of light from the mirror on the contact lenses is recorded.

There were several different variants of this technique. Some set-ups placed a mirror directly onto the sclera (Adler & Fliegelman, 1934), others required tight fitting and heavy contact lenses (Riggs et al., 1954), whilst yet others used suction to hold the lenses in place (Alfred Yarbus, 1967), generating pressures greater than 150 mmHg, which after a short time causes headaches, even when the cornea is anaesthetised and can lead to corneal abrasions if the lens is jolted (Barlow, 1963). Some labs standardly used a local anaesthetic to minimise the discomfort due to the contact lens and minimise the associated blinking and thereby lens slippage (Pritchard, Heron & Hebb, 1960).

Generally speaking, the more secure the lens was, the better the eye tracking results, as evidenced by the fact that when the respective set-ups are used for fading experiments, fading occurs faster and more completely for the more secure suction lenses (Barlow, 1963). This technique limited participant comfort. Not only did it lead to the above described issues, but often lenses left a circular depression of the sclera after the experiment had finished (Ditchburn & Drysdale, 1977). As it prohibits blinking, it required participants to hold their eyelid up during the experimental session which is uncomfortable. The issues around participant comfort and eye safety made testing large numbers of participants unsuitable, and monetary reasons further allowed this way of eye tracking to become obsolete, as "the cost of providing a large number of subjects with contact lenses is prohibitive" (Ditchburn, Fender, Mayne & Pritchard, 1956). Thus, only small numbers of participants could be tested for each experiment.

Stabilised retinal images

One way in which contact lens methods have been very effective is their contribution to our knowledge of vision with a stabilised retinal image. Using contact lenses any image can easily be

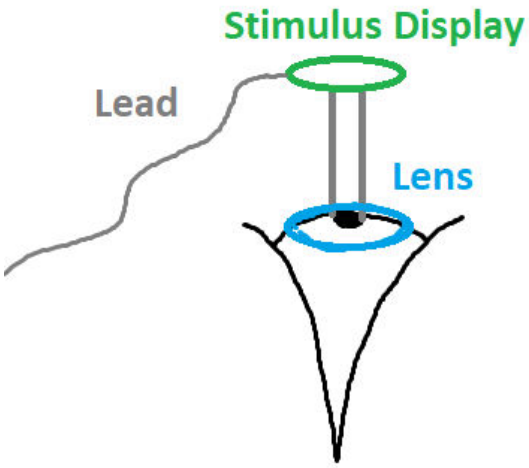


Figure 1.5: The original image is redacted due to copyright. Diagram of an observer wearing a contact lens for eye movement recording and image stabilisation. Note: the observer is lying down so that gravity can aid the lens staying in place. Adapted from (Pritchard,1961).

held stationary on the retina, as the lens, depending on the security of its fit, will move with the eye, thereby preventing relative motion of the image. A similarly good stabilisation is practically impossible to achieve using digital methods. Other stabilisation techniques allow anatomical features of the eye (e.g. vessels/iris) to be optically stabilised, which is useful in showing the effect stabilisation has on the visual percept, however these methods prevent the careful manipulation of stimuli (Ditchburn et al., 1956).

1.5.2 Scleral coil

Scleral coil eye trackers are highly accurate, but rely on participants wearing lenses that contain a metal coil, across which a magnetic field is generated by surrounding coils (Remmel, 1984). Motion of the coil in the magnetic field induces a current, which is measured via a cable connected to the coil in the eye. This cable and the lens may be uncomfortable for the wearer (for an example see Fig. 1.6). Also scleral coils have been shown to reduce the speed of saccades beyond what is explicable by the weight of the lens or the necessary scleral anaesthesia

In animal research scleral coil eye trackers are frequently used with the metal ring necessary for the induction of current sewn to the sclera (e.g. Collewijn & Van Der Mark, 1972). This makes their recordings more accurate than corresponding measurements in humans. However, it is an invasive procedure which is gradually becoming replaced by using video-based tracking techniques on animals (e.g. Blanchard, Wilke & Hayden, 2014).

Any technique using contact lenses, such as scleral coil or plane mirror eye tracking, is limited by how well the lens fits the participant's cornea and it is often not possible to completely eliminate slippage of the lens, leading to artefacts in the recording (Barlow, 1963).

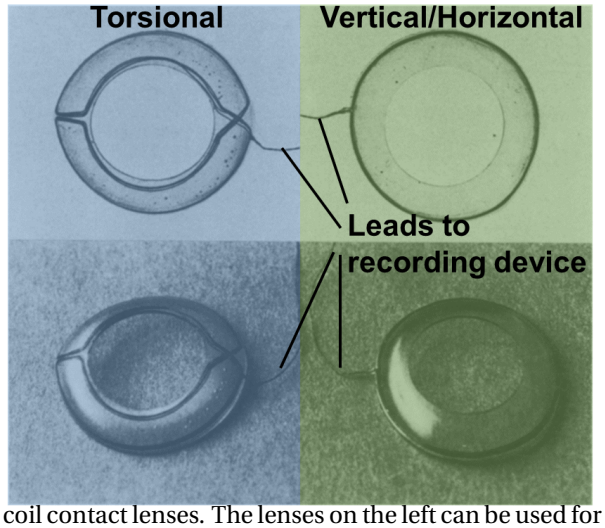


Figure 1.6: Photo of scleral coil contact lenses. The lenses on the left can be used for rotational eye movements,while the ones on the right would provide standard horizontal and vertical position measures. The diameterof the central hole is 11.3 mm. Adapted from (Collewijn et al., 1985). Reprinted by permission from: Springer, Experimental Brain Research, Human ocular counterroll: assessment of static and dynamic properties from electromagnetic scleral coil recording, Collewijn et al., 1985.

1.5.3 Electrooculograms

Electrooculograms (EOGs) record eye movements by detecting changes in the retino-corneal standing potential, which is typically recorded using electrodes placed above and below the eye (for an example see Fig. 1.7), although other methods, including in-ear electrooculography have been used (Hládek, Porr & Brimijoin, 2018). They assume that the eye acts as a dipole, with the front of the eye being the positive and the back of the eye the negative pole. To extract eye-movement data it has to be assumed that any recorded changes in this potential are due to eye movements, not other artefacts, such as noise from the skin potential response (Shackel, 1967). Whilst useful for recording large eye movements, as the method isn't limited by large rotational angles, its spatial resolution struggles with recording fixational eye movements. The fact that no equipment needs to be placed in front of the eye makes EOGs a useful tool in the field, for example when studying eye movements while driving (Galley, 1993).

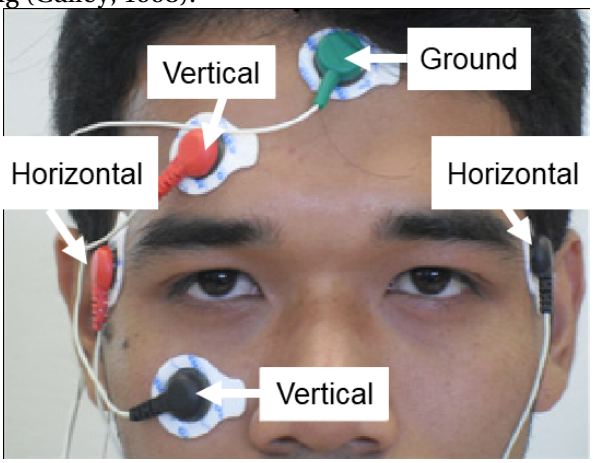


Figure 1.7: Photo of EOG used for interacting with a computer interface. Adapted from (Aungsakun et al., 2011). Reprinted by permission from: Springer, Communications in Computer and Information Science, Robust eye movement recognition using EOG signal for human-computerinterface, Aungsakun et al. 2011.

1.5.4 Dual Purkinje Image trackers

Dual Purkinje Image DPI eye trackers do not require the fitting of uncomfortable lenses (see Fig. 1.8) and are good at separating displacements of the corneal reflection that are due to translation of the eye from those caused by rotation of the eye. They compare the first and fourth Purkinje reflections (front surface of cornea and back surface of lens) that originate in different planes in the eye and their overall accuracy is of the order of 1' (Crane & Steele, 1985). However, the underlying assumption that the eye is spherical only holds to some approximation and errors occur particularly frequently when the participant moves their head (Körding, Kayser, Betsch & König, 2001). DPI eye trackers are the current gold standard for eye tracking. However, few are in use, as they are difficult to maintain. Additionally, binocular eye movement recordings are only possible with these eye trackers when two separate but synchronised systems are available.

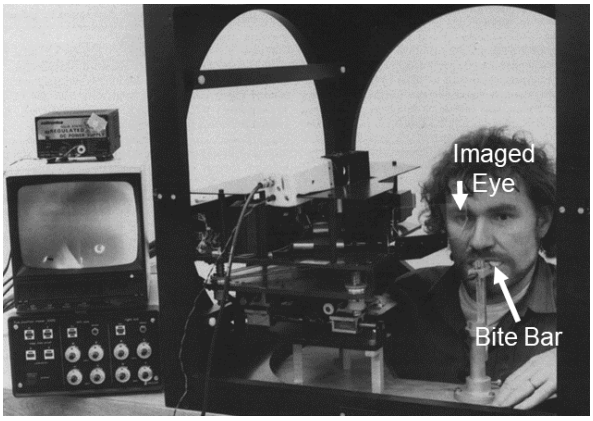


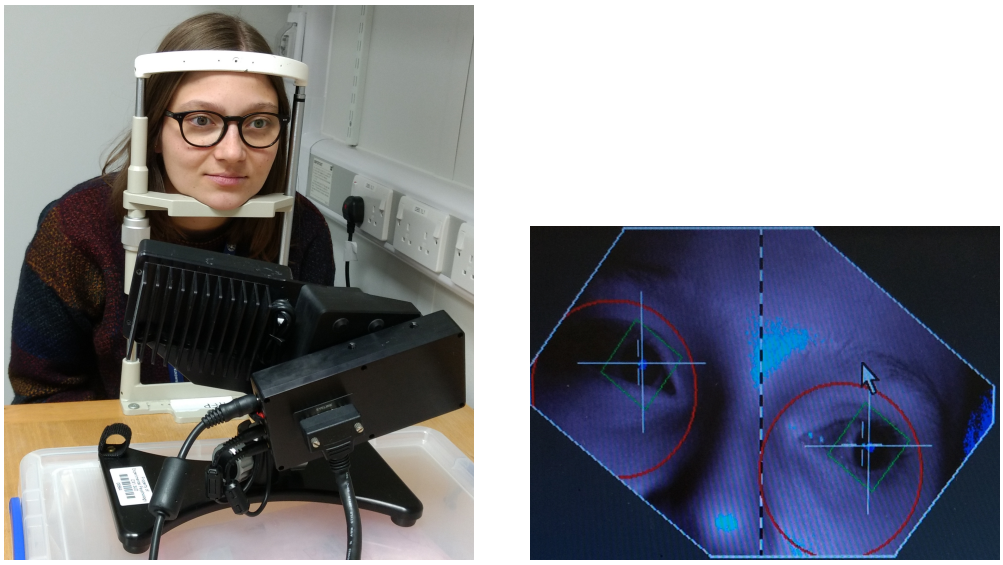
Figure 1.8: Photo of DPI eye tracker. Adapted from (Deubel & Bridgeman, 1995).

1.5.5 Limbus trackers

Limbus Trackers were developed early on as a non-invasive way to record eye movements. They work by measuring the difference in reflection intensity between the iris and sclera (e.g. Tse, Baumgartner & Greenlee, 2010; Zuber & Stark, 1965), as when the eye moves the location of the boundary between iris and sclera relative to a stationary reference also changes. Therefore, eye movements can only be recorded in the horizontal dimension, as two reference points would be needed for two dimensional recordings, but the top (or bottom) of the iris is usually obscured by eyelids. Given the difficulty of tracking iris position using average reflectivity, limbus trackers often have a low spatial resolution.

1.5.6 Video-based trackers

Since the late 1990s video-based eye trackers, which analyse video data of the eye to extract gaze position, have become available. They usually use the relative changes of the pupil compared to the coneal reflection, measured during a calibration stage, to infer the position of the eye relative to a target plane. They are now widely used (e.g. Otero-Millan et al., 2008; Siegenthaler et al., 2014) due to their comparatively easy set-up and maintenance, allowing for data collection on many different participants with relative ease (see Fig. 1.9). Whilst more convenient than older eye tracking methods, they can be limited in spatial and temporal resolution. Eye tracking remains a compromise between tracking resolution and accuracy, and participant comfort.



(a) Participant during eye tracking.

(b) Example of tracked eyes: note the selected pupil and corneal reflex.

Figure 1.9: Example of the video-based eye tracker EyeLink 1000.

Video-based eye trackers have made eye tracking more readily accessible outside the specialist oculomotor community. Now microsaccades are used as a tool by cognitive scientists as a measure of cognitive processes, such as attention (see Fig. 1.10).

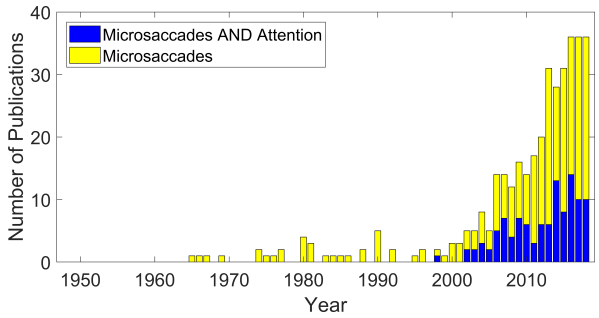


Figure 1.10: Numbers of papers that contain either the search term 'microsaccades' or 'microsaccades AND attention' in abstract, title or keyword searches in Scopus, from 1948 to 2018.

The Eyelink 1000 by SR research systems is one of the leading video-based eye tracking systems

and reports an accuracy during head mount use of 0.25-0.5° and a root mean square sampling resolution of 0.05° for microsaccades (SR Research). However, without optimal set-up and calibration large errors can be induced in pupil and corneal reflection trackers simply by changes in pupil size, independent of the supplier of the system (Brisson et al., 2013; Nyström et al., 2016).

Even under optimal set-up conditions there is no video-based eye tracker that can detect tremor. Any tremor-like signal in the data from these eye trackers originates from equipment noise.

1.5.7 Other eye trackers

Other eye tracking methods have been used to study eye movements. For the majority it is not necessary to go into any detail, as they have not been used to study fixational eye movements. However, there are some exceptions.

In 1952 Barlow published an article on fixational eye movements using a new recording technique. In this set-up a droplet of mercury was placed on the sclera and used as a reflective surface, akin to mirrors used in contact lens set-ups. Blinking had to be suppressed whilst the droplet was on the sclera.

Nowadays, we have every reason to avoid putting mercury in contact with any part of the human body, but it was not until the mid- to late 1950s that mercury was identified as a poisonous substance, coming to prominence due to large numbers of people suffering from neurological symptoms in Minamata, Japan (Takeuchi, Morikawa, Matsumoto & Shiraishi, 1962; McAlpine & Araki, 1958).

Another method for eye movement recording that is encountered occasionally is the piezoelectric technique. First described by Bengi and Thomas (1968), this method depends on the pressure exerted by the eye during movement. A small piece of rubber or latex is connected to the eye (usually using a perspex face mask to stabilise it, see Fig. 1.11) and its displacements, assumed to be solely due to eye movement, will be recorded by a piezoelectric element, which will give off a voltage depending on the total displacement of the eye. To record in two directions, two sensors touching different parts of the sclera (e.g. directly below and nasally for vertical and horizontal movements) are required. Blinks have to be avoided.

1.5.8 AOSLO

AOSLOs are a comparatively new and rare high-resolution eye tracker. They work by capturing images of the live human retina at single-cone resolution. As they raster-scan across the retina to generate such an image, there is a temporal difference between the scan lines within an image is

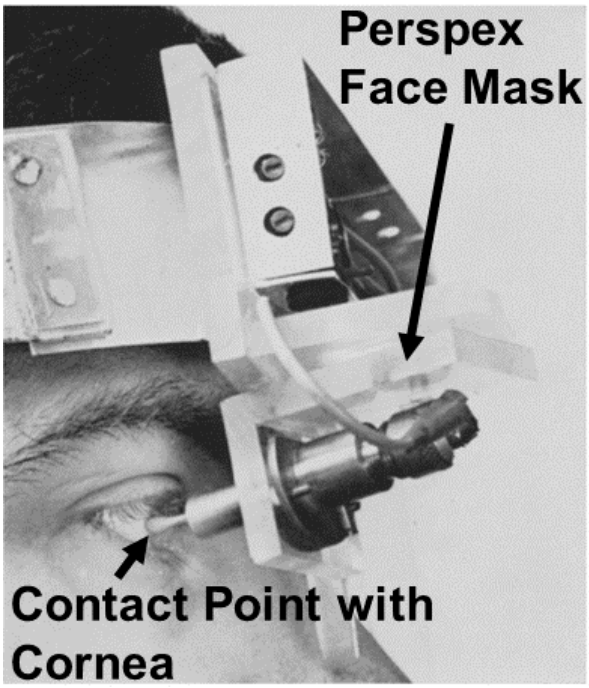


Figure 1.11: Photo of piezoelectric strain gauge method for eye tracking. Adapted from (Bengi & Thomas, 1968).Reprinted by permission from: Springer, Medical & Biological Engineering, Three electronic methods for recording ocular tremor, Bengi, H. & Thomas, J. G., 1968.

introduced. If the eye moves during this time, characteristic sheering is induced, which can be processed to extract the eye movement. The adaptive optics component of the AOSLO is not strictly speaking necessary for eye tracking and image capture, but does significantly reduce noise in the images. For this thesis a custom-built AOSLO was available, which remains under development.

One reason it is desirable to use AOSLOs for eye tracking is that they do not simply estimate the rotation of the eye in the head, but rather detect shifts of the retinal mosaic directly, which is more important when studying how the visual stimulus is sampled by photoreceptors. As the AOSLO eye trace is directly referenced to the retinal mosaic, it does not matter whether the recorded movement stems from the eye muscles or head positioning - it is any shift of the retinal mosaic with reference to the stimulus that is recorded. It should be noted, however, that movement can directly affect image quality, e.g. if the movement of the eye distorts the eye's lens. Additionally, using an AOSLO for eye tracking is beneficial, as the accuracy of eye movement recordings is comparable to that of the highest resolution eye trackers (contact lens mirror or DPI trackers), whilst participant comfort is not compromised. AOSLO tracking is also free from some of the assumptions made by other eye trackers, like the spherical structure of the eye (DPI trackers), or the direct correspondence to reflection intensity (limbus trackers).

1.6 Thesis Overview

The first three experimental chapters of this thesis will present work focussed on improving microsaccade detection. Chapter 2 presents the manually classified data collected as part of this thesis on two different eye trackers: the video-based Eyelink1000 and the AOSLO. It will explore the differences in the available eye trackers and the data they provide and discuss the consequences of these idiosyncrasies for the study of fixational eye movements. In Chapter 3 a new microsaccade detection method based on the correlations between the velocities in the two eyes will be presented. This method is particularly suited to finding microsaccades in data recorded from video-based eye trackers, or similar, as it requires simultaneous data recorded from both eyes with a relatively good spatial resolution. To automate data analysis for the high-resolution AOSLO eye tracker a second new microsaccade detection method is presented in Chapter 4, which uses only monocular data and is reliant on thresholds for speed and path smoothness.

The binocular microsaccade detection method is used in Chapter 5 to study the effect of stimulus structure on fixational eye movements. Specifically, it investigates if fixational eye movements actively respond to differences in stimulus eccentricity or orientation. The findings from this experiment are followed up in Chapter 6 in which the contributions of possible mechanisms that our visual systems could employ to provide an error signal to maintain stability are assessed. Specifically, unreferenced motion thresholds and centre estimation ability are assessed as candidate mechanisms for fixational stability. Whether, the spatio-temporal change is intensity (flux) on the retina plays a role in fixational stability is examined in Chapter 7 by manipulating the amount of blur for circular targets and comparing measures of fixational stability. Data from both eye trackers are used for this.

Lastly, Chapter 8 will compare the relative importance of microsaccades compared to drift in maintaining a stable fixation position. Traditionally microsaccades have been considered responsible for correcting errors induced by drift. However, the presence of contradicting evidence merits a closer examination of the claim.

For all experiments in this thesis participant numbers were not based directly on power-calculations but were determined by practical considerations. Different considerations affected experiments using the Eyelink1000 and the AOSLO. For experiments using the Eyelink1000 approximately 20 participants were available post-exclusion, which is a large enough number to compare effects across participants and comparable to the number of participants conventionally recruited for experiments of this nature. For experiments using the AOSLO, the main practical limitation was the technical development of the system itself meaning that the instrument was available only

towards the end of the DPhil. For this instrument in particular each participant would generate in the order of 120GB of data and computational time to extract eye movement measures was also a consideration. The experiments on the AOSLO represent a considerable advance in the field, but nonetheless the relatively limited participant numbers (n 6-14) limit the conclusions that can be drawn at a population level. It was decided, however, that analysis of data at the participant level was less useful to the field since there is not enough population-level context within which individual differences in fixational eye movements could be interpreted.

Ultimately, this thesis aims to make contributions to the study of fixational eye movements in two main fields: microsaccade detection and our understanding of the active process of vision using fixational eye movements. This thesis presents two new microsaccade detection tools and makes labelled eye movement data available for use in developing future microsaccade detection methods. Additionally it provides evidence of an interaction between the visual stimulus and fixational eye movements.

Chapter 2

Manual Microsaccade Detection and Eye Tracker Differences

Abstract

This chapter examines the two eye trackers available in the lab for their suitability to study different aspects of fixational eye movements. One eye tracker is a video-based Eyelink1000 and the other is a bespoke Adaptive Optics Scanning Laser Ophthalmoscope (AOSLO), which records high resolution images of the live human retina. Both eye tracker work-flows are described and all major sources of error are discussed. To compare the eye trackers for their ability to represent the fixational eye movements studied, two different tests were conducted, each on a representative dataset for both eye trackers. Firstly, data of "following responses" in response to target movement were evaluated. Secondly, microsaccades were manually detected in the datasets. These manual classifications are used in Chapters 3 and 4 to optimise the performance of new microsaccade detection methods.

2.1 Comparing Data

In the study of fixational eye movements, two choices are of central importance to the validity of any conclusions. The first question is which eye tracker to use and the second, how to segment the captured data, if segmentation is required. Often these choices are forced by availability: eye trackers are often prohibitively expensive and require at least some specialist knowledge to set up correctly to yield the best possible data. Similarly, data segmentation is often dictated by which methods are available for the type of eye tracking data that were collected (sampling frequency,

number of eyes recorded) and by which methods have been programmatically implemented. Recently, some progress has been made in comparing which eye trackers work best with which microsaccade detection methods (Nyström et al., 2017), however more formal comparisons are desirable.

The reason these choices are so important, is that either of them alone, as well as the combination of the two, can influence results significantly. If, for example, noisy data from an eye tracker are not smoothed, many microsaccade detection methods might struggle (Nyström et al., 2017). Or, if an eye tracker lacks resolution of the smallest microsaccades, studying microsaccades using this tracker would be a risky choice, as some important information may be lost at capture. However, currently, little data that formally makes these comparisons are available. Data that would be useful, would be in-depth characterisations of eye trackers, which are only commonly available for commercially available eye trackers, such as the Eyelink, as well as labelled datasets of eye tracking data, from different eye trackers and labs, which can be used to develop and test microsaccade detection methods.

2.2 Description of Eye Trackers

Before discussing the implications of individual eye tracker features on data collection and interpretation, an overview of the eye tracker work flow, including the likely sources of error are given.

2.2.1 AOSLO

Answering questions about the interaction of retinal structure with the visual stimulus requires a way of tracking the retinal motion, in terms of displacement of the photoreceptor mosaic with respect to the retinal image, in response to a stimulus. Using an AOSLO we aim to measure fixational eye movements by imaging the retina with single-cone accuracy (Sheehy et al., 2012; Stevenson et al., 2010), without compromising participants' comfort, For an example of the image quality achievable with the Oxford AOSLO, see Figure 2.1.

AOSLOs work by projecting an eye-safe laser beam into the participant's eye and recording the intensity of the light reflected from the retina. The laser scans across a rectangular area of the retina, by sinusoidal motion in the horizontal direction and a saw-tooth motion in the vertical direction (slow scan, with a linear ramp and a fast fly-back period). The light is focussed on a particular plane in the retina, in this case the photoreceptor layer, by a set of curved mirrors and reflected light is collected through a pinhole in a confocal imaging system. Fine-tuning of the focus is achieved via

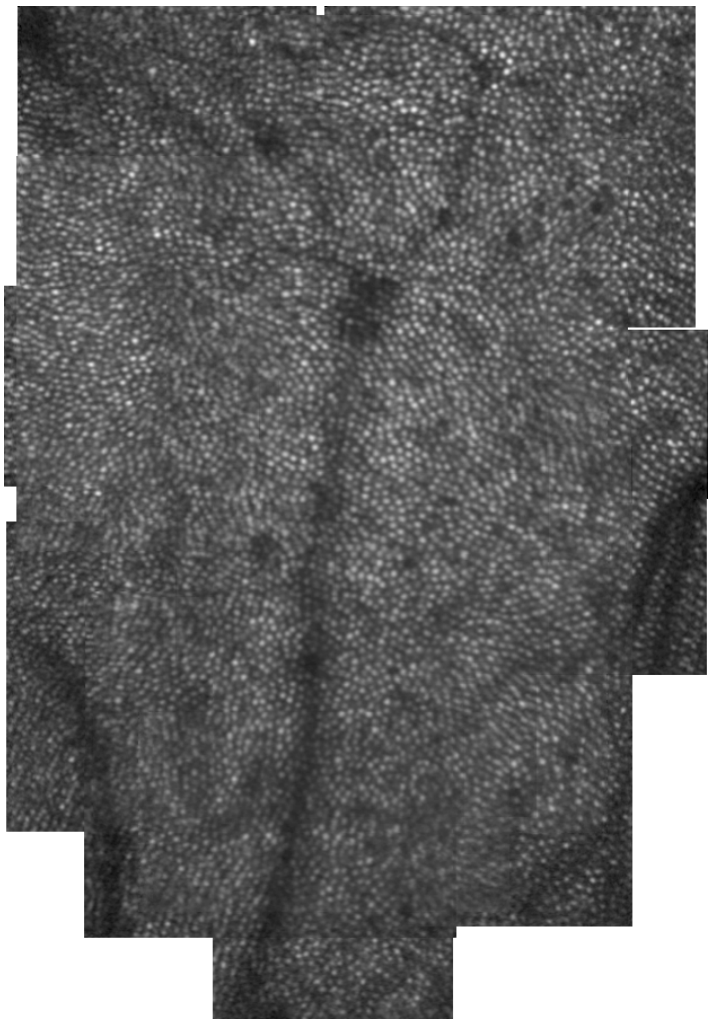


Figure 2.1: Montaged image of the author's retina captured as part of the data for Experiment Two, Chapter 7. This was taken at an approximate retinal eccentricity of 3 degrees from the fovea laterally.

an adaptive optics system, which alters the shape of a deformable mirror to compensate for the optical imperfections in front of the photoreceptors (mainly stemming from the lens and cornea), which are detected by a wavefront sensor. As a result of the AOSLO's set-up, it is only possible to image one eye at a time. Imaging both eyes simultaneously would require two synchronised AOSLO systems.

Before imaging participants using an AOSLO, it is very important to set them up optimally, so that the best possible images can be obtained, as eye tracking will only be possible if the recorded images contain enough retinal structure. Correct alignment with the system and a stable head position, maintained using a bite bar, are required (see Fig. 2.2). As the deformable mirror in the Oxford AOSLO can only correct about .5 dioptre of refractive error, participants who have refractive errors greater than about .25 dioptre require additional correction to be imaged successfully. For this we either use a set of optician's trial lenses, which have the slight disadvantage that they are never as well adjusted to a participant as would be possible with professional glasses or contact lenses, or the participant's own glasses or contact lenses. Extra care needs to be taken, so that no

undesirable reflections are introduced by these lenses.

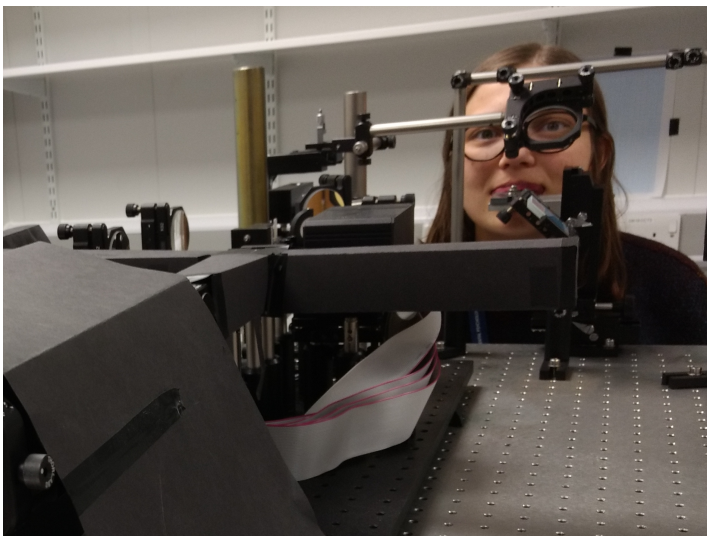


Figure 2.2: Participant during eye tracking with the AOSLO.

The data output from an AOSLO system need a large amount of post-processing to be able to obtain usable eye movement traces. The AOSLO records light at the confocal pinhole as a function of time, and the retinal images are reconstructed from this data stream, with reference to the position of the scanning mirrors at that time. Given that the scanning happens in a predictable way this information can help us remove the sheer caused by movement of the eye. There are several ways in which eye motion might be extracted from the resultant image, but all of them require comparison to an image with no motion. Finding such an image is difficult, as with a human eye we can never be sure it was completely still. One important step is to find an objective way to find a frame with little motion. Previously this has been done by averaging a number of frames with little apparent motion (Stevenson et al., 2010). Now our lab is in the process of developing more sophisticated methods of arriving at a reference frame, including using many overlapping locations to create a larger reference, to allow more accurate eye tracking, even when the movement was large. For data presented in this thesis a manual montaging method was used, to create reference frames at least two times the size of the scan patch. For this, frames in a number of overlapping locations were manually aligned using image processing tool Gimp, then exported to MATLAB, where pixel values were averaged at each location. This was done, so that as many data points as possible could be used to estimate the relative brightness of each pixel and therefore arrive at a more representative image of that retinal location.

Another important step is to select a method of extracting the eye movements that gives accurate results. Currently, systematically cross correlating horizontal strips of the image (Stevenson et al., 2010; Stevenson & Roorda, 2005) is the most common one. However, recent work in our lab has shown that a dense optical flow method (Farnebäck, 2003) can provide more satisfactory results.

For a schematic explanation of eye movement extraction from AOSLO data please refer to Figure 2.3.

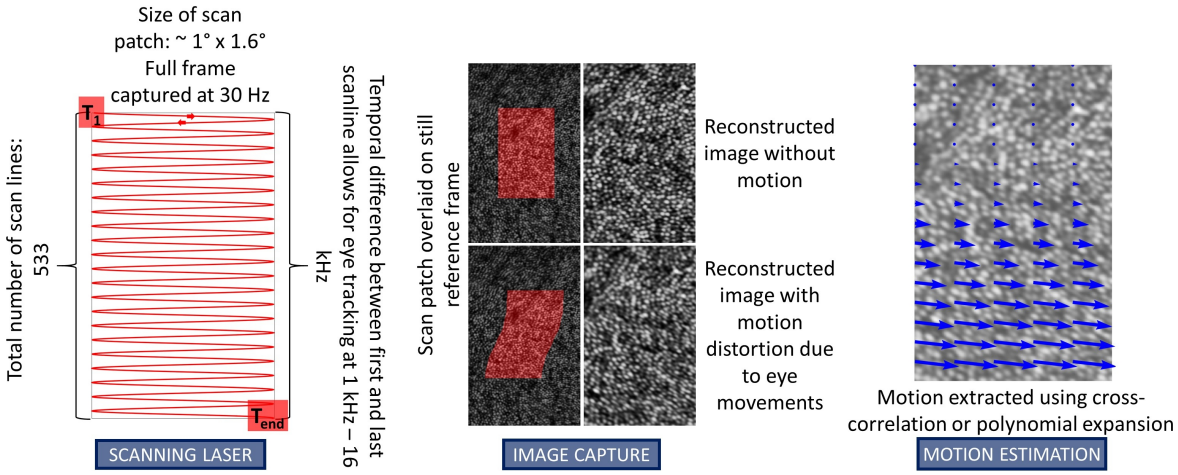


Figure 2.3: Schematic description of motion extraction from AOSLO recordings.

A diagrammatic work flow for data capture, eye movement extraction, eye movement processing and microsaccade detection is shown in Figure 2.4. Boxes highlighted in orange represent work completed by the author of this thesis, while boxes in black represent procedures developed by collaborators on this project. The red circles with white letters highlight the following sources of error:

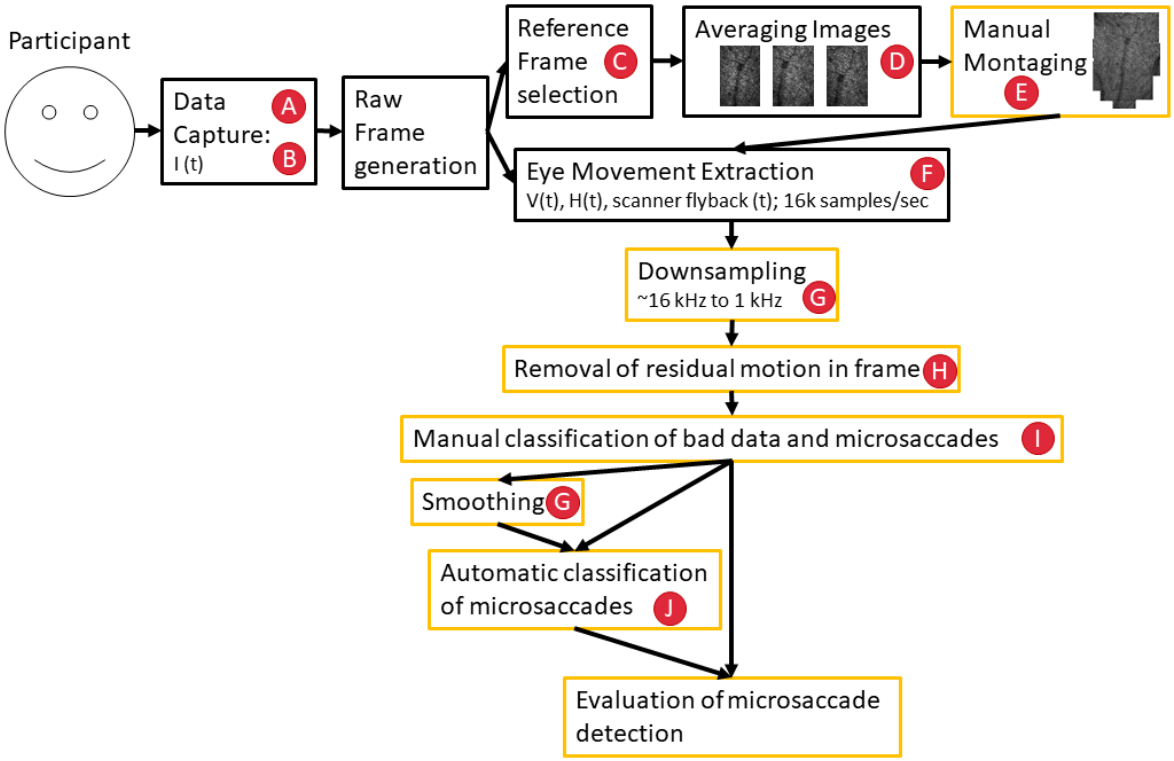


Figure 2.4: Schematic description of the work flow for AOSLO eye tracking. All boxes highlighted in orange represent work completed by the author of the thesis. Boxes in black represent work done by collaborators on this project. The red circles with white letters link to the sources of error, described in the list in the main text.

A ***Gathering Any AOSLO Data:*** During data capture on the AOSLO a variety of factors influence the resultant image quality. They can be broken down into two areas: participant dependent and AOSLO dependent factors. For a participant to give good retinal images their optical refractive errors need to be well-corrected so that the remaining aberrations can be corrected by the AOSLO. Not all aberrations are due to a fixed refractive error though, some change with time, such as the tear film, which, when drying out can lead to increased aberrations. The other participant dependent factor is their retinal reflectivity. The more reflective cones in the retina are, the easier it is to capture good images on the AOSLO. The reflectivity of cones appears to vary between participants, but also over time, depending on cone angle and stage in its cell cycle. A related participant factor is pupil size. For other AOLSOs it is customary to pharmacologically dilate the pupil, as a larger pupil allows for more light to enter the eye and better image capture. On the Oxford AOSLO, however, dilation of the pupil is rarely used. Without dilation fluctuations in pupil size occur, leading to changes in the recorded images, as the diffraction limit changes, which imposes hard limits on the image quality. But imaging without dilation also allows for better comparability between psychophysical experiments done with and without AOSLO eye tracking, as well as greater participant comfort: dilating drops can sting and the resultant dilation leading to blurry vision and light sensitivity for hours after use.

Factors relating to the AOLSO are (i) its optical alignment, which can fluctuate with small changes in temperature, (ii) the stroke of the deformable mirror, which in Oxford is comparatively small, (iii) the properties of the amplifier used to amplify the output, and (iv) the 850 nm wavelength of the light source, which is longer in most comparable systems. Having a longer wavelength is less disruptive in a psychophysical task, but shorter wavelengths improve diffraction.

B ***Gathering Montage Data:*** When capturing images to create a montage to reference experimental eye movements against several things need to be considered. Firstly, the montage has to be large enough to cover the whole area of the retina that may later be imaged. Thus, if the task involves fixating a stationary target, it is likely that a smaller montage would be sufficient, compared to a task that involves following a moving target. Secondly, a balance between number of overlapping frames and time input needs to be struck: the more images are available for a montage, the theoretically better the resulting montage. However, capturing these images takes time and it is not desirable to spend too much time on montage compared to data capture in any given experimental session. The montage also acts as a cal-

ibration of the eye tracker. As the eye movements are always referenced to the same montage, data recorded at different times during the experiment can always be referred back to the same underlying retinal position. However, no formal linking between the montage and the displayed stimulus is undertaking, therefore the central position of the stimulus relative to the output coordinates from eye tracking needs to be estimated in other ways (in this thesis the median fixation position for a given period is used).

C ***Reference Frame Selection:*** Selecting a reference frame for motion correction is an error-prone procedure, as the eye is never completely still during image capture. To ensure that an objective measure is used to select the reference frame, several image statistics may be used. After a reference frame has been selected, all frames collected at that retinal location are motion corrected against it and averaged to create a retinal image with an improved signal-to-noise ratio. For an example of a raw retinal image compared to an automatically motion-extracted and averaged one see Figure 2.10.

D ***Creating Averaged Image:*** These averaged images are important as they create a less-noisy version of the imaged retinal location, which is important for creating montages of a reference location. This process is affected by the method used to average the images. It is important for images to be correctly aligned and motion reduced against the selected reference frame. Bad frames with too much noise or residual motion need to be discarded.

E ***Creating Manual Montage:*** Creating a manual montage is an error-prone procedure, due to the implicit bias of the observer. Often the motion-corrected averaged images created in the previous step still contain some residual motion. By manually aligning the images the creator of the montage has to make decisions on which image represents a more accurate version of the ground truth to align the other images to. Also, at this stage it is often necessary to discard noisy images, or crop areas of the images that do not represent the cone mosaic well.

F ***Eye Movement Extraction:*** Extracting the eye movements within raw frames by comparing them to a reference montage is dependent chiefly on the image quality of both the raw frame and the montage. If either is too noisy, no meaningful correlation can be established between the two and the eye movement extraction will fail. This results in random noise in the eye trace output. The other aspect of this is that the retinal location imaged in the raw frames from the experimental run also needs to be present in the montage, as only those locations within the montage can be successfully correlated. Automatically identification of regions where tracking failed is currently under development.

G ***Downsampling/Smoothing:*** Downsampling and smoothing the data introduce similar sources of error and present with similar dilemmas. Downsampling the trace is best done by averaging over a number of samples, to reduce the noise in the data. As the AOSLO trace is fragmented into small chunks of continuous recording, because no data are captured during the scanning mirror's fly-back region, smoothing and downsampling the data face the question of whether to temporarily interpolate over the fly-back region. If the data are not interpolated, then the downsampled movement trace will be more noisy at the edges of every captured frame, while the smoothing will remove samples from the edges of the frame. Interpolating can prevent these two effects, but does not represent the true movement present during that time. In either event after the downsampling or smoothing has taken place, the fly-back regions should be masked out to remove these estimated samples.

H ***Removal of Residual In-Frame Movement:*** As the montaging process is not perfect there is often some constant error in the montaged image. The largest component of this which is constant across the whole montage is a rotational offset, however smaller, regional errors are also likely to be present. When extracting eye movements against this montage, the same error will be systematically introduced in the eye movement trace, as any rotational factors are constant and the eye usually does not shift sufficiently far across the montage for substantial local errors to be introduced. This can sometimes be visible as a movement pattern that repeats in every image frame between the blank fly-back regions. By averaging all corresponding samples across frames, the average motion contained in every frame can be found. If this residual motion is then subtracted from each frame, a trace without the constant error between the montage and the raw frames is generated.

I ***Manual Classification:*** As tracking errors can occur, as discussed in F, those not automatically removed need to be manually excluded. This is a subjective process. Similarly the manual detection of microsaccades in this data is also difficult. The AOSLO tracking often fails for fast microsaccades, as the image of the photoreceptor mosaic becomes so distorted that it cannot be reliably placed on the reference frame, resulting in uncertainty in the eye-position estimate. This presents a dilemma for the manual coder whether or not to include microsaccades for which part of the trace is missing due to tracking failures.

J ***Automatic classification of microsaccades:*** The automated classification of microsaccades for AOSLO data is currently under development (see Chapter 4). As with any microsaccade detection method, the setting of parameters is crucial in achieving good results. For this, a well-pre-processed eye trace is needed, as well as accurate manual microsaccade labels for

training and testing.

With these sources of error it needs to be noted that errors earlier in the data capture and analysis chain affect all subsequent steps. Despite this long list of potential sources of error capturing eye movement data is a worthwhile undertaking, as the resulting eye traces have a significantly better spatial resolution than most commercially available eye trackers. AOSLO eye tracking is a field still in its infancy with improvements being made to all stages of the process, from the instrument, to data processing and analysis. By improving the data we can capture researchers can start asking different questions about fixational eye movements, which could not be addressed with lower-resolution or more noisy data.

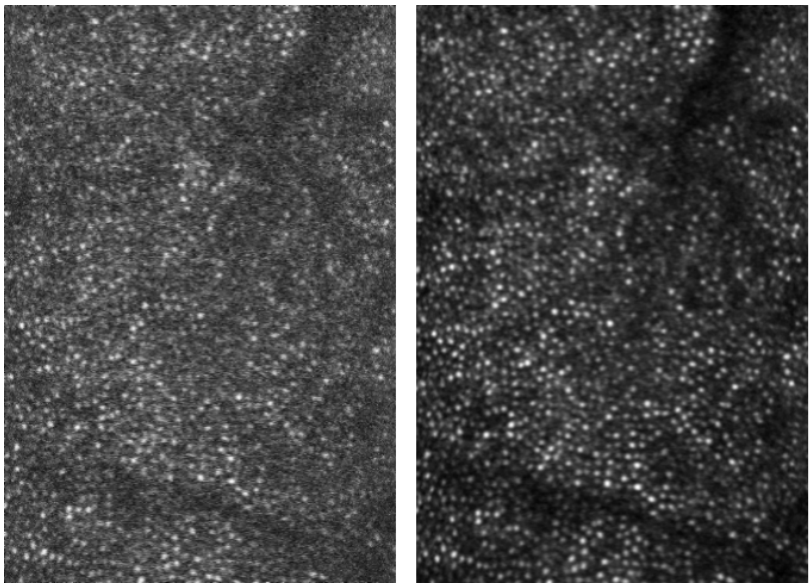


Figure 2.5: Example of a raw frame and the corresponding averaged and motion-reduced frame. On the left the noisier raw frame can be seen, on the right is the corresponding averaged and motion reduced frame. Frames like the averaged motion reduced frame were used to generate the reference montage, while frames like the one on the right were collected during the task and referenced to the montage to extract eye movements.

2.2.2 Eyelink1000

The Eyelink1000 (SR Research) is a video-based eye tracker very commonly used in eye movement research. These trackers estimate the position of the eye in the head by comparing the relative changes in pupil and corneal reflection depending on the eye position in the target plane during a calibration phase. The version available for this thesis is the Eyelink1000 with a 2 kHz extension, meaning that binocular data can be recorded at 1000 Hz and monocular data at 2000 Hz. As this eye tracker is a commercial one, the work flow for this eye tracker is simpler than for the AOSLO (see Fig 2.6). The sources of error are as follows:

A ***Eye Tracker Calibration:*** Without an accurate calibration, the results of the eye tracking will

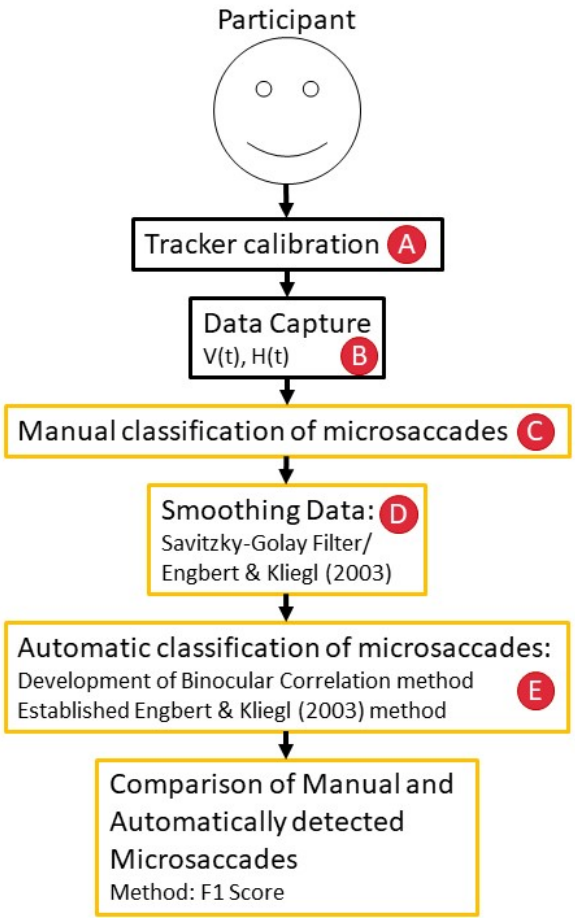


Figure 2.6: Schematic description of the work flow for Eyelink1000 eye tracking. All boxes highlighted in orange represent work completed by the author of the thesis. Boxes in black represent work done by collaborators on this project. The red circles with white letters link to the sources of error in this step, described in the list in the text.

not be accurate. Firstly, the distance between the participant and the screen, as well as the size of the screen need to be entered into the eye tracker, so that accurate estimations of angular rotation of the eye can be made. Then the participant needs to be recorded with the eye tracker while fixating a dot, which will trace a grid pattern on the screen. This will be repeated once for calibration. At this stage it is crucial that the errors in the estimation of eye position that the tracker incurs are acceptably small, otherwise a second calibration attempt should be made. For the calibration to give satisfactory results it is important that the Eyelink1000, the participant and the screen are well aligned with each other and that a sufficiently large calibration grid is used to cover all areas of the screen used during the task, and also to reduce estimation errors. Any consistent errors in calibration will affect all data collected and can introduce errors such as a systematic misalignment of the recorded eye positions on the screen with the actual eye positions on the screen.

B ***Data Capture:*** At data capture, assuming the eye tracker is set up correctly, most sources of error stem from the participant. Participants may not be tracked well by this eye tracker if they

are wearing mascara, as this can be mistaken for the pupil, due to the reflectivity thresholds the eye tracker uses. Glasses may also cause difficulties if they reflect the tracker's infra-red light source poorly or throw shadows over the eye. When participants have very large pupils or become tired their eye lids may cover part of their pupil which leads to tracking failures, as the eye tracker relies on fitting an ellipse to the pupil. Some participants also struggle to stay still enough on the headrest and thereby introduce tracking errors or failures. One source of error that stems from the eye tracker software, is that changes in pupil size lead to recorded changes in eye position, even when the eye did not move.

C ***Manual Classification of Microsaccades:*** Manually classifying microsaccades is a time consuming process. Observer bias for both detection thresholds and microsaccade lengths can influence the data. Decisions also have to be made about how the data are presented to the coder and what pre-processing of the data should occur.

D ***Smoothing:*** What type of smoothing is applied and how much the data are smoothed can significantly affect subsequent analyses. Data from the Eyelink1000 are generally not suitable for automated microsaccade detection unless smoothed (Nyström et al., 2017).

E ***Automatic classification of Microsaccades:*** Two methods are used in this thesis. The first is an existing microsaccade detection method by Engbert and Mergenthaler (2006), which is an improvement on the earlier, but better-known version by Engbert and Kliegl (2003). The second method is one developed as part of this thesis, known as the binocular correlation method. For both detection methods choosing the correct parameters to optimise microsaccade detection is important. Also, microsaccade detection is always associated with some error rate, which has to be accepted.

2.3 Aims

To answer these questions for two eye trackers available in the lab (AOSLO and Eyelink1000) data was collected on both instruments, sometimes simultaneously, and subsequently manually labelled. Using this manually labelled data, microsaccade occurrences and properties can be compared across trackers, as well as across different microsaccade detection methods (see Chapters 3 and 4). Additionally correlating drift traces between eye trackers can also give us information about how accurately smaller and slower eye movements are captured. The manually coded data will be made available online, so that other researchers can use it to improve microsaccade detection methods, or any other analysis on eye movement data.

With regards to the two available eye trackers in the lab we predict that the AOSLO will be able to resolve drift accurately, and potentially some tremor, too, as the AOSLO eye movement extraction method is very reliable when the image shifts are small and slow. Similarly, the smallest microsaccades may also be successfully captured using the AOSLO, while larger microsaccades may be lost, as the shift in eye position results in so much sheering that it cannot be referenced to the montage, or falls off it. By comparison, we expect the Eyelink1000 to be able to capture large microsaccades well but struggle with the smallest microsaccades and drift. It is already known that the Eyelink1000 cannot be used to track tremor.

2.4 Direct Comparison of AOSLO and Eyelink1000

The two eye trackers available in the lab that have sufficient resolution to study aspects of fixational eye movements are the commercially available Eyelink1000 and the custom-built AOSLO. For video-based eye trackers, such as the Eyelink1000, a lot of information is available on their strengths and weaknesses and ability to track fixational eye movements. It is known, for example, that tremor cannot be resolved using these eye trackers (Mergenthaler & Engbert, 2007), or that pupil size can confound eye position (Brisson et al., 2013). However, the same is not the case for the AOSLO, as these are rarer instruments and, even though certain parameters are the same across similar devices, since it is a bespoke setup, its individual features need to be carefully explored and evaluated. For this purpose data were simultaneously recorded from the AOSLO and Eyelink1000 in the lab and subsequently compared.

The data examined in this Chapter were collected as part of Experiments One and Two in Chapter 7. In both experiments participants were fixating circular stimuli which, after a variable time period, moved up or down (Experiment One), or left or right (Experiment Two). In Experiment One only data collected from the Eyelink1000 are analysed, this data are used in manual microsaccade classification and for showing how well following-responses to the shift in the stimulus are recorded. In Experiment Two simultaneous Eyelink1000 and AOLSO recordings were made. Of the data collected as part of Experiment Two, only the AOSLO data are manually classified, the accompanying Eyelink1000 data are only briefly compared to the AOSLO data to establish how closely the two recorded traces resemble each other. The comparison of how well both eye trackers capture the following-responses to the shift in the image is undertaken on the manually labelled datasets.

2.4.1 Methods

Movement traces of the same eye were recorded simultaneously with the AOSLO and Eyelink1000 in five participants. This data are part of Experiment Two, Chapter 7 in which participants were asked to fixate small circular targets of three different levels of blur which moved after a variable interval to the left or right. The Eyelink1000 was set up on the same optical bench the AOSLO is built on to record data simultaneously. This resulted in an acceptable but not optimal placement of the Eyelink1000, as it was forced to deviate slightly to the left from being placed in the centre between the participant and display monitor. One feature of the task was an induced movement of the target after a variable 2-3 s interval. The targets could move by either 3', 9' or 27'.

For direct comparisons only those trials in which, on visual inspection, both the AOSLO and Eyelink1000 gathered data of an adequate quality were considered. Factors which may have led to less than optimal data quality were the added light from the Eyelink and AOSLO combined, potentially drying the eyes more and leading to more blinking and optical aberrations the AOSLO has to compensate. For the Eyelink the sub-optimal setup, as well as the fact that calibration of the Eyelink was difficult, as sometimes parts of the AOSLO equipment obscured the view of the Display monitor, rendering some locations on the screen invisible.

Data Analysis

The data from the Eyelink1000 and AOSLO was temporally synchronised using flags sent to both systems. For the Eyelink1000 its inbuilt system for messages was used, while the AOSLO trace was aligned using the signal from a photodiode which received input from a small rectangle on the bottom right of the display monitor. This rectangle was programmed to change luminance depending on what part of the trial was being displayed.

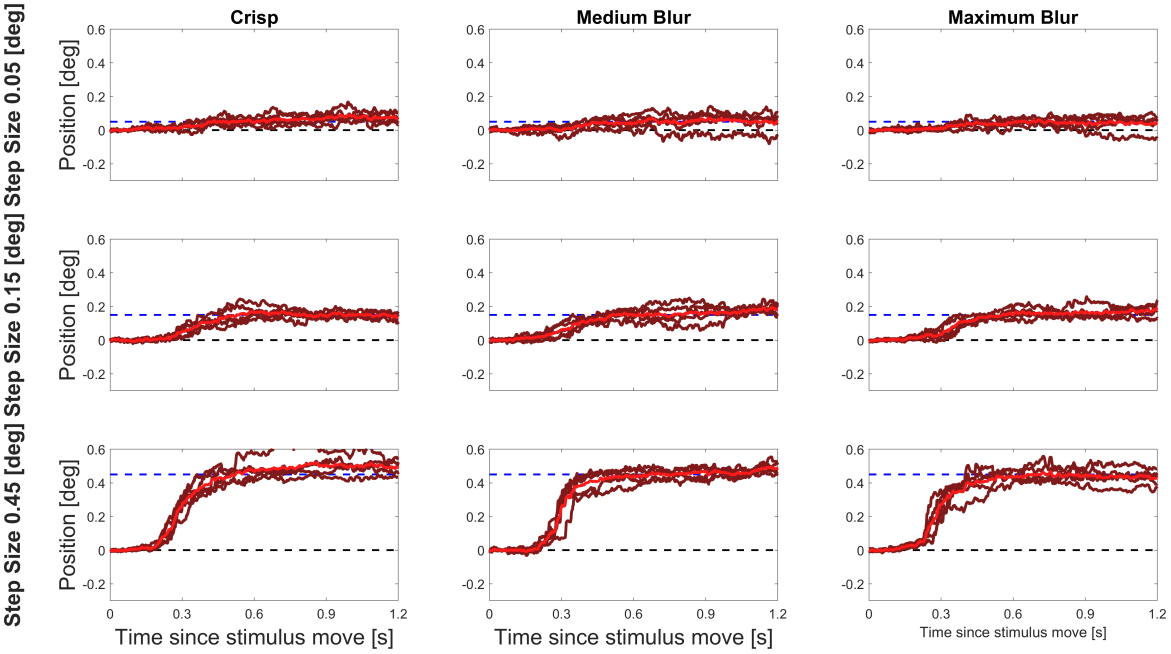
To compare the two systems the 2-dimensional eye traces are examined qualitatively for similarity and comparisons of the recording of the following response of the eyes to the target movement are made.

2.4.2 Qualitative Interpretation of the Data

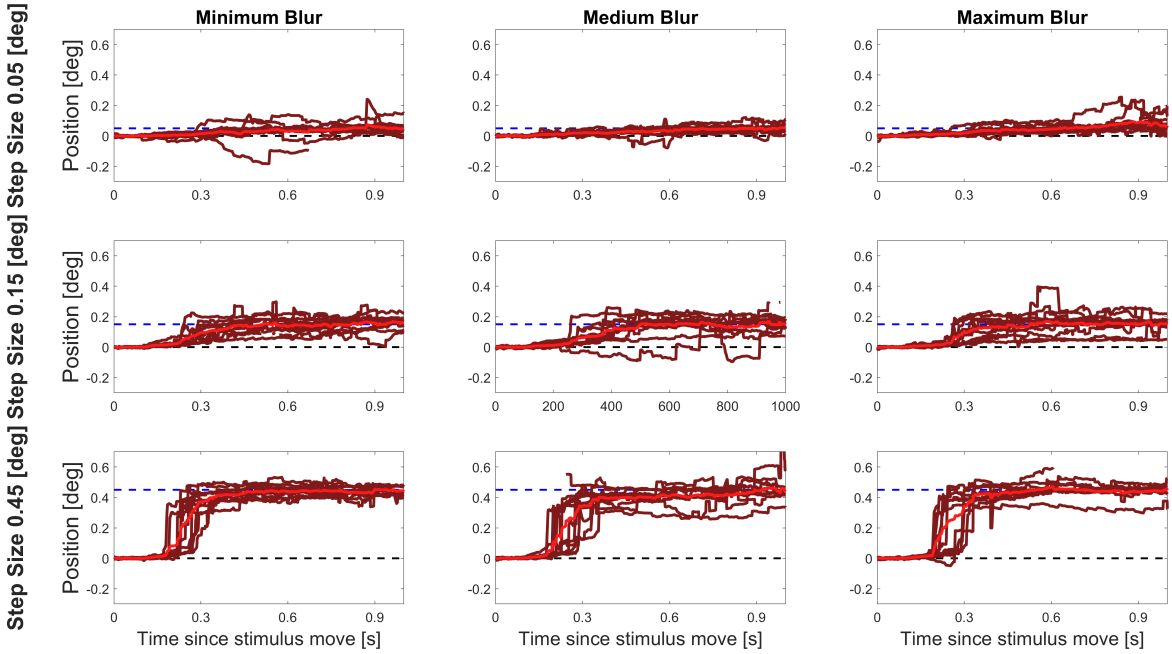
In Figure 2.7 the following-responses of all participants recorded on both the Eyelink1000 and the AOSLO in the experiments are shown. It is clear from inspecting the traces that the both eye trackers make reasonable recordings of fixation position since, in all stepsize and blur conditions the following-responses appear proportional to the induced target shift. It can also be seen that on the AOSLO recordings each individual participant's latency in responding to the target shift with a

saccade is more clearly discerned, while for the Eyelink that information is hidden by noise. For the AOSLO the participant's individually averaged dark-red traces appear to not always follow the target's movement very closely. This may be for a variety of reasons: Some of the lines that follow the target poorly may have been overly influenced by tracking failures, which were not removed properly, or by bad alignment of the trace to the starting position at 0. There are also fewer trials contributing to each AOSLO trace, as a third fewer trials were captured, but also because the timing of the AOSLO recording was not as easily controlled. The AOSLO does not always capture the same length of time after the movement of the target and two factors have been identified as contributing to this. The first factor is the way the AOSLO recording was triggered in this experiment: a signal was sent to the AOSLO to start recording via the photodiode and, due to the complex nature of this system the time it takes for the AOSLO to trigger recording is variable. As the AOSLO is only capable of recording a maximum of 5 s of continuous data, this means that if the AOSLO triggered the recording particularly fast, less time after the target movement could be captured. The second factor is the reliability of eye movement extraction. As the AOSLO records eye movements by comparing the recorded cone mosaic structure against the structure in a reference image, there are a number of situations which may impair this, some of which are linked to movement of the eye. The most common is that the image quality deteriorates to a point where not enough structure is present for this comparison to be successful. This may occur due to (i) optical factors such as refractive error, induced by a previously well-focussed participant focussing on a different plane, (ii) aberrations caused by a number of factors in the front of the eye, such as an insufficient tear-film, or (iii) diffraction effects caused by a smaller pupil, in response to higher luminance levels, changes in attention, or partial occlusion by an eyelid. Non-optical factors may be that the eye moved to a position where it no longer matches sufficiently well to the reference frame it is being compared to, leading to an erroneous position estimate. This may be because of the quality of the underlying reference frame: for this task a manual montage of several adjacent retinal locations was used as a reference frame, however it was not always possible to use only the highest quality images, and it is not impossible that relative motion errors were introduced by decisions made during the reference frame montaging. A second option is that the eye moved sufficiently fast for the sheering introduced into the image to be too great to be compared to the reference frame automatically. Another option is that the eye moved sufficiently far, for too large a portion of the frame, to no longer overlap with the reference frame. When any of these issues occur the data from the ASOLO were automatically excluded in a first pass and manually in a second pass. This may have led to more data missing after the target moved, compared to prior to the movement. This is a potential

systematic bias in AOSLO data and needs to be considered when interpreting the data.



(a) Following-responses of the five participants recorded on the Eyelink1000 in Experiment One, Chapter 7. The targets moved either up or down, for the purpose of this plot both upward and downward motion have been aligned.



(b) Following-response of all 11 participants who completed Experiment Two in Chapter 7 and whose data were analysed recorded using the AOSLO. The targets moved either left or right. For the purpose of this plot both left and right motion have been aligned. This plot shows the data downsampled to 1000 Hz to remove noise. A moving mean filter of size 0.01s was also applied to smooth over the flyback region. These data appear more noisy than the Eyelink data above, which is mainly because there were fewer AOSLO traces to average and the averaged traces were of variable lengths so some jumps are caused by individual traces ending.

Figure 2.7: Following-responses recorded using the Eyelink1000 (top panel) and the AOSLO (bottom panel). The black line indicates the starting position of the target and eye traces were aligned to this by taking the median fixation position in the first 0.1 s after the target moved as the centre of fixation. The blue line represents the target destination relative to the centre of fixation. All movements have been adjusted so that direction of target movement (up or down / left or right) becomes irrelevant. The dark red lines indicate the median movement of each participant of at least 3 trials at any given time point, the bright red line indicates the median movement of all participants at any given time point.

The direct comparison of a well-captured trace across the two eye trackers (Fig. 2.8) shows

that both record broadly similar events. However, the Eyelink1000 trace appears more noisy and more variable than the AOSLO trace. Position 1 shows a microsaccade detected by both eye trackers in both the horizontal and vertical components of the trace. This is promising as it shows broad agreement between the eye trackers. However, in position 2 the Eyelink1000 shows a systematic decrease followed by a systematic increase in the horizontal position, which is not reflected in the AOSLO data. It is a known feature of the Eyelink that calibration can drift and that changes in pupil size can affect position estimation (Brisson et al., 2013). In this experiment pupil size was not recorded, so it cannot be substantiated if that was the underlying reason for the spurious positional drift. Position 4 indicates two parts of the horizontal Eyelink trace which may be classified as very small microsaccades. However in the first instance the AOSLO data agree with the Eyelink, while in the second instance they do not show a microsaccade-like movement. As the AOSLO produces highly accurate data for small eye movements, we can be reasonably confident that no microsaccade occurred, but that the event in the Eyelink trace was caused by noise. Position 5 indicates a similar event in which the Eyelink trace may be manually labelled as a microsaccade, when there is not one present in the AOSLO data. In position 3 the vertical component of a microsaccade, clearly visible in the AOSLO trace, cannot be made out in the Eyelink trace. It is present in the horizontal component, but it has to be assumed that a solely vertical microsaccade of the amplitude in the vertical AOSLO component would have been missed at this point in the Eyelink data. For both the missed and spuriously detected microsaccades in the Eyelink, it may be argued that recording binocularly could help decide if a given event was a true detection or not, however how to weigh binocular information adequately is another matter.

The correlated traces show a good baseline agreement between both eye trackers. For both the vertical and horizontal components the mean correlation coefficient R is positive for both correlation window sizes. To be able to correlate the traces the AOSLO data were downsampled from its native ca 16 kHz to match the Eyelink sampling rate of 1 kHz.

When examining the same traces as in Figure 2.8, plotted as a two-dimensional paths it is striking how much less noisy the AOSLO data appear. The eyes appear to follow the target well and across both trackers the rough shape of the fixations is similar, however a much greater area is covered by the Eyelink trace.

During manual labelling of the data it was noted that there are certain recurring patterns in the AOSLO data within trials and participants (see Fig. 2.10). These patterns occur consistently within each recorded frame. As they are repetitive and linked to the timing of the frames, this motion must represent residual motion between the reference frame and the sampled frame. There are several



Figure 2.8: Example of eye movements recorded by the Eyelink1000 and the AOSLO during one trial for participant P3. The blue lines represent the eye positions of the right eye. The red line indicates the moving correlations between both eye trackers for a window size of 200 ms, while the green line indicates the moving correlations for the shorter window size of 100 ms. The dotted lines correspond to the mean correlation coefficients for both correlation window sizes.

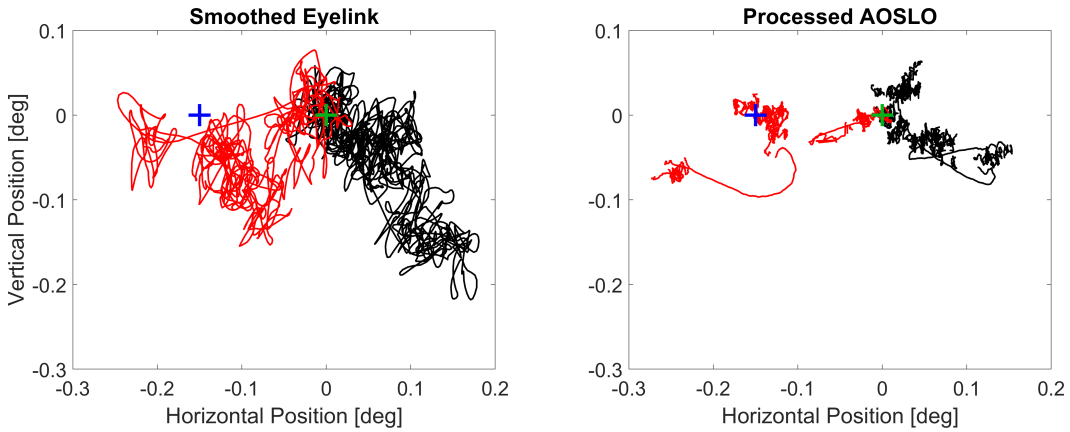


Figure 2.9: Example of eye movements recorded by the Eyelink1000 and the AOSLO during one trial for participant P3.The assumed fixation position in green was calculated based on the median of positions in black. The blue cross indicates where the target moved to relative to that assumed initial fixation position.

possible origins of this residual motion. It may be that the reference frame is distorted in some systematic way, or that the retina has changed in some way between the capture of the reference frame and the sampled frame. Changes to the retina may be its position and torsional rotation, as even though a bite bar is used to capture AOSLO images, small changes in eye position will have relatively large effects of the precise location of individual photoreceptors. For two participants, changes to the retina were also of a temporal nature, as, due to experimenter error, the images used to create the montage had to be taken several days after the data were initially recorded. This temporal difference would have led to substantial changes in the reflectivity of individual cones (Pallikaris, Williams & Hofer, 2003) as well as a different alignment of the eye with the optical system.

As this residual movement is reasonably consistent across a trial, it was removed by taking the median movement across all frames as a function of position within the frame and removing it from each frame.

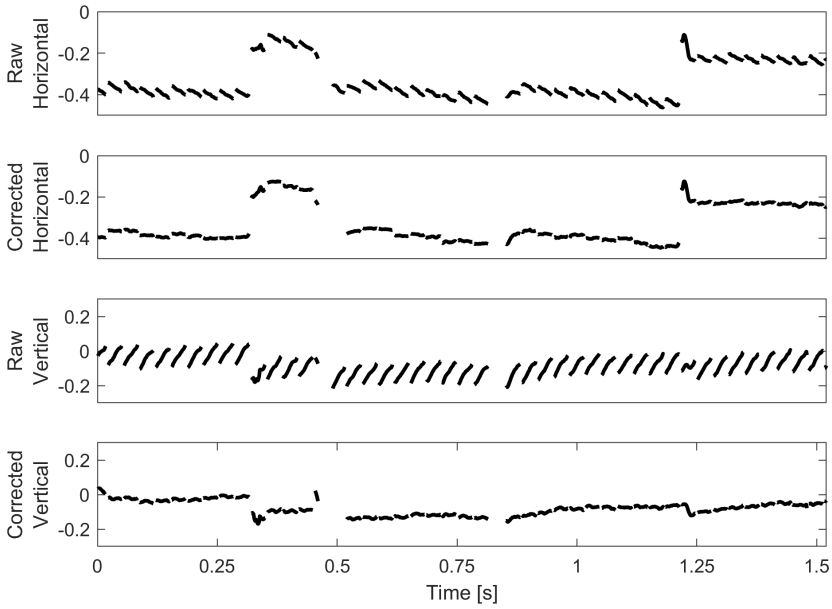


Figure 2.10: Example of the raw eye movement trace, compared to the trace when the residual in-frame motion has been removed. This section of data was chosen, as the effect is particularly noticeable here.

2.5 Manually Labelled Datasets

2.5.1 Methods

Eye movement data were captured on both the Eyelink and AOSLO as part of Chapter 7. The manually coded Eyelink data were recorded in Experiment One of Chapter 7, while the AOSLO data came from Experiment Two.

Manual Data Classification

The author manually classified microsaccades based on vertical and horizontal position traces. Only the position traces were shown (and not for example velocity or binocular correlation profiles), as this is the data microsaccade researchers always have available and that has historically been used for microsaccade identification. This was also intended to stop the manual coder relying on information that may bias the results in favour of a detection mechanism relying on the same information. To the best of the author's knowledge, no automated microsaccade detection method relies on the visual appearance of eye traces and therefore this may prevent biasing the data for or against any particular detection method.

For both eyetrackers these traces were presented without prior smoothing. Horizontal and

vertical position for one eye was displayed at a time and microsaccades could be selected by double-clicking on the beginning and end of the microsaccade. The selected section was then highlighted. If the coder was not happy with the highlighted trace the displayed trial could be cleared and classification attempted again.

Ideally more than one coder would classify microsaccades, as for example done by Nyström et al. (2017). For large numbers of coders the average bias should tend to zero. However, even small numbers of coders allow for the calculation of inter-coder reliability, which can be a useful metric in determining if the coders were detecting broadly similar events, suggesting that true microsaccades were found.

Eyelink data classification

For the Eyelink data, periods of 200 ms before and 300 ms after blinks were excluded before manual classification, due to the distracting saccade-like artefacts that are induced by the partially occluded pupil. In the experiment that the data came from the target moves after a 2-3 second interval. For the purposes of this manual identification, only the time prior to the target move was displayed and classified. This means that 2-3 s of data were displayed to the manual coder at a time. The data were presented in a window no smaller than 1° in vertical extent, so that no bias was induced by displaying a trace without large microsaccades , potentially leading to the wrongful identification of noise as a saccadic event. However, sometimes very large saccades were recorded, and if that was the case the window was extended to accommodate these saccades. This means that during those trials, a similar problem applies, in that the manual coder may have overlooked saccades they would usually have detected, because the spatial resolution of the display had changed. As this only applied to a very small number of trials, this is accepted as a source of error.

Identification was undertaken on a 24" screen with the data being displayed using MATLAB. The white space on the screen was minimised so that the eye movement trace could be displayed as large as possible to allow for best microsaccade detection.

At total of 5 participant's data were manually classified, resulting in approximately 2000 s of data. For these participants all available trials were classified.

AOSLO data classification

For the AOSLO data the whole recorded trial from the point the target appeared to the point when the AOSLO stopped recording, either before or after the target moved was displayed. At the point the target moved a red line was shown. The window size was fixed at 2 deg, to accommodate any

movement of the eye in response to the largest target shift of 27' comfortably. These data were manually classified on a 27" monitor using MATLAB and white space was similarly minimised. The data were extracted at a sample rate of 16 010 samples/sec and the raw data were presented to the coder. Subsequently it was discovered that to minimise velocity noise it is useful to downsample the data to 1000 samples/sec. This is used for all analyses of the data in this thesis, however, it would have had little effect on the coder's microsaccade ratings, as velocity information was not presented.

A total of 14 participants were available for microsaccade classification in this experiment. Microsaccades were manually detected in all trials for all participants resulting in approximately 5000 s of classified eye movement data. Additionally all data where tracking was overly noisy or poor was manually excluded. An example of resultant labels in a trace from participant P3 is presented in Figure 2.11.

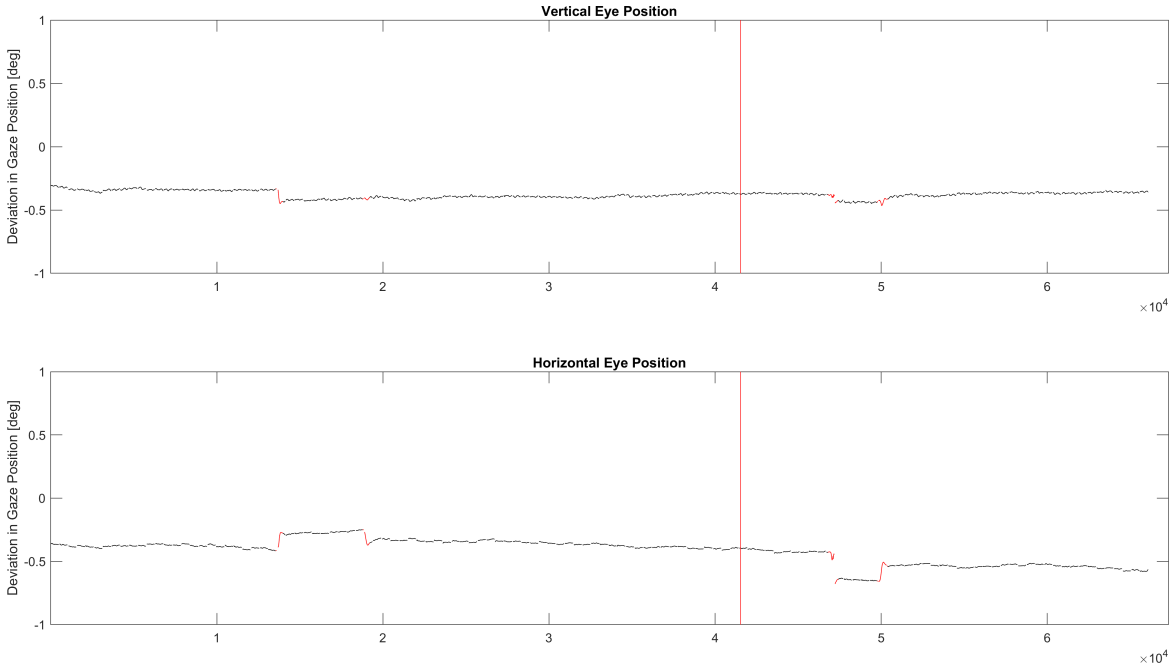


Figure 2.11: Example of manually classified microsaccades in AOSLO data for participant P3. The black trace represents the processed eye movements while the red highlights represent detected microsaccades.

2.6 Discussion

For the improvement of eye movement data analysis it is important that more and more varied datasets of labelled eye traces are made available to research. The Eyelink data from this chapter will be made publicly available in an upcoming publication. The labelled AOSLO data from this chapter will also be published as part of a paper on the interaction between eye movements and blur.

From the direct comparison between the Eyelink1000 and the AOSLO it can be gathered that examining the smallest eye movements using the AOSLO is preferable to the Eyelink1000, as it allows for potentially highly accurate data that are directly referenced to the retinal mosaic. Both the AOSLO and Eyelink1000 have their respective and complimentary limitations: The AOSLO is most likely to fail when larger and faster movements occur, while the Eyelink struggles to accurately represent drift as well as the smallest microsaccades.

These differences should also be taken into account when analysing and interpreting data from both trackers. Given the higher levels of noise in the Eyelink data, and the potential for binocular recording, any automated microsaccade detection method would ideally rely on data from both eyes to confirm the occurrence of a microsaccade. For the AOSLO, given its high precision, it may be better to use hard threshold values for microsaccade detection, as both tracking failures and non-microsaccades may be excluded.

Another feature to consider is that the AOSLO can generate eye-movement data at a much higher temporal frequency than the Eyelink1000. At more than 16 000 samples/second the AOSLO offers a higher temporal resolution than can conceivably be necessary for the study of fixational eye movements. Indeed, this leads to unacceptably large amounts of noise in the sample-to-sample velocities and so is downsampled to 1000 samples/second to resemble the Eyelink1000 data. Whether or not it is necessary to downsample by this much is not clear, it may be that downsampling to 4000 or 2000 samples/second would also give acceptable sample-to-sample velocities and is an avenue worth exploring in the future.

Chapter 3

Binocular Microsaccade Detection

Abstract

This chapter explores a new microsaccade detection method that exploits their binocular nature. The binocular correlation method for microsaccade detection is validated on two datasets of binocular eye-movements, recorded using video-based systems: one collected as part of this study, and one from Nyström et al. (2017). Comparisons between detection methods were made using precision-recall statistics. This confirmed that the binocular correlation method performs well when compared to manual coders and performs favourably compared to the commonly used Engbert and Kliegl (2003) method with subsequent modifications Engbert and Mergenthaler (2006). The binocular correlation microsaccade detection method is easy to implement and MATLAB code is made available to download.

Microsaccade research has experienced one major change in its history: the shift from historical eye trackers, which relied heavily on complex optical set-ups, to modern video-based eye trackers that depend on the underlying image-processing software for tracking. The greater ease of recording large amounts of eye tracking data from many different people using video-based eye trackers brought with it changes in the types of questions researched, and the way the collected data are processed.

Automated microsaccade detection became essential in dealing with the large amounts of data that could be collected with digital and easy-to-use eye trackers, as manually coding each microsaccade became too time intensive. Several automated detection methods have been put forward, with the most widely used being the Engbert and Kliegel (Engbert & Kliegl, 2003; Engbert & Mergenthaler, 2006) adaptive velocity threshold method (EK). Others include methods combining

velocity and linearity thresholds (Martinez-Conde, Macknik & Hubel, 2000) and unsupervised clustering of velocity and acceleration samples (Otero-Millan, Castro, Macknik & Martinez-Conde, 2014). An ideal microsaccade detection method would correctly identify all microsaccade periods, be easy and fast to implement and be driven by our theoretical understanding of what constitutes a microsaccade. To decide which of two detection methods is optimal, systematic comparisons should be carried out.

3.1 Why microsaccade detection is difficult

To study microsaccades it is crucially important to be able to detect microsaccades with high accuracy in the eye movement data. At a first glance it should be easy to separate microsaccades from other fixational eye movements, as they are typically larger, faster and smoother over space than drift and tremor. Similarly it should be easy to distinguish them from eye movements of visual exploration, such as smooth pursuit or larger saccades, that occur only in response to targets moving, in the case of smooth pursuit, or are much larger and faster, in the case of saccades.

However, in practice, it is hard to detect microsaccades accurately (i.e. with high precision and recall compared to a manual coder). It is hard to separate microsaccades from drift and tremor, as the smallest and slowest microsaccades strongly resemble periods of drift/tremor in velocity space - the most used and obvious separation criterion, especially in noisy data. It is also hard to distinguish microsaccades from larger saccades, as they lie on a continuum and we have no convincing reason to draw a distinguishing line between microsaccades and larger saccades. This, in particular, poses a problem for studies on the free exploration of a visual scene: is a small saccade target-directed, or is it an involuntary microsaccade?

3.1.1 Detecting large saccades

To justify looking for a better way of detecting microsaccades, it appears necessary to first turn to the detection of larger saccades, as it has been established that microsaccades are fundamentally just smaller saccades (e.g. Otero-Millan et al., 2008). Therefore it would seem logical to use the same detection methods for locating them in eye-movement data.

The majority of large saccade detection mechanisms are based on simple velocity or acceleration thresholds (e.g. Krauzlis & Miles, 1996). Some even use further derivatives of velocity, such as jerk (Wyatt, 1998). Often they provide satisfying results, however it is important to consider which types of movement are being deselected: simple thresholds are sufficient to separate saccades from fixations, however not necessarily from smooth pursuit. It should be noted that there is no

immediate need to separate smooth pursuit movements from fixational eye movements. Whilst the slowest movements that elicit smooth pursuit are well below 5°/sec (Robinson, 1965; Rashbass, 1961), in most fixation tasks we can rule out smooth pursuit. It is known that smooth pursuit can not wilfully be induced without a target (Becker & Fuchs, 1985), and no stimuli that could elicit such a response are available during the task.

However, more recently adaptive threshold mechanisms have been developed, such as the one proposed by Liston, Krukowski and Stone (2013), which uses a moving median velocity threshold and clustering of candidate traces. Similarly, a new method by Behrens, MacKeben and Schröder-Preikschat (2010) also uses an adaptive acceleration threshold informed by preceding samples.

Another way in which the focus of saccade detection differs from microsaccade detection is that there is a greater focus on identifying exactly when a saccade begins and ends (e.g. Nyström & Holmqvist, 2010; Krauzlis & Miles, 1996), as those sections may contain important information about landing position and glissades. When identifying microsaccades it is difficult to accurately pinpoint start and end points, as the microsaccades themselves stand out less from the rest of the data and are shorter in duration, meaning that the samples at either end make up a larger percentage of the total trace, resulting in a larger potential error.

To the best of my knowledge there are no saccade detection mechanisms that use anything other than velocities or derivatives thereof as the main identifying feature. As velocity does not sufficiently separate drift from the smallest microsaccades, these velocity-based thresholds will, most likely, not be sufficient to identify microsaccades in the data and alternative and complimentary detection methods need to be considered. Useful principles that are apparent from the detection of large saccades are that velocity and its derivatives are important features of the eye movement data and that adaptive methods can provide potentially better detection results for individual participants than methods with fixed thresholds.

3.1.2 Established microsaccade detection methods

Manual detection

Historically, manual detection used to be the only method of detecting microsaccades. The earliest eye-movement traces were all recorded via analogue methods. As this meant that the data were not available digitally, manual analysis was required. In this way microsaccades were often detected visually as abrupt steps in the eye trace (see Figure 3.1), described by Armington and Bloom (1974) as having a “characteristic step-like shape”. Manual microsaccade detection is a very time-consuming and subjective process, which is why it has been replaced by automated microsaccade detection

methods.

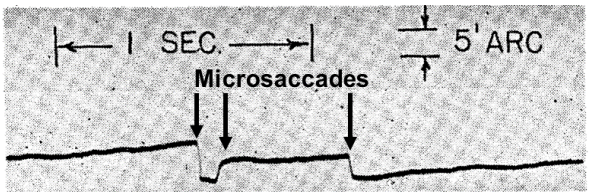


Figure 3.1: Example of eye movement trace containing microsaccades. Eye movement recordings were made using a contact lens mirror technique. Adapted from (Cornsweet, 1956).

One of the issues associated with manual microsaccade detection is its reliance on the personal biases of the coder and the data presented to the coder. A bias to report spikes in velocity as microsaccades may be induced when velocity information is available, potentially at the expense of reporting step-like changes in the position trace. The only way to reduce the amount of bias, is by having many manual coders and averaging across them, in the hope that some would be more conservative and some more liberal. To reduce any biases or errors associated with the data available to the coder, the way of data presentation should be carefully considered. To be as assumption-free as possible, the observer should have access to only the horizontal and vertical position of one eye at a time. Having information about both eyes could bias the coder to consider binocularity of microsaccades. Similarly, the coder should not have access to the velocity or acceleration traces, to prevent the coder putting weight on those types of information. This would resemble microsaccade detection from the analogue age more closely and may help to reduce the systematic changes in reported microsaccade features. Special care should be taken to fix the spatial and temporal resolution of all traces a coder would encounter, so as not to change the influence of noise or large movements on detection.

Manual detection nowadays is usually only used when a ground truth is needed to evaluate the performance of an automated microsaccade detection method. Not only it is hard to control the biases of the coders, but it is also too time intensive to be suitable to analyse the large amounts of data it is now possible to collect with modern eye trackers. It should be noted though, that manual coding does not represent a true ground truth and that it is desirable to also use other methods of evaluating the performance of detection mechanisms.

Threshold methods

The simplest ways of identifying microsaccades is by setting hard thresholds for e.g. velocity or acceleration. Most early attempts at automated microsaccade detection used threshold criteria. Boyce (1967) used two velocity thresholds: a peak velocity threshold (2° /sec) which had to be exceeded, as well as a second, lower threshold (1° /sec) that was used to define the beginning and

end of a microsaccade. Other groups have also used threshold criteria. For example Martinez-Conde et al. (2000) used a velocity threshold of 3° /sec, allowed a maximum deviation from a straight line by 15° and any detected microsaccades had to be between 3' and 2° in size.

Threshold-based microsaccade detection has the advantage that it is relatively simple to implement and quick to run. However, it suffers from a number of issues, which has limited its widespread use in recent years.

Firstly, finding the correct threshold(s) to use is difficult, as many eye tracking set-ups have their own quirks in systematically over- or underestimating e.g. velocity. This is complicated further by the fact that there is a reasonable amount of individual variation, both in the features of an individual's eye trace, and in how well the eye tracking works for an individual. In video-based systems pupil size can influence the quality of the eye tracking (Brisson et al., 2013; Gagl, Hawelka & Hutzler, 2011), whilst on an AOSLO system refractive errors and positional stability of the eye can impact the quality of tracking. The amount of noise present in a given eye-movement recording is also important to consider, as tracker noise may mask microsaccades, but also create false ones.

Secondly, threshold-based microsaccade detection methods have typically limited themselves to a relatively small number of thresholds. This, however, means that they usually have to set values that are quite well-adapted to the particular dataset they are using and therefore lack generalisability. Using thresholds on a number of different properties can constrain the microsaccade space better and be helpful in creating detection mechanisms that are transferable between eye trackers.

Lastly, most thresholds that have been used in the literature are lower- or upper bounds only. Boyce (1967), for example, only set minimum velocity thresholds, but empirically it is known that there must be an upper velocity thresholds to microsaccades as well. This could be defined as (i) the smallest peak velocity that, according to the main sequence relationship, can no longer belong to a microsaccade (ca 100° /sec for a movement of .5° or ca 200° /sec for a movement of 1° Duchowski et al., 2017), (ii) the smallest peak velocity belonging to a saccade larger than the eye tracker can detect (400 ° /sec, assuming a maximum trackable range of 10° Bahill et al., 1975), or (iii), at the upper end, the highest achievable velocity of any eye movement (ca. 700° /sec achievable during a 40° saccade Harris & Wolpert, 2006). Any velocities recorded that are higher than the first threshold, must belong to larger saccades or smooth pursuit, whilst any velocities larger than the second threshold must be measurement errors and do not represent true eye movements. The same logic applies to other features of microsaccades, for example, minimum measurable microsaccade distances are limited by the tracking resolution whilst minimum duration is limited by the recording frequency.

Engbert and Kliegl

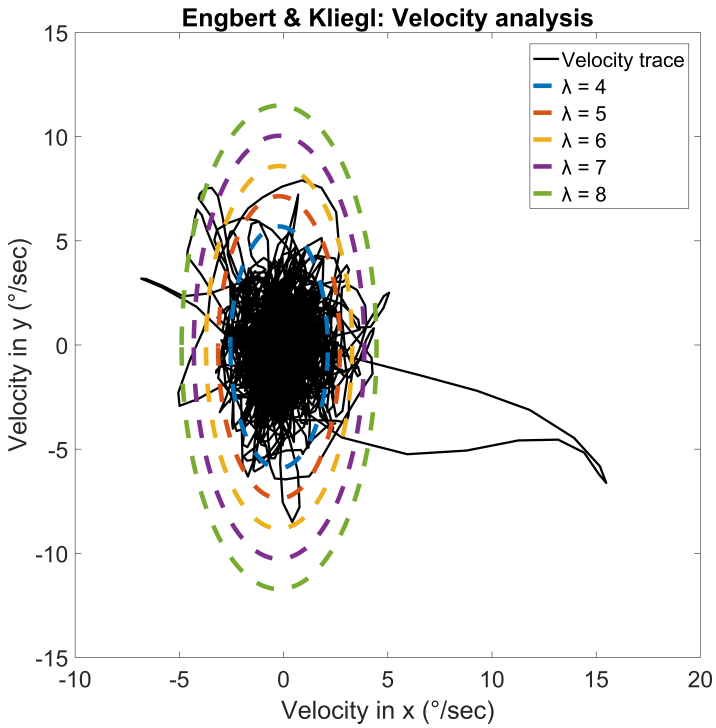
Engbert and Kliegl (2003) published the first widely adopted, and still commonly used microsaccade detection method. Many studies have reported adjustments to this method (Engbert & Mergenthaler, 2006; Thaler et al., 2013). For clarity and consistency we consider the EK method as described in 2003, unless explicitly stated otherwise.

The EK method calculates a smoothed velocity trace for each trial and microsaccades are defined as samples in which the velocity exceeds a threshold. Thresholds are based on median velocities and a multiplier λ. On a polar plot of velocities, an elliptical boundary is used to accommodate differences between vertical and horizontal velocities (see Fig. 3.2 for explanation). After thresholding, (i) a minimum duration criterion is applied and (ii) only those microsaccades occurring in both eyes are considered. For different studies and tracker sampling frequencies some aspects of the method vary, such as the exact way of calculating the velocities, and the minimum microsaccade duration (Engbert & Kliegl, 2004; Nyström et al., 2017).

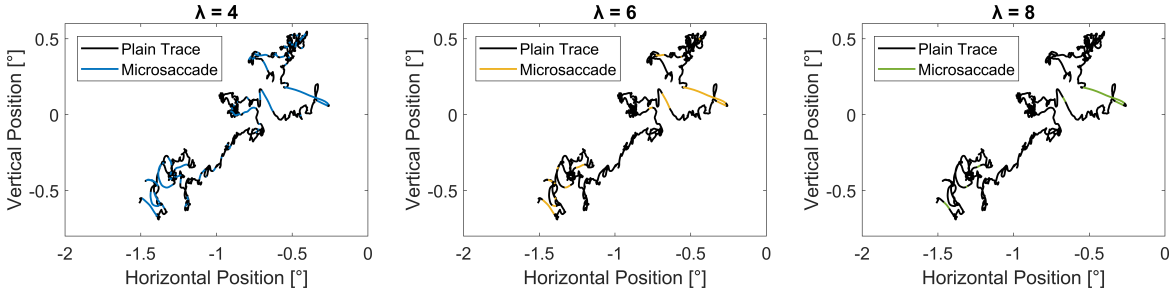
Although widely used and accepted, the EK method is not without limitations. Since it relies primarily on velocity as an identifying feature of microsaccades, it is vulnerable to spurious increases in velocity resulting from various sources of measurement noise. To protect against inherent noise in the data, the EK method applies a fixed multiplier to the median-based velocity threshold for a particular dataset. The original 2003 paper further aimed to reduce misidentifications by requiring one sample overlap between microsaccades in both eyes. However, this binocularity criterion has been omitted when only monocular data were available (Betta, Galfano & Turatto, 2007; Dimigen et al., 2009; Otero-Millan et al., 2011; Thaler et al., 2013). Ultimately, using velocity as the main identifier of microsaccades may not be optimal and other avenues to detecting microsaccades should be considered.

Unsupervised Clustering

In 2014 Otero-Millan et al. published a novel microsaccade detection method, which used a machine learning technique called unsupervised clustering to distinguish microsaccades from spuriously detected samples. At the base of their system is a simple threshold method for selecting candidate microsaccades: they find a peak velocity threshold that gives them a microsaccade detection rate of five per second. Each candidate microsaccade section is defined as including all those samples before and after the identified velocity peak which stay above a velocity greater than 3° /sec. This set of data is chosen, as it is considered to contain all true microsaccades as well as some spuriously detected periods in the data.



(a) The horizontal and vertical velocities in one eye are plotted against each other and an ellipse with a median multiplier λ for both vertical and horizontal velocities is fitted. Any samples outside the ellipse are considered to be microsaccades, if the corresponding timepoint in the other eye also contains a microsaccade.



(b) Three examples of how the chosen λ can change detection results. Standardly a λ of 6 has been recommended. Data in this figure are taken from participant P3 collected as part of the experiment described in Chapter 2.

Figure 3.2: Example of microsaccade detection using the EK method.

Then the selected candidate sections are clustered by an unsupervised system according to their peak velocity, as well as the first and final acceleration peaks occurring in the microsaccade candidate section. However, as the raw values are all very small the logarithms are taken of the values and then transformed into z-scores. The clustering is allowed to produce either 2, 3 or 4 clusters, and the cluster with the largest average microsaccade magnitude is finally chosen as the cluster of true microsaccades.

Based on this, unsupervised clustering is a good way of identifying microsaccades, because it is free from the setting of arbitrary cut-offs, but rather is data-driven in its threshold selection. One downside to this method is the assumption that the cluster with the largest microsaccade magnitude is the correct one. Perhaps this could be improved by selecting the cluster based on its fit on the main sequence. Another downside to the unsupervised clustering method is that

the method is difficult to implement from scratch - whilst Otero-Millan et al. have provided a ready-made implementation, for anyone hoping to tweak or adjust this method, it will still be a complex undertaking.

3.1.3 Formally comparing detection methods

To establish which detection method is best suited to the detection of microsaccades formal comparisons should be made. In fields other than eye movement research classification mechanisms are usually trained on a set of labelled data, i.e. data that represent a ground truth, and then tested on another set of labelled data, that it was not exposed to during refinement of the technique. This is standard practice, especially in computationally driven fields like neural networks (e.g. Mazurowski et al., 2008). The reason to train and test on separate datasets is that any detection method should be sufficiently generalisable to also apply to previously unseen data. At the same time, to achieve this, the training set also needs to include enough diversity, similar to the level one would expect in novel datasets.

Providing training and testing datasets with enough diversity is a challenge in eye movement research. Few datasets are publicly available and even fewer of these contain manual labels for the data, which is the closest we can get to a ground truth. The reason for this, beyond the slow adoption of data sharing in science, is that manual labelling is barely ever done on eye tracking data nowadays, as it is too time consuming. In recent years there have been two examples of manually classified eye movement data. Otero-Millan et al. (2014) manually classified some eye movement data, which was done by inspecting the velocity and acceleration traces and double clicking velocity peaks belonging to microsaccades, the program then extended these microsaccades over subsequent successive samples until the velocity of the eye fell below 3° /sec. An obvious issue with this method is that saccade start and end points are not manually identified, and that a large emphasis is placed on the velocity and acceleration information, rather than position. Also, this dataset is not accessible online. Another dataset, which is available online, was classified by Nyström et al. (2017). This classification was done by three independent observers based on position data, and is a suitable candidate for training and testing microsaccade methods. The old datasets, which stem from a pre-digital age and were manually classified are not available to researchers now. Also, any manually classified dataset will be biased by the coder who made the judgements. In a perfect world, each available dataset would have multiple coders rate the trace, as an aggregate of more people should represent a more bias-free set of data, according to regression to the mean.

Given the absence of readily available datasets to conduct formal comparisons, several other

techniques to estimate how well a detection method performs on eye tracking data have been proposed. Qualitative comparisons are often used. These include visually inspecting the main sequence relationship, but also more formalised comparisons of the distribution of peak velocities and amplitudes, for which a distribution more similar to a normal distribution is regarded as desirable (Otero-Millan et al., 2014). Another option is to compare the overall number of detected microsaccades between different detection methods, as done by Nyström et al. (2017), which, however, does not necessarily establish how many of these detections were successful.

As a result of the limited data and quantitative approaches to microsaccade detection, none of the established methods have been thoroughly tested and compared. Ideally in the future more researchers will make their data available online and provide manual labels for it. Of particular importance would be the provision of data from a variety of eye trackers and at different sampling frequencies, as this variety is present in the literature but not reflected in the testing of detection methods. With the BC method and data provided here I hope to provide a starting point for this field to expand.

3.1.4 Possible features of microsaccade detection mechanisms

The central question to address before developing a new microsaccade detection method is which feature(s) of microsaccades should be used as the main criteria. From the literature on microsaccades five stable features of microsaccades arise:

1. They occur simultaneously in both eyes.
2. They follow a main sequence relationship between peak velocity and distance.
3. They are ballistic in nature.
4. They are smoother than drift.
5. Their frequency is dependent on task instructions and can also be suppressed after stimulus onset.

Additionally, some physical parameters of microsaccades are also characteristic of them: their velocity profiles, as well as their duration and size (see Table 1 on page 31).

Not all of these features will prove to be useful detection tools, as for example, the dependence of microsaccades on task instruction could, at most, be used as a weak validation method. However, binocularity, the main sequence relationship, their ballistic nature and the physical parameter space they span can be used to our advantage in detecting microsaccades.

3.2 The binocular correlation method for microsaccade detection [1]

The binocular correlation (BC) method for microsaccade detection finds microsaccades based on peaks in the moving correlation values between the speeds of both eyes, as microsaccades are known to occur simultaneously in both eyes. As this method is new, its parameter space needs to be thoroughly explored before recommendations for other users may be given. Here the binocular correlation method is refined based on data from two independent datasets and systematic comparisons to manual microsaccade labels and a commonly used microsaccade detection method are made.

3.3 Methods: Optimising the binocular correlation method

3.3.1 Participants

Five observers with normal or corrected-to-normal vision were recruited for this research. They all gave informed consent and the experiment was conducted in accordance with the University of Oxford's ethical review process (CUREC Approval Reference: R56329/RE001). The first author participated in this experiment and is identified as P1.

3.3.2 Materials

Eye movements were recorded using an Eyelink 1000 eye tracker (SR Research) with a 25 mm lens. The tracker was brought to a distance from the eye of 55 cm for P1 and P2 and 35cm for P3-P5 to maximise the size of the pupil in the tracker's field of view, for better microsaccade detection. The participants' heads were kept stable using a chin and forehead rest. Participants viewed three circular stimuli of different levels of Gaussian blur (see Fig. 3.3) and matched summed intensities, which had a full-width at half-maximum of 19' at a distance of 175 cm. The matched dioptric blur was estimated to be [2] 0.20 D of blur for the sharpest stimulus, 0.47 D for the medium blurred stimulus and 0.74 D for the blurriest target. Stimuli were generated using MATLAB and displayed with 10-bit resolution on a Display++ driven via a ViSaGe graphics system (Cambridge Research Systems).

[1] Part of this work is currently under review in the Journal of Eye Movement Research. This chapter expands on the paper. I have only reproduced work here that is my own.

[2] The estimation of blur was conducted by Dr Laura Young, a post-doc in the group. For this a few unknown quantities were estimated: the pupil size was estimated at 3.5 mm, and the display was assumed to be monochromatic at 550 nm. All stimuli were compared against a completely unblurred circle of the same FWHM.

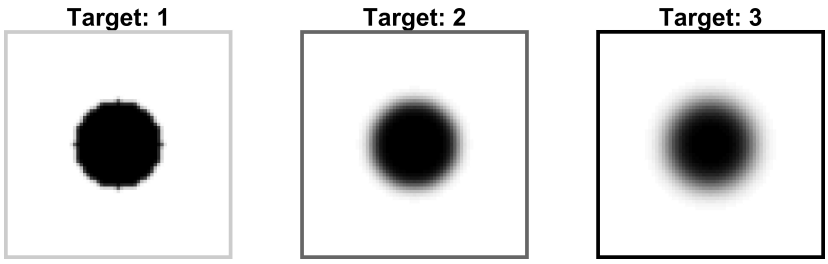


Figure 3.3: Example of the stimuli used during the experiment. The stimuli are defined within a square area where each side measures 48' while the FWHM of each stimulus is 19'.

3.3.3 Procedure

Stimuli were presented for an initial duration of 2 s plus a randomly generated interval of up to 1 s. After this interval the target randomly moved up or down in steps of either 3', 9' or 27' and the onset of movement was indicated to the participant using a beep. Observers were instructed to look at the target and follow it with their eyes. Between trials, 9 s of dynamic grey scale noise was displayed on the monitor to prevent after-images. Participants completed 15 repeats of nine trials of 5 s each, resulting in a total of 675 s of data per participant. Only the first phase before the target moved was considered in this analysis, as the movement in response to the target would contaminate the microsaccade trace and was used to stop participants from focusing too heavily on keeping their eyes still. This resulted in a total of between 403 s and 409 s of data for each participant. An analysis of the data with regards to the blur of the targets is described in Chapter 7 and examples of the following-responses to the movement of the targets are part of Chapter 2.

3.4 Microsaccade detection

The data collected by the above method will henceforth be referred to as the Oxford dataset. A published dataset by Nyström and colleagues (2017) (henceforth Lund dataset) was also included in the analyses to increase the variability of the data used for training, testing and validating the microsaccade detection methods. The subset of the Lund dataset used here contains manual microsaccade labels for fixation data from 4 participants. In the Lund dataset the fixation stimulus was a white cross on a grey background viewed continuously for 200 s. Eye movements were recorded at 1000 Hz using the Eyelink 1000 Plus.

Pre-processing

Before analysis, horizontal and vertical position data were first smoothed. Two methods of smoothing were compared: (i) the smoothing method supplied with the EK method published by Engbert (2006) and (ii) the Savitzky-Golay filter (3rd order, frame length 21 ms) as described by Nyström

and colleagues (2017), and recommended because it preserves high frequency components of the signal well, without amplifying noise. Blink periods were removed, as well as 200 ms before and 300 ms after each blink, to avoid any unwanted artefacts from a partially occluded pupil. Three different ways of detecting microsaccades were employed: manual coding, as well as the EK and BC methods.

Manual coding

For the Oxford data, the first author manually classified microsaccades. The procedure emulated that used in early experiments with analogue eye trace recording, where microsaccades were originally reported. Importantly, the manual coder did not have access to binocularity or velocity cues, so classification could remain as bias-free as possible. The full horizontal and vertical position traces up until the target movement were displayed for each trial (e.g. Fig. 3.5, panels 1 and 3: blue and red lines would be displayed separately). Microsaccades could then be selected by double clicking on the beginning and the end of identified saccades. The height of each figure, corresponding to the vertical or horizontal eye position, was fixed at a minimum of 1° in size, ensuring that all displays were of the same maximum spatial resolution. Data from each eye were presented separately. For further analysis, only binocularly detected microsaccades were considered.

For the Lund dataset the published manual classifications by both coders (columns: *ms_type_c1* and *ms_type_c3*) were combined using a logical OR operation. This method of combining the two coders was chosen, as it gave best performance of the EK method compared to using logical AND.

Automated EK

The EK detection method as published by Engbert (2006) was used for microsaccade detection and different values for lambda (3 to 9 in steps of .5) were considered.

Automated BC

To identify microsaccades using the BC method, moving correlations between the speeds in the left and right eye have to be calculated. The speeds in both eyes are defined as the absolute velocities calculated from the first derivative as returned by the Savitzky-Golay filter, or by taking the first derivative of the smoothed positions returned by the smoothing supplied with the EK method. It is important to note here that the key variable is speed, not velocity, as it is not necessarily the case that the direction of the eye movement in both eyes is always well correlated during a

microsaccade (Van Horn & Cullen, 2012). In early piloting of this method, we assessed if correlating the accelerations between both eyes could improve the accuracy of this technique and found no improvement on microsaccade detection when including an acceleration criterion.

A threshold is applied to the coefficient of determination R^2 of speed between the two eyes. This results in a trace that has selected periods of high correlation, which depend in duration and prominence on (i) the underlying microsaccade, (ii) the size of the correlation window (ω) and (iii) prior smoothing. Too little smoothing leaves the data too noisy to analyse, while too much smoothing may remove all evidence of the smallest microsaccades, as well as artificially increasing correlation between both eye traces. Using a larger ω results in less prominent and wider periods of interest, as they correlate across more non-microsaccade samples. This, however, has to be balanced with the overall reduction in noise. As such, smoothing and the size of ω interact in the BC method. This is akin to how data smoothing and the way of calculating the moving velocity in the EK method interact and in this case some papers have proposed different velocity calculations to accommodate different tracking frequencies (e.g. Nyström et al., 2017). Both the EK method's velocity calculation and the BC method's ω essentially act as an additional level of smoothing.

Since the periods of high correlation extend beyond the microsaccade duration by an amount that depends on the size of ω (see Figure 3.4), a set number of samples are removed from the beginning and end of the periods of high correlation .

The method can be summarized in three steps:

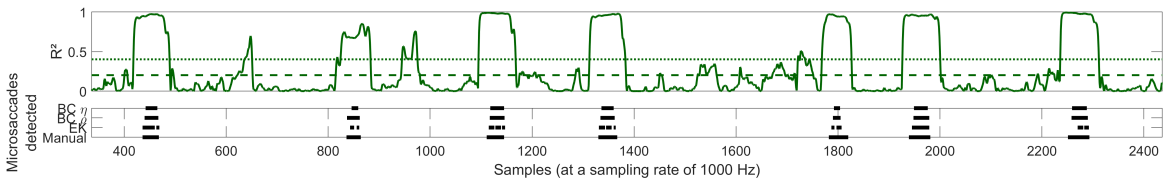
1. Calculate the coefficient of determination (R^2) for an moving correlation window between speed for left and right eyes.

2. Apply a threshold value to R^2; high R^2 values identify periods containing a microsaccade.

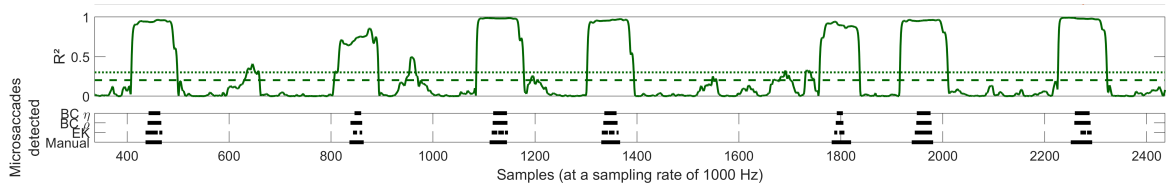
3. Remove the first and last N samples from the detected microsaccade, where N is half of ω.

The BC detection method consequently has two main parameters that can influence the successful detection of microsaccades: ω and the threshold for R^2 values. For any given set of thresholds, the size of ω will determine how many microsaccades are identified. Larger values of ω may result in smaller microsaccades going undetected, as they are swamped by adjacent noise, as well as a false merging of two neighbouring microsaccades. Shorter durations of ω may lead to the spurious identification of short bursts in correlation among noise as microsaccades. A threshold for the R^2 values needs to be set, as this influences the number of identified microsaccades. There are two ways of choosing such a threshold value, both of which are explored. The first option is to select a fixed threshold value and apply this to all data. This method we refer to as BCρ, where the threshold

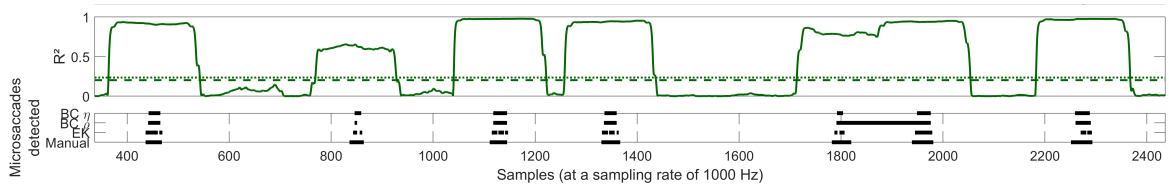
value is specified by a parameter ρ for which threshold = ρ^2. The second option is more similar to the EK method, in that a variable threshold value is chosen, based on a median multiplier, which we refer to as η, and consequently refer to this version of the BC method as BCη (where threshold = η * Median of the R^2 values). In the next section a systematic approach to optimizing these parameters is described. The Oxford data (mean microsaccade duration for manual coder: 34 ms / 34 samples at 1000 Hz (the sampling rate of the data used), for other features, please refer to Table 1, page 31), as well as an example implementation of the BC method for MATLAB will be made available upon publication of this research.



(a) Detected microsaccades, thresholds, and spikes in correlation for an ω of 45 ms.



(b) Detected microsaccades, thresholds, and spikes in correlation for an ω of 95 ms.



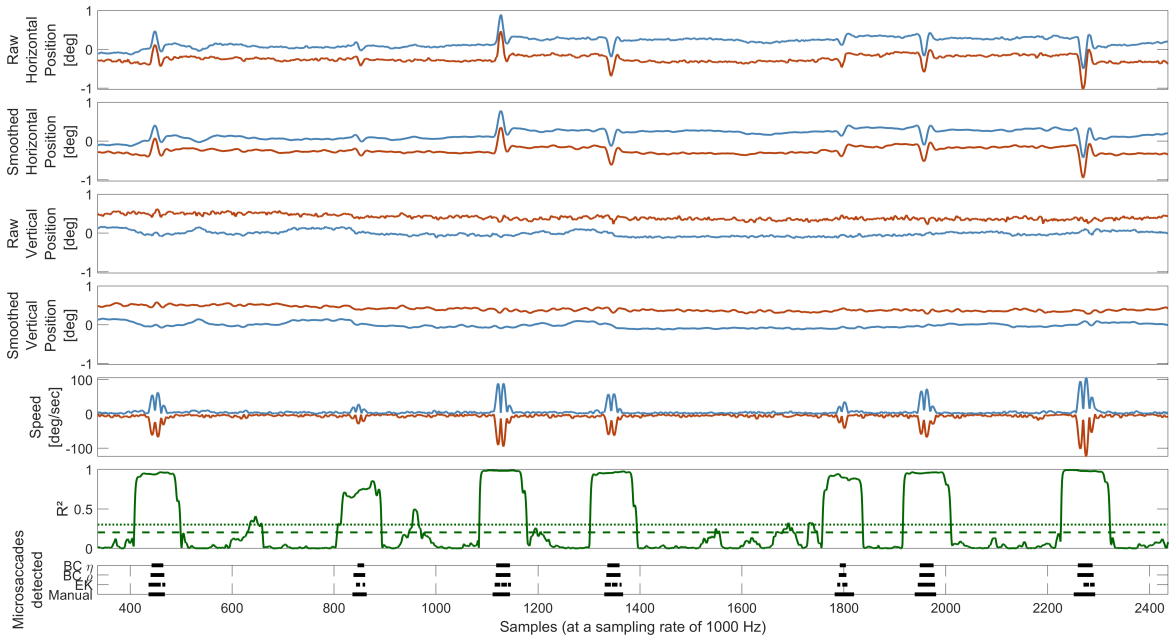
(c) Detected microsaccades, thresholds, and spikes in correlation for an ω of 155 ms.

Figure 3.4: The effect of ω on microsaccade detection. The thick black lines indicate when a given detection method identified a microsaccade. The green solid line represents the moving correlation of the speeds between both eyes with an ω of 65 ms. The corresponding finely dashed green line represents an η value of 7 and the coarsely dashed green line indicates a ρ value of .45.

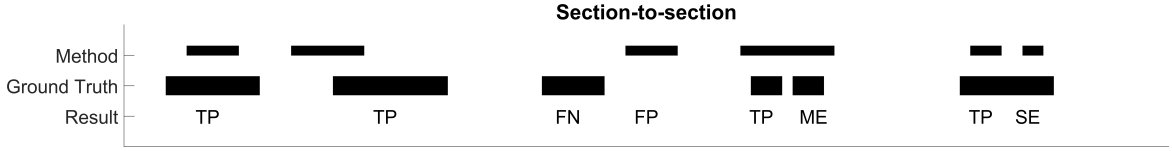
3.5 Comparison of Detection Methods

To compare the performance of the BC method with the established EK one, we used Precision-Recall (P-R) curves. P-R is an objective and established way to evaluate classification performance, but to our knowledge has not yet been used to quantify the performance of microsaccade detection methods, although it has been used in evaluating the similarity between manual coders (Hooge, Niehorster, Nyström, Andersson & Hessels, 2018; Nyström et al., 2017). P-R curves plot precision against recall:

$$Precision = \frac{TruePositives}{TruePositives + FalsePositives} \tag{3.1}$$



(a) Comparison of microsaccade detection methods and their mapping onto smoothed eye-movement data, speed and correlation profiles for P4. The red lines indicate data from the left eye and the blue lines indicate data from the right. The green solid line represents the moving correlation of the speeds between both eyes with an ω of 65 ms. The corresponding finely dashed green line represents an η value of 7 and the coarsely dashed green line indicates a ρ value of .45. A total of just over 2000 samples or 2 seconds is shown. Note: Speed in the left eye is represented as negative to facilitate readability of the graph.



(b) Graphical explanation of how the ground truth and detection method were compared. TP refers to true positives, FN to false negatives, FP to false positives, ME to merged events, and SE to split events. Please refer to the main text for a full discussion.

Figure 3.5: Example of eye trace and microsaccade detection.

$$Recall = \frac{TruePositives}{TruePositives + FalseNegatives} \tag{3.2}$$

The therefore give an indication of a method's performance by relating how many correct identifications, misses and false positives occurred. As there is no available ground truth specifying which data samples represent a microsaccade, manually coded classifications were used, as they are the current gold standard to approximate ground truths. Using P-R curves is advantageous compared to receiver operator characteristic curves in imbalanced datasets (Saito & Rehmsmeier, 2015). As microsaccades are a relatively rare occurrence in eye movement data we decided on the use of P-R to evaluate the performance of the two methods.

The F1 score, based on the Sorenson-Dice coefficient for comparing the similarity of two samples (Dice, 1945; Sorensen, 1948), can be used to quantify P-R performance and is given by:

$$F1 = 2\frac{Precision * Recall}{Precision + Recall} \tag{3.3}$$

Precision and recall can either be determined on a sample-to-sample or section-to-section basis. When comparing methods on a sample-to-sample basis each data sample is assigned a binary value: 1 for being part of a microsaccade and 0 for not being part of a microsaccade. These are then compared sample-to-sample to a similarly coded ground truth. Looking at the data on a section-to-section basis, each data point is still assigned a binary value, but sections are only taken as successful identifications if there is at least one sample overlap between those microsaccade samples identified using one method and those identified in the ground truth. Sample-to-sample data might be useful in identifying how accurately start and end points of saccades match between different detection methods. However, none of the three detection methods is likely to be accurate in identifying the edges of a microsaccade. Therefore, using sample-to-sample data would lead to additional variability associated with the performance of the different methods and so we chose not to consider it. Comparing identified microsaccades section-to-section is a more robust method and more strongly indicates whether individual microsaccades were identified correctly.

Section-to-section comparisons assess if any microsaccade in the ground truth overlaps with any microsaccade detected by the detection method by at least one sample. If there is any overlap between the ground-truth and method-detected microsaccade, this is counted as a true positive. There are two possible special cases which are included in the analysis in this Chapter: merged events and split events. In a merged event two or more microsaccades in the ground truth are represented by only one microsaccade by the detection method. This is labelled as one true positive and one or more merged events. Split events occur when a single microsaccade in the ground truth is represented by two or more microsaccade in the detection method. This would be counted as a single true positive and one or more split events. For a graphic description of this, refer to Figure 3.5. Thus, section-to-section comparisons were used to evaluate the performance of the different detection methods.

As the BCρ method has two parameters that need to be set (ω and η), the interaction between different parameters was first freely explored using fixed values. Sizes of ω between 15 ms and 155 ms in 10 ms steps were considered. For any given ω exactly half of the number of samples in the window were removed from the beginning and the end of a detected microsaccade. The values for η varied between .25 and .75 in .05 steps. This resulted in a total of 165 parameter combinations.

The parameter space for the BCη method was also explored, using the same ω sizes as for BCρ. The value of the median multiplier η was varied between 3 and 9 in .5 steps, the same values which were used to vary the EK method's λ.

To find the best possible combinations of type of smoothing and detection parameters a training-

and-testing strategy was used. To test the data, two participants out of the nine available ones (five from the Oxford dataset and four from the Lund dataset) were reserved. All possible combinations were tested sequentially, resulting in a total combination of 36 unique pairs. In each case, the remaining participants were used as training participants and the parameters with the best mean F1 score across those seven participants were taken as the training recommendation. To find the most suitable overall parameters, the 36 parameter recommendations were averaged (either λ, ω, η, or ρ) and the most similar value used to explore the data was chosen as the final recommendation. Strictly speaking, as ω interacts with η or ρ, taking the mean of those values is not useful. However, on inspection of the data all recommended values were found to be very similar and so the means were taken as representative.

To give an estimation of how transferable parameter estimations are from one dataset to another, the parameters were trained on one of the two datasets and then tested on either itself or the other dataset.

Parameters that gave the highest F1 score across all participants from both the Oxford and Lund datasets were identified as optimal parameters.

3.6 Results

The box plots of the best parameters for the EK method, the BCη, and BCρ methods are shown in Figure 3.7, as well as the standard recommended EK method with a λ of 6. The difference in recommended parameters and spread of F1 scores depending on whether EK smoothing or a Savitzky-Golay filter was used can be determined by comparing the two different panels. On inspection it appears that using a Savitzky-Golay filter for smoothing results in higher, and less spread out F1 scores for all methods. This is also supported by Figure 3.6, which shows higher F1 scores for the Savitzky-Golay smoothed data plotted in black, compared to the EK smoothed data in red. Due to the small number of available participants no test of statistical significance were conducted.

When considering the data smoothed using the Savitzky-Golay filter, the best performing EK λ for 1000 Hz data was 7. For the BCρ method an ω of 65 and a ρ of .45 performed best, while for the BCη an ω of 65 and an η of 7 were optimal (see Fig. 3.7).

The resulting physical features of microsaccades determined using manually coded data, the EK method and the BC methods are given in Table 1 (p. 31, shaded grey). Where minimum or maximum values are required the mean across all microsaccades' maximum or minimum values was taken. For microsaccade distance we reported the diagonal of the smallest rectangle that

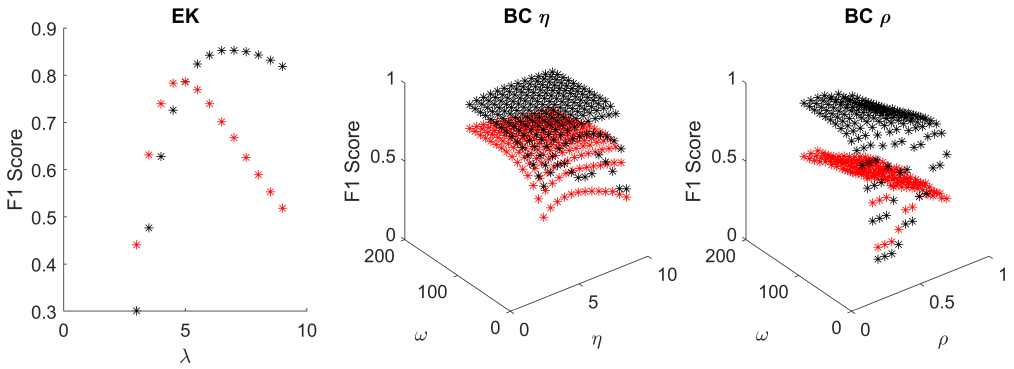
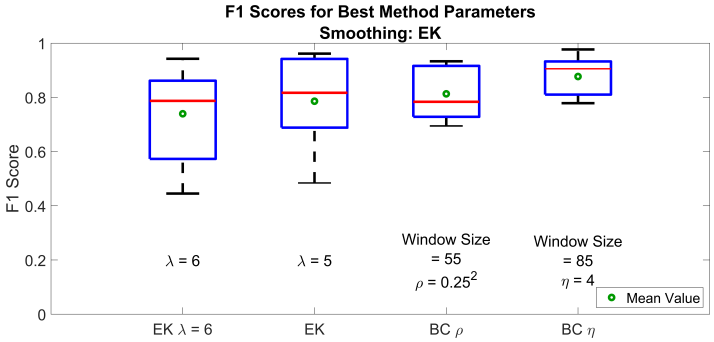
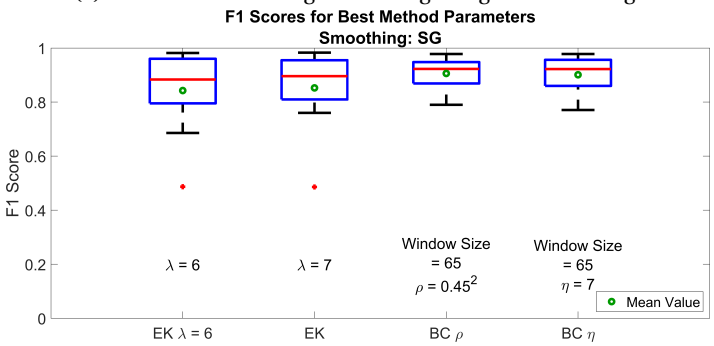


Figure 3.6: Plots showing the interaction between the different microsaccade detection parameters and the F1 score. In black data points smoothed using the Savitzky-Golay filter are shown while in red data points smoothed using the EK smoothing are given.

contains the full microsaccade trace.



(a) Results from training and testing using EK smoothing.



(b) Results from training and testing using Savitzky-Golay smoothing.

Figure 3.7: Comparison of the EK and the BC methods using the F1 score. The box plots show the spread of F1 scores for the 9 participants (5 from the Oxford dataset and 4 from the Lund dataset). For box plots the edges of the box represent the 25th and 75th percentiles, the line in the centre represents the median, while the errorbars show the most extreme values not considered outliers. Outliers are plotted as separate asterisks. Below the box plots the parameters used are given. They represent the optimal parameters as identified during the training and testing phases, apart from the EK $\lambda = 6$, which is given for context, as $\lambda = 6$ is often a suggested starting value.

Microsaccade main sequences were plotted for all Oxford data. Microsaccade distance was estimated using the difference between the points created by the most extreme horizontal and vertical points (see Fig. 3.8). The main sequence plots for all detection methods appear to fall reasonably well on a line in the log-log plot, not dissimilar to unity. The BC method includes some smaller and slower microsaccades, compared to the manual coder. These may be real microsaccades that are below the detection threshold of the manual coder, but are successfully

picked up by the BC method. If this were the case, these samples would lower the apparent precision value of the BC method, as they would be counted as false positives. Visual inspection of the data suggests that this is the case, however, it remains possible that some of these may also be false detections.

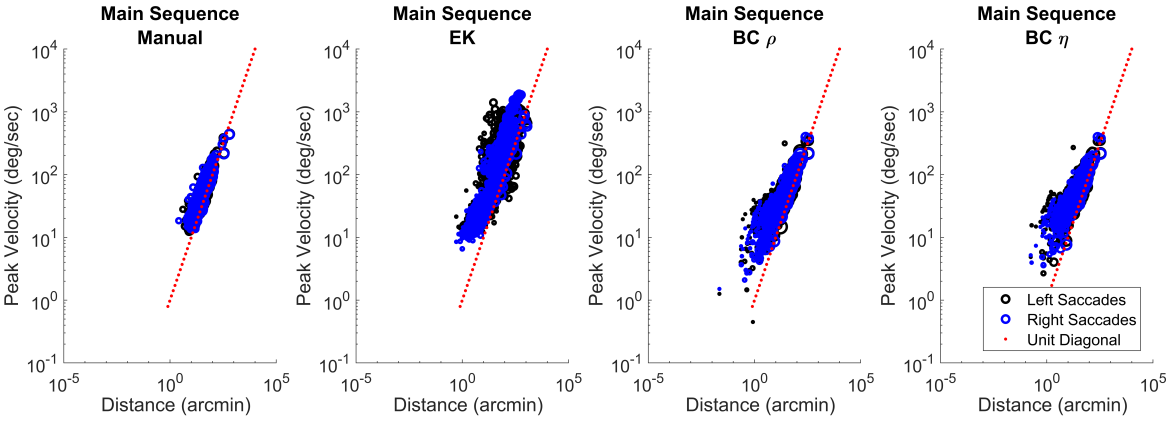
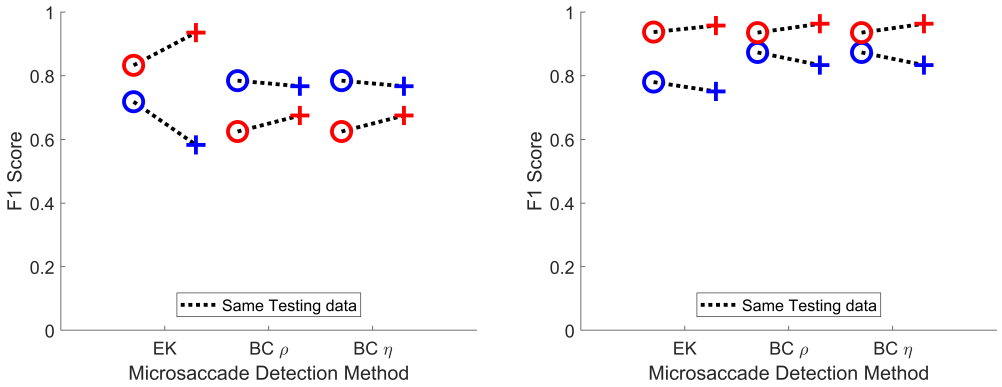


Figure 3.8: Microsaccade main sequences for the Oxford dataset using Savitzky-Golay smoothing. For the EK method a λ of 7 was used. For both BC methods an ω of 65 was used. η was set to 7, while ρ was set to $.45^2$.

The transferability of the different detection methods from the Oxford to the Lund dataset and vice versa is shown in Figure 3.9. On visual inspection transferability appears to be better for data smoothed using a Savitzky-Golay filter compared to the EK smoothing.



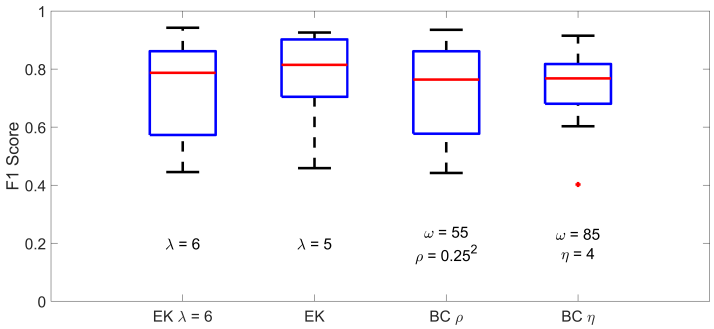
(a) Transferability of optimal method parameters from one dataset to the other when using EK smoothing.

(b) Transferability of optimal method parameters from one dataset to the other when using Savitzky-Golay smoothing.

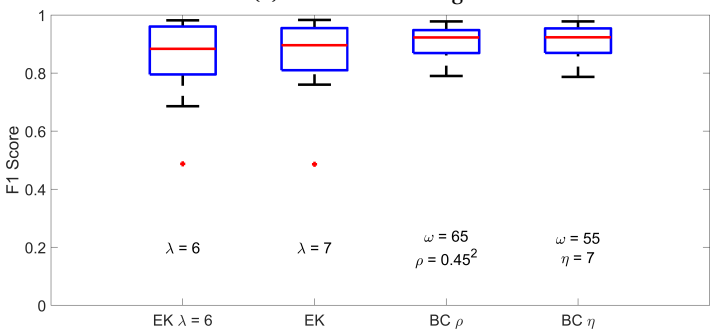
Figure 3.9: Transferability of the different detection methods between datasets. The symbols indicate which dataset was used to train on: 'o' indicates Oxford training data and '+' indicates Lund training data. The colour indicates which data were tested: blue for Oxford test data and red for Lund test data.

The absolute best achievable values for both detection methods and smoothing types are very similar to the ones given by the training and testing method (see Fig.3.10).

For the best achievable values the merged and split events can be seen in Figure 3.11. From the figures it is clear that the EK method produces more split events compared to the BC methods, while the BC methods produces more merged events than the EK method. It appears that the BC methods produces comparatively fewer merged events than the EK method produces split events.



(a) For EK smoothing



(b) for Savitzky-Golay smoothing.

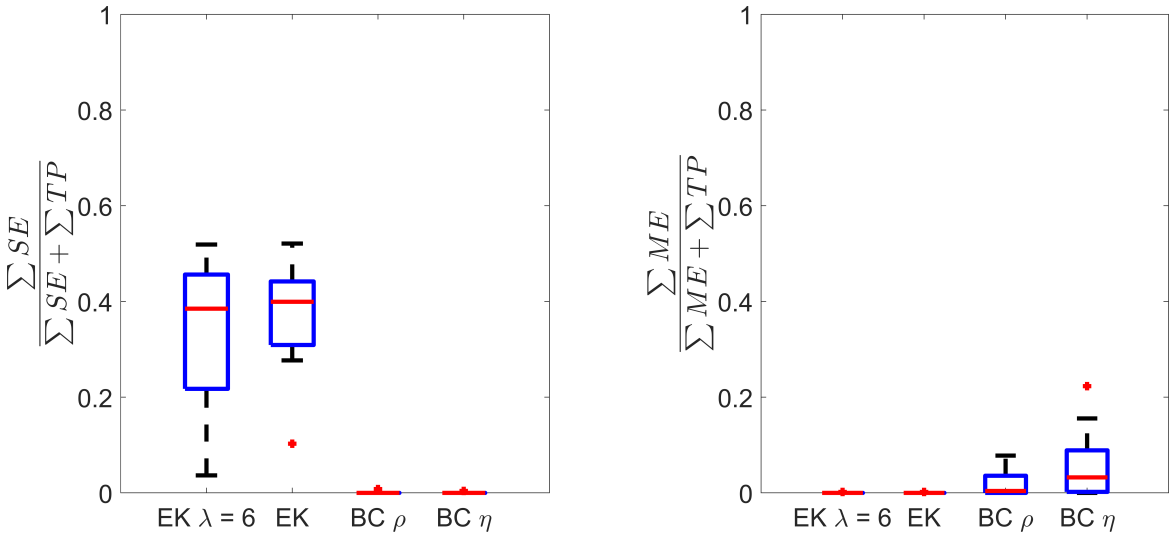
Figure 3.10: Best parameter values and corresponding F1 scores.

The figures show the same trends irrespective of what type of smoothing was used.

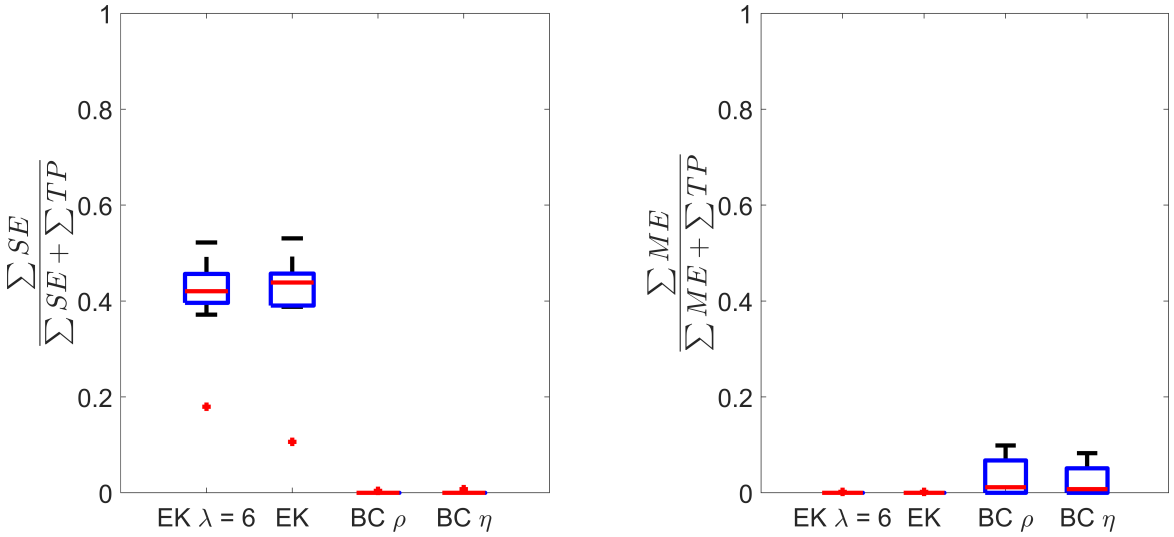
3.7 Discussion

Correctly identifying microsaccades is important in many areas of research, from trying to understand the visual system (Barlow, 1952), to medical research (Fried et al., 2014) and studies on attention (Gowen, Abadi, Poliakoff, Hansen & Miall, 2007; Tse, Sheinberg & Logothetis, 2002). Over time, our understanding of what makes a microsaccade has developed significantly, yet there have been few attempts to improve microsaccade detection based on our advances in knowledge. The EK method relies on the theoretical basis that microsaccades are outliers in velocity space and uses a simple binocularity criterion as a way of rejecting noise. The presented BC method relies on the temporally synchronous nature of microsaccades between the two eyes, and considers speed data, which is expected to be correlated between the two eyes during microsaccades. Other candidate characteristics for theory-driven methods of microsaccade detection are their characteristic ballistic motion, the main sequence relationship between their peak speed and distance travelled, as well as a combination of the physical parameters that limit them.

The BC method presented here is a new way of classifying microsaccades. Because speeds in both eyes are more correlated during microsaccades than during drift and tremor these correlations can be used to successfully identify relevant periods in the data. Based on the data available for this study, the best parameters to use on unknown data are an ω of 65 ms and a fixed threshold



(a) For EK smoothing



(b) for Savitzky-Golay smoothing.

Figure 3.11: Best parameter values and corresponding merged and split events.

ρ of .45[2]. Whilst there was no large difference between the BCρ and BCη methods, the box plots for BCρ were smaller, indicating a smaller interquartile range and therefore more consistency between participants, which is useful for microsaccade detection. If adjustments to these values are necessary, it would be advisable to stay within the middle of the range of tested ωs. Too small an ω will result in some noise being misclassified as a microsaccade and too large an ω will produce lower correlation signals that may not be detected above the background values (see Figures 3.6 and 3.4). After choosing an ω, good performance can be achieved by tuning the ρ value.

The BC method focusses on a different feature of the microsaccade trace compared to the EK method and it may therefore be possible to choose which method to use depending on the experiment. For example, the BC method may be used when deliberately analysing only binocular microsaccades, while the EK method can be used to investigate potential monocular microsaccades.

In direct comparison, both microsaccade detection methods performed well on two separate

sets of data, the Lund dataset (Nyström et al., 2017), and the Oxford dataset. From the comparison to the default value of the EK method in Figure 3.10 it is obvious that a λ of 6 is a good starting value, which can be further improved with knowledge of the dataset. Perhaps a technique similar to the unsupervised clustering method proposed by Otero-Millan et al. (2014) could be employed to optimize detection by combining the BC and EK methods. Preselecting candidate microsaccades using a liberal λ for the EK method and then choosing only those candidate microsaccades with the highest binocular correlation values may improve performance. One benefit offered by the binocular correlation method is that the height of the correlation peak may be used as an indicator of confidence in the correct identification of the microsaccade.

P-R is a useful tool for studying the effectiveness of microsaccade detection methods. No microsaccade detection method is without issue, including the manual detection we used as a ground truth. However, using a weighted F1 score, it would be possible to select methods that are favourable because they are either biased to high recall or high precision. Having a high precision value may be useful in isolating only microsaccades from data, which may be particularly relevant for studies on covert attention, where drift periods are of no interest and contamination of data with them should be avoided. Alternatively, when research is interested in drift properties, and contamination with microsaccades should be avoided, biasing a method towards high recall may be beneficial.

As the field of microsaccade research continues to grow and develop, reporting a variety of physical microsaccade parameters can contribute to the development of future detection techniques and increase the comparability of results between studies. It remains important for the progress of the field that we keep evaluating the research methods we use, from tracking setups to task design, participant instructions and detection mechanisms. One crucial side to this is that it is desirable for more researchers to make their eye tracking data available, including manual coding of microsaccades, where possible. Only with more diversity in the data available to train and test detection methods can we truly evaluate performance and make informed choices in the quest to optimize microsaccade detection.

Chapter 4

Monocular Microsaccade Detection

Abstract

In some situations binocular eye tracking is not possible, so a single monocular trace has to be used for analysis of eye movements. Here, development of a new method, for use on high-resolution data from an adaptive optics scanning laser ophthalmoscope (AOSLO), is reported. This method primarily relies on the smoothness of the data trace and a velocity threshold. As AOSLO eye tracking is a developing field, this Chapter discusses tools for improving AOSLO eye-movement analysis and future directions for this research. Eventually, this microsaccade detection method would benefit from formal training and testing once more data are available.

4.1 Why monocular microsaccade detection is important

Microsaccade detection is easier the more information is available. As a consequence, it is desirable to have access to binocular eye movement traces, as microsaccades occur in both eyes at the same time. This fact can be exploited to improve detection (see Chapter 3). However, in some cases binocular eye movement recordings may not always be possible, making monocular detection methods an important tool for the study of fixational eye movements.

One common reason for a lack of binocular data is that some eye trackers are heavily dependent on a complex optical setup, as is the case with AOSLOs, DPI trackers or historical trackers depending on contact lenses, such as scleral coils or contact lens mirror trackers. In these cases binocular recordings are only possible if two of the required systems are available. This may be hard to achieve due to associated maintenance and set up costs. A further reason may be that binocular eye tracking limits the available temporal frequency of eye tracking, as it does for some video-based trackers,

and it may be judged to be more desirable to have higher temporal resolution tracking, rather than data from both eyes, especially in tasks depending on exact timing of stimuli. Lastly, even when binocular eye tracking is being used, there can be occasional or systematic tracking failures for one eye. A common reason for this is often the geometry of glasses, which might slip during a recording session, or scratches on only one side of a pair of glasses, therefore complicating binocular eye tracking. Moreover, monocular eye tracking might be used in experiments that require occlusion of one eye or for participants for whom only one eye is suitable for eye movement analysis.

Monocular microsaccade detection can still exploit most features of microsaccades for detection and therefore can still be reliable. As with binocular tracking, it is possible to adjust thresholds to make the classification more or less liberal, depending on the purpose of microsaccade detection. When setting thresholds it is therefore important to establish if it is more important to detect all potential microsaccades, or only those that definitely are true microsaccades. Also, monocular tracking benefits from having highly accurate and low noise trackers, to compensate for the lack of binocular data.

4.2 Related problems in other fields

Whilst eye movements can not be directly compared to other motor activities, there are certainly movement patterns similar enough to eye movements to be of interest. For example an algorithm effective at detecting whether or not a person is currently travelling in a car, based on their GPS signal, should be good at separating a person walking from a car in slow traffic. This may be considered a problem similar to that of classifying movements at the border between slow and small microsaccades vs. fast and large drift and tremor.

The most similar path-analysis problems stem from biology, where paths of organisms ranging from bacteria to different types of animals are analysed. What these have in common with monocular eye tracking is that only a single trace is available to make decisions about the state of that path at a given time. Moreover, as summarised by Taylor-King, van Loon, Rosser and Chapman (2015) these biological movement traces all exhibit two different phases: a long distance movement phase and a local or resting state. The same can be said for fixational eye movements. While we distinguish between three types of fixational eye movement, two of these, drift and tremor, occur together and are slower and can therefore be classified as a local motion, whereas microsaccades lead to larger retinal displacements. Often the same classification is used when talking about larger saccades as well, with a classification into *fixations* which include microsaccades, drift and tremor and larger movements like saccades or smooth pursuit.

Commonly researchers have been trying to classify, describe, and simulate the movement patterns of these diverse organisms. As many of them exhibit movement paths akin to random walks, diffusion processes are frequently used (Visser & Kiørboe, 2006; Taylor-King et al., 2015). However, there are not yet many suggestions for automatically segmenting these traces into their large- vs. small scale components. Rosser et al. (2013) suggested the use of Hidden Markov Models to separate larger from smaller scale movements. Hidden Markov Models can be used to estimate the transition probabilities between different states of a model, in this case the long and short range states. The *hidden* aspect of the model is that the exact state is not explicit, but can only be estimated from the observed behaviour. Hidden Markov Models have also been used to segment larger saccades from fixations during reading in humans (Macas, Lhotska & Novak, 2013), however they have not yet been applied to microsaccades. Often the features of interest in the movement trace are similar across disciplines and include speeds of movement, distances travelled, curvature of paths and angles of orientation. Segmenting the paths using these features is done across disciplines and perhaps working on segmentation methods that can generally exploit these characteristics will be beneficial to many different fields.

It is important that awareness of segmentation in path analysis between different fields of research is fostered, as the paths and computational issues are in many cases similar. An example for cross-disciplinary exchanges should be the field of image analysis, as many approaches to image analysis have proven useful in a diverse range of fields. In the future Hidden Markov Models may be used to separate microsaccades from drift and tremor. However, before more complex models are used, it may be argued that we should first establish the basic features of interest and optimise classification using only those. This may also be helpful in identifying which features should be made available to more computational types of data analysis, akin to the unsupervised clustering method used by Otero-Millan et al. (2014), or neural network/deep learning based methods. In this thesis we will consider specialised threshold criteria to detect microsaccades in eye movement data.

4.3 The monocular microsaccade detection method

At the core of the new monocular microsaccade detection method is the concept that, in systems with low noise levels, loosely constraining multiple different parameters to segment microsaccades from drift and tremor can provide better microsaccade detection results than relying on fewer, more tightly constrained parameters. Currently, microsaccade detection methods rely on just a few, tightly constrained parameters to detect microsaccades. Most commonly a monocular version of

the EK detection method is used to detect microsaccades when tracking data are only available for one eye (e.g. Betta et al., 2007; Dimigen et al., 2009; Otero-Millan et al., 2011; Thaler et al., 2013). This has the disadvantage that it is not as robust as also relying on the criterion that the saccade has to be detected in both eyes, which the method originally required (Engbert & Kliegl, 2003). To counteract the loss of this criterion it could be argued that higher velocity limits should be used, yet that could lead to missed microsaccades.

Another aspect of many microsaccade detection methods is that they only consider very few parameters. While this can be effective, it is often challenging to find the correct ones, e.g. the best velocity threshold, for each participant, as there can be large variations between people. The most basic microsaccade or saccade detection method is a minimum velocity threshold (e.g. Boyce, 1967; Rucci & Desbordes, 2003), sometimes combined with duration, or distance criteria (e.g. Ko et al., 2010; Poletti & Rucci, 2010). Similarly, many additions to the basic EK method have considered a single additional threshold value, such as a *minimum* duration, distance or linearity criterion (e.g. Thaler et al., 2013). In reality any parameter that applies to a movement trace has a lower and upper value. It is true that, for example, the *maximum* duration of a microsaccade should largely be irrelevant as microsaccades are generally short events and the lower threshold is more meaningful for excluding noise from being detected as microsaccades. However, including the less used threshold can also protect against unintentional errors, such as characteristic failures in data collection (for example, when eye tracking fails for the AOSLO, it usually results in impossibly high eye velocities), or bugs in analysis codes. Thus, whenever a lower threshold value is used, adding an upper value should also be considered and vice versa.

The monocular microsaccade detection method presented here is specifically under development to detect microsaccades in AOSLO and other high-resolution eye tracking data. As it is not adaptive in any way, it is of great importance that eye position data are relatively accurate, low-noise, and well-calibrated so that realistic velocities and positions can be extracted. Additionally, the method is designed to work with unsmoothed, or only minimally smoothed (by downsampling) AOSLO data, contrary to the requirement of many microsaccade detection methods developed for video-based eye trackers (Nyström et al., 2017). The monocular microsaccade detection method requires several features to be extracted from the data. It is necessary to determine the sample-to-sample velocities and accelerations, which can be extracted from the first and second derivatives of the Savitzky-Golay filter, as well as the sample-to-sample angle of movement.

The following five steps are used to extract microsaccades from the data.

1. Identify all samples that follow a sufficiently smooth trajectory to plausibly be part of a

microsaccade.

2. Identify all samples above a minimum (and below a maximum) velocity.

3. Find all runs of samples that fulfil both point 1 and 2.

4. Check that all remaining candidate microsaccades last for a minimum duration.

5. Merge any remaining candidate microsaccades that are not well-separated temporally.

6. Check that all candidate microsaccades have a minimum duration or number of samples.

Some parameters can be safely estimated using previous data: the maximum velocity should be chosen in accordance with possible eye speeds and tracker idiosyncrasies; the minimum duration of microsaccades should be set in relation to the temporal resolution of the tracker and/or plausible microsaccade length (4); and the permissible gap between microsaccades that are merged can be estimated based on convention in the field (5). The values that need to be determined for successful use of this method are the parameters relating to the smoothness of the eye trace (1); and the minimum velocities (2).

Establishing the smoothness of a trajectory is not trivial and multiple options are available. The simplest method would be to allow a maximum angular deviation from a straight line. This, however, has the disadvantage that zig-zagging motions are evaluated by the same standards as continuously curved movements. In practice we would like to deselect zig-zagging motion and allow for curvature (i.e. sustained angular deviation), as microsaccades only exhibit the latter property. Yet, as eye trackers are not perfect, a small amount of zig-zagging should be permissible for microsaccades, as even a perfectly linear eye motion would likely result in a small amount of angular difference between samples, due to measurement errors or noise.

Thus, a combination of two angular criteria was used: a permissible local angle and consistent-curve angle. The local angle decrees how much zig-zagging of the signal is permissible from sample to sample, whilst the consistent-curve angle regulates how much of an angular curvature is acceptable, if the difference is in the same direction as the previous sample, i.e. curving in one direction. The local angle is set to a smaller value than the consistent-curve angle. Therefore a given sample may violate the local angle criterion, but if the consistent angle criterion is met, it will still be considered smooth enough to be part of a microsaccade (see Fig. 4.1).

This method of detecting microsaccades in monocular data therefore has three parameters that can be altered to meaningfully tune classification performance. These are the two smoothness criteria: the locally allowed deviation from a straight line (local angle) and the permissible angle

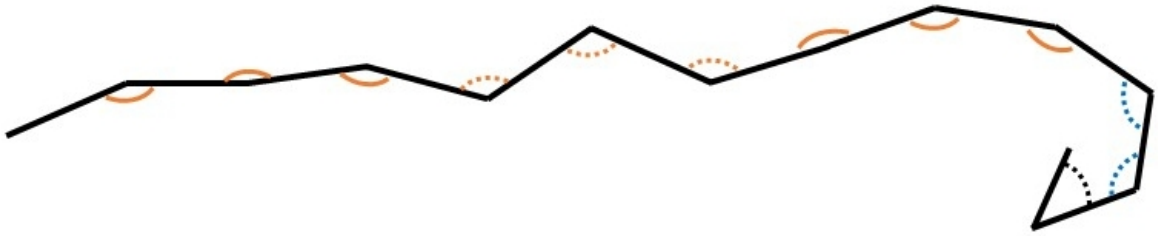


Figure 4.1: Examples of different sample-to-sample angles and how local and consistent-curve angle criteria are applied. On the left the movement(black) zig-zaggs. The local angles are highlighted, with solid lines representing those judged to be sufficiently small that they may be part of a recorded microsaccade trace. The dashed lines represent the angles which exceed the local angle criterion. The orange dashed lines also do not pass the consistent-curve angle criterion, as they do not form part of a movement curving in the same direction. Towards the right the movement becomes curved. The blue dashed lines indicate angles that fail the local angle criterion but pass the consistent-curve angle criterion, as they both curve in the same direction successively. The black dashed line indicates an angle between successive samples with fails both the local and consistent-curve angle criteria, despite continuing to curve in the same direction.

within a sustained curve (consistent-curve angle); and the minimum velocity. In addition five parameters were fixed: the minimum duration of microsaccades was fixed as 3 ms, while the minimum permissible gap between microsaccades was set to 20 ms. An unlikely maximum duration of 1 s was also set. A maximum velocity threshold of 120° /sec was chosen, as this should correspond to a microsaccade size of approximately 0.6° (Duchowski et al., 2017) and no larger saccades were expected. A minimum microsaccade distance of 3' was chosen. This distance was calculated by adding each sample-to-sample distance.

Moreover, exploring the feasibility of this method can tell us something about how uniformly these parameters are distributed in the population. If all participants have similar threshold values it will be relatively easy to identify adequate parameters for this method. However, if that is not the case, it suggests larger individual variation in these parameters, which may require additional adjustment of thresholds for each participant.

4.4 Methods

AOSLO eye-movement recordings from Experiment Two, Chapter 7 were used to develop this microsaccade detection method. Manual microsaccade labels were available for all 14 participants, a detailed description of which can be found in Chapter 2. Two microsaccade detection methods were compared to this assumed ground truth: The monocular microsaccade detection method presented in this chapter and the Engbert and Kliegel (EK) (2003) method. Both methods were used on all of the data.

4.4.1 Data Preparation

As AOSLO data with a sample rate of 16 000 samples/sec are comparatively noisy in the velocity component, and both methods used to detect microsaccades in this chapter rely on velocity estimates, the AOSLO data were downsampled to a sample rate of 1000 samples/sec. The automatically and manually detected tracking failures were replaced with NaNs, however the flyback periods (ca 3 ms long, 30 times/s) were spline interpolated, to allow for better smoothing and easier comparison to the manually classified microsaccades. Interpolating these flyback periods improves the smoothing, as otherwise more samples either end of a frame are removed. Interpolating also benefits the comparison to the manual microsaccade detection, as the flyback regions now will not interrupt a string of samples identified as a microsaccade and will therefore probably reduce the number of false positives detected. However, a decision was made against also interpolating the missing data due to tracking failures, as these represent larger gaps across which the spline interpolation would not represent a good approximation of the actual movement across its whole range. The data were submitted to automated microsaccade detection with prior smoothing (Savitzky-Golay filter, order: 3, framelength: 21 ms) and without.

4.4.2 Refinement of Detection Methods

Different possible values for the three parameters (local angle, consistent-curve angle and minimum velocity) were assessed. The exploration of the parameter space was done iteratively, guided by the experimenter: a set of threshold values was investigated and their performance examined. If the optimal values from this set were at the boundaries of one or more of the parameters the search for an optimum was extended in this direction. Eventually a total of 624 different parameter combinations was tested. For the local angle, the explored values ranged from 0.1° to 5° . For the consistent-curve angle, values between 1°and 18° were analysed. Minimum velocity values between 0.5° /sec and 9.7° /sec were considered.

For the EK method 25 different values for λ were analysed ranging from 3 to 15 in steps of 0.5.

The F1 scores for both methods were calculated based on the Sorenson Dice coefficient for comparing the similarity of two samples (Dice, 1945; Sorensen, 1948) (see Equation 4.1). Then the best F1 scores achievable with the EK and monocular detection method for either smoothed or unsmoothed data were compared and discussed.

$$F1 = 2\frac{Precision * Recall}{Precision + Recall} \tag{4.1}$$

4.5 Results

Both the EK method and the monocular microsaccade detection method performed well on the data. Both methods performed better on the unsmoothed data (see Fig. 4.2). How the different parameters influenced F1 scores can be see in Figure 4.3. It appears that for the monocular microsaccade detection method the velocity threshold has the largest impact on improvements to the F1 score. The fact that performance is similar for both the EK and the monocular microsaccade detection method suggests that no adaptive velocity threshold is needed for high-resolution AOSLO data and that most participants have a similar velocity threshold that optimally separates microsaccades from the drift and tremor component.

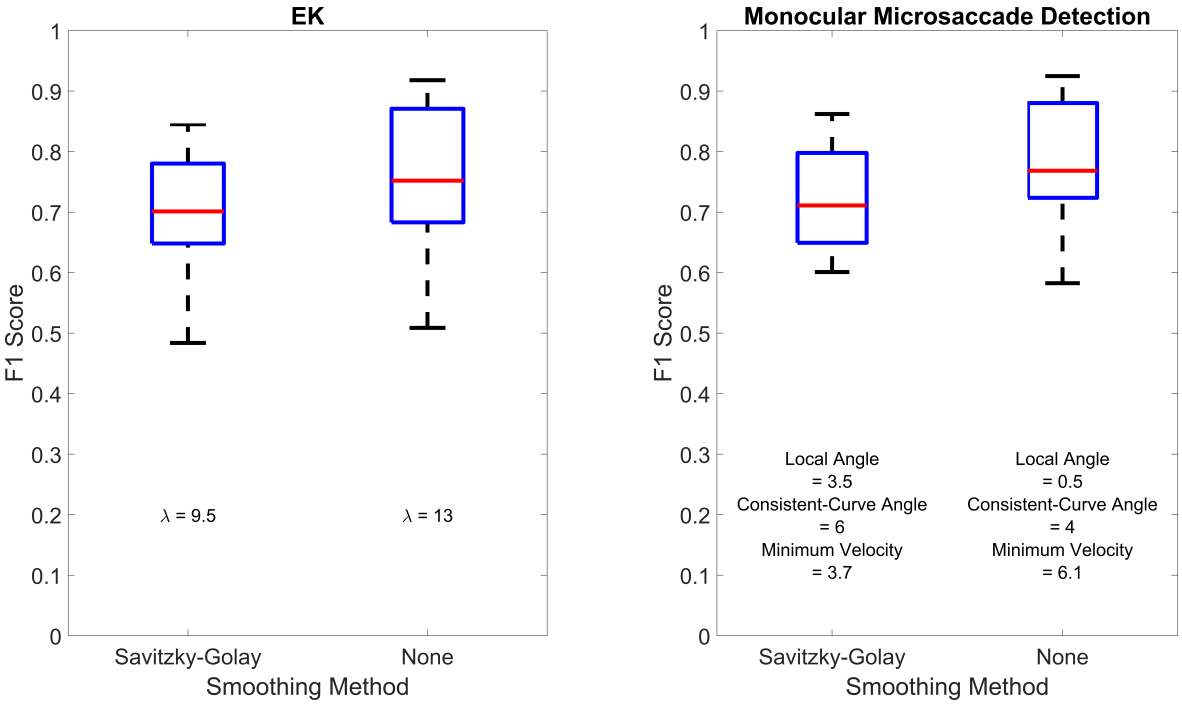


Figure 4.2: Box plots of highest recorded F1 scores for a given detection method and smoothing type.

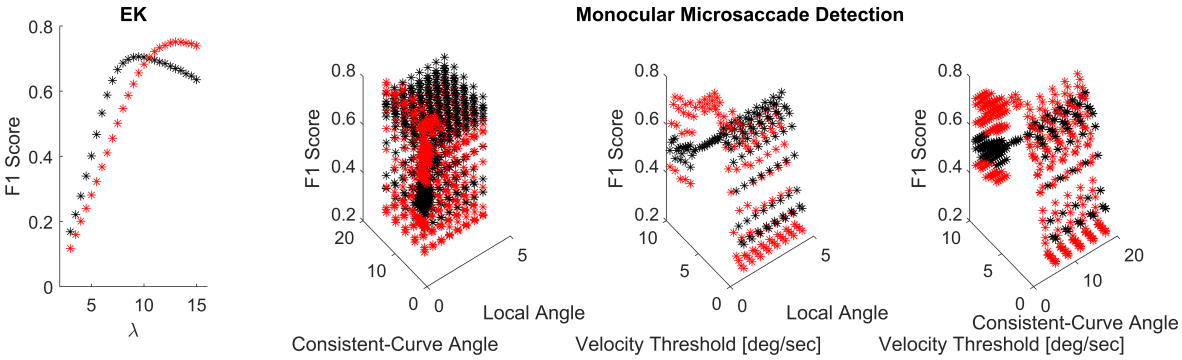


Figure 4.3: Influence of the different parameters on the F1 score. Data points in red belong to the unsmoothed data, while data points in black represent the smoothed data. The leftmost panel shows the different values for λ that were explored. The three panels on the right show the different combination of parameters used in the monocular microsaccade method.

A microsaccade main sequence for participant P3 is shown in Figure 4.4. An example of the raw

and smoothed position and velocity data, as well as the microsaccade detections by the manual coder, the EK method and the monocular detection method can be seen in Figure 4.5. The eye tracking worked particularly well for this participant (P3) (Fig. 4.5 (a)), as almost all microsaccades in the displayed section of the eye movement trace are well captured and not interrupted by tracking failures.

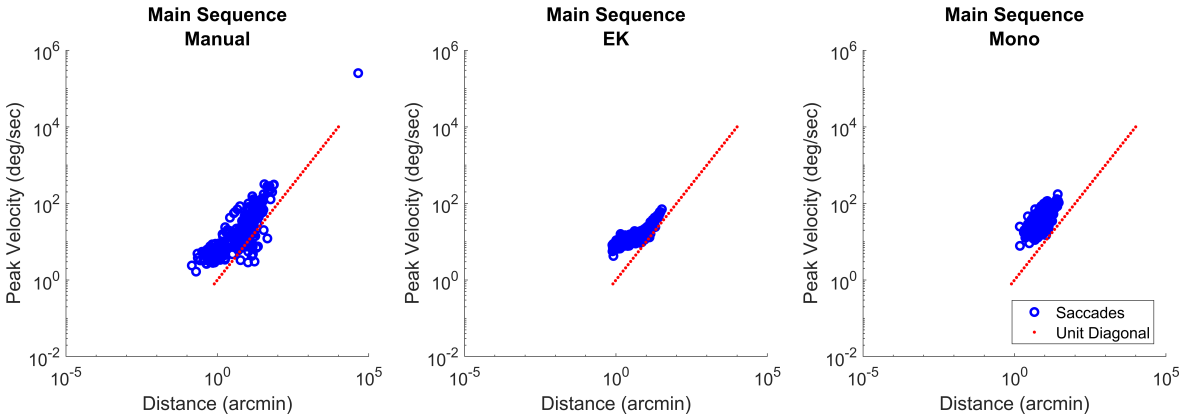


Figure 4.4: Microsaccade main sequences for participant P3. The three panels show the main sequences on (i) the unsmoothed data with manual labels, (ii) the microsaccades detected using the EK method on the smoothed data, and (iii) the microsaccades detected using the monocular detection method on the unsmoothed data.

4.6 Discussion

The monocular microsaccade method is a new way of detecting microsaccades in the type of high resolution eye movement data provided by the Oxford AOSLO. This system has a number of idiosynchasies and the eye movement extraction and microsaccade detection remains under development in the lab. The F1 scores obtained by the monocular microsaccade detection method are promising and suggest that further improvements in both eye movement extraction and this detection method can lead to accurate automatic microsaccade detection in the data available through this eye tracker.

The manually detected microsaccades do not fall perfectly onto the main sequence described in the literature and observed on outputs from other eye trackers and manual microsaccade detections. There are several factors contributing to this. The most important one is that, especially during larger microsaccades, tracking often fails. This has three main consequences. The first one is that microsaccades may be missed by automated detection methods that were detected by the manual coder, leading to a ceiling effect in the achievable F1 scores. The second consequence is that both peak velocity and microsaccade distance may be misrepresented due to the lack of the highest velocity data. A third reason for the unexpected shape of the main sequences lies in

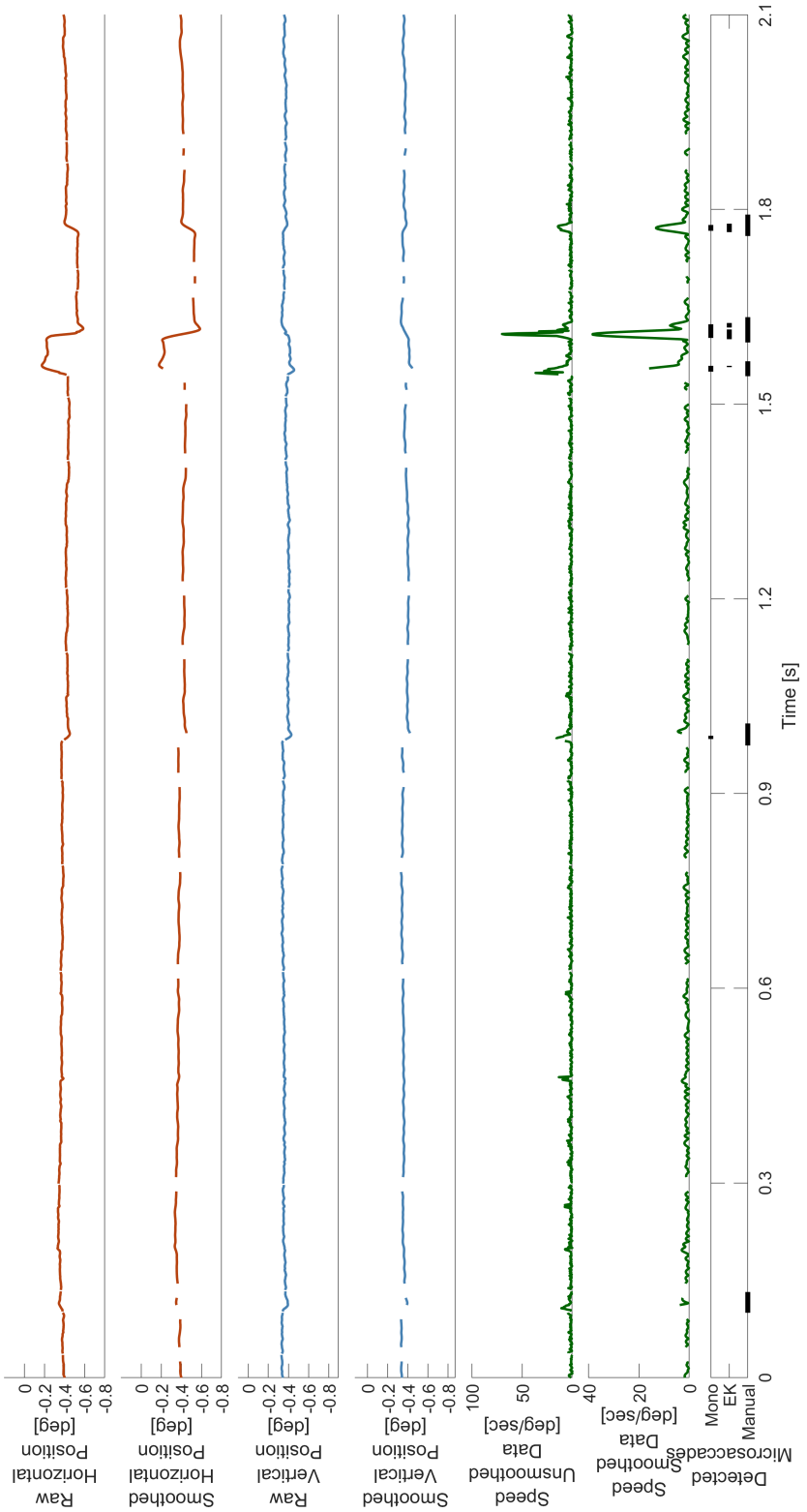


Figure 4.5: Example of microsaccade detection on AOSLO data for participant P3. A time window of just over two seconds is displayed during which several microsaccades occurred.

inconsistencies in microsaccade classification in the presence of tracking failures in the data. As microsaccades were classified before tracking failures were removed, some microsaccades have start and end points which lie at the beginning and end of a tracking failure (which are mostly due to large microsaccades). At the time of classification this problem was known, but it was unclear what the best way of manually classifying these data would be, especially, as sometimes partial

microsaccades are retained before or after tracking failures.

To improve automatic microsaccade detection for AOSLO data, changes to both eye movement extraction and classification are desirable. The manually excluded data, which provides labels for tracking failures, can be used to improve the automatic exclusion of tracking failures by acting as a ground truth to train the exclusion method against. To further improve eye movement classification a stricter formalised procedure should be used in which firstly all tracking failures are excluded (or it is confirmed that the automated exclusion method has worked). Then two separate labels should be used for microsaccades: one for all completely captured saccades and one for partially captured microsaccades. At the level of eye movement extraction it would be beneficial to get a more accurate representation of the flyback regions, as the labelled flybacks do not 100% cover all NaN samples during flyback regions. This leads to gaps in the smoothed data, and therefore may lead to worse microsaccade detection for these data.

By improving data quality and manual labels it should be possible to automatically identify microsaccades in the AOSLO data using the monocular microsaccade detection method, which already shows some promise in detecting microsaccades. Two potential additions could be made to the detection method. The first is to not simply set a velocity threshold for all data samples, but a two-fold threshold: one lower velocity threshold applied to all the data and a second, high threshold, which must be met by at least one sample within a microsaccade. This second threshold is analogous to setting a peak velocity threshold. The second addition could be a test for an acceleration profile. It is known that microsaccades should first accelerate, then cross through a point of no acceleration and then decelerate. The requirement that a microsaccade must contain such a profile could be added. Initially, an acceleration criterion was explored and dropped for the binocular correlation method, as the data were too noisy, however the downsampled AOSLO data contains, compared to most eye trackers, very little noise and thus an acceleration criterion may be worth exploring.

One remaining issue is the question of missing microsaccade segments. This will remain an issue with the AOSLO data for the foreseeable future, as the tracking fails when the movement is so large that the sheering induced by the motion distorts the image of the retina to the extent that it cannot be compared to the reference frame. When studying the nature of microsaccades it may be necessary to exclude those saccades. However, when studying the interaction between microsaccades and blur for keeping the eyes on target, it is essential that these intervals are considered as saccades and not integrated into a drift trace. Irrespective of how the data are to be analysed these instances need to be detected and classified, which is inherently difficult for microsaccade

detection methods that rely on features of the data such as speed, as those key pieces of information are missing from these saccades. In the future it may therefore be worthwhile to explore other microsaccade detection methods which may have the capability to deal better with partially missing microsaccades. One candidate would be the use of neural networks, which can learn to imitate human classification performance. One such network which is available was published by Bellet, Bellet, Nienborg, Hafed and Berens (2019), which claims to be able to achieve human-level performance in saccade detection.

Chapter 5

Fixational Eye Movements and Stimulus Structure

Abstract

It is known that fixational eye movements can provide, potentially epiphenomenal, performance benefits in certain tasks, such as judging the orientation of a grating (Rucci et al., 2007) or preventing peripheral Troxler targets from fading (Martinez-Conde et al., 2006). There have also been many reports that microsaccade frequency or direction can change in response to task instruction and stimuli. However, this interaction between fixational eye movements and the visual stimulus has not been thoroughly explored using modern eye tracking equipment and analysis techniques. Here, two experiments are presented that examine the effect of either presenting a visual stimulus at varying levels of retinal eccentricity or presenting a grating stimulus at different orientations and spatial frequencies. It is found that fixational eye movements become less stable the greater the eccentricity of stimulus presentation, and that the eyes are less stable along the grating compared to perpendicular to it. It is also found that the presence of a fixation helper can offset any influence of peripheral information and stabilise gaze. These findings suggest that microsaccades and drift are both influenced by the visual stimulus and several potential mechanisms for this are discussed.

5.1 The structure of the visual field

Humans have a foveating visual system. This means that there is a marked difference between visual processing in the centre of our visual field and the periphery. The fovea exhibits several

special features, all enabling high resolution daylight vision. There, the spatial resolution of daylight vision is highest, with cones being smaller and more tightly packed than anywhere else in the retina. To maximise spatial sampling and accommodate more photoreceptors the fovea lies in a dip in the retina, called the foveal pit. The relative amounts of different photoreceptors - the three different cone types used during daylight vision and the rods used to see in low-light conditions - vary across the retina. In the fovea there are no rods which we use to see in low light conditions (Hecht, Shlaer & Pirenne, 1942; Osterberg, 1935). Depending mainly on retinal eccentricity distributions of cones and rods vary. Other factors that influence relative densities of rods and cones are age (Panda-Jonas, Jonas & Jakobczyk-Zmija, 1995) and individual factors (Song, Chui, Zhong, Elsner & Burns, 2011). The highest density of rods is found at approximately 20° (Osterberg, 1935). Rods account for approximately 60 million photoreceptors in the human retina, whilst cones make up only around 3 million (Jonas, Schneider & Naumann, 1992). Estimates of these values vary, with Wandell (1995) quoting 5 million cones and 100 million rods and Osterberg (1935) suggesting 110-125 million rods and 6.3-6.8 million cones. These ratios of rods outnumbering cones further highlight the imbalanced distribution of both across the visual field. Differences in cone distribution are also found dependent on retinal eccentricities. There are three different cone types: short, middle and long-wavelength receptors, often abbreviated as S-, M- and L-cones. The M- and L-cones share more evolutionary history than the S-cones (Neitz & Neitz, 2011), which helps to explain these differences. Between 90% and 95% of cones are L- and M-cones, which are distributed in relatively irregular patterns within individuals (Hofer et al., 2005). S-cones, however, are very regularly spaced in the human retina (Hofer et al., 2005). Somewhat surprisingly, there are also no S-cones in the very centre of the fovea - the foveola (Curcio et al., 1991).

The receptive field size of retinal ganglion cells increases with eccentricity (for example, as estimated from dendritic fields of primate midget ganglion cells by Dacey (1993)), and does so for each sub-type of retinal ganglion cell (Field et al., 2010), such that each sub-type provides an efficient tiling of the visual field (Gauthier et al., 2009). The local density or spacing of adjacent receptive fields is important for understanding spatial sampling. The dependence on eccentricity is sufficiently ordered and predictable that it is possible to summarize in a predictive equation (Watson, 2014). Furthermore, this eccentricity dependence is additionally shown in cortical receptive field sizes (for example, as estimated with neuroimaging techniques to recover a model of the population receptive field by Dumoulin and Wandell, (2008)). These are some of the driving factors for a phenomenon called cortical scaling (Cowey & Rolls, 1974): more cortical area is assigned to the centre of vision than the periphery. From these structural differences between central and

peripheral vision alone it is clear that there are likely to be fundamental differences in the use of the central and peripheral retina for vision. This knowledge should be taken into account when considering oculomotor behaviour in response to different stimuli, as their spatial structure will interact with our retinal structure.

The periphery also differs from the fovea in visual task performance, which can be explained by the physiological differences between the two. For tasks requiring high acuity, the fovea always performs better than the periphery (e.g. grating acuity, vernier acuity (De Valois & De Valois, 1991), reading and matching letters (Yu, Legge, Wagoner & Chung, 2018; Williams & Lefton, 1981)). However, the rate at which visual task performance drops off is not equal across all tasks. Movement perception, for example, is known for its relatively slow drop-off in the periphery (Tynan & Sekuler, 1982), probably as a result of the evolutionary need to be vigilant of motion in the periphery. However, claims about the special status of motion in the peripheral retina are often exaggerated (for a detailed discussion see Finlay, 1982). Centrally fixated targets tend to be stationary, and if they are not, their motion is usually not their feature of interest, but something to be compensated using smooth pursuit eye movements, for which fading is not an issue due to the minute discrepancies between the target movement and the following response of the eyes. Rather, movement retains its importance in the periphery: optic flow is used to estimate relative positions when walking, while the movement of individual features in the environment can signal approaching predators, or friendly parties. Similarly, an advantage for flicker perception has also been shown in the periphery (Hartmann, Lachenmayr & Brettel, 1979).

However, it is often hard to make direct comparisons between foveal and peripheral vision, as tasks can rarely be matched completely for different retinal locations. Therefore, it is central to evaluations of visual task performance to consider whether or not and to what extent physiological differences between the centre and periphery of vision were taken into account.

5.2 The periphery and fixation

In almost all everyday tasks and psychophysical visual experiments peripheral information is available and might contribute to fixational stability and behaviour. However, little is known about how the peripheral retina contributes to fixation behaviour. In the majority of psychophysical experiments measuring eye movements it is simply assumed that the central fixation stimuli are the only relevant pieces of information that may influence fixation behaviour. Previous studies have found that task-irrelevant (Galfano et al., 2004) and spurious targets (Deaner & Platt, 2003) can bias eye movements, suggesting that peripheral visual information does contribute to fixation

behaviour. Yet there has been no in-depth analysis of whether peripheral information alone is sufficient to stabilise gaze, and how such stabilisation may differ from that achieved via central targets, as well as biases exhibited when central and peripheral targets are present.

In patients with central vision loss the periphery is the only available source of visual information. Fixational stability is often poor after the loss of foveal vision (Midena et al., 2004) and specific training is often used to build a new preferred retinal locus for fixation (Déruaz et al., 2006). This provides evidence that visual feedback is important for maintaining fixation, and that the periphery can be used to stabilise gaze, even if this is less effective than when the central retina is used.

5.3 Factors influencing fixational stability

Factors that might be of interest in this context are the eccentricity and spatial structure of targets. The eccentricity of the target is of interest, as this property may shed light on whether or not fixation stability based on peripheral information also follows a type of M-scaling. M-scaling can be used to scale stimulus properties according to a function describing the changes in anatomy, physiology or performance according to eccentricity. One common target function for M-scaling is the cortical magnification factor for which various equations have been proposed (e.g. Rovamo & Virsu, 1979). There are a number of other possible scaling factors which could be used to M-scale a stimulus, for example (i) Ricco's area which is a psychophysical measure of summation area for threshold targets as a function of eccentricity (e.g. Rovamo & Raninen, 1984) and (ii) size thresholds for letter identification, which increase rapidly with greater eccentricity (e.g. Klein, Berry, Briand, D'Entremont & Farmer, 1990). Some form of M-scaling would be expected because of the characteristic physiological and psychophysical changes from the fovea to the periphery if visual information is used to stabilise the eyes. Target patterns may also be of interest, as it should be expected that, if fixational eye movements are in any way influenced by the stimulus, they should exhibit different motion patterns depending on spatial anisotropy in the target. For example, eye movement differences may be expected when viewing horizontal compared to vertical gratings. This is because movement in the direction of the grating will result in less signal that the stimulus has changed, compared to movement perpendicular to the grating component (see Fig. 5.1).

There are two hypotheses we aim to test:

1. A visual target presented closer to the fovea will have a greater influence on fixational stability. We would expect this, as the aim of fixation, generally speaking, is to retain alignment of the visual axis with the visual target. Both spatial and temporal sensitivity are higher in the fovea, therefore, potentially providing stronger signals of change.

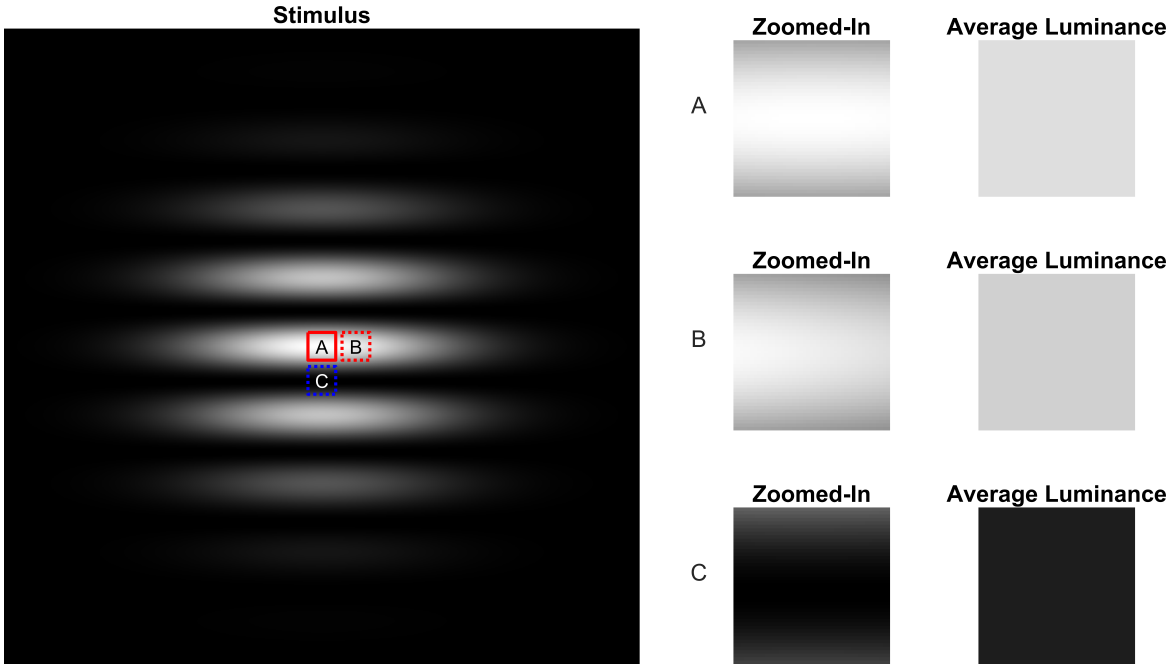


Figure 5.1: This figure shows examples of 7 pixels of horizontal/vertical movement across a horizontally aligned grating. Movement perpendicular to the grating (A to C) results in much grater luminance changes for the same amount of motion compared to motion along the grating (A to B).

2. A visual target with a grating component should bias eye movements in the direction of the grating. This is because there is less information about a possible position change when moving along a grating than perpendicular to it.

5.4 Assessing fixational stability

Being able to successfully separate an eye movement trace into its microsaccade and drift components is only the first step in quantitatively analysing fixation behaviour. Having access to information regarding the microsaccades and drifts in an eye trace leads to the question: which metrics are important in assessing eye stability? Which metrics should be examined in greater detail to extract important differences between different conditions?

These metrics can be divided into those applicable to (i) microsaccades, (ii) drift or (iii) the eye movement trace as a whole. To compare microsaccades between different conditions it is useful to compare their overall frequency, as it is known that microsaccade frequency can change drastically under different task instructions, a feature which may extend to different fixation stimuli as well. Similarly one feature out of peak velocity, duration or distance should also be examined. As the three are closely related due to the main sequence relationship it may be assumed that only one is necessary to analyse as any trends should be borne out in a similar pattern in the other two. For the purposes of the following experiments only microsaccade distance will be considered, as this is most easily related to the visual stimulus. Microsaccade direction is also of interest, as it

is known that it is naturally biased along the horizontal (e.g. Hermens & Walker, 2010) and can change in relation to peripheral targets (Hermens & Walker, 2010), and as such may exhibit changes in response to stimuli in any chosen task.

For drift many of the same features as for microsaccades are relevant, however some for different reasons. Drift distance is of interest, as it quantifies the total displacement of the retinal image due to drift and should therefore be included. Duration is often not discussed, with microsaccade frequency, being a related and more prominent value. However, peak velocity during drifts, at least for data derived from video-based eye trackers is of little interest, as it is highly influenced by noise in the system and the inability to record tremor. Moreover, to the best of our knowledge, drift peak velocity is not important beyond separating it from microsaccades (or, perhaps, when trying to investigate differences between drift and slow control). Drift direction should also be examined, as there are reports of drift being biased by the target (St. Cyr & Fender, 1969) and a moving background grating (Murphy et al., 1975), and thus may indicate that drift is susceptible to differences between tasks.

Measures applicable to the whole eye trace are generally measures of spread. Several different methods have been used historically to quantify this and each method highlights slightly different aspects of fixation behaviour. At the most simple level is the interquartile range (IQR). The IQR simple gives a measure of the statistical dispersion of the data relative to the median. The root mean square (RMS) error is similar in nature to the IQR, however it has the advantage that it allows for errors to be calculated in relation to any given point, e.g. the first sample, mean or median of the data, or the centre of the stimulus (see Eq. 5.1). Which of these references is most appropriate is at the discretion of the experimenter, but, for example comparing fixational errors to the centre of the target necessitates great trust in the accuracy of the eye tracker. Equally, determining that the first position is in fact the position of the target is making a substantial assumption about the abilities of the observer. Lastly there are two measures of the total area covered by the eye movements. Firstly, the bivariate contour ellipse area (BCEA) and secondly the isoline area (ISOA) (Castet & Crossland, 2012). The BCEA is a measure relying on the eye position data following a Gaussian distribution, which can not normally be guaranteed. Because of this uncertainty it is desirable to use an ISOA, which fits an irregular outline to the positions. Both area measures give an idea of the size of the area needed to cover a set percentage of position samples, usually taken to be 68%.

$$RMS = \sqrt{\frac{\sum (data - reference)^2}{number\ of\ data\ points}} \tag{5.1}$$

Another issue for establishing parameters for fixational eye movements is the problem of blinks

and missing data. In some tasks trials can be too long to ask participants to suppress blinks. When a blink occurs most eye trackers have a way of labelling the relevant interval as missing data so it can be excluded during post-processing of the data. It is also customary to exclude some samples before and after each blink, as most eye trackers can suffer from artefacts induced by a blink such as a partially occluded pupil (video-based eye trackers), slippage of the contact lens (contact-lens mirror and scleral coil eye-trackers) or spikes in electric activity from muscles (EOGs). Often it is not possible to automatically determine if a missing stretch of data is due to a tracking failure or a blink. Therefore exclusion of samples around missing data caused by tracking failures inflates the number of samples that can not be used for meaningful analyses. Moreover, these missing data raise the question of how to handle missing samples when talking about the frequency of visuo-motor events like microsaccades. One can either calculate rate referring to the time the data were being recorded for, i.e. trial length, ignoring missing data, or accounting for it. There is no correct answer to which of the two is best, however, it is best to ascertain that there is no difference in the missing data for different conditions to rule out an effect on the overall direction of the results.

Two experiments were conducted. Experiment One focussed on the difference in fixation of central vs. peripheral Gaussian targets. Experiment Two examined the influence of gratings of different orientations and spatial frequencies. A detailed account of the experimental set up is given for Experiment One, while for Experiment Two only those aspects that were changed are highlighted.

5.5 Experiment One: Eccentricity

The first experiment in this chapter aims to establish the importance of eccentric information for visual stability and address the first hypothesis formulated earlier. Eye traces were collected while peripheral information was displayed either with or without a central fixation target. It would be expected that peripheral information is less good at keeping the eyes stable, the further from fixation the information is presented. Also it may be expected that the presence of a central target additionally to the peripheral information would increase stability. If there is an influence of peripheral information even when a central target is present, this may have implications for how visual set-ups should be configured when investigating eye movements.

5.5.1 Methods

Participants

Participants gave informed consent and the experiment was conducted in accordance with the University of Oxford's ethical review process (CUREC Approval Reference: R62306/RE001). A total of 29 participants' data were recorded for this experiment. Of these, two participants were excluded from further analysis as only one eye had been trackable for the experiment. A further 8 participants were excluded post data-collection as their data did not meet the criteria for inclusion described below.

Setup

Stimuli were displayed on a gamma corrected Display++ (Cambridge Research Systems) in 10 bit resolution. The display was placed 175cm from the participant, therefore subtending a vertical extent of 12.8° and a horizontal extent of 17.3 ° . Stimuli were generated in MATLAB and presented using ViSaGe++.

An Eyelink1000 (SR Research) was used to record eye movements binocularly at 1000 Hz. It was used in its desktop-mount configuration with a 35 mm lens at a distance of 50 cm. Standard calibration and validation procedures were followed. At the beginning of each recording block the eye tracker was calibrated and only calibrations in which at least one eye was labelled as *good* and neither eye was labelled *bad* were accepted.

The visual environment of the testing room was made as dark as possible, so that the visual stimulus could be perceived in isolation. For this, a dark tablecloth was used to cover the surfaces immediately in front of the participants and all status lights from keyboards and electronic devices were covered. This was sufficient for some subjects to, without being prompted, report the autokinetic effect, i.e. illusory motion of targets in space, which is expected in a completely dark environment (Schweizer, 1857). This is reassuring, as the Display++ is a backlit monitor, however the presence of illusory motion indicates that any light coming from the display is not interfering significantly with the overall impression of darkness in the room and isolation of the fixation target from any other visual frame of reference.

Stimuli

The basic stimulus for this task was a simple Gaussian blob with a standard deviation of 0.1° and maximum luminance contrast (minimum screen value: 0.129 cd/m^2, maximum value 91.04 cd/m^2, measured using a Cambridge Research Systems SpectroCAL). A small target is desirable, as it closely

mirrors most targets in use in fixation tasks (Thaler et al., 2013). Moreover, small targets ensure that the target borders, which may be important for fixational stability do not fall far from the eccentricity at which the centre of the target is displayed. Thus ensuring that a centrally presented target actually elicits a behavioural response relevant to the centre of the fovea, as opposed to a response of a more peripheral area and vice versa for more peripheral targets. At the same time it is also important that the stimulus does not contain spatial frequencies that are so high as to be detected more efficiently in the centre of the fovea compared to the peripheral retina. Before stimulus presentation it was therefore checked that the majority of the power in the stimulus was carried in spatial frequencies between 0 and 8 cycles per degree (c.p.d.) (see Fig. 5.2) as previous research (Rovamo, Virsu & Näsänen, 1978) suggests that those frequencies should be visible at all eccentricities the stimuli were presented at.

These Gaussian shapes were presented at three different eccentricities. When presented foveally (0°) a single Gaussian target was presented. At 3° and 5° two Gaussian shapes were presented in horizontal alignment, each at the relevant eccentricity from the fovea.

Procedure

The task took a total of 1 h and was divided into 5 recording blocks. In each block there were twelve 30 s trials separated by 7 s breaks (for a graphic description, see Fig. 5.3). Two beeps during the last second of the break indicated to the participant that the trial was about to begin. Before recording, participants were instructed to always look in the centre of the whole stimulus, meaning either the centre of the central stimulus or the middle between the two peripheral stimuli. To avoid participants always directing their gaze at the same position the centre of the stimuli was decided randomly for each trial out of a combination of 3 horizontal and 3 vertical positions (-1° , 0° or +1° from centre). Each trial was divided into two equal 15 s periods. In one period a central fixation helper (a 2x2 px (pixel) dot) indicated where the participant was supposed to be looking, in the other interval this helper was absent. Within each recording block the same number of trial combinations with regards to stimulus eccentricity and dot order was presented, but the order was shuffled for each block.

Data Analysis

The data were first smoothed using a Savitzky-Golay filter (order: 3, framelength: 21 ms) and blinks, as well as 200 ms before and 300 ms after each blink, were removed to prevent recording artefacts caused by a partially occluded pupil to influence the analysis. The first 1.7 s were also excluded

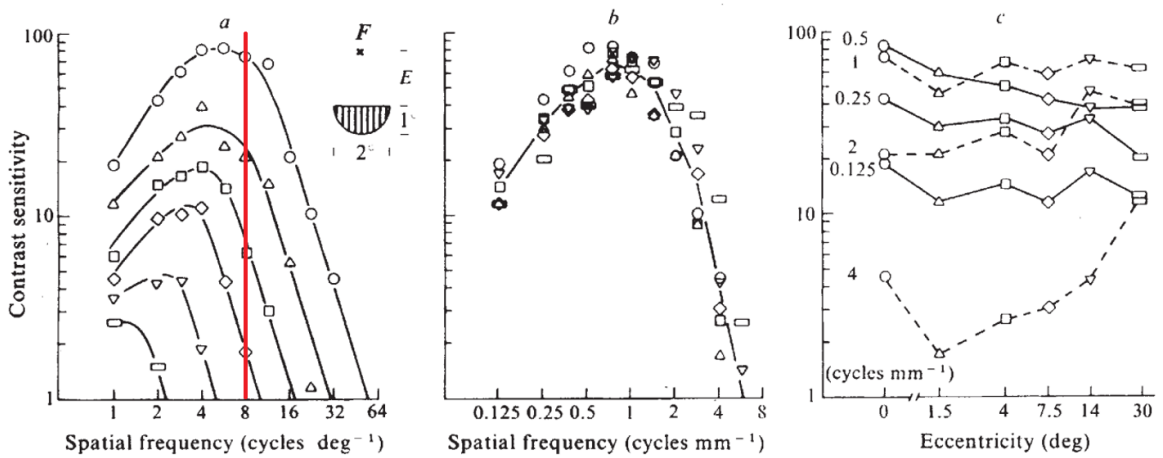
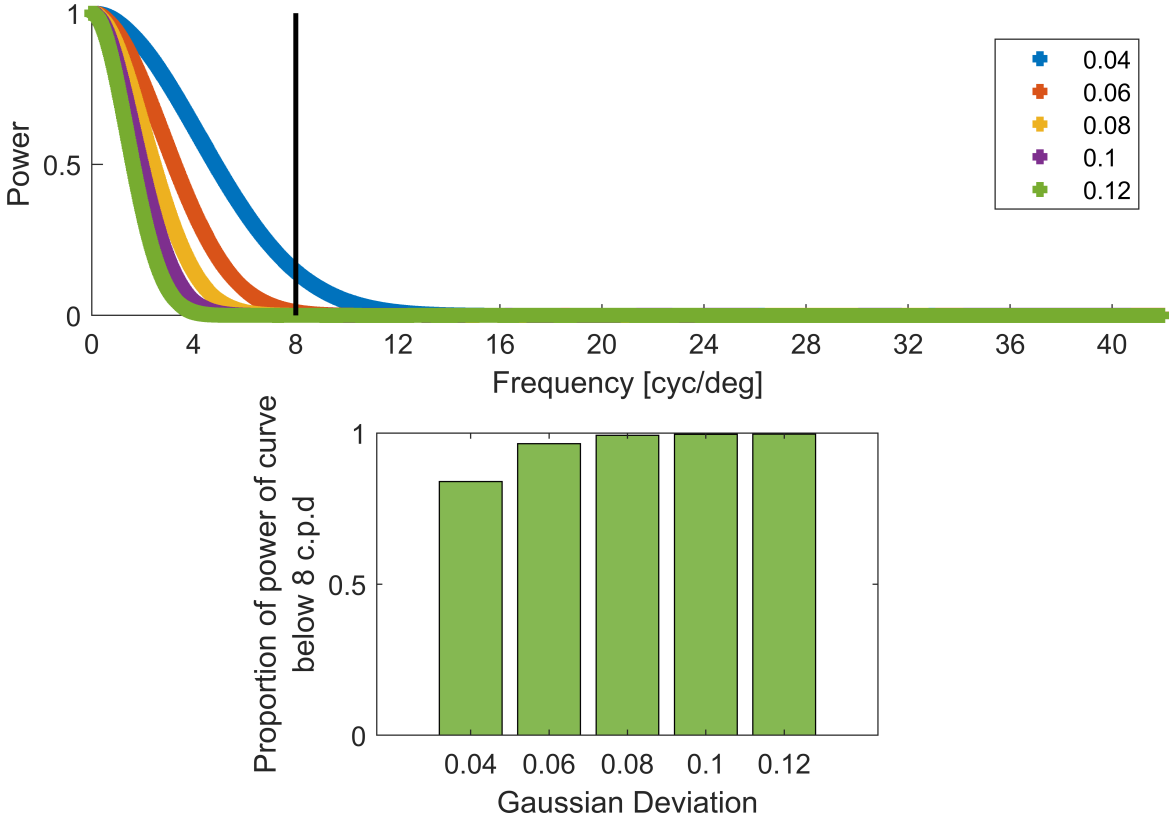


Fig. 1 Contrast sensitivity as a function of spatial frequency and eccentricity (E) in the lower visual field. *a*, The retinal images of various sinusoidal test gratings were similar at different eccentricities as shown in the inset. Spatial frequency indicates the bar density of gratings in cycles per degree of visual angle and eccentricity refers to the angular distance between the fixation point (F) and the nearest edge of the semicircular vertical grating. Curves represent values of E as follows: ○, 0°; △, 1.5°; □, 4°; ◇, 7.5°; ▽, 14°; ■, 30°. *b*, Cortical projections of the test gratings were similar at different locations. The symbols are as in *a* regarding eccentricity in the visual field. Spatial frequency indicates the estimated bar density in cycles per mm on the primary visual cortex. *c*, Part of the data of *b* replotted to reveal the expected improvement of sensitivity as a function of E at high cortical spatial frequencies.

(a) Contrast sensitivity functions depending on target eccentricity (Adapted from (Rovamo et al., 1978). The red stripe indicates 8c.p.d. below which the majority of spatial frequencies in the stimuli used for this experiment fell.



(b) Example of spatial frequencies contained in Gaussian patches dependent on standard deviation of the Gaussian.

Figure 5.2: Information based on which the deviation of the Gaussian target was chosen.

from further analysis, as during this time the participants located the new target centre, which was randomly chosen for each trial, leading to greater instability. Also during this time, the known effect of microsaccadic suppression following stimulus onset would have occurred. Then microsaccades and drifts were separated using the binocular microsaccade detection method described in Chapter 3. Here the binocular correlation method with a fixed speed correlation threshold ρ was used. The

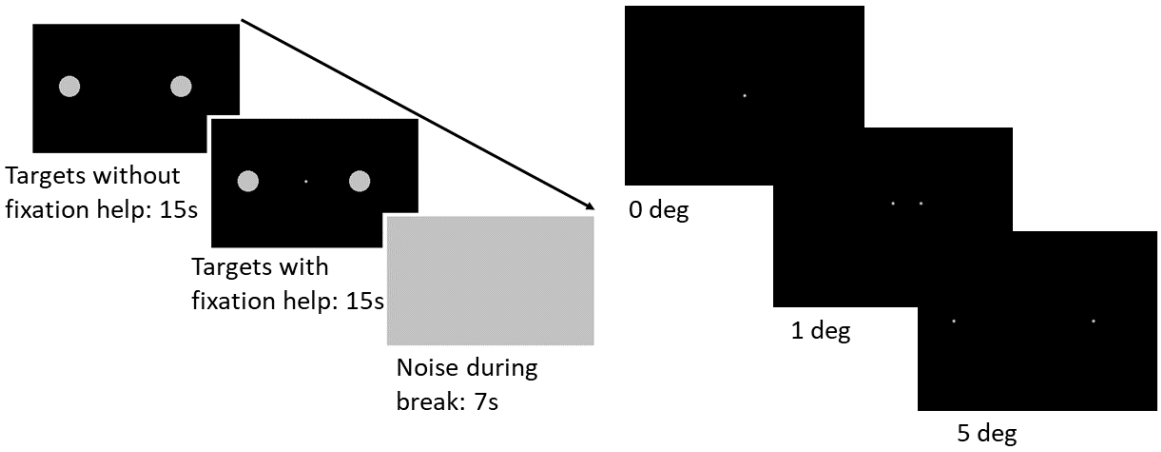


Figure 5.3: This figure shows the trial sequence of events schematically on the left side. On the right the stimuli are shown in relation to the monitor size.

correlation window size was set to 65 ms and the parameter ρ was set to .45 R^2.

Next trial intervals for which more than 50% of data are missing (due to blinks, exclusion around blinks or tracking failures) are excluded, as well as those trials in which the difference in missing data from the left and right eye exceeds 2% of the whole trial. In the final data analysis only those participants for whom more than 66% of trials were accepted were included.

The data were then prepared for statistical analysis. For all dependent variables (microsaccade frequency, microsaccade distance, amount of missing data, RMS to median, difference in fixation position when fixation helper was present compared to when absent) a mean value was calculated for each participant which was then used in further significance testing. If no trials were excluded then a total of 45 trials would contribute to each value for each participant. These data were then analysed using two-way repeated measures ANOVAs with the independent variables of eccentricity (0° , 1° , 5°) and presence of fixation helper (present, absent). No analysis was undertaken to estimate if the order of fixation helper presentation had an effect, as trials were counterbalanced and this did not form part of a hypothesis that was being tested. As a precaution it was tested if there was a significantly different amount of time missing between the different conditions. If this were the case, subsequent analyses may have been biased by differing amounts of data between the groups.

For all hypothesis-driven statistical questions the dependent variables of RMS to the median of fixation, as well as microsaccade distance and frequency were analysed. In a separate one-way repeated-measures ANOVA the difference in the median of the fixation position while the fixation helper was present compared to when it was absent was examined. All data that were subjected to ANOVAs were first tested for normality using Kolmogorov-Smirnov tests. If the data were not normally distributed a log10 transform was applied, as in most cases the data had a strong right

skew, because the values could only be positive, like distance or duration. It was then confirmed that this transform achieved a data distribution not significantly different from normality. In the results section data are clearly labelled if statistical tests were conducted on the transformed data. Appropriate follow-up tests on the significant effects were conducted. If these were undertaken Cohen's d is given as the difference of the means divided by the standard deviation of the all values.

The time course of the RMS error was also explored by calculating the RMS to the median for each 500 ms section of the trial. This was done in two separate ways: one local and one global. For the local RMS error over time each 500 ms section was compared to the median of fixation within the same time period. For the global RMS error over time the 500 ms section was compared to the median within the same trial interval (i.e. while the fixation helper was present/absent). Examining the RMS error over time can identify if differences in fixational stability arise over time, or whether they are present from the outset.

5.5.2 Results

Participant Exclusion

Post-exclusion 19 participants were eligible for inclusion in further analysis, for exact proportions of usable trials, please refer to Fig. 5.4.

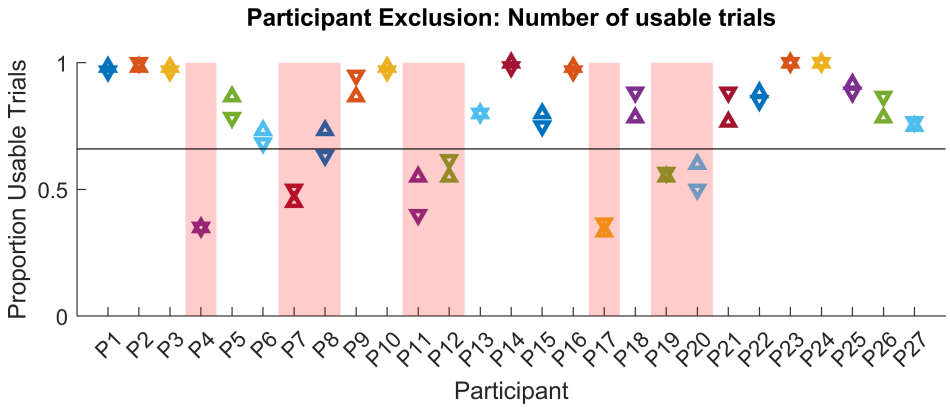


Figure 5.4: Figure showing the exclusion of participants based on missing data. The upward pointing triangle for each participant represents the proportion of usable trial intervals when the fixation helper was present while the downward pointing triangle represents the proportion of usable trial intervals when the fixation helper was absent. All participants who have at least one point that lies below the reference line were excluded and are shown shaded in red.

Missing Data

The first analysis undertaken on the data was a two-way repeated-measures ANOVA to identify if the number of missing data samples were evenly distributed between the different conditions. For this the number of missing samples within a trial were averaged for all 45 trials in that condition.

No main effect or interaction effect reached significance in this analysis (see Fig. 5.5).

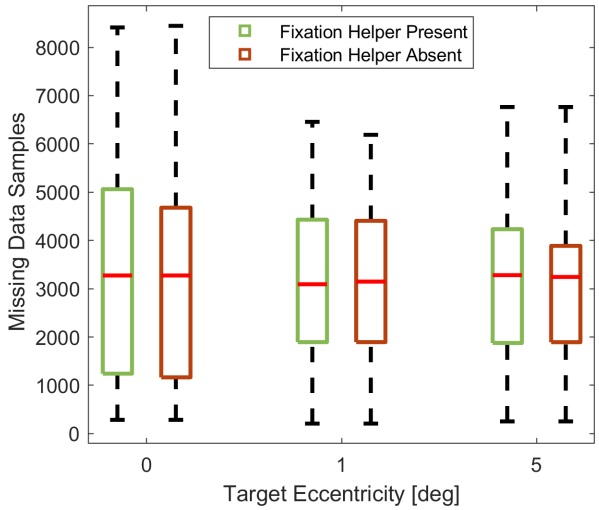


Figure 5.5: Box plot of number of missing data for each experimental condition.

RMS over Time

The change in RMS error over time was investigated. Two ways of calculating this value were used. Firstly, the local RMS error within a 500 ms time period was calculated. This gives an estimate of short term fixational stability. The change in this measure can be see in Figure 5.6. The second measure is a global RMS error where the reference point is not the median within the 500 ms, but rather the median of the whole trial interval. The results for this can be see in Figure 5.7. In both figures the red shading indicates data excluded at the beginning of the trial from all other analyses. It is during this excluded time that participants have a higher RMS value. The local RMS error within a 500 ms time period is consistently lower than the corresponding RMS error to the global trial median. Also, the RMS values during the excluded time period at the beginning, appear larger when the fixation helper is absent, compared to when it is present. For the global RMS values no difference between the three target eccentricities is obvious when the fixation helper is present. When the fixation helper is absent is does appear that for the majority of the trial the RMS error of the most central target is lowest, followed by the targets displayed at 1° and lastly the targets displayed at 5° . There also seems to be no systematic deviation from the median position, once the final fixation location has been reached. For the local RMS values there appears to be no consistent trend depending on target eccentricity.

RMS to Median

The two-way ANOVA for the RMS error relative to the median of fixation was conducted on the data after a logarithm of base 10 was applied, as the raw data failed the assumption of normality

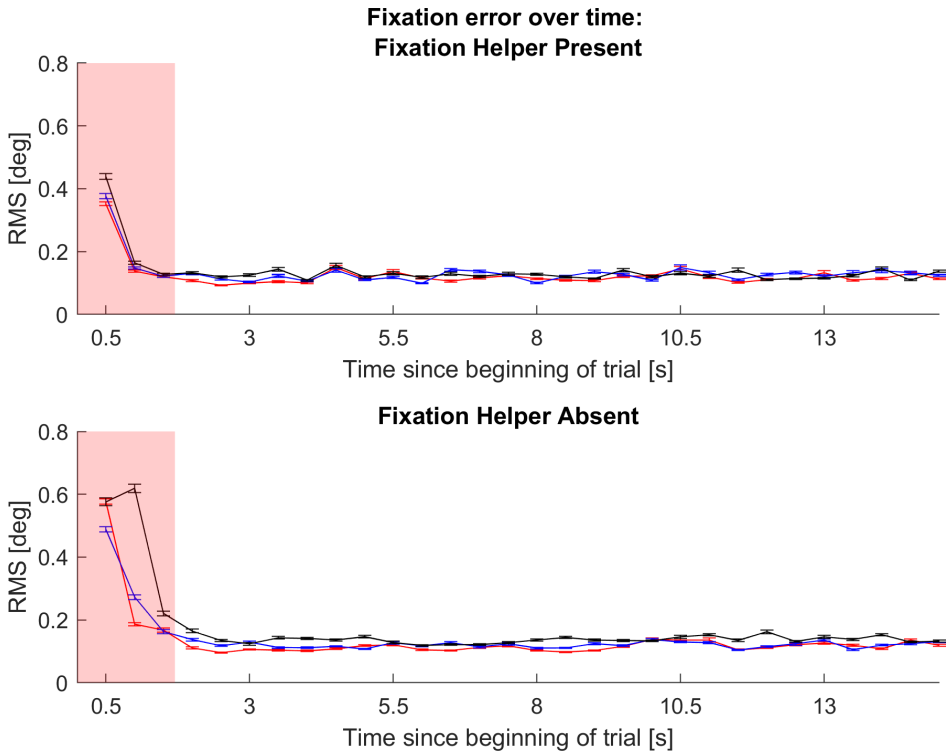


Figure 5.6: This plot shows the temporal progression of the local RMS error. The top panel shows the RMS error for the 15s of the trial when the fixation helper was present and the bottom panel for when it was absent. RMS values are averaged over 500 ms relative to the median of the same time period. Error bars represent the standard error of the mean. The red shading indicates the beginning of the trial, which was excluded from all other analyses. The red line represents the RMS error over time when the target was presented centrally, the blue line refers to targets presented at 1° , while the black line indicates targets presented at 5° .

due to its rightward skew. This RMS error is represented by a single average for each trial, which is then averaged within the same condition for the same participant. This ANOVA revealed significant main effects of eccentricity ($F(2,36) = 17.656$, $p < .001$, $\eta^2 = .495$), presence of fixation helper ($F(1,18) = 18.481$, $p < .001$, $\eta^2 = .507$), and an interaction effect of the two ($F(2,36) = 7.088$, $p = .003$, $\eta^2 = .283$). For a graphical representation of these results please refer to Figure 5.8. In the figure the effect across participants can be seen on the left, while the effect within participants (calculated by demeaning each participant's data) can be seen on the right.

Further analysis of the main effect of eccentricity using paired t-tests between all conditions (0° and 1°, 1° and 5°, and 5° and 0°) revealed significant differences between 0° (M = 0.381, SD = 0.135) and 1° (M = 0.402, SD = 0.150)($t(37) = -2.065$, $p = .046$, $d = 0.146$), as well as between 1° and 5° (M = 0.464, SD = 0.196)($t(37) = -3.585$, $p = .001$, $d = 0.354$) and between 0° and 5° ($t(37) = -4.114$, $p < .001$, $d = 0.482$). These follow up t-tests can be run without correction for multiple comparisons, as the main effect in the two-way ANOVA was significant (Cardinal & Aitken, 2006).

The interaction effect between target eccentricity and presence of a fixation helper was further explored using two one-way ANOVAs in an analysis of simple effects. The one-way ANOVA on data with a fixation helper present showed no significant difference between the different eccentricities

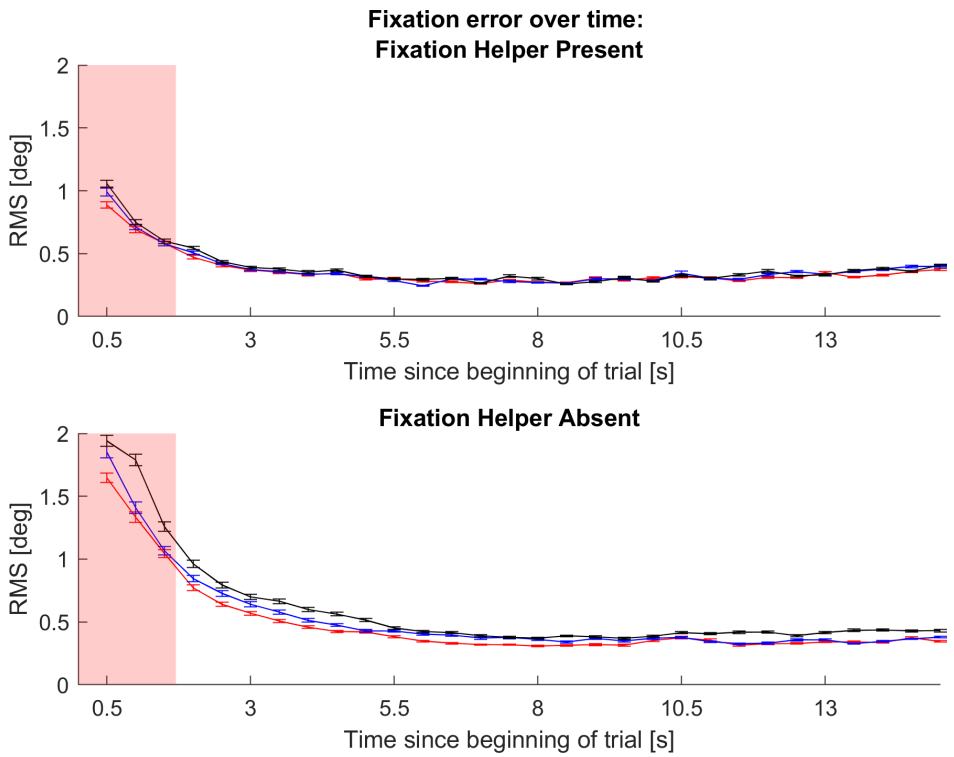


Figure 5.7: This plot shows the temporal progression of the global RMS error. The top panel shows the RMS error for the 15s of the trial when the fixation helper was present and the bottom panel for when it was absent. RMS values are averaged over 500 ms relative to the median of the trial. Error bars represent the standard error of the mean. The red shading indicates the beginning of the trial, which was excluded from all other analyses. The red line represents the RMS error over time when the target was presented centrally, the blue line refers to targets presented at 1° , while the black line indicates targets presented at 5° .

($F(2,36) = 2.074$, $p = .140$, $\eta^2 = .103$). The second one-way ANOVA on the RMS values for the times when no fixation helper was shown showed a significant main effect of eccentricity ($F(2,36) = 8.734$, $p = .002$, $\eta^2 = .507$). When followed up by paired t-tests there was no significant difference between targets displayed centrally (M = 0.390, SD = 0.143) compared to 1° (M = 0.410, SD = 0.137) ($t(18)$ = -0.433, $p = .169$). A significant difference was found between targets displayed at 1° and those displayed at 5° (M = 0.524, SD = 0.210) ($t(18)$ = -4.261, $p < .001$, $d = 0.618$), as well as between targets displayed at 0° and those displayed at 5° ($t(18)$ = -4.101, $p = .001$, $d = 0.707$).

Microsaccade Distance

A logarithm to base 10 was applied to the dependent variable of microsaccade distance before analysis, as the data were skewed to the right and the normality criterion was not met. Analysis of the transformed data revealed significant main effects of eccentricity ($F(2,36) = 31.965$, $p < .001$, η^2 = .640), presence of the fixation helper ($F(1,18) = 93.970$, $p < .001$, $\eta^2 = .839$), as well as a significant interaction effect between the two ($F(2,36) = 10.949$, $p = .002$, $\eta^2 = .378$).

Further analysis of the main effect of eccentricity on microsaccade distance showed a significant difference between the 0° (M = -0.493, SD = 0.192) and 1° microsaccade distances (M = -0.437, SD =

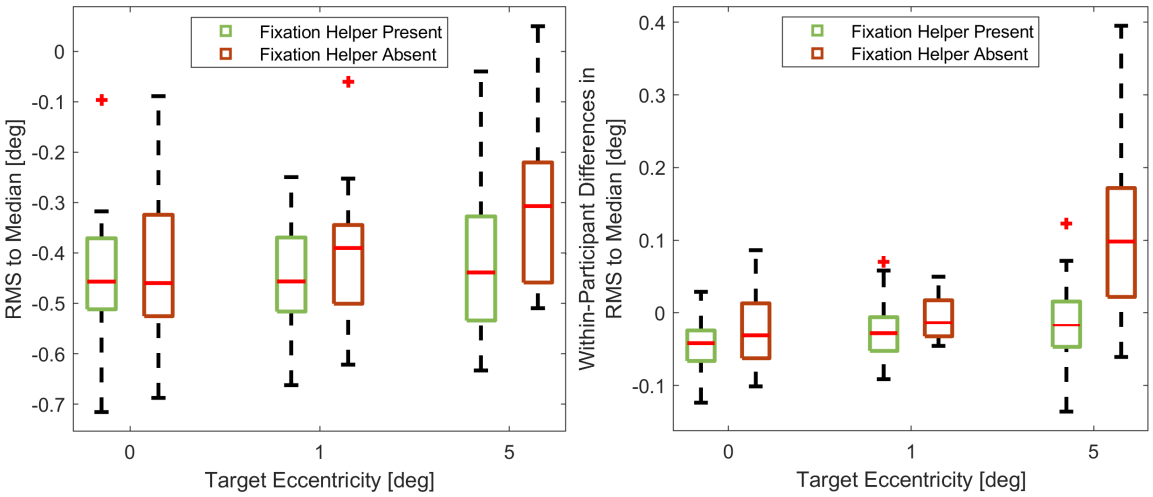


Figure 5.8: Box plots of RMS error to the median of fixation for all ANOVA conditions. On the right hand side the effects across participants are shown, while on the left the within-participant differences are displayed.

0.191) ($t(37)$ = -2.554, p = .045, d = 0.291). The microsaccade distance in the 5° (M = -0.311, SD = 0.268) condition was significantly larger compared to the 0° condition ($t(37)$ = -5.080, p < .001, d = 0.732) and the 1° condition ($t(37)$ = -4.830, p < .001, d = 0.528) (see Fig. 5.9).

Investigating the interaction effect between target eccentricity and presence of fixation helper for microsaccade distances with a one-way ANOVA with the independent variable of target eccentricity while a fixation helper was present revealed no significant main effect of eccentricity ($F(2,36)$ = 1.359, p = .284, η^2 = .138).

The second follow-up one-way ANOVA for microsaccade distances when comparing different eccentricities while the fixation helper was absent was significant ($F(2,36)$ = 35.566, p < .001, η^2 = .807). Follow-up t-tests on this data showed significant differences between all combinations. Microsaccade distances for targets presented centrally (M = -0.454, SD = 0.212) were significantly different from those for targets presented at 1° (M = -0.330, SD = 0.155) ($t(18)$ = -3.931, p = .001, d = 0.643), as well as from those targets presented at 5° (M = -0.148, SD = 0.185) ($t(18)$ = -7.954, p < .001, d = 0.947). The difference in microsaccade distances was also significant between targets presented a 1° and 5° ($t(18)$ = -7.397, p < .001, d = 1.224).

Microsaccade Frequency

No significant main effect of fixation helper presence ($F(1,18)$ = 3.156, p = .093, η^2 = .149) was found in a repeated measures two-way ANOVA on microsaccade frequency. The main effect of eccentricity reached significance ($F(2,36)$ = 3.156, p = .093, η^2 = .149), as well as an interaction effect between the target eccentricity and presence of a fixation helper ($F(2,36)$ = 5.837, p = .012, η^2 = .407) (see Fig. 5.10).

Follow-up t-tests on the main effect of eccentricity on microsaccade frequency showed signific-

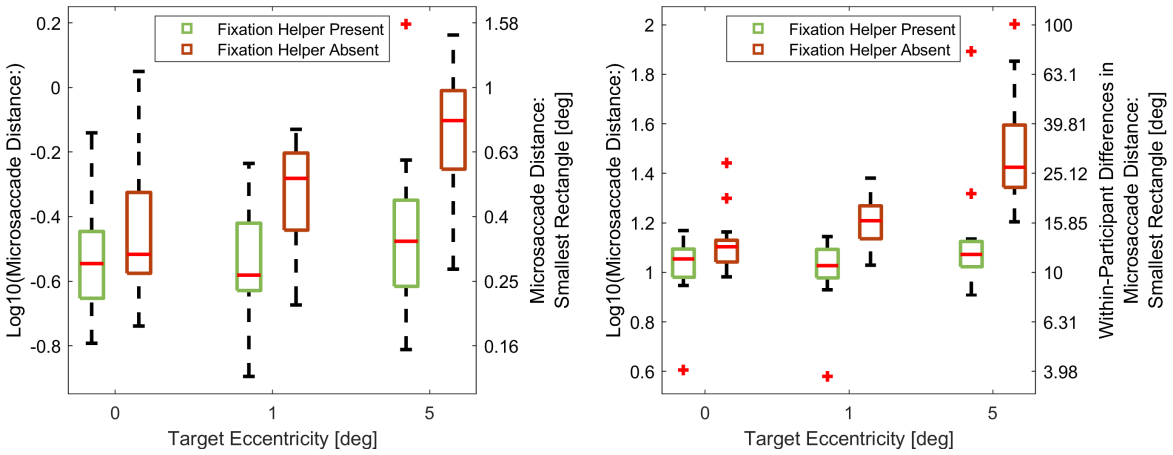


Figure 5.9: Box plot of microsaccade distances for the different experimental conditions. On the right hand side the effects across participants are shown, while on the left the within-participant differences are displayed. The scale is in log format, with raw values given on the left-hand-side y-axis, as the data needed to be transformed to achieve normality for significance testing.

ant differences between targets presented centrally (M = 0.855, SD = 0.053) and at 1° eccentricity (M = 0.762, SD = 0.052) ($t(18) = 3.154$, $p = .003$, $d = 0.288$) and also between targets presented centrally compared to targets at 5° (M = 0.780, SD = 0.050) ($t(18) = 2.309$, $p = .027$, $d = 0.237$). The difference between the means of microsaccade frequency for 1° and 5° targets did not reach significance ($t(18)$ = -0.739, $p = .465$).

A follow-up one-way ANOVA on the data for the three different eccentricities when the fixation helper was present revealed no significant main effect, while a follow-up one-way ANOVA on the data for the three different eccentricities while the fixation helper was absent revealed a significant main effect of eccentricity ($F(2,36) = 5.553$, $p = .014$, $\eta^2 = .395$). Paired t-tests to follow up this effect showed a significant difference in the microsaccade frequencies between targets presented centrally (M = 0.868, SD = 0.323) and targets presented at 1° (M = 0.711, SD = 0.329) ($t(18) = 3.164$, $p = .005$, $d = 0.475$). A further significant difference was found between targets presented centrally and at 5° from fixation (M = 0.706, SD = 0.277) ($t(18) = 3.142$, $p = .006$, $d = 0.527$). No significant difference was found between targets presented at 1° and 5° ($t(18) = 0.120$, $p = .906$). Unlike for previous differences, here there were significantly *more* microsaccades for the central target, than the eccentric targets.

Fixation Position

The magnitude of the difference between the median fixation position when the fixation helper was present in a trial compared to when the fixation helper was absent was calculated. The means of this difference within each participant were compared using a one-way repeated measures ANOVA (see Fig. 5.11). A significant main effect of eccentricity was found ($F(2,36) = 10.813$, $p < .001$, η^2

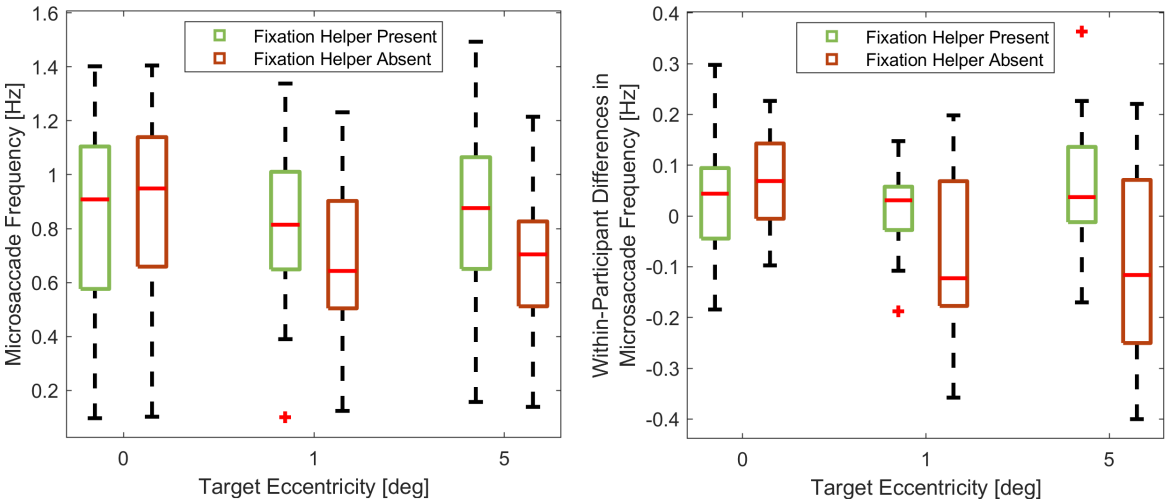


Figure 5.10: Box plot of microsaccade frequencies for the different experimental conditions. On the right hand side the effects across participants are shown, while on the left the within-participant differences are displayed.

= .375). Follow-up t-tests showed significant differences between 0° (M = -0.254, SD = 0.227) and 5° (M = -0.117, SD = 0.176) ($t(18)$ = -2.180, $p < .001$, $d = 0.648$), 1° (M = -0.197, SD = 0.201) and 5° ($t(18)$ = -2.658, $p = .016$, $d = 0.420$), and between 0° and 1° ($t(18)$ = -2.180, $p = .043$, $d = 0.270$), further mirroring the pattern observed in other variables.

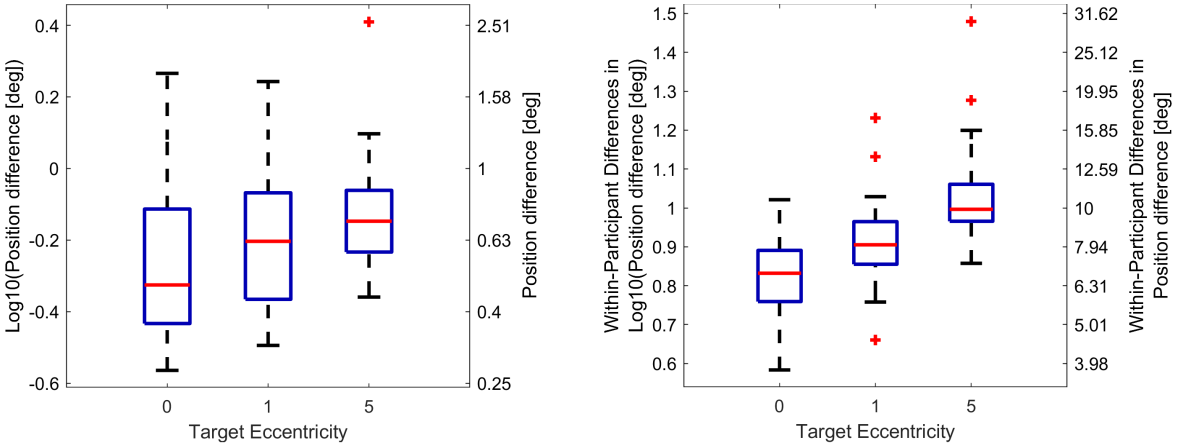


Figure 5.11: Box plots of the difference between the median fixation position when the fixation helper is present and when it is absent by eccentricity. On the right hand side the effects across participants are shown, while on the left the within-participant differences are displayed. The scale is in log format, with raw values given on the left-hand-side y-axis, as the data needed to be transformed to achieve normality for significance testing.

5.5.3 Discussion

This experiment examined the potential influence of peripheral information on fixational stability. The results confirmed the hypothesis that fixational stability uses peripheral information, as both RMS errors and microsaccade distances were increased with increased eccentricity. Therefore more central targets are more effective at stabilising gaze. It was also possible to show that in the presence

of a central target (the fixation helper) there is no impact of peripheral information on fixational stability. None of the measures used in this task showed significant effects of eccentricity, while a fixation helper was present, when investigating the interaction effect between target eccentricity and presence of fixation helper. This is of particular interest to other studies relying on a central fixation target to stabilise gaze, as uncontrolled peripheral information does not appear to have a large potential to influence results.

The results of the RMS error are in line with the two hypotheses stated earlier: that equal targets will result in less stability the further from fixation they are presented, as well as that a fixation helper increases fixational stability. It is yet unclear if peripheral information improves overall stability beyond a central target, as participants in this experiment were never shown the central fixation helper by itself. If it were the case that simply more visual information always leads to greater stability, then the eyes should be less stable with just the fixation helper and no peripheral information. In either case, future studies could map out the relative amount of influence of peripheral information on fixational stability to determine its characteristic change across the retina and compare this to other visual functions. This may lead to predictions about which underlying pathways and processing stages are shared between the fixation stability mechanism and other visual functions.

When examining the microsaccade component an almost identical pattern is observed for microsaccade *distance*. This suggests that microsaccade distance is at least to some degree influenced by visual feedback. Microsaccade *frequency*, on the other hand, displayed a completely different pattern. Microsaccade frequency was higher while the fixation helper was present, and for the central target, compared to when the fixation helper was absent and the targets eccentrically presented. This suggests that when not fixating on a target, but using only peripheral information, microsaccades occur less frequently, but when they do, they are larger.

The error in the difference between the median fixation position in each trial between the half during which the fixation helper was present compared to the half when it was absent further supports the hypothesis that equal targets presented at greater eccentricity have less of a stabilising effect, as the positional difference, and thereby participants estimation of the centre of the targets, increased with eccentricity.

The local RMS error over time appears relatively stable, suggesting that there are no systematic changes to fixational stability when viewing the same stimuli over a prolonged period of time. Considering, however, the global RMS error over time in a trial, the effects observed in the RMS error means become apparent: With a fixation helper no differences between the eccentricities is

apparent, but without it, more central targets appear to be more stable. The initial spike in RMS value can be explained by participants moving their eyes to their preferred fixation location.

5.5.4 Potential Underlying Mechanisms

Now that it is established that peripheral visual information can influence the behaviour of both the overall nature of fixational eye movements, and of microsaccades in particular, it is of interest which underlying system this depends on. There are several possibilities. One possible system may be the movement detection system, as fixational eye movements introduce movement of the visual stimuli on the retina. Movement perception can be either referenced, when stationary visual anchors are present to link the motion to, or unreferenced, when there are no visual anchors available for the movement. In this experiment movement due to fixational eye movements was effectively unreferenced to other visual stimuli, as apart from the fixation stimuli the room was dark. Therefore it would be interesting to explore if unreferenced motion thresholds in response to the same stimuli from this experiment are predictive of the amount of variation between fixational eye movements at the different eccentricities. Should similar thresholds be found this would be correlational evidence that the movement detection system, or information feeding into it plays a role in extracting signals to feed into the fixational eye movement system. If the unreferenced motion thresholds in these conditions are very different in both size and relative proportion to the reported measures of fixational stability, this would be evidence that it is a different system providing the feedback that eye position has changed.

The exact interaction between peripheral and central visual information on fixational stability also requires further investigation. It is unclear exactly how information from different eccentricities is combined to signal a positional shift. Here it may also be of note that the visual information may affect different types of movement, or their features, differently: microsaccades became larger, but less frequent with peripheral information (Fig. 5.10).

5.6 Experiment Two: Orientation

For the second experiment in this chapter the orientation and spatial frequency of large Gabor-like targets were tested for their influence on fixational eye movements. The assumption is that, if some form of visual feedback is used in stabilising fixational eye movements the instability will be greater along the bars of the grating, as there is less information available in the stimulus about a change in position compared to movements perpendicular to the bars of the grating.

The stimuli used in this experiment were Gabor-like, as they faded to a background of black

and had peaks of white (see Fig 5.12), as opposed to the usual Gabor structure of having both black troughs and white peaks fading to a background of grey. These stimuli were chosen, so that the background luminance of the monitor could remain as dark as possible, to prevent visible structure at the edges of the screen that the participants could use to stabilise their gaze. The equations describing these stimuli are:

$$GaussianModulation = e^{-\frac{x}{sd}^2-\frac{y}{sd}^2} \tag{5.2}$$

$$SineModulation = sin(ph + sf * pi * \frac{x}{n}) \tag{5.3}$$

$$OverallModulation = GaussianModulation * SineModulation \tag{5.4}$$

Here x represents the horizontal position, y the vertical position. sd refers to the standard deviation of the Gaussian. The phase of the sine modulation is given by ph and sf refers to the spatial frequency while n refers to the pixel this sine modulation value is assigned to. All values are expressed in pixel units.

Three widely spaced spatial frequencies were chosen, as there was no prior research suggesting a particular frequency would be well suited to study the effects of grating orientation.

All differences from the protocol of Experiment One are listed below.

5.6.1 Methods

Participants

27 participants' data were recorded for this experiment. Of those 22 participants had also provided data in Experiment One. Two participants were excluded from further analysis as only one eye had been trackable for the experiment. A further 5 participants were excluded post data-collection as their data did not meet the quality criteria for inclusion described in section 5.5.1. This resulted in a total of 14 participants contributing data to both Experiments One and Two.

Stimuli

The stimuli in this experiment consisted of Gabor-like targets of three different spatial frequencies (3.5 c.p.d. , 7 c.p.d. , and 12 c.p.d.). The stimuli were similar to Gabor patches, however, instead of having light and dark peaks fading to a mean grey, they had bright lines fading to a dark background (see Fig. 5.12). These targets had a standard deviation of 2.5° and spanned approximately 10.2° .

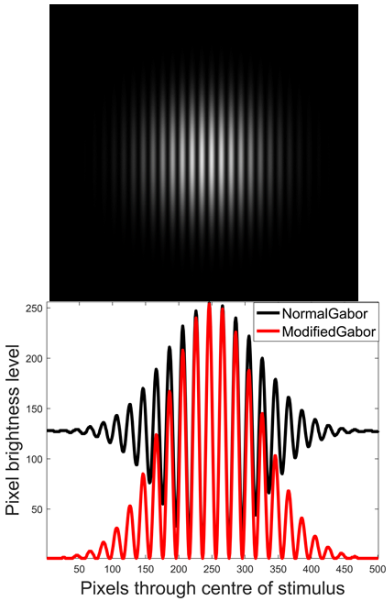


Figure 5.12: Example of the grating stimulus in our study, compared to a Gabor. The top panel shows a stimulus similar to how it would have appeared in the task (note that this image will not be a faithful reproduction of the calibrated stimulus presented on a gamma-corrected display. The bottom panel shows the modulation of the pixel level of the Gabor-like stimulus (black) compared to a Gabor (red) of the same size.

Procedure

Each trial in this experiment consisted of a single 30 s interval followed by 7 s of break during which dynamic greyscale noise was shown (for a graphic description of timings see Fig. 5.13). The participants were instructed to fixate the centre of the stimulus and not to look at the periphery of the stimulus, such as to avoid the visible edges of single lines of the Gabor-like patch.

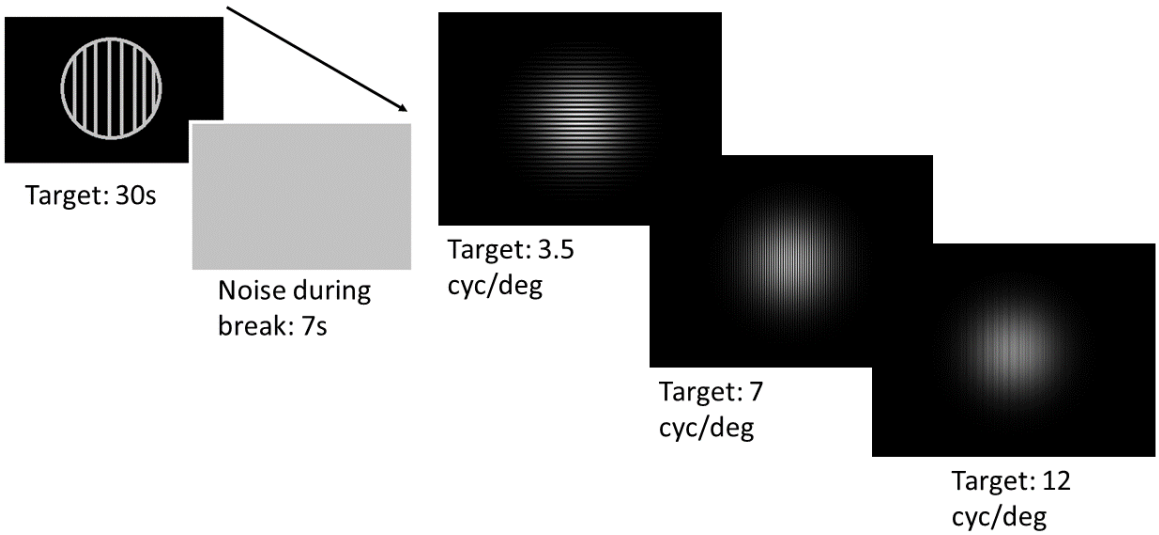


Figure 5.13: This figure shows the trial sequence of events schematically on the left side. On the right the stimuli are shown in relation to the monitor size. Note that at the spatial resolution available in printing, spatial aliasing effects may be present that were not present in the displayed experimental stimulus.

Data Analysis

Firstly it was established that the proportions of missing data are not significantly different between the different conditions, so that an imbalance can not adversely affect subsequent analyses.

The extracted dependent variables were subjected to two-way repeated-measures ANOVAs with the independent variables of grating orientation (vertical or horizontal) and spatial frequency (3.5 c.p.d. , 7 c.p.d. , or 12 c.p.d.). Particular interest was placed on the relative instability of gaze in the direction of, or perpendicular to, the grating. Therefore, to estimate this, the ratio of horizontal and vertical RMS error to the median was used as the dependent variable. A two-way repeated-measures ANOVA was also conducted on the overall RMS error to the median values to establish if any particular combination of frequencies or grating orientations was better able to stabilise fixation.

As fixation stability may also depend on the size of a cycle in the displayed grating the ratio of RMS error to the peak-to-trough distance was also compared. If participants used the flux provided by the grating then their fixational stability should systematically be related to the cycle of the grating, a relationship which would be expected to be constant for all frequency conditions.

5.6.2 Results

Participant Exclusion

Post-exclusion 20 participants were eligible for inclusion in further analysis. For exact proportions of usable trials, please refer to Fig. 5.14.

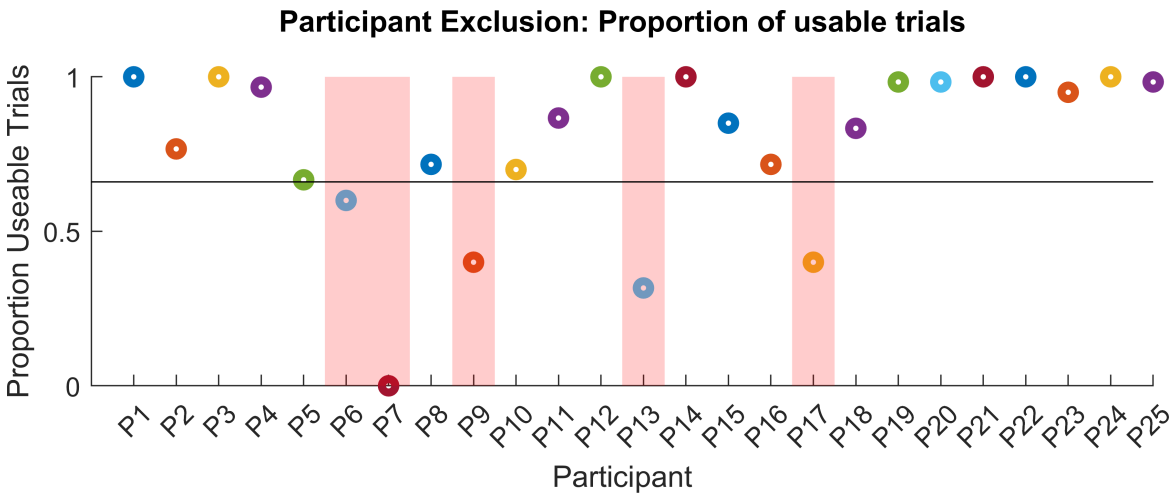


Figure 5.14: Figure showing the exclusion of participants based on missing data. The circles represent the proportion of usable trial intervals when the fixation helper was absent. All participants whose marker lies below the reference line were excluded and are shown shaded in red.

Missing Data

When comparing the amount of missing data in the different categories no significant differences were found (Fig. 5.15).

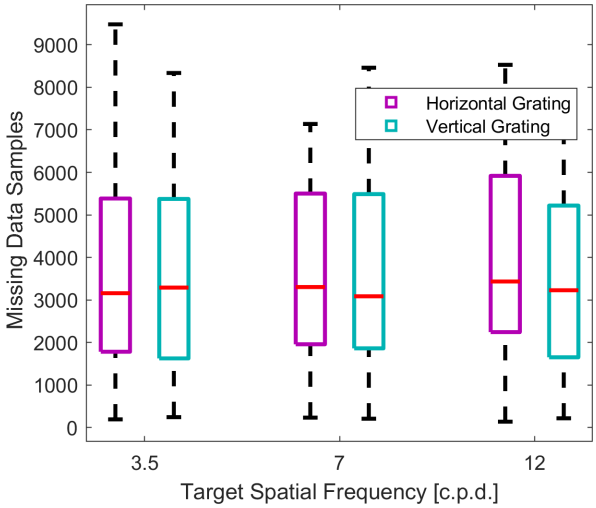


Figure 5.15: Box plot of the amount of data missing from all trials that were included in the analysis.

RMS over Time

A plot of the time course of overall RMS error every 500 ms is shown in Figure 5.16. Two ways of calculating this value were used. Firstly the local RMS error within a 500 ms time period was calculated. This gives an estimate of short term fixational stability. The change in this measure can be seen in Figure 5.16. The second measure is a global RMS error where the reference point is not the median within the 500ms, but rather the median of the whole trial interval. The results for this can be see in Figure 5.19. In both figures the red shading indicates data excluded at the beginning of the trial from all other analyses. It is during this excluded time that participants have a higher RMS value. The local RMS error within a 500 ms time period is consistently lower than the corresponding RMS error to the global trial median.

The ratio of the local horizontal and vertical RMS errors (Fig. 5.18) and the global horizontal and vertical RMS errors (Fig. 5.19) was also calculated over time. These plots do not show the same elevation in error at the beginning of the trial, indicating equal amounts of error in both cardinal directions. Differences in spatial frequency or vertical compared to horizontal gratings are not immediately obvious.

RMS Ratio

When examining the ratio between vertical and horizontal RMS error of the whole trial significant main effects of grating orientation ($F(1,19) = 22.655$, $p < .001$, $\eta^2 = .544$) and spatial frequency were

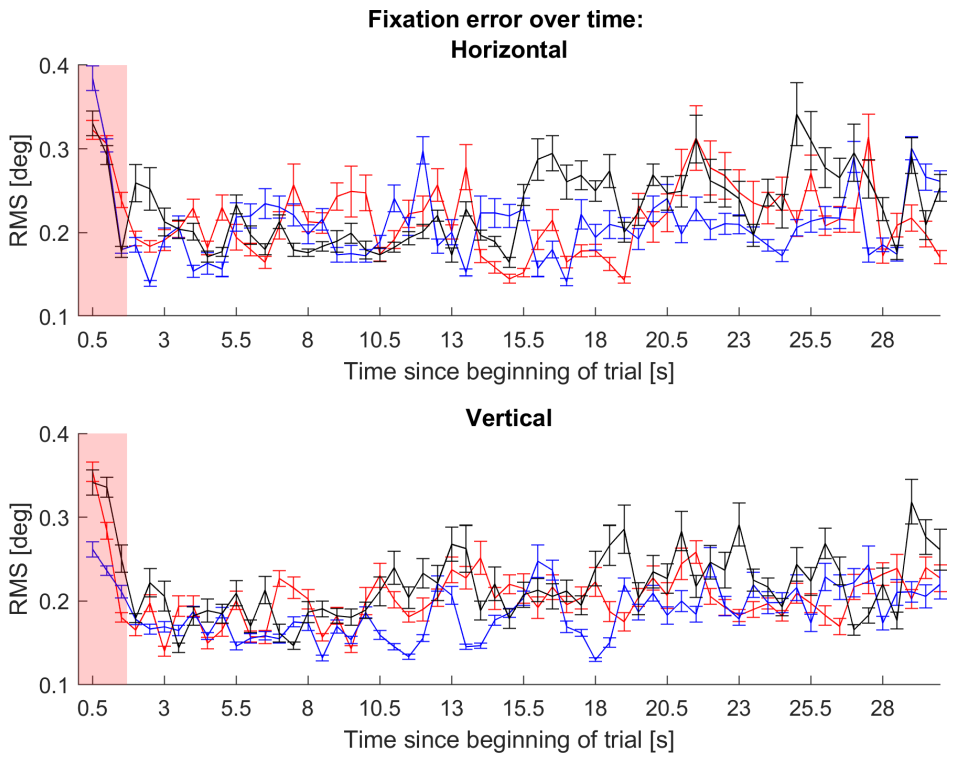


Figure 5.16: This plot shows the temporal progression of the local RMS error. Trials with a horizontally aligned grating are shown in the top panel and trials with a vertically aligned grating are shown in the bottom panel. The RMS error is taken to the median of the local 500 ms period. The red shading indicates the beginning of the trial, which was excluded from all other analyses. The red line represents the RMS error over time when the grating had a spatial frequency of 3.5 c.p.d., the blue line refers to targets with a spatial frequency of 7 c.p.d., while the black line indicates spatial frequencies of 12 c.p.d.

found ($F(2,38) = 4.533$, $p = .025$, $\eta^2 = .335$)(see Fig. 5.20). The interaction effect between the two did not reach significance.

Follow-up paired t-tests on the main effect of spatial frequency on RMS error ratio revealed significant differences between 3.5 cyc/° (M = 1.117, SD = 0.332) and 7 cyc/° (M = 1.058, SD = 0.332) ($t(39) = 2.166$, $p = .036$, $d = 0.179$) as well as between 7 cyc/° and 12 cyc/° (M = 1.155, SD = 0.383) ($t(39) = -3.104$, $p = .004$, $d = 0.269$), but not between 3.5 cyc/° and 12 cyc/° ($t(39) = -1.059$, $p = .296$).

RMS

When examining the RMS error a significant main effects of grating orientation ($F(1,19) = 6.120$, $p = .023$, $\eta^2 = .244$) and spatial frequency were found ($F(2,38) = 3.481$, $p = .041$, $\eta^2 = .155$)(see Fig. 5.21). The interaction effect between the two did not reach significance.

Follow-up paired t-tests on the main effect of spatial frequency on RMS error revealed a significant difference between 7 cyc/° (M = -0.2811, SD = 0.205) and 12 cyc/° (M = -0.255, SD = 0.213) ($t(39) = -2.532$, $p = .015$, $d = 0.127$). Neither the difference in mean RMS values between cyc/° (M = -0.275, SD = 0.213) and 12 cyc/° ($t(39) = -1.915$, $p = .063$), nor between 3.5 cyc/° and 7 cyc/° ($t(39) = 0.521$, $p = .605$) reached significance.

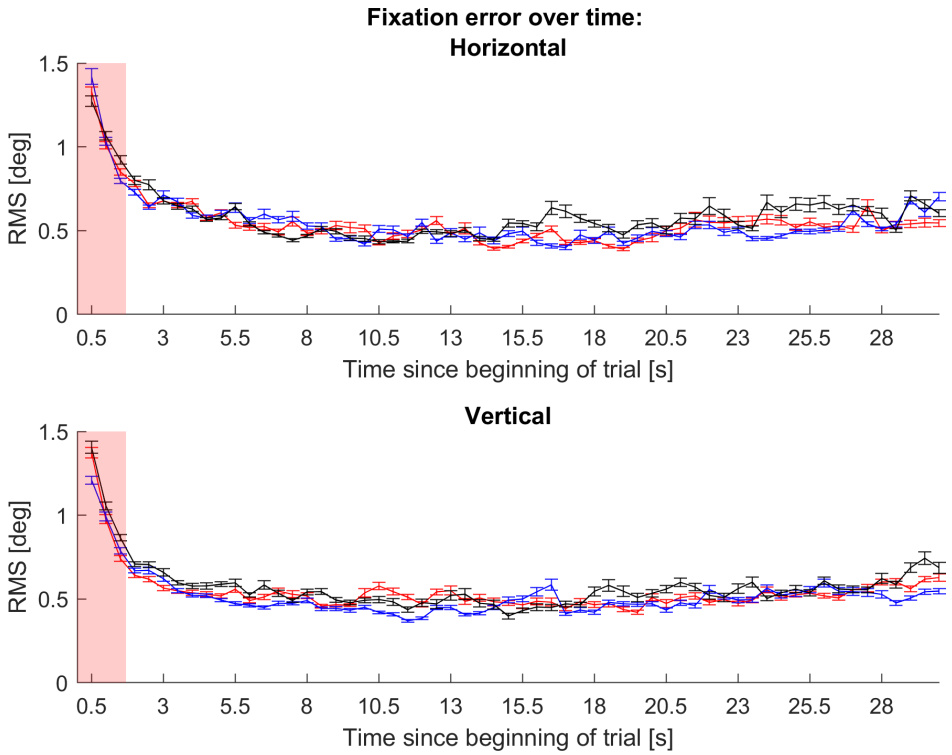


Figure 5.17: This plot shows the temporal progression of the global RMS error. Trials with a horizontally aligned grating are shown in the top panel and trials with a vertically aligned grating are shown in the bottom panel. The RMS error is calculated to the global trial median. The red shading indicates the beginning of the trial, which was excluded from all other analyses. The red line represents the RMS error over time when the grating had a spatial frequency of 3.5 c.p.d., the blue line refers to targets with a spatial frequency of 7 c.p.d., while the black line indicates spatial frequencies of 12 c.p.d.

RMS error compared to peak-to-trough distance

The ratio of RMS error within a trial to the peak-to-trough disctance of each of the grating frequencies shows little similarity across them. For the lowest frequency grating the peak-to-trough distance was 13 px, and the mean RMS error was 0.61°, resulting in a ratio of 0.047. For the grating with a spatial frequency of 7 c.p.d. the peak-to-trough distance was 7 px and the mean RMS error was 0.59°, resulting in a ratio of 0.085. For the highest spatial frequency grating the peak-to-trough distance was 4 px and the RMS error was 0.64°resulting in a ratio of 0.16.

5.6.3 Discussion

The results confirm the main hypothesis that grating orientation influences fixational eye movements, with greater instability being observed in the direction of the grating. This is further evidence that fixational eye movements are indeed influenced by the spatial structure of the visual stimulus.

The results of the RMS error over time suggest that at the beginning of each trial participants' RMS errors were greater, due to finding their preferred location on the target. However, during this initial phase there was no spike in the RMS error ratio between vertical and horizontal movement directions, suggesting that the uncertainty in both directions is approximately equal.

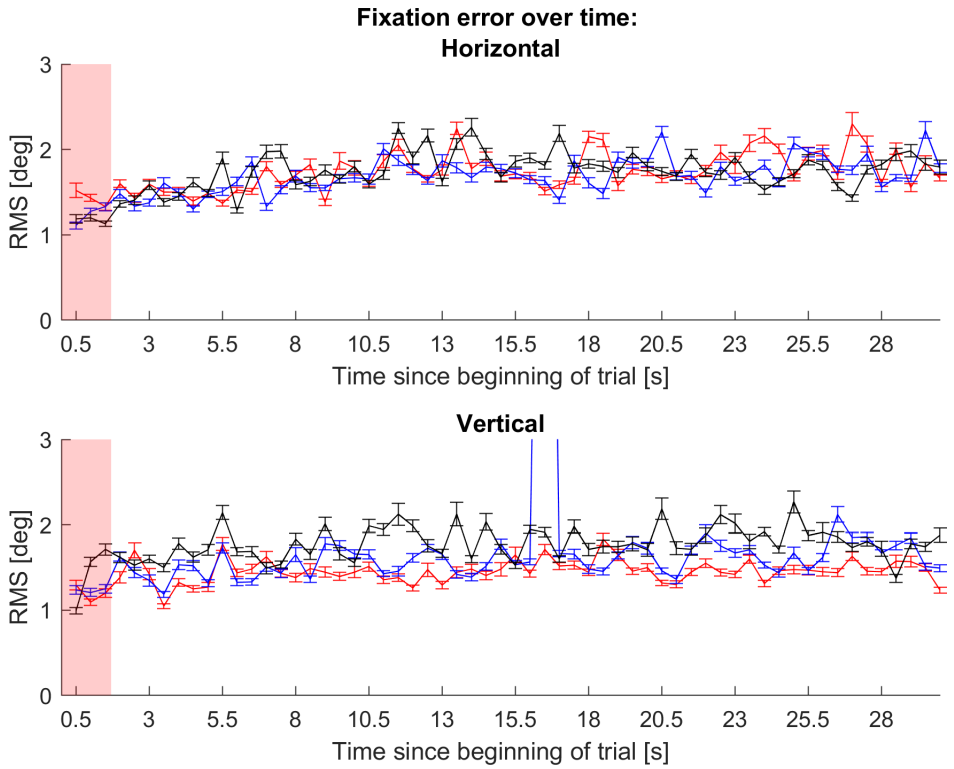


Figure 5.18: This plot shows the temporal progression of the local RMS error ratio. Trials with a horizontally aligned grating are shown in the top panel and trials with a vertically aligned grating are shown in the bottom panel. The RMS error is taken to the median of the local 500 ms period and the ratio of both cardinal directions is taken. The red shading indicates the beginning of the trial, which was excluded from all other analyses. The red line represents the RMS error over time when the grating had a spatial frequency of 3.5 c.p.d., the blue line refers to targets with a spatial frequency of 7 c.p.d., while the black line indicates spatial frequencies of 12 c.p.d.

The three chosen frequencies change fixational eye movements significantly. Three different levels were chosen because the optimal range for testing the hypotheses related to grating orientation was not known, so no hypotheses about these frequencies were made. The spatial frequency with the overall best fixational stability, as measured by RMS error is 12 c.p.d., however, the three spatial frequencies were very similar, so no firm recommendations for future use may be based on this exploratory analysis. As no interaction effect was observed for the different RMS error ratios, it can be assumed that over some range of spatial frequencies the directionality of the effect of grating direction on RMS error is constant. This will be bounded by our ability to perceive differences in the grating stimulus and thereby relate to our contrast sensitivity function (CSF). While it is theoretically possible that the relative influence of a grating component on fixational stability could be traced by exploring the range of the CSF at this point there is little to suggest any benefit in doing so. A better understanding of which factors influence fixational stability can help create stimuli optimised for fixational stabilisation, as necessary for e.g. field tests and retinal imaging, however, it is unlikely that a grating stimulus would be used, as it would bias fixational eye movements, as described here.

Additionally the effect of the spatial frequency appears not to be directly linked to the size of

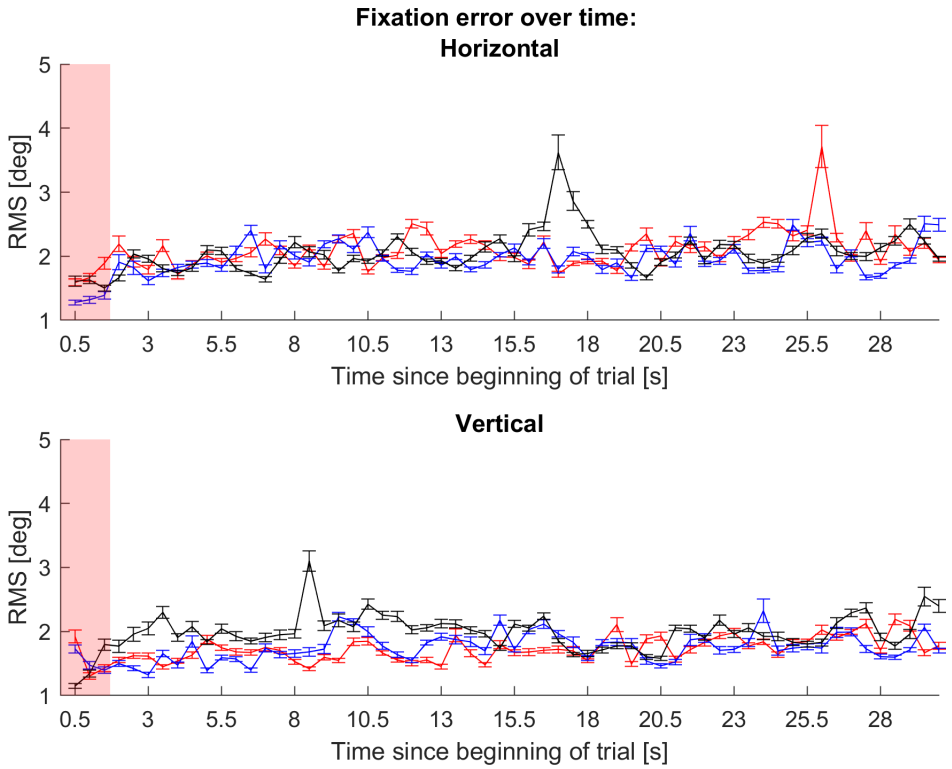


Figure 5.19: This plot shows the temporal progression of the global RMS error ratio. Trials with a horizontally aligned grating are shown in the top panel and trials with a vertically aligned grating are shown in the bottom panel. The RMS error is calculated to the global trial median and the ratio of both cardinal directions is taken. The red shading indicates the beginning of the trial, which was excluded from all other analyses. The red line represents the RMS error over time when the grating had a spatial frequency of 3.5 c.p.d., the blue line refers to targets with a spatial frequency of 7 c.p.d., while the black line indicates spatial frequencies of 12 c.p.d.

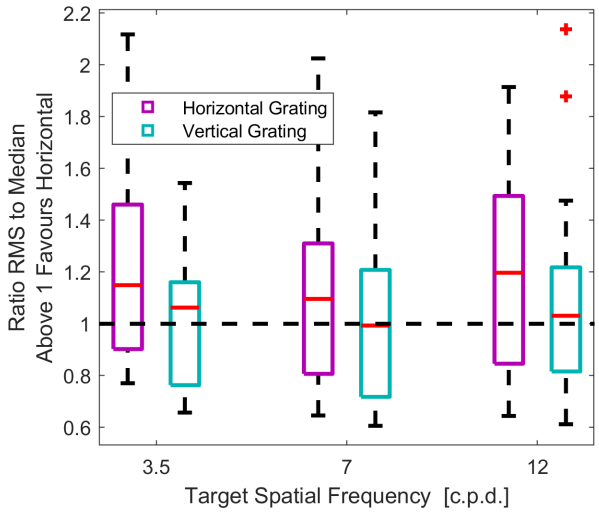


Figure 5.20: Box plot of RMS error ratios for the different experimental conditions.

a cycle, as the ratios of RMS error to cycle length were variable between the conditions. This is evidence that flux, i.e. the shift required to change the luminance by a certain amount is not what drives fixational stability in this case.

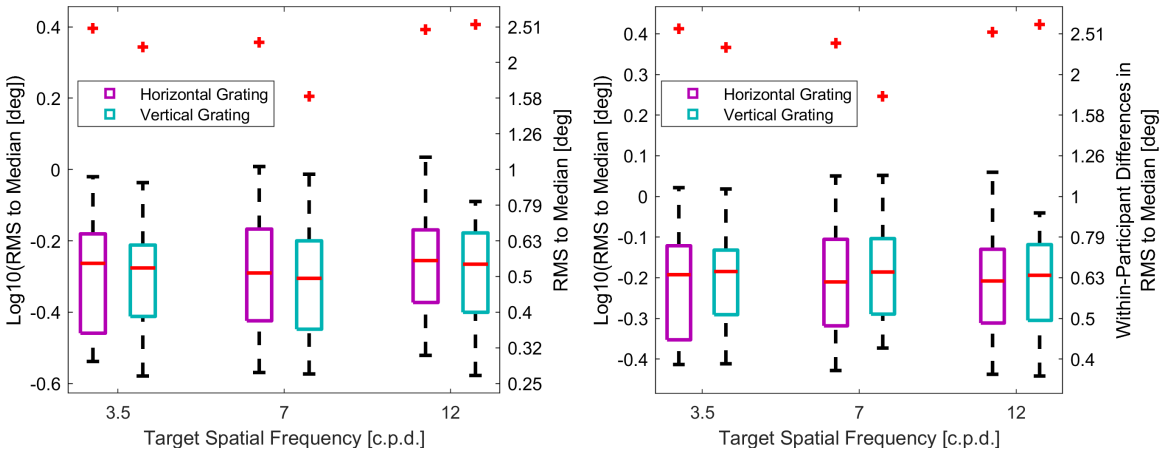


Figure 5.21: Box plot of RMS error for the different experimental conditions. The right side shows the raw values for all participants, while the left side shows the within participant effects.

5.7 Overall Discussion

The aim of the two experiments presented in this chapter was to establish if there is a measurable interaction between the visual stimulus and fixational eye movements. The first experiment examined the influence of eccentricity on fixational stability. If visual feedback influences fixational eye movements, then identical stimuli presented further peripherally should be expected to lead to less stability, as the visual system generally has a lower spatial resolution in the periphery. The second experiment tested whether the internal structure of the stimulus influences fixational eye movements. If visual feedback plays a role in stablising gaze during fixations, then differences between vertically and horizontally aligned gratings should be observed: errors should be greater in the grating direction than perpendicular to it.

The data collected shows both of these hypotheses to hold. Therefore fixational eye movements as a whole are influenced by the visual stimulus. This is intuitively appealing, as a combination of two systems (one proprioceptive and the other relying on external feedback) would probably create the most reliable stabilisation. A proprioceptive system is needed to hold fixation in complete darkness (Skavenski, 1971), or absence of external information. However, when visual information is available, this can be used to stabilise gaze.

Theoretically this may mean that some individuals with a faulty proprioceptive system exhibit normal or near-normal fixational eye movements when a fixation target is present. However, in the absence of a target, their eye movements would be abnormal. A search for any reported cases of such an eye movement disorder revealed no evidence this has ever been recorded. There are two possible explanations for this. Such a disorder may be subtle and hard to study, as most would not be aware that their eyes are significantly less stable in complete darkness. Third parties would also usually not be able to notice it, as in our world usually the only times we can experience the

absence of visual information is in complete darkness, in which case no-one around us can notice any differences in eye movements. Alternatively, this dissociation between eye movements with and without visual targets never occurs, either because the proprioceptive system never suffers from abnormalities, or because the proprioceptive system is so fundamental to controlling eye position, that a failure in that system leads to disorders of eye stability even in the presence of visual targets.

The results of these two experiments suggest that stimulus structure, as well as the eccentricity of visual features influence our fixational stability. What remains unclear is the exact mechanism via which this takes place, and which factors might influence these effects. If visual transients are important, then blurred stimuli should lead to less fixational stability than those with sharp edges. However, if uncertainty is derived from the error associated with estimating the current and/or desired centre of fixation, stimuli that are more spread out in one dimension than the other would result in less stability in the spread out dimension, assuming that this spread would make it harder to estimate the centre. Estimating fixational stability may depend on a number of local or global mechanisms, the exact nature of which requires further research.

Based on these findings an optimal stimulus for inducing fixational stability would feature a central target, as Experiment One has highlighted the marked improvement in fixational stability in the presence of the 2x2 px fixation helper. This is expected, given the foveating nature of our visual systems. If further benefit may be derived from adding peripheral information is unclear. Moreover, a directionally biased stimulus, such as a grating should also be avoided, as the results from Experiment Two suggest that it will bias instability. It is unclear if therefore a circular target is preferable, or, if a target with several radial arms may be optimal, as there would be no particular bias in any direction, while still containing more information about movement relative to the radial arms than in a circle.

Chapter 6

How Does Fixational Stability Correlate With Unreferenced Motion Thresholds and Centre Estimation Abilities?

Abstract

Recent evidence has shown that fixational eye movements behave differently in response to different visual stimuli. It remains unknown which aspects of the visual stimulus drive these changes and which neural mechanisms execute them. In this experiment two mechanisms are investigated for their relative contribution to fixational stability: the ability to estimate the centre of a stimulus and the unreferenced motion thresholds in response to the stimulus. Centre estimation may be important as the visual system needs to compute the desired fixation position and keep this updated during fixation. The ability to detect a stimulus shift may be relevant for fixation stability, as the information of the stimulus shift on the retina needs to be detected to be acted upon. It was found that both centre estimation and unreferenced motion thresholds correlate well with measures of fixational stability. This suggests that both contribute to fixational stability.

6.1 Potential factors in fixational stability

There are a limited number of mechanisms we could theoretically employ to help us maintain fixation. They can be broadly categorised into mechanisms relying on proprioceptive feedback and those relying on visual input. As it is beyond the scope of this thesis to examine proprioceptive

feedback for eye position, we will further examine those mechanisms for fixational stability that rely on visual feedback.

Chapter 5 provides clear evidence that fixational stability relies, at least in part, on visual information. The particular features studied in Chapter 5 were the eccentricity of the visual information and the orientation of its borders. It was shown that (i) greater eccentricity of available information leads to greater instability and (ii) that the eyes are less stable along the bars of a grating. However it remains unclear which underlying mechanisms analyse visual information with regards to the information it can provide on fixational stability. One possible mechanism would extract the change in position of the image on the retina. The visual system has dedicated processing mechanisms for extracting a change in position over time, namely motion detection mechanisms. One possibility is that the visual feedback to eye-position also makes use of these processing mechanisms. Another possible contributing factor to determining eye position could be a direct estimation of the position of a feature of the stimulus, such as its centre. If it is harder to estimate the centre of a stimulus for whatever reason, it may also be harder to keep gaze directed at this estimation of the centre.

In this chapter the change in RMS error in response to stimuli of different eccentricities will be compared to the changes in unreferenced motion thresholds and the changes in centre estimation error in response to the same stimuli. If the rate of change with eccentricity is similar for these mechanisms, it suggests that they rely on at least partly shared underlying processing steps. The central question is if the M-scaling (first described for grating acuity in Cowey & Rolls, 1974), which refers to the psychophysical correlate of the cortical magnification of a given property at a given eccentricity, for fixational stability correlates with the M-scaling for unreferenced motion thresholds and/or centre estimation ability. It is important that the actual values of each measure are not important, but that their characteristic change across different eccentricities matters, as different processes exhibit characteristically different M-scaling and that these changes are also dependent on the underlying physiology (e.g. De Valois & De Valois, 1991; Dumoulin & Wandell, 2008; Song et al., 2011).

6.1.1 Motion Perception

The detection of motion is central to our ability to interact with the world: it allows us to judge the speed of oncoming cars and estimate when we have poured enough water into a glass. The central problem in motion perception is how to go from local signals of change at retinal level to a global percept of motion in a given direction. A simple model for local motion extraction was described by Reichardt (1961): Two spatially offset detectors that feed into one node can detect a specific

direction and speed of movement, if a delay is added to the connection from one detector to the node. However, this only provides a local motion signal, the combination of these is necessary for a global percept of motion. The aperture problem characterises the difficulties in the integration of local motion signals, by confounding direction and speed for a local motion detector. There are two possible ways the information may be integrated globally: by vector summation or as an intersection of constraints. Based on experiments where the two methods would predict different motion directions, given the motion is perceived as coherent, rather than two gratings sliding across each other, human participants seem to follow intersection of constraints (Adelson & Movshon, 1982).

In the experiment in this Chapter, the moving stimulus was not designed to isolate first, second or third order motion, as both the luminance and features shifted congruently. If fixational stability correlates well with motion thresholds, then it may be of interest to isolate the type of movement presented. This would allow for more in-depth conclusions about which underlying processing mechanisms support fixational eye movements, as different types of motion may be processed at different stages in the visual stream.

6.1.2 Unreferenced Motion

In most every day situations, motion is always referenced to the moving or stationary nature of other objects in our visual environment. We can tell that a fly is moving across a window pane, as not only is its image on our retina displaced in time (assuming we do not move ourselves, or track the fly using smooth pursuit) but also due to its relative position to the window frame, or other known stationary objects. Therefore, even if we were to move our vantage point, we can deduce that part of the motion of the fly on our retina is due to its own movement, rather than ours, by referencing the position of the fly to that of the window pane. This is a typical example of referenced motion. Another example that has a bearing on our behaviour is, for example, the interpretation of optic flow when we move. Optic flow was first introduced as a concept by Gibson (1958) to explain how we actively navigate our environment. The super-importance of visual information in this, at least for healthy observers, was demonstrated compellingly by experiments in which visual information incongruous with the proprioceptive feedback was presented. Participants frequently appeared to correct their posture in response to the visual information, overriding the proprioceptive information (Lishman & Lee, 1973). This illustrates the importance of interpreting motion of the visual image to influence our own motor behaviour. Could motion detection, or underlying processing steps also contribute to fixational stability?

To test this hypothesis, the same stimuli as in Experiment One, Chapter 5 were presented to observers, this time in a two-alternative interval forced choice (2afc) motion direction discrimination task. What is special about the stimuli in this experiment is that both times, in the original version and the new version, they were presented in near-complete darkness without (much) visual context[1]. Therefore it is difficult to separate movement of the eye from movement of the object, which is frequently reported as the autokinetic effect (Schweizer, 1857). The autokinetic effect was spontaneously reported by some participants in the original experiment, suggesting that the room was sufficiently dark to remove visual anchors which may prevent the autokinetic effect. Movement without external references is called unreferenced motion. While unreferenced motion thresholds are already known to increase in the periphery (Levi, Klein & Aitsebaomo, 1984), the aim of this experiment was to establish unreferenced motion thresholds for the specific stimuli used. If unreferenced motion thresholds scale with eccentricity in a similar way to the instability measured in the previous experiment, this would suggest that the same underlying neural system might detect both unreferenced motion as separate from movement of the participant's own eyes, as well as trigger eye movements to correct for fixational error. If the motion thresholds scale differently with eccentricity, then other mechanisms must be responsible. It should be noted that this scaling does not have to be of the same magnitude, but rather the pattern in which it changes from the centre to the periphery is important. To investigate this relationship the current chapter presents newly collected data on the same task as in Chapter 5 and also on tasks relating to centre estimation and unreferenced motion thresholds.

6.1.3 Centre Estimation

Another possible mechanism would be one estimating the centre of a given stimulus. Under this hypothesis, one reason fixational stability might have been lower for more eccentric targets is that the constantly-updated estimation of the centre of the stimulus would be more variable, the further the targets are in the periphery. If this was the main driving force then the uncertainty attached to estimating the centre of each type of target would be expected to scale in a similar way with eccentricity as measures of fixational stability.

6.1.4 Complexity of determining the underlying mechanisms of fixational stability

As our understanding of fixational stability is still relatively limited, any evidence, including that presented in this Chapter, is likely to be correlational only. This limits the strength of any conclusions

[1] As the Display++ is a backlit monitor a very small amount of light was present in the room, however the table surface of the setup was covered in black cloth and the room itself was blacked out.

that can be drawn from this. Additionally, there is a more differentiated argument to be made about the contributing factors in fixational stability. Firstly, it is unlikely that there is a single underlying mechanism driving fixational stability, given the plethora of potential cues available. Secondly, there is good reason to believe that what drives fixational stability in the microsaccade component is not the same as in the drift component. Large saccades are drawn to the centre-of-gravity of stimuli (Coren & Hoenig, 1972), and the same may be true for microsaccades, while there is no evidence that this assumption should hold for drifts. Additionally the changes in the different measures of stability across the different target eccentricities did not appear similar in Chapter 5 Experiment One. Therefore the unreferenced motion thresholds are unlikely to correlate well in their relative proportions to both drift and microsaccade statistics.

6.2 Methods

6.2.1 Participants

A total of nine participants who also contributed data to Chapter 5 took part in this experiment. Only those participants whose data met inclusion criteria in the previous experiment(s) were contacted to take part. Their informed consent was given (CUREC Approval Reference: R62306/RE001) and they were compensated for their time.

6.2.2 Set Up

This experiment used the same arrangement of equipment as in Experiment One, Chapter 5. Stimuli were displayed on a Display++ at 175cm from the participants. Eye movements were recorded binocularly at 1000 Hz using an Eyelink 1000.

6.2.3 Stimuli

The visual targets were identical to those described in experiment 1 in Chapter 5, without the fixation helper. In this experiment, motion was added to the stimuli. As sub-pixel motion was required, a shift of the target was programmatically introduced in the Gaussian target. To find out how small a shift could be adequately presented, the requested shift was compared to the actually achieved shift, which was calculated using the 'regionprops' function with the option 'Weighted Centroid' in MATLAB. Then the ratio of actual shift/ requested shift was taken. The smallest possible shift that could be accurately represented on the display monitor was determined to be .05 pixels (see Fig 6.1). All step sizes were capped at that lower limit.

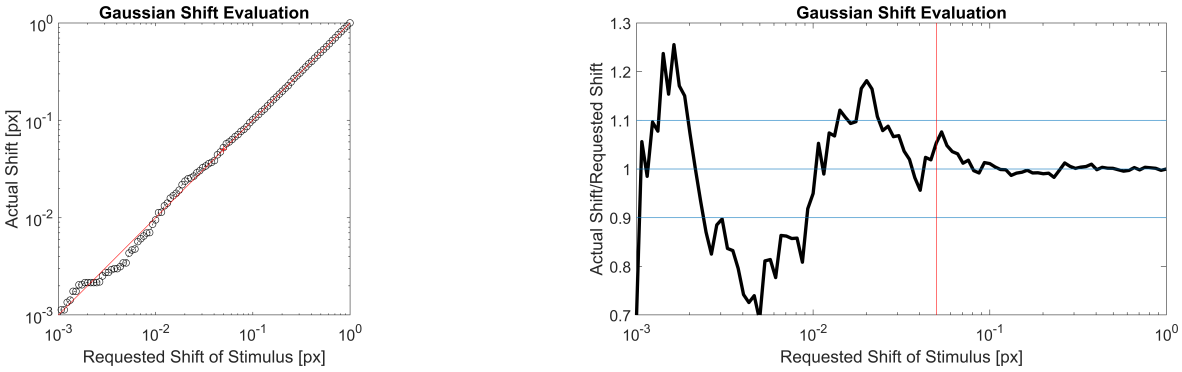


Figure 6.1: Comparison plots of actual step size in pixels compared to requested step size in pixels. The red cross in the left plot and the red line in the right plot indicate the chosen cut-off value of 0.05 px.

6.2.4 Procedure

There were three types of task in this experiment. The first was a 2afc task to determine motion-direction thresholds and the second was a fixation task, similar to the one in Experiment One, Chapter 5. These two tasks were interleaved, although depending on timing, on occasion two blocks of the 2afc motion threshold task were completed back-to-back, omitting the observation task. All participants performed a minimum of four repeats of the 2afc task and four repeats of the observation task, although some participants completed more repeats. The third type of task was a mouse-click task completed once at the end of the testing for a participant.

During the 2afc task participants were asked to respond in which of two temporal intervals the targets moved to the right (see Fig 6.2). In a given trial, one interval contained a two-frame motion stimulus to the right and one interval a two-frame motion stimulus to the left. The order of the interval was randomised. They could indicate their response using the up arrow for the first interval and the down arrow for the second interval. The up and down arrow buttons were chosen over the left and right arrow buttons to avoid any cognitive conflict given the targets were moving to the left and right, also known as the Simon effect (Simon & Wolf, 1963). In each block, 90 trials were presented. Each trial consisted of a first interval lasting up to 1 sec, a 0.5 sec black screen to indicate the transition between the two intervals and a second interval identical to the first one, except that the motion direction was reversed. Participants could input their response as soon as the last targets disappeared. There was no time limit on responding. After the response they received auditory feedback followed by a 1 sec interval during which greyscale dynamic noise was shown. In each block, 9 different combinations of target eccentricity and step size could be tested, resulting in 10 trials for each step size-target combination. After each block the results were plotted using the MATLAB Psignifit toolbox (Schütt, Harmeling, Macke & Wichmann, 2016) and the experimenter manually selected the step sizes to be tested in the next round of testing. This was done to most efficiently get a good estimate of an individual's complete psychometric function.

To prevent observers directly looking at the eccentric targets and thereby viewing stimuli at a different eccentricity to the one intended, participants were eye tracked. At the beginning of each interval the eye tracker determined if the participant was looking within a central region, and only if their gaze fell in this region would the target movement be initiated. In case tracking failed, or participants were not fixating accurately, the trial would progress without the eye tracker trigger after 1 sec. The criterion for whether or not a participant was fixating centrally was set so that participants' gaze had to fall within 1.79 ° of the centre for 5 consecutive samples. These 5 consecutive samples could also themselves not be further from each other than 0.42 °Ṫhis was to ensure that participants gaze was stable enough in its chosen position to trigger the movement, as it is not desirable for the system to trigger the movement before the eyes have become relatively stable.

In the fixation task participants were shown the same stimuli as in Experiment One in Chapter 5, but without the fixation helper. They were shown the targets for 30 consecutive seconds with the instruction to fixate the centre of all targets.

In the mouse-click task each stimulus was presented ten times for a maximum of ten seconds. Trials were separated by a 2 sec break during which dynamic noise was shown. A 5x5 px pointer with a black outer ring and a white 3x3 px centre was presented and the initial position of the mouse was randomised to 153 possible positions, all of them away from the centre of the stimulus which the participant had to indicate. The position of the stimulus was randomly chosen each trial to fall either ±1.79° , ±2.38° , or ±2.98° vertically and horizontally from the centre position. Participants were instructed to use the mouse to click on the centre of the stimulus, i.e. where they had been instructed to look previously. The click-position of the pointer was recorded.

6.2.5 Analysis

Firstly the data were examined to establish if the eye position was sufficiently central and stable in a large proportion of trials for subsequent analysis to be meaningful. This was determined by the proportion of trials and trial intervals that were automatically triggered after checking for fixation position.

Eye movements from the fixation task were analysed for their fixational stability based on the RMS error. This metric is analogous to the one used in Experiment One in Chapter 5. RMS was chosen as the primary metric of stability as it combines both microsaccade and drift components. This outcome variable will also be referred to as the RMS within trials, as the error is calculated for each trial separately.

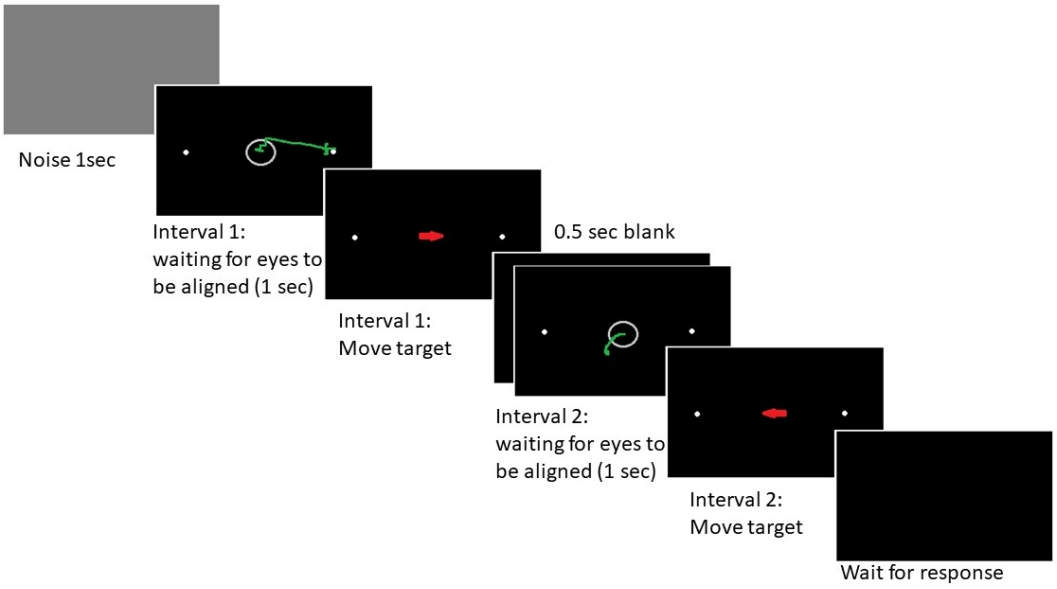


Figure 6.2: Graphical representation of the trial sequence during the 2afc task. The arrows in the centre of the screen were not present during the task and are used here to indicate the movement direction of the targets. Similarly the large circles and green lines were not present during the task, but here represent the acceptable fixation position and eye movements respectively.

A second instability metric was also employed: the RMS error of the median position between trials. This provides an estimate of how close to their other fixation loci participants returned their gaze each trial. Subsequently this will be referred to as the RMS between trials, as it measures the difference in median fixation position across trials.

The positional data from the mouse-click experiment were analysed for the RMS error to the real centre of the stimulus. This differs from the analysis done on eye position, as there the median within a trial was taken as the reference. The reasons the centre of the screen was chosen for the mouse-click task are that (i) the participant was receiving direct visual feedback of where the mouse was on the screen in relation to the stimulus, while during the eye tracking drifting of the calibration may have affected eye position estimation and (ii) during the mouse-click task only a single best-estimate value was recorded, so there were no within-trial reference values.

The data from the 2afc task were the most complex to analyse. Initially the psychometric responses were plotted, in Psignifit (Schütt et al., 2016). The step size matching the inflection point in the curve, i.e. the conventional discrimination threshold, was determined and the confidence intervals recorded. The step size associated with this inflection point is taken as an estimate of the unreferenced motion threshold for these stimuli. Traditionally a 75% correct value would be used, however as the Psignifit toolbox takes into account a lapse rate, the inflection point is not always aligned with that threshold value and it is assumed that the inflection point is more meaningful.

In a second step the data were analysed by combining the movement of the stimulus with the recoded eye movement to reveal the actual movement of the stimulus on the retina. This analysis

introduced too much noise in to the data and was subsequently disregarded.

To assess how much of the variance in the RMS error can be explained either by the unreferenced motion threshold or by centre estimation using a mouse respectively, an analysis of covariance and linear regression was run. For this the procedure described by Bland and Altman (1995) was followed, which allows to separate repeated observations within one participant while still considering the outcome variables across participants.

6.3 Results

6.3.1 Automatic Triggering Success

Figure 6.3 shows the spread of the proportion of successfully triggered trials for all participants. On visual inspection it appears that the first trial interval was more likely to be successfully triggered compared to the second interval.

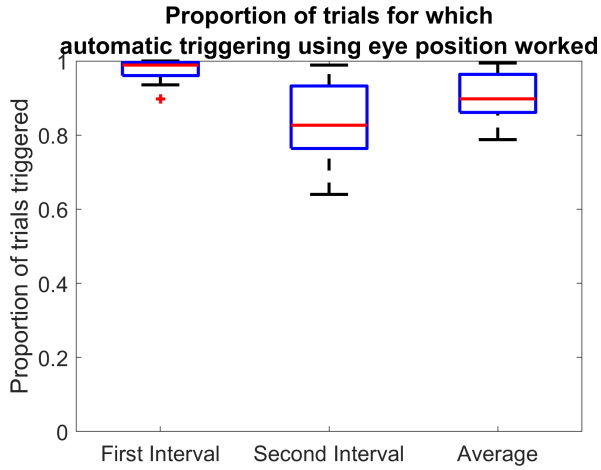
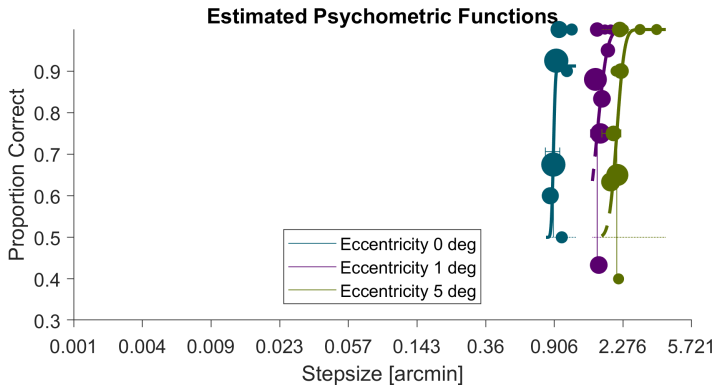


Figure 6.3: Box plots of the proportion of trials that were successfully triggered during the experiment for all participants.

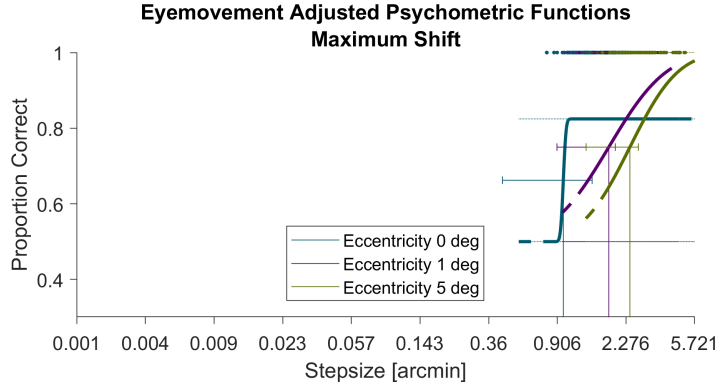
6.3.2 Comparison of Stability Measures

Accounting for eye position when considering the psychophysical data did not yield satisfactory results. For all participants the 95% confidence intervals on the threshold estimates became much larger, suggesting that the movement correction was not a useful way of representing the psychometric data. It was therefore decided to run all subsequent analyses on the psychometric thresholds derived without accounting for eye movements. An example of the effect of including eye movements on the psychometric functions can be found in Figure 6.4.

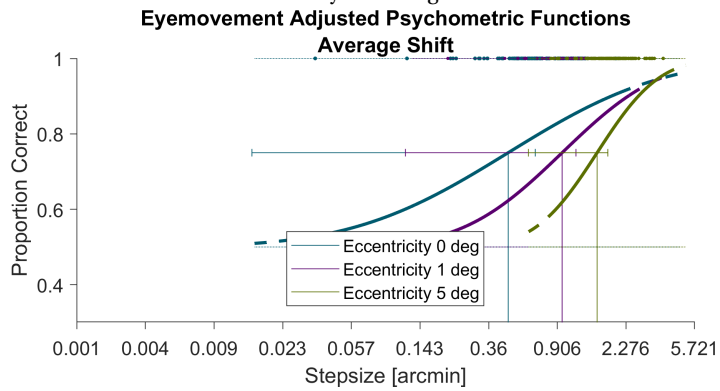
Next the correlations within subjects for repeated observations were examined (Bland & Altman, 1995). When examining how much variance within the RMS error within trials can be explained by



(a) Participant P3X's psychometric function without accounting for eye movements.



(b) Participant P3X's psychometric function when considering the step-size as the *maximum* difference within 5 ms before and after the target moved between the combined eye and target traces.



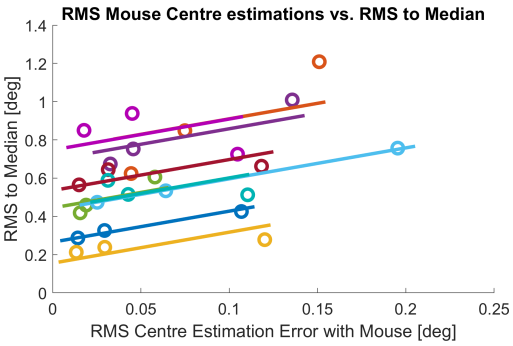
(c) Participant P3X's psychometric function when considering the step-size as the *average* difference within 5 ms before and after the target moved between the combined eye and target traces.

Figure 6.4: Comparing raw psychometric functions with eye movement adjusted ones under two different methods of performing the adjustment. Both methods lead to much more finely-spaced stimulus step sizes and failed to change the psychometric functions in favourable ways. Both have larger error bars than the raw psychometric data.

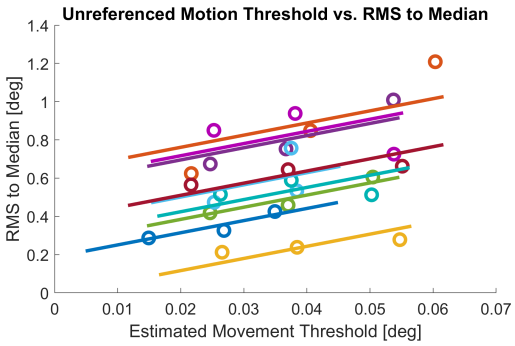
the RMS error on the centre estimation using the PC mouse it was found that 41.9% of variance could be explained in this way ($r = 0.647$, $p = .003$) (see Fig. 6.5). For the RMS error between trials 18.6% of the variance could be explained by the RMS error on the centre estimation using the mouse, which was not significant ($r = 0.431$, $p = .068$)(see Fig. 6.5).

When examining the unreferenced motion threshold as a covariate, 40.7% of the variance in the RMS error within trials can be explained ($r = 0.638$, $p = .003$)(see Fig. 6.5). When considering the

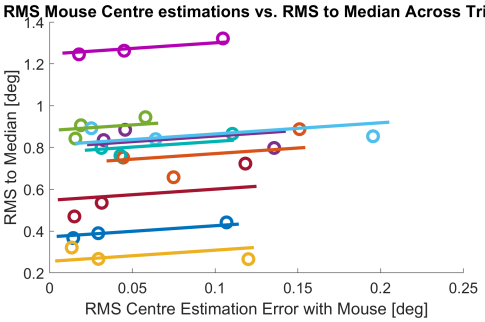
RMS between trials as the dependent variable 30.6% of covariance can be explained (r = 0.553, p = .013)(see Fig. 6.5).



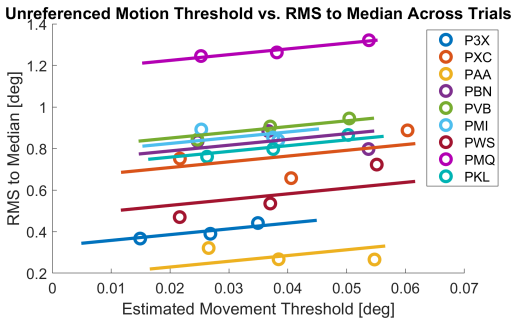
(a) Plot of all participants' RMS centre estimates using the mouse compared to each participants' RMS error to the median of fixation within trials.



(b) Plot of all participants' unreferenced motion thresholds compared to each participants RMS error to the median of fixation within trials.



(c) Plot of all participants' RMS centre estimates using the mouse compared to each participants' RMS error to the median of fixation between trials.



(d) Plot of all participants' unreferenced motion thresholds compared to each participants RMS error to the median of fixation between trials.

Figure 6.5: Comparison of the correlation between the RMS error, unreferenced motion thresholds and centre estimations. For each participant three data points are plotted, one for each target eccentricity. The lines represent the regression lines defined by the best slope when accounting for all participants and each participant's individual intercept in line with the method reported by Bland1995 (1995).

6.4 Discussion

Both the RMS on the centre estimation using a mouse pointer and the unreferenced motion thresholds correlate well with the participants' RMS errors within and between trials, except for the non-significant correlation between the mouse centre estimation and the between-trial RMS. The centre estimation may be more related to fixation stability within a trial, rather than fixation consistency between trials, as assess using the between-trial RMS. The findings suggest that both underlying mechanisms, unreferenced motion thresholds and mouse centre estimation could be related to how we keep our eyes on target, especially fixation stability.

It should be noted that adding eye movement information to the estimation of the unreferenced motion threshold added noise, rather than removing it. This is surprising as eye motion and target motion should interact. There are several possible explanations for this. Either relative motion of eyes and target was irrelevant, as the movement was referenced against the sparse remaining visual

information in the room. This would be a slightly dissatisfying reason, as great care was taken to eliminate any visual information. However, the visual setup in this experiment, and in Chapter 5 was identical, so any comparisons between these experiments would remain valid, even if the movement was not entirely unreferenced. This option also appears unlikely given the subjective reports of the autokinetic effect by some participants. The alternative explanation for this is that either the eye tracker did not track these fine movements accurately enough, thereby actually introducing noise. This would not need to be a great error to have some effect, as the movement threshold was in the range of .8 -2 arcmins, so even small errors in reported eye position would add a lot of noise to the position estimation. A third possibility is that in this case it is simply not valid to account for eye position as simply as was done, given the nature of the task: the eyes will have moved different relative amounts compared to the stimuli in both trial intervals of the 2afc task, and simply averaging this movement may not be a valid estimation of the eye-movement-corrected stepsize. Potentially, more sophisticated ways of estimating how the eye movement could have influenced performance are necessary.

Another interesting finding in the eye movement data was the difference in automatic triggering between the first and second interval. It appears that the second interval failed to trigger much more frequently than the first. This may be because on some trials participants were certain of their response after the first interval and then focussed less well on the task/the screen in the second half. It may also be a result of a natural following response after the movement in the first interval, which is then not fully corrected in time for the second interval.

Ultimately, it appears that both unreferenced motion thresholds and the RMS error on the centre estimation using a mouse are related to changes in eye stability. This suggests that the most likely way that eye position is maintained is supported either by several mechanisms, or by a mechanism common to both of the correlating measures we used.

In the future it would be interesting to consider these types of effects with a range of targets that display different patterns in fixational stability in the hope that these patterns are borne out across other measures, too. If fixational eye movements differ during a vernier acuity task, it would be interesting to see if the effect on eye movements scales in a similar way in the periphery as the M-scaling of vernier acuity. Another promising route for exploring fixational stability would be to consider effects on drift and microsaccades separately, to learn more about their differing subcortical (and potentially cortical) origins.

Chapter 7

Fixational Eye Movements and Gaussian Blur

Abstract

Given that fixational eye movements display different behaviours in response to different visual stimuli, there must be a signal associated with the stimulus that is extracted by the visual system to actively guide eye movements. There are many different possible candidate signals and combinations thereof that could help us fixate. One such candidate signal is the amount of optical flux (i.e. the change in intensity at each location, per unit of retinal displacement, which provides a proxy for the local change in signal due to movement of the target on the retina). This signal also requires some global integration for the direction of a shift to be detected. One way of changing the amount of flux available in the visual scene is to introduce blur. As the border of a stimulus becomes softer, the sensory array needs to move further to receive the same amount of signal change compared to a crisper stimulus. In this experiment small circular targets were presented foveally with three different levels of Gaussian blur. Eye movement recordings were made using both a video-based eye tracker and an Adaptive Optics Scanning Laser Ophthalmoscope (AOSLO). Fixational stability in response to the stimuli was evaluated by comparing the root mean square (RMS) errors of eye position. No significant differences between the eye movements in response to the different targets were found. This suggests that blur and consequently flux does not play a large role in stabilising eye position, although it can not be ruled out that at greater retinal eccentricities, or greater levels of blur, differences may be found.

7.1 Does Gaussian blur interact with fixational stability?

Effective eye movement control requires some input from the visual scene to maintain fixation on target, as fixational eye movements increase in the absence of such signals, e.g. in the dark (Cornsweet, 1956), and are influenced by aspects of the stimulus like eccentricity and orientation (see Chapter 5). Therefore the properties of the stimulus boundary itself may influence the stability of fixational eye movements. If movements are used to generate a fixed minimum amount of change in the response of the sensor-array, sharp boundaries would require smaller movements than gradual boundaries (see Fig 7.1). However, if eye stability depends on the centre-of-gravity of the stimulus summed over a large area, blur of the boundary should only minimally affect eye-movements. The experiments described in this Chapter are aimed at answering that question.

A previous study by Ukwade and Bedell (1993) found that fixational stability decreased significantly with increases in blur, suggesting that this degradation in the visual information does interact with fixational stability. However, Ukwade and Bedell used a Limbus tracker, which are known to have quite poor spatial resolution and an examination of their results reveals only a small and noisy increase in positional error for blurrier targets. Another study by Vikesdal and Langaas (2016) varied spherical defocus between -3 and 5 D. They recorded monocular eye movements at 120 Hz and an accuracy of 0.3° and found small changes in fixational stability as estimated by a bivariate contour ellipse area (BCEA). These previous investigations found an effect of blur using comparatively low-resolution (both temporal and spatial) eye trackers. To further investigate the influence of blur on fixation stability there is merit in using a high resolution eye tracker like the AOSLO.

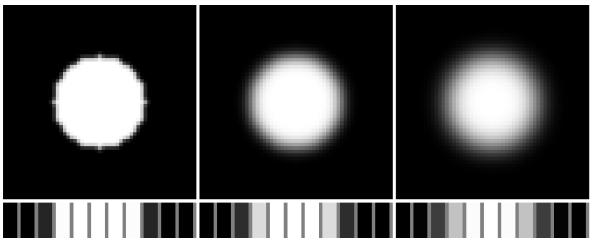


Figure 7.1: Example of a possible local summation of luminance signals for the three stimuli used in the experiment.

If the feedback signal for maintaining eye stability is derived from transient signals of edges, it should be expected that stimuli with a sharper border will result in greater fixational stability than stimuli with a blurrier border, because for blurrier stimuli a small displacement of the image on the retina will lead to a smaller transient signal. Alternatively, if the signal that maintains eye stability is instead derived from integrating the centre-of-gravity of stimulus intensity, little differences between symmetric stimuli that are equated in their overall luminance is to be expected. If that

were the case this would be a further point of similarity between fixational eye movements and larger-scale movements, as it has been shown that large saccades are biased towards the overall centre of gravity of a target (Coren & Hoenig, 1972). Further evidence that blur may influence fixational eye movements is that target blurriness predicts how quickly a fixated target undergoes perceptual fading (Bachy & Zaidi, 2014). Could the same edge-based visual signals be used maintain fixation? Martinez-Conde et al. (2006) showed that, for the blurry peripheral visual information available during Troxler fading (Troxler, 1804), microsaccades can counteract the fading of the visual targets. This is consistent with early research that showed the size of a voluntary movement to be crucial in determining whether or not the movement could restore visibility of faded Troxler targets (Clarke & Belcher, 1962). However, it is not clear that such stimuli have a causative effect on microsaccade generation, or what their effect on the drift component of fixation is.

At this point there is more experimental evidence that target borders should play a role in fixational stability, as the results of Chapter 5 indicate the importance of the structure of the visual stimulus for fixational stability. Previous findings in Chapter 5 and by Ukwade and Bedell (1993) suggest that a difference in fixational stability should be borne out in the RMS error of fixation. Based on the findings of Martinez-Conde et al. (2006) it may also be expected that more and larger microsaccades occur in response to the blurriest target. However, other research suggests that there should not be a significant difference in the microsaccade component, given that microsaccades are not triggered by fixational error signals (see Chapter 8, Collewijn and Kowler (2008)). Microsaccades are also more likely to behave like large saccades, and therefore be biased most by the centre of gravity of a visual object (Coren & Hoenig, 1972) than other features like blur. Given this evidence it can be expected that the overall instability of the trace expressed as RMS will increase with increased target blurriness, while there is conflicting evidence as to whether or not there should be measurable changes to microsaccade rate or distance.

Whether the estimation of the centre of gravity or a detection of local flux (perhaps by local motion detectors) is more important leads to different predictions for blurry targets. If we assume the stimuli are sampled by a coarser receptor grid (see Fig. 7.1) then the overall estimation of the centre of gravity should not be affected, as long as the targets have the same full width at half maximum (FWHM), no matter how gradual the transition at the edge. Therefore it would be sampled by the same number of receptors, which would lead to approximately equal centre estimations. However, when considering local intensity changes, i.e. flux, to be the most important signal, then a blurrier stimulus provides less information than a sharper one.

A simple way of manipulating flux in a stimulus is to apply an amount of Gaussian blur. The

blurrier a border, the smaller the local flux signal. Gaussian blur is not identical to the dioptric blur commonly caused by defocus of the lens of the eye. However, given some assumptions, an approximate correspondence can be established.

7.2 Choice of eye tracker

As the effect of a difference in blur on fixational stability may be quite small, and predominantly borne out in the drift and tremor component of the eye trace both Eyelink1000 and AOSLO recordings were made. This was done, as the Eyelink1000 lacks tremor and drift resolution, while the AOSLO is better able to resolve those, but struggles with larger microsaccades. One advantage the AOSLO brings is that it effectively provides an objective assessment of the visual acuity of the observer. Only those participants with optimal or very close to optimal acuity can be imaged on the Oxford AOSLO, as the deformable mirror, which is used to correct any remaining optical aberrations in the image captured from the eye (note, this has no impact on the vision of the observer), can only compensate around a quarter of a dioptre. Participants therefore must wear an optical correction close to optimal. Thus, using the AOSLO to study the perception of Gaussian blur allows us to implicitly ensure good visual acuity, as any participants without adequate acuity (either corrected or uncorrected) are not able to provide images, and therefore eye tracking data, on the AOSLO. Therefore, the Gaussian blur in the image must only have been minimally altered by optical imperfections of the participants' eyes.

In principle for participants who are not presbiopic the different levels of blur may elicit different accommodative responses. However, as noted, the system can only tolerate (i.e. provide good retinal images) a discrepancy of up to ca 0.25 D between accommodation to the screen distance (for which the AOSLO was calibrated) and the accommodative state of the observer. Given that there were no consistent differences in tracking failures between the different blur conditions we have evidence that any accommodative response was small and would have had minimal effect on the retinal image blur of the targets.

7.3 Experiment One

In Experiment One blurry targets moved up and down, while eye tracking with the AOSLO and Eyelink1000 was done separately. This served as a pilot experiment for Experiment Two in this Chapter. Also data from the Eyelink1000 were used to train and test the binocular microsaccade detection method described in Chapter 3. The data from the AOSLO were not analysed, but

used to improve various stages of the AOSLO work-flow. Since the AOSLO data were collected for Experiment One, substantial updates to the AOSLO and AOSLO eye movement extraction mean that it does not represent the current capabilities of the AOSLO accurately and is therefore also unsuitable for the study of the influence of blur on fixational stability. Full details of the AOSLO procedure are given in Experiment Two.

7.3.1 Methods

Participants

Five participants completed the AOSLO part of this experiment. Seven participants completed the Eyelink part of this experiment. One had to be excluded due to bad tracking performance. Of the remaining six, two had participated in the AOSLO experiment. All had normal or corrected-to-normal vision and gave their informed consent before taking part in the experiment (CUREC Approval Reference: R56329/RE001).

Setup

All stimuli were displayed on a Display++ (Cambridge Research Systems) monitor with 10 bit resolution, driven by a ViSaGe++. The monitor was placed at a distance of 175 cm from the participant and subtended 12.8° x 17.3° .

Eyelink1000

When recording on the Eyelink1000 all recordings were made at 1000 Hz binocularly. Participants used a chinrest with a forehead rest to stabilise their head position.

Stimuli

The stimuli in this experiment were disks of three different levels of blur, with at least a single pixel displayed at maximum intensity, equated for overall luminance (see Fig. 7.2). The stimuli all had a FWHM of 19'. An estimation of the amount of blur in each stimulus compared to a completely unblurred stimulus was undertaken[1]. For this a few unknown quantities were estimated: the pupil size was estimated at 3.5 mm, and the display was assumed to be monochromatic at 550 nm. All stimuli were compared against a completely unblurred circle of the same FWHM. Based on these calculations the sharpest stimulus had 0.20 D of blur, the medium blurred stimulus 0.47 D and the blurriest 0.74 D.

[1] The estimation of blur was conducted by Dr Laura Young, a post-doc in the group.

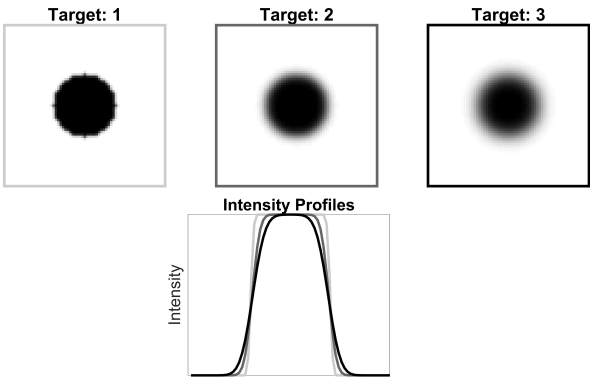


Figure 7.2: The stimuli used in this experiment and their corresponding luminance profiles. The bounding square around each stimulus is 48' (0.8°) while the FWHM of each stimulus is 19' (0.32°).

Procedure

Participants completed ten blocks of nine trials while being tracked on the AOSLO and 15 blocks of nine trials while being tracked on the Eyelink. Each trial lasted approximately 5.5 seconds followed by a 10 sec interval (for a graphic description, see Fig 7.3). During the break dynamic greyscale noise was shown. Before the onset of the target a placeholder was briefly shown for 1.2 s. Each trial consisted of the target being displayed for 2 s plus a random interval of up to 1 s. After this the target randomly moved up or down by either 3', 9' or 27' and stayed in this new position for 3 s. Participants were instructed to follow the target with their eyes. The starting position of the target was not randomised, so that for AOSLO eye tracking the stimulus would not shift outside of the created reference montage.

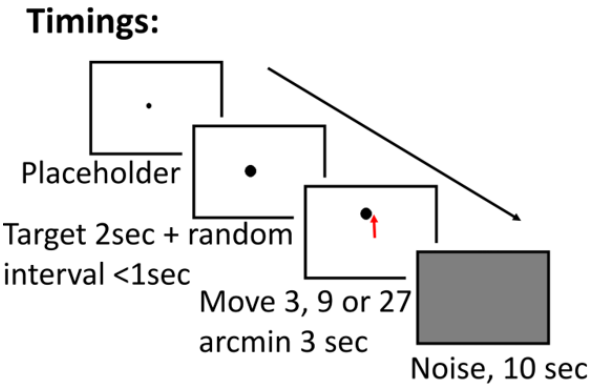


Figure 7.3: Timing of stimulus presentation during the experiment. Note that the target is marked as moving up, but it could have moved either up or down in Experiment One (and either left or right in Experiment Two) and the red arrow was not presented.

Data Analysis

The resultant eye movement data from the Eyelink1000 are smoothed using a Savitzky-Golay filter (framelength: 21 ms, order: 3). Blinks, as well as 200 ms before and 300 ms after each blink were removed to prevent recording artefacts caused by a partially occluded pupil to influence the analysis.

The first 0.5 s were also excluded from further analysis, as the stimulus onset was followed by a characteristic drop in microsaccade frequency. The data were separated into microsaccades and drift/tremor using the binocular correlation method for binocular Eyelink1000 data, with the same parameters recommended in Chapter 3.

Three stability factors were extracted: the frequency of microsaccades, the size of microsaccades and the root mean square (RMS) error. These were all calculated by taking the mean values across all trials for one participant in a given condition. Additionally, the time course of the RMS error was examined. No tests on statistical significance were undertaken, as there were not enough participants to average over.

7.3.2 Results

Visual inspection of the RMS errors within trials (Fig. 7.4) for the three different targets does not show any striking systematic trends in fixational stability related to target blurriness. The same is true for the RMS error over time both relative to the median within a 33 ms time period (Fig. 7.5) and the median within a trial (Fig. 7.6). For the RMS error over time, an initial a dip and a subsequent increase in instability can be observed.

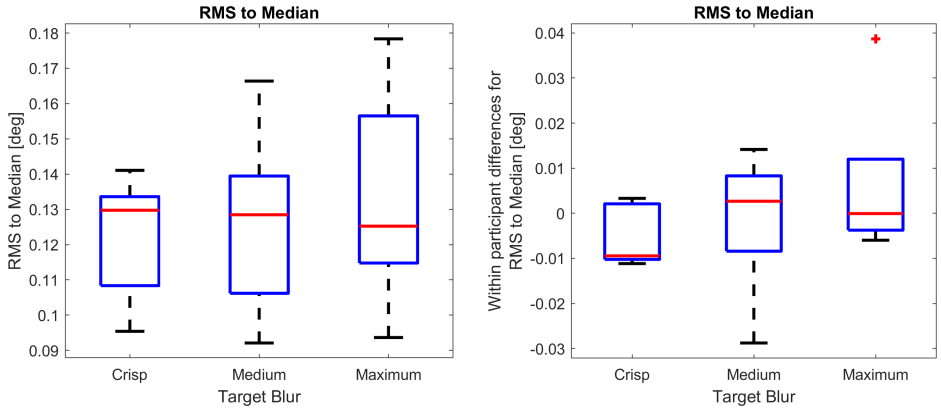


Figure 7.4: Box plots of the RMS error within trials of five participants in response to the blurry stimuli. On the right the box plot shows the effect across all participants, while on the left the effect within participants is highlighted.

7.3.3 Discussion

It is not possible to base firm conclusions on the data from these five participants, however the data do not confirm the hypothesis that more blur leads to less stability. As for the time course of the RMS error the initial spike in RMS can be explained by the participants finding their preferred fixation position on the target. The dip following this may be due to saccadic suppression following stimulus onset (Engbert & Kliegl, 2003; Rolfs et al., 2008; White & Rolfs, 2016) while the subsequent rise in RMS values most likely represents the baseline instability in fixation for the given targets.

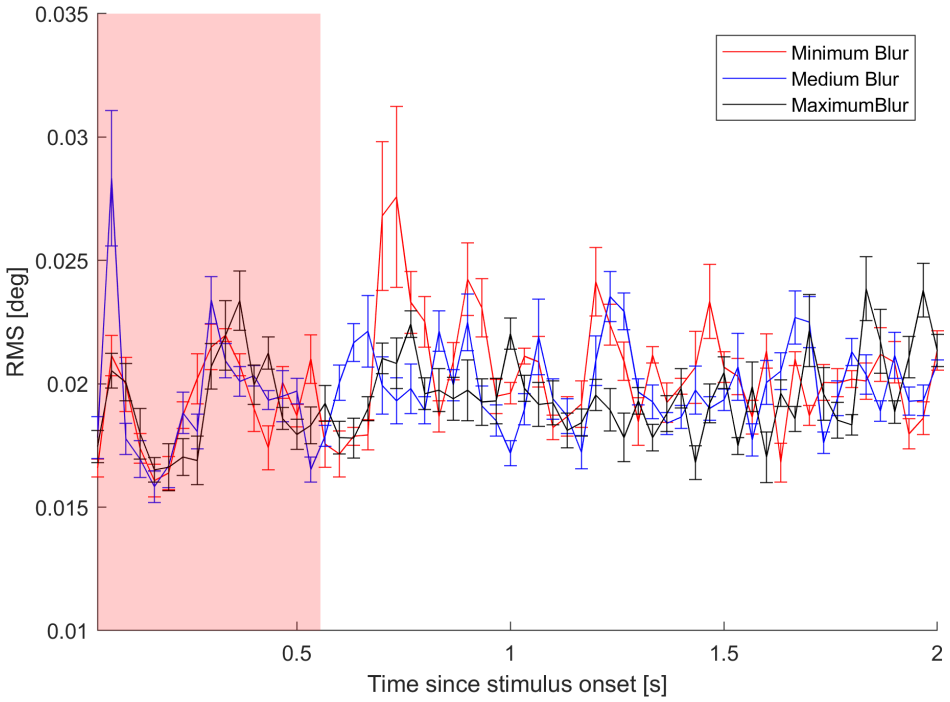


Figure 7.5: Local RMS error over time across five participants. The error was calculated over successive 33 ms periods relative to the median of the same time period. The error bars represent the standard error of the mean. The red shading indicates the beginning of the trial, which was excluded from all other analyses. The red line represents the RMS over time for the target with minimal blur, the blue line refers to targets of medium blur , while the black line indicates targets of the maximum amount of blur.

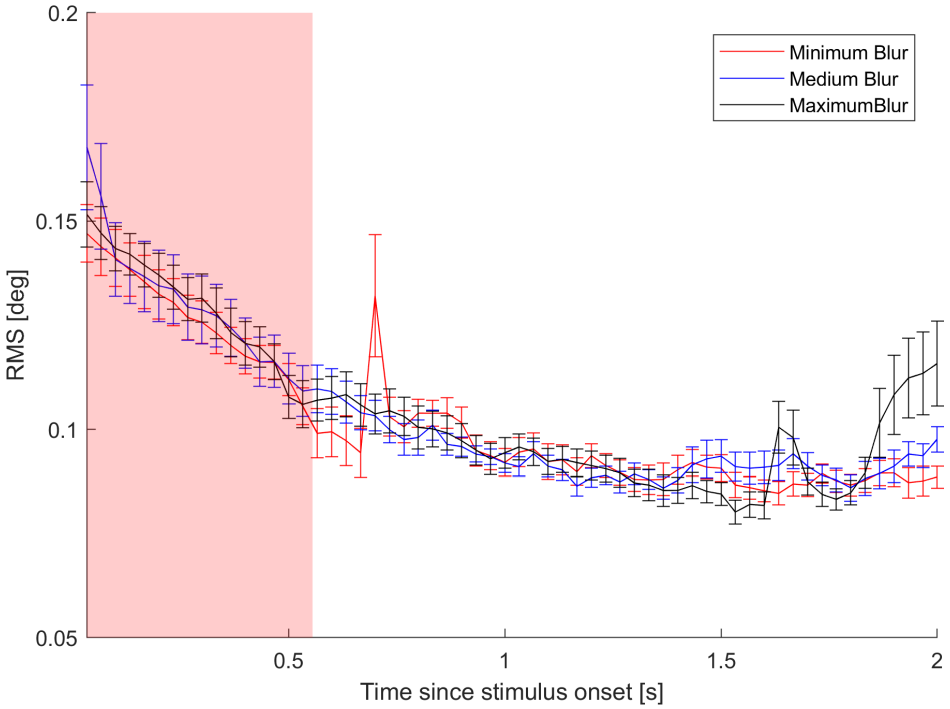


Figure 7.6: Global RMS error over time across 5 participants. The error was calculated over 33 ms relative to the median of the whole trial. The error bars represent the standard error of the mean. The red shading indicates the beginning of the trial, which was excluded from all other analyses. The red line represents the RMS over time for the target with minimal blur, the blue line refers to targets of medium blur , while the black line indicates targets of the maximum amount of blur.

As no clear trend is shown it is worthwhile investigating any potential differences with more participants on a higher accuracy eye tracker. This prompted Experiment Two in this chapter.

7.4 Experiment Two

In Experiment Two the blurry targets moved horizontally and, for the first six participants, when possible, eye tracking was done simultaneously on the same eye with both the AOSLO and Eyelink1000. The change from vertical to horizontal movement was made as it was established that large shifts in eye position are more easily extracted from AOSLO data when they are horizontal, due to the asymmetry in the vertical and horizontal scan pattern. This is also more applicable to the study of microsaccades which predominantly fall along the horizontal (Moshel et al., 2008). The Eyelink data collected in this experiment are not discussed further here, as it was collected to compare the AOSLO and Eyelink traces in Chapter 2.

7.4.1 Methods

Participants

A total of 14 participants completed this experiment. All gave their informed consent (CUREC Approval Reference: R62306/RE001) and had normal or corrected-to-normal vision. The data from the first six participants were collected by the author, while the subsequent eight participants were tested by Allie Hexley, a DPhil student in the lab.

AOSLO

When using the AOSLO for eye tracking, the 16 010 samples/second sampling rate was downsampled to 1000 samples/second to reduce noise. To ensure sufficient stability of the head position custom bite bars were made for each participant. At the beginning of each recording session an oversized reference frame of the retina was created to improve eye tracking quality. This reference frame covered twice the area of the normal AOSLO scanpatch, i.e. increasing in size from 1.6 x 1 ° to 3.2 x 2 °Ṫhese images were later used to manually create an oversized reference frame for motion extraction. The AOSLO was set up to record in bursts of 5 sec. However, due to the scanning mirror properties, a few samples (approximately 3 ms) are lost during each flyback region, approximately 30 times a second.

All participants had a bite-bar fitted and a for the creation of a reference montage a grid of the retina around the desired tracking position was imaged.

Setup

The Eyelink1000 was positioned on the same optical table as the AOSLO. Safety calculations for the combined exposure from the AOSLO photodiode and Eyelink1000 LED illuminating panel were

completed. It was determined that over two hours of continuous imaging with a 9 mm pupil a total of 15% of the maximum permissible exposure (MPE) would be reached when combining light from the AOSLO with a power of 100 μW (11.7 % of MPE) and the light from the LED panel with a partial cover on it (3.3 % of MPE). These are conservative estimations, as imaging with the AOSLO and Eyelink simultaneously was usually around 1h of imaging and participants were instructed to keep their eyes closed during trial breaks. Also, most participant's pupils were below 9mm in diameter, due to the comparatively high light levels in the room during the experiment. Lastly, laser power was kept well below 100 μW during the experiment with most being around 80 μW. It is unclear how much light exposure would damage individual participants, however the MPE is defined to be 10% of the amount of light that has a 50% chance of damaging the tissue in the eye in any way. Staying below 15% of that exposure is considered safe.

All other aspects of the setup with regards to display and stimuli were identical to Experiment One in this chapter.

Procedure

The procedure was identical to the one described in Experiment One, apart from a deviation at the beginning of the trial. After a trial break the experimenter manually triggered the next trial while monitoring the AOSLO image quality, to increase the probability that the data collected for a given trial were going to result in a usable eye movement output.

Data Analysis

Manual montages were created for each participant. Of those, three montages were completed by other members of the lab.

All tracking failures in the AOSLO data were manually removed before analysis. For a detailed explanation of this process, please refer to Chapter 2. Then the residual motion within each frame in a trial was subtracted from each frame in that trial.

To assess fixational stability RMS error and RMS error over time were used. Direct measures relating to microsaccades were dropped, as the AOSLO fails to adequately track larger microsaccades (see Chapters 2 & 4). As such this would have overly biased these measures.

7.4.2 Results

Three participants were excluded, because too much data were missing from more than 1/3 of trials (see Fig. 7.7). One further participant (P10) was excluded after further analyses, as their data

represented an implausibly large outlier, leading to violations of the normality assumption.

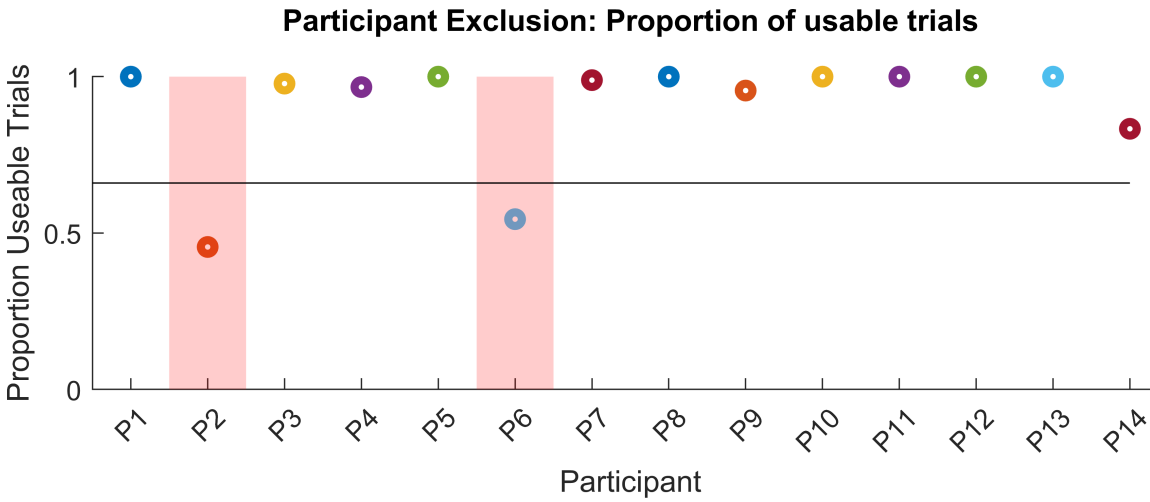


Figure 7.7: Figure showing which participants were automatically excluded due to too much missing data. One further participant P10 was excluded, as their data were too large an outlier.

Comparing the mean number of missing samples from each of the blur conditions using a one-way repeated-measures ANOVA, no significant difference was found ($F(2,10) = 1.232$, $p = .308$, $\eta^2 = .087$).

The one-way repeated-measures ANOVA test for the RMS error within trials (Fig. 7.8) showed no significant difference between the 3 groups ($F(2,10) = 0.537$, $p = .593$, $\eta^2 = .051$). Considering the RMS error of the consistency of fixation position across trials (Fig. 7.9), again, no main effect was found ($F(2,10) = 1.437$, $p = .261$, $\eta^2 = .126$)

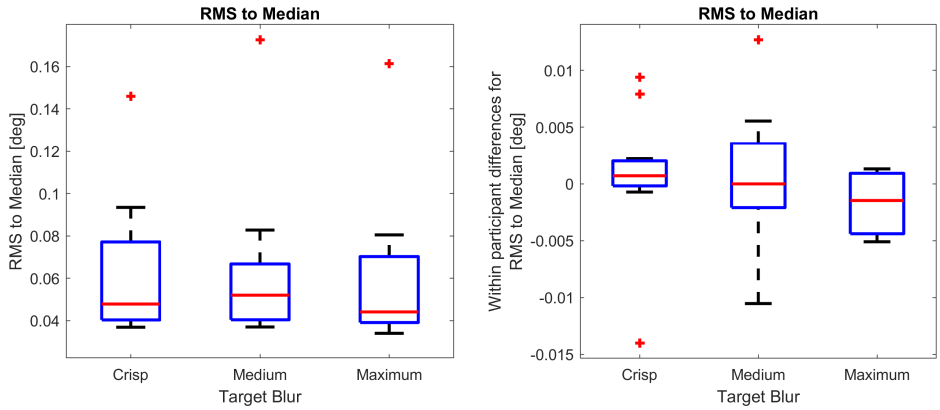


Figure 7.8: RMS error within trials of 11 participants in response to the blurry stimuli. The left hand panel shows the data across participants and the right hand panel shows the data within participants.

The local (Fig. 7.10) and global (Fig. 7.11) RMS errors over time were also plotted. Both graphs exhibit initial drops in the RMS value after stimulus onset that occur within the time period excluded from further analysis. The graph of the local RMS, which shows the in-frame RMS error compared to the median of the same frame does not appear to show any consistent trends for the three different target blur levels. The global RMS error over time, calculated as the RMS error within a frame

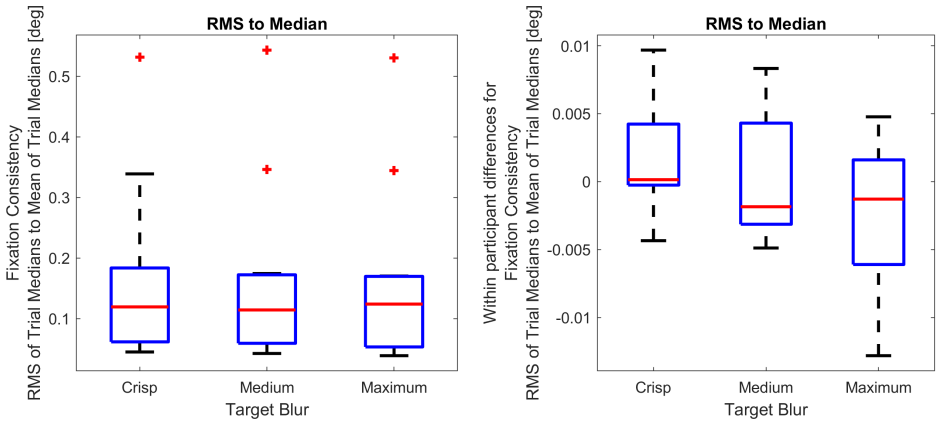


Figure 7.9: RMS error across trials within trials of 11 participants in response to the blurry stimuli. The left hand panel shows the data across participants and the right hand panel shows the data within participants.

compared to the trial median position, shows a similar picture of no consistent trend in which blur level leads to the lowest RMS error.

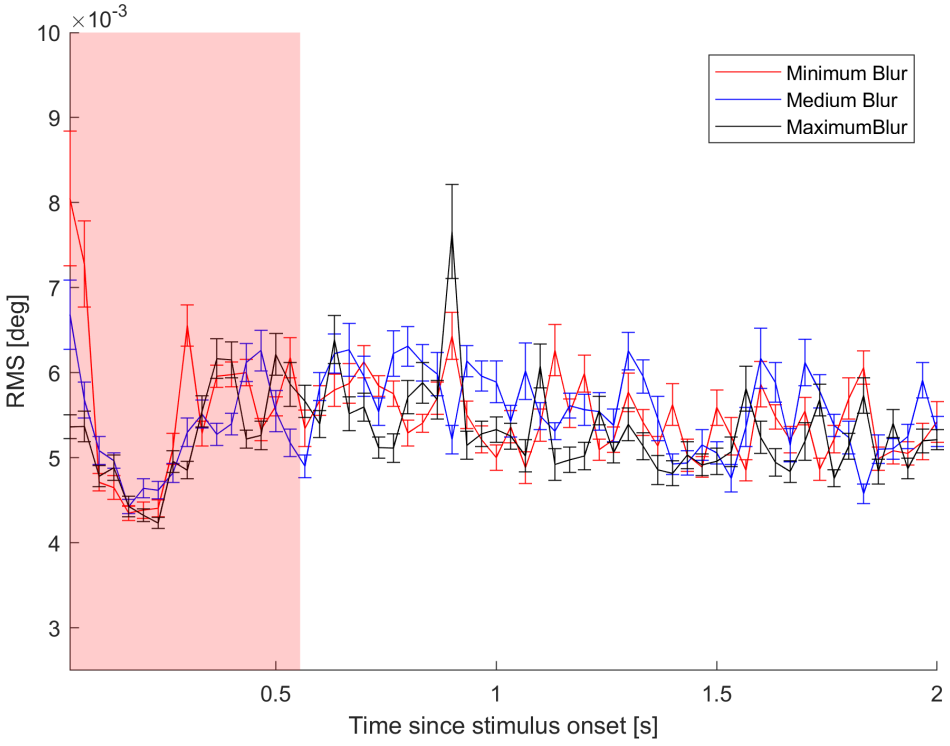


Figure 7.10: Local RMS error over time across 11 participants. The error was calculated over 33 ms relative to the median of that time period. The error bars represent the standard error of the mean. The red shading indicates the beginning of the trial, which was excluded from all other analyses. The red line represents the RMS over time for the target with minimal blur, the blue line refers to targets of medium blur , while the black line indicates targets of the maximum amount of blur.

7.5 Follow Up: Experiment Three

A brief follow-up experiment was conducted in which eight participants were asked to indicate the centre of the three blurry stimuli with a mouse click. Each stimulus was presented a total of 10 times for a maximum of 10 sec in the same experimental setup as described for the Eyelink data in

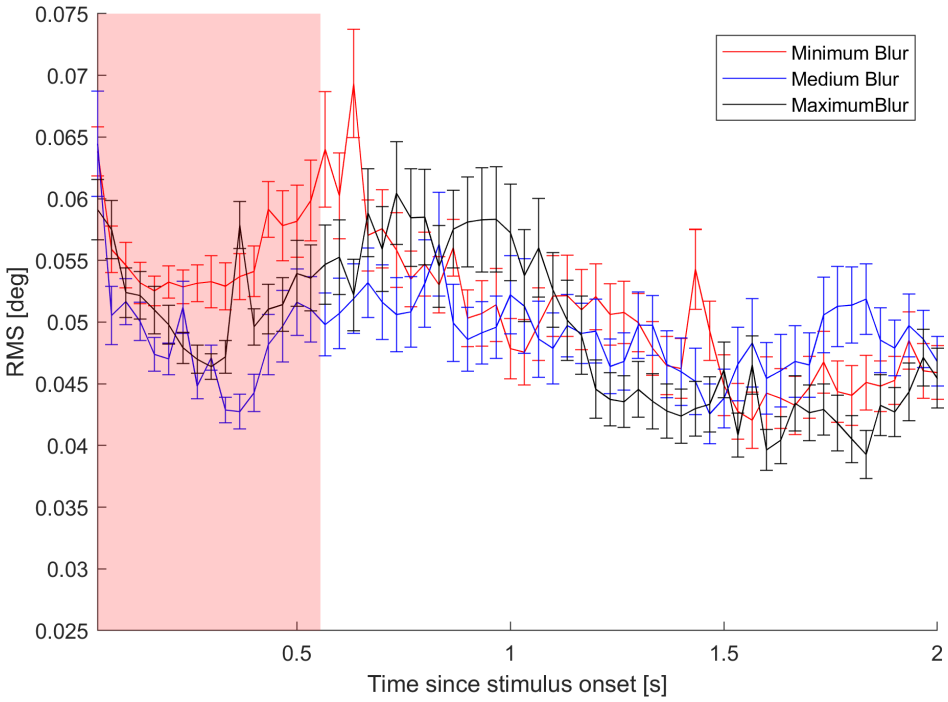


Figure 7.11: Global RMS error over time across 11 participants. The error was calculated over 33 ms relative to the median of the whole trial. The error bars represent the standard error of the mean. The red shading indicates the beginning of the trial, which was excluded from all other analyses. The red line represents the RMS over time for the target with minimal blur, the blue line refers to targets of medium blur , while the black line indicates targets of the maximum amount of blur.

Experiment One in Chapter 7. The total distance from the centre of the stimulus to the estimated centre was calculated per trial and then averaged. When comparing the mean estimates of the eight participants using a repeated measures one-way ANOVA a significant difference between the targets was revealed ($F(1,7) = 6.875$, $p = .034$, $\eta^2 = .496$). Follow-up paired t-tests revealed that only the difference between the crispest stimulus (M = 1.30, SD = 0.43) and the blurriest stimulus (M = 1.47, SD = 0.36) is significant ($t(7) = -2.6221$, $p = .034$, $d = 0.436$) (Fig. 7.12). The difference is not clearly visible in the figure as the ANOVA considers within subject variation, while the figure shows the data averaged across participants.

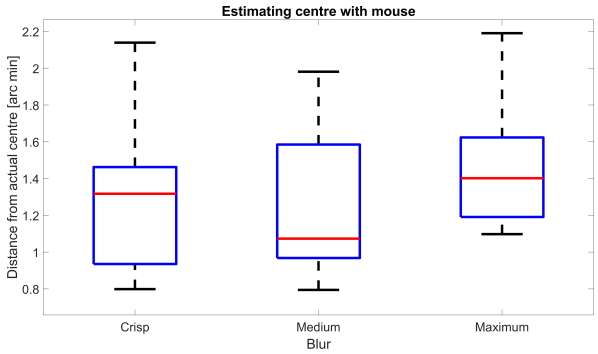


Figure 7.12: Box plots of the stimulus centre estimates using mouse clicks. Ten centre estimations were collected for each blur level from each participant and the mean distances from the actual centre were averaged and are given here.

7.6 Overall Discussion

Both the pilot Experiment One, and Experiment Two, on the influence of blur on fixational stability failed to provide any evidence that blur affects fixational stability. This is somewhat surprising, given that previous reports suggested such a relationship to exist (Ukwade & Bedell, 1993; Vikesdal & Langaas, 2016) as well as the fact that other aspects of the visual stimulus, such as eccentricity and orientation do influence stability.

There are several possible reasons why these experiments have failed to show a systematic difference in fixation behaviour. One possible reason for this is that the error signal determining fixational stability is not triggered by the amount of local flux in an image. An explanation consistent with the fact that grating orientation influences the amount of error in a given direction from Experiment Two in Chapter 5 would be that rather than using transient signals to estimate positional error, the visual system estimates a desired fixation position based on the two-dimensional shape of the stimulus. If the stimulus is asymmetric, like the bars of the grating, then the estimation of the centre point is less accurate in the direction in which the borders fall more eccentrically. As the stimuli used here are symmetrical and not of substantially different spatial extents this could explain why no difference in fixational stability was observed. An account of fixational stability that takes into account centre estimation is also consistent with the findings from Chapter 6, as the estimation of the centre of the stimulus using the mouse was a significant predictor of the RMS error of the eye trace for a given target. For this experiment the results of the follow-up experiment 3 tested this and revealed only a very small increase in centre estimation error, which may account for why no significant difference in eye stability was found.

Another possible reason for the null findings in this chapter may be that the stimuli were simply too similar and that more extreme levels of blur may be required to have a noticeable effect on fixational stability. It is known that humans can tolerate relatively moderate amounts of blur during daily activities, Chung, Jarvis and Cheung (2007) were able to show that around 2D of spherical refractive error did not lead to severe impairments in reading performance, which is substantially more blurred than the stimuli used in this experiment. Additionally, all targets were comparatively small, with borders falling close to the fovea, such that, even though blurry, the retina may have been sensitive enough to extract sufficient information about position from the available data.

7.6.1 Natural occurrence of blur during fixation

One reason it is interesting to study blur is that it is the most common reason for sub-optimal vision in the population: refractive error. The most common types of refractive error are spherical errors

such as myopia, or near-sightedness, and hyperopia, or far-sightedness. Another common cause is astigmatism, in which the amount of defocus is greater along one meridian. These refractive errors can usually be corrected with glasses or contact lenses.

Humans are very sensitive to blur, with the just noticeable difference in blur falling somewhere around the 0.3D mark (Atchison, Fisher, Pedersen & Ridall, 2005). However, levels of tolerable blur are much higher and depend on personal preference and task. Most humans have some level of refractive error with 76 % of US adults wearing some form of vision correction according to the Vision Council of America and studies showing that around 60% of people have a measurable level of astigmatism (Satterfield, 1989). A population study in Finland examining the habitual levels of visual acuity revealed that while in the under 75s a large proportion of the population have vision equal to or better than 20/20, more than 15 % of adults have visual acuity worse than 20/20 rising to more than 75% in the over 75s. Not all of the impairment in visual acuity in this study will be caused by optical errors giving rise to blur in the image. However, it can be assumed that a large proportion of it will be due to uncorrected refractive error. Yet what amount of blur merits correction is a personal preference, with humans being able to perform day-to-day tasks including ones requiring near and far vision such as reading and driving with some ease even with some dioptric blur. Chung et al. (2007) examined reading speeds of observers while varying defocus from 0D to around 4D. Up to around 2D of spherical refractive error did not lead to severe impairments in reading performance. Even when no refractive error is present any object not at the distance the eye is focussed at, will be out of focus and (for younger participants who are not yet presbiopic) accommodation may be used to bring the object into focus.

Refractive error usually remains temporally constant over large stretches of time, allowing the observer to adapt to their individual level of visual acuity. In all experiments that induce refractive error in the participants or visual stimuli, the onset of said error is sudden compared to the development of real refractive error. Therefore only limited conclusions can be drawn about the behaviour participants would exhibit if they had time to adjust to those levels of refractive error. In the proposed experiment blur is used as a way of manipulating the amount of flux in a given retinal location caused by the movement of the eye across the stimulus. Any differences in fixational eye movements in response to stimuli of different levels of blur may hold true for induced blur, however may not extend to scenarios in which this level of blur is constant. A way of adapting fixational eye movements to a constant level of blur may be to up-regulate the relative contribution of other information about eye position and down-regulate information based on flux.

To further probe the role optic flux plays in fixational stability further experiments are needed.

One way to extend the findings from this experiment would be to include more drastic levels of blur, or, alternatively, to change the amount of visual flux by other means. One option would be to increase flux by using targets with irregular sharp borders. Another factor to manipulate would be stimulus size, as there may be sizes, corresponding to retinal eccentricities,for which differences in flux may show greater effect.

Chapter 8

Position Correction due to Microsaccades and Drift

Abstract

The part of the eye movement trace that is chiefly responsible for keeping our eyes on target remains a topic of debate. Microsaccades have long been proposed to correct for the random error introduced by drift, however, evidence of long, stable fixations without microsaccades contradicts this claim. In this chapter, eye movement traces collected during fixation tasks are examined. The corrective power of both the microsaccade and drift components is assessed using a range of new measures for this purpose. It is found that drift has significant corrective properties. In the future it would be useful to further examine the temporal aspects of the interplay of microsaccades and drift.

8.1 Historical Debate

Ever since different parts of the fixational eye movement trace have been described, researchers have asked questions about the purpose of and interaction between the different types of movement. As large saccades help us relocate our line of sight to targets of interest, it is an obvious extension to assume that microsaccades would serve a similar purpose on a smaller scale, i.e. that microsaccades would relocate our gaze to the desired target position after it had moved away from that position due to drift. The popularity of this proposal is apparent in the following passage from Boyce (1967)(p. 294):

> *The most widely accepted model of the fixation control system postulates that fixation is maintained by the operation of a simple position-control servomechanism. Owing to*

> *instability in the oculomotor system the visual axis drifts away from the target thereby producing an 'error', i.e. a disparity between the desired direction and the actual direction of the visual axis. This error is reduced by a saccadic eye movement.*

This theory has enjoyed an undue amount of popularity, given the weight of historical evidence contradicting it. One reason it has proved popular to this day is that other information about drift and microsaccades seems to tie in well with it. It appears plausible that microsaccades should be the only correcting factor, given that they are the only type of eye movement for which there is any firm evidence that it may be, in part, supported by subcortical brain regions and perhaps the cortex. With access to visually-based, proprioceptive, and motor signals the cortex would presumably be able to determine that the eye position has strayed from its desired point and trigger a signal for a microsaccade to correct this. Even without cortical input, the binocular nature of microsaccades suggests some extra-ocular inputs, while drifts have typically been described as being uncorrelated between the two eyes (Krauskopf, 1960), suggesting no extra-ocular input. Because of this drift has often been hypothesised to be nothing but slight noise in the eye muscles. However, there is some evidence that drift may exhibit some relationship across both eyes (for a review see Rolfs, 2009).

The evidence that this view of microsaccades correcting positional error introduced by drift is wrong has been available for some time. Steinman et al. (1967) were able to demonstrate that participants could voluntarily reduce their microsaccade rate without training, simply by following task instructions. During those longer intervals without microsaccades no great positional error was induced, counter to what would be expected if drift was the cause of error that could only be corrected by microsaccades. Nachmias (1959) was also able to show, that while microsaccades corrected some errors in some directions, in other directions the positional correction due to drift was "appreciable". Moreover, he found that the amount of positional error was a worse predictor for microsaccade occurrence than the amount of time that had passed since the previous microsaccade. More recently Cherici et al. (2012) found that drift appeared to be the main component keeping the eyes on target, not microsaccades. Similarly Poletti et al. (2013) found that when removing microsaccades, the remaining drift motion did not significantly deviate from the centre of the screen, which they chose as a reference point. In combination the available evidence suggests that, while microsaccades do somewhat correct position, the same is true for drifts. Also the (in-)ability of microsaccades to correct positional error is not their main feature of interest.

8.2 Defining Drifts and Microsaccades

When comparing drifts and microsaccades it is important to be clear about how both of these movements were defined as different methods and assumptions may lead to drastically different

results. Defining what is meant when referring to a microsaccade is simpler compared to drifts, as microsaccades visually stand out from the eye movement trace as small, abrupt shifts in position. However, defining drift is not as simple. Historically it was accepted that drifts inhabit the space between two saccades (Nachmias, 1959), but for the purpose of measuring drift this method was rarely used. It was more common to select parts of the eye movement trace of a fixed duration at fixed intervals, checking that these do not contain microsaccades (e.g. Nachmias, 1959, 1961; Cornsweet, 1956). Doing this, however, loses a lot of information about drifts, as their meandering movements (Cherici et al., 2012) can not be adequately expressed by completely straight lines. Therefore removing potentially large parts of them at the beginning and end of the drift movement, makes it unlikely that one can accurately predict the start and end points of the drift by the remaining movement. Most surprisingly, however, the same papers also discuss drift rate, which should be identical to microsaccade rate, but do so while not recording single drifts, but rather fixed intervals containing drift.

Today, with the help of automated microsaccade detection methods the central problem of defining microsaccades and drift does not disappear. Careful considerations need to be made before comparing these two features of the eye movement trace. Classification-induced over or underestimation of microsaccade length may significantly influence the results of a comparison. For example, by underestimating microsaccade length the first and last samples, which may be used to calculate positional improvement in relation to the movement, may be assigned to drift when they in fact belong to microsaccades. This has the potential to make a movement appear more or less corrective than it really is. One way to counteract this effect is to manipulate how conservative the automated detection method is at identifying microsaccades. By comparing more liberal with more conservative measures both the length and number of identified microsaccades may change. If this manipulation leads to different outcomes, it suggests that microsaccade detection for this purpose would best be done manually to avoid any detection-method bias. Manual ratings are not bias-free, but are the best available method to assign microsaccade labels.

8.3 Measures of Corrective Power

A central problem for determining how effective a certain type of movement is for correcting gaze position is the type of measure used to quantify corrective power. This is because most features of the trace only tell a part of the story. For the purpose of this Chapter we will assume that the median measured fixation position during a consecutive recording of eye movements in response to the same stimulus is the desired *centre* of fixation. Selecting the median fixation position is desirable

compared to selecting the centre of the visual target, as eye trackers usually lack the calibration accuracy required to use this measure. Also participants will choose individual preferred fixation points, which may not fall in the centre of the stimulus, but on some other part of it. Additionally their preferred retinal locus may not align perfectly with the visual axis measured by most eye trackers. Choosing the median of fixation also protects the analysis from outliers in eye position, unlike selecting the mean, as done by Cornsweet (1956).

8.3.1 Measures used in previous research

Historically, papers assessed whether or not microsaccades corrected for drift by a range of measures. The most common ones are:

- Distance from the centre of fixation when a movement is initiated.
- Difference between the distance from the centre of a movement at the start compared to the end of a movement.
- Angle with regards to the centre of fixation that a movement goes out in.
- Rate of occurrence of this movement during different stimulus conditions (e.g. a movement occurring more during stabilisation may be seen to attempt to counteract fading, but not for correcting position, as during fading the position of the stimulus on the retina is constant).

A further suggestion is to calculate whether there was a set distance from the desired fixation position which triggered a saccade (St. Cyr & Fender, 1969). If there is a set distance this implies that the movement is corrective in nature and triggered by retinal image shift. However, Nachmias (1959) was able to show that while there was some predictive power in the distance from the desired fixation point, the time since the last microsaccade was a much bigger predictor. This, in turn, suggests that microsaccades are not primarily triggered to correct errors in fixation position. A second measure used in previous texts is the direction of the movement relative to the desired fixation point (e.g. Cornsweet, 1956).

The reason why none of these approaches are ideal is that they capture very little about the actual movement. Simply how far the eye was from desired fixation when the movement started, or the angle at which it moved, does not reveal if the following movement actually corrected for eye position. It is entirely possible, that the movement over- or undershot the target significantly. Therefore more complex measures should be considered, which relate the movement back to the desired point of fixation.

Any method of quantifying the corrective power will be flawed, as it is impossible to capture all features contributing to how corrective a movement is. These factors include not only the size and direction of the movement, but also the shape of its path (Does it turn back on itself? How much does it meander?), the relative position of the desired target location, and the time-course of the different movements.

8.3.2 Measures used in this Chapter

Start-To-End-Error

The simplest measure that captures something meaningful about the corrective power of a movement is to calculate a ratio between the distance to the centre of fixation from the start of the movement and from the end of the movement. This is a modification of a measure used by Cornsweet (1956), which calculated the change in distance, but not the ratio. That way if a movement was correcting it will have a value greater than 1, if it was neutral it will be exactly one, and if the movement has increased the distance to the centre of fixation it will be a value below 1 (see Fig. 8.1). This measure will be called the Start-To-End-Error.

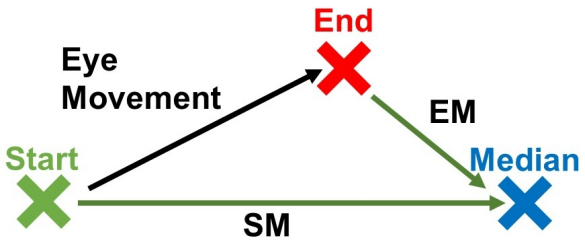


Figure 8.1: Graphical explanation of the Start-To-End-Error measure. To obtain the ratio between the distances from the start of the movement to the median of fixation and the end of the movement to the median of fixation the ratio of $\frac{|SM|}{|EM|}$ is taken.

Movement-Towards-Median

To compare movement directions and amplitudes relative to the median of fixation, all movements were normalised so that the ideal movement towards the median would be represented by a motion vector between 0,0 and 0,1 and the recorded movements are expressed relative to this (for a graphical representation of this please refer to Fig. 8.2). The Movement-Towards-Median is then given by the distance along the axis of the median needed to reach the end point of the actual movement when drawing a line with a right angle to the axis of the median. From this new representation of the movements it is possible to compare both movement direction and magnitude of movement. This measure will be referred to as the Movement-Towards-Median.

While it is possible to represent the Movement-Towards-Median graphically, any formalised

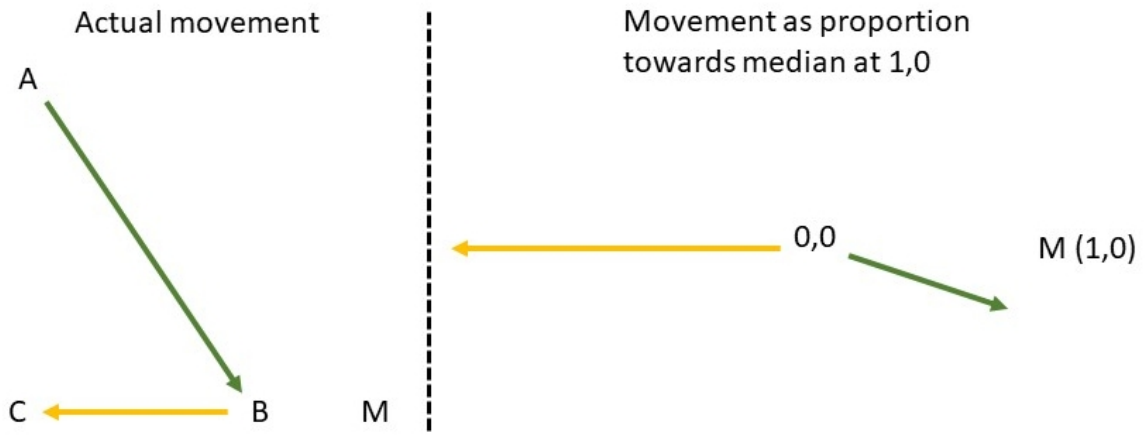


Figure 8.2: Graphical explanation of the Movement-Towards-Median measure. On the left two movements are plotted between points A and B and B and C as they were recorded. On the right the same two movements are plotted as their Movement-Towards-Median measure. This measure fixes the optimal movement as a movement originating from 0,0 out to the median at 1,0. All movements are scaled in relation to the optimal movement for both direction and magnitude.

analysis will be broken down into the direction and magnitude component. When comparing the movement direction the most obvious choice is to use circular statistics and compare if the mean direction of the drifts/microsaccades is different from the direction of the optimal movement towards the median. However, circular statistics are more difficult to perform, as there is less information on them available and fewer statistics packages supply implementations of these tests. In this thesis the circular statistics toolbox for MATLAB is used (Berens, 2009). Before using parametric tests in circular statistics, it has to be established if the data follow a von Mises distribution (similar to a wrapped normal distribution and the assumed underlying distribution for parametric tests on circular data). To test if this assumption is met, a Rayleigh test (circ_ rtest) is performed and if the null hypothesis is rejected, the data can be assumed to stem from a von Mises distribution. To test if a distribution of angles is significantly different from a reference angle a mean angle test can be conducted (circ_ mtest). To establish if two distributions of angles are different from each other a Watson-Williams test can be used (circ_ wwtest).

Other than for display purposes the magnitude of this movement will not be further analysed. Instead the Optimal-Achievable-Movement, a related measure described in the next paragraph, will be used.

Optimal-Achievable-Movement

To compare movement magnitudes a new metric called the Optimal-Achievable-Movement was devised. This metric is calculated by representing the optimal movement towards the median by a movement from 0,0 to 1,0 and scaling the actual movement accordingly. The actual movement

is then projected onto the axis on which the optimal movement lies by dropping a perpendicular line from the end point of the actual movement onto the meridian. The resulting line between 0,0 and the intersect is called the Optimal-Achievable-Movement (see Fig. 8.3). In this way the best possible outcome is an Optimal-Achievable-Movement of 1, which would mean that the eye moved an optimal amount towards the target, given the direction of movement. It would have a score greater than 1 if the eyes overshot and between 0 and 1 if the eyes undershot. Any movement with a score smaller than 0 went in the opposite direction to the median and did not have the opportunity of improving fixation.

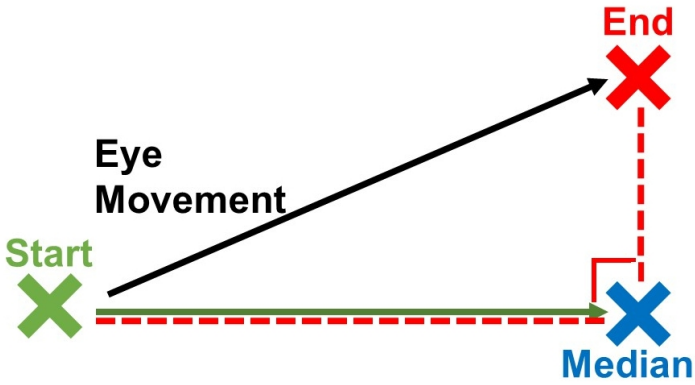
Statistical tests on the Optimal-Achievable-Movement can be conducted in two ways. Either a movement is compared to the reference of 1 with the null hypothesis: The movement's Optimal-Achievable-Movement is not significantly different from the optimal score of 1. Or the Optimal-Achievable-Movement can be compared between two different groups, e.g. microsaccades and drift.

8.3.3 Missing Information

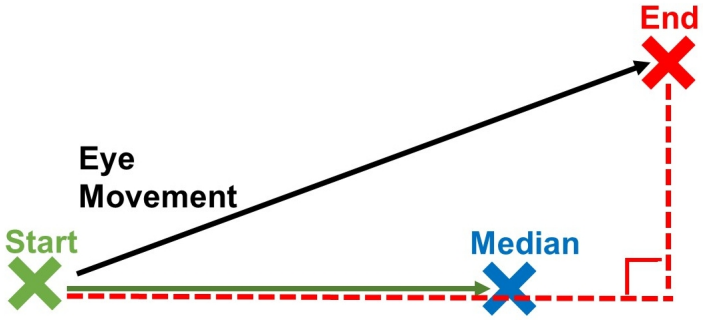
Of course, these measures do not completely capture how corrective either microsaccades or drift, or any type of movement is, but they capture a lot of the available information. One missing piece of information is the time course of these movements. Examining the time course may reveal if either microsaccades or drift correct for the other, or if a more intricate interplay takes place. If indeed microsaccades were correcting for drift then they would be triggered once a certain deviation from the desired position had occurred. The same is true, if it is in fact drift that is the more correcting component. One can imagine a scenario in which microsaccades disrupt the drifting of the eye without having any positive effect on the overall centredness of the eye trace. In that case the microsaccade trigger is unrelated to the eye position in relation to the centre of fixation and again, the time course of these movements would be irrelevant.

Another piece of missing information is the interplay between both eyes in maintaining fixation as discussed in St. Cyr and Fender (1969). With the video-based eye tracker used to collect the data in this Chapter, it is unlikely that such fine differences would be represented well enough for analysis. This type of analysis also depends on such highly accurate calibration that it would be an ambitious undertaking to achieve even with highly accurate data from both eyes, as choosing the central reference points for each eye becomes even more important.

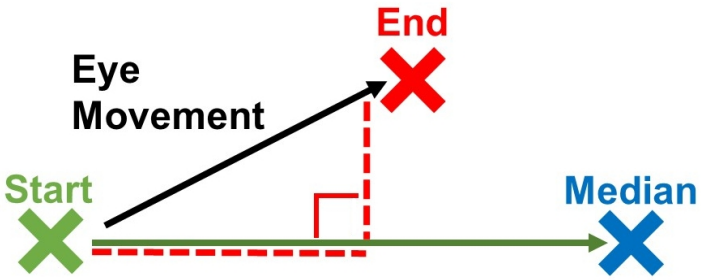
Given previous reports of microsaccades not being closely linked to corrective movements it is expected that while microsaccades may display some corrective power, drift will also display



(a) Example of movement where the actual eye movement is projected optimally onto the optimal movement. This scenario should result in a numeric value equal to 1.



(b) Example of the actual movement of the eyes overshooting. This scenario should result in a numeric value greater than 1.



(c) Example of the actual movement of the eyes undershooting. This scenario should result in a numeric value between 1 and 0.



(d) Example of the actual movement of the eyes going in the opposite direction of the target and therefore inducing error into the position. This scenario should result in a numeric value smaller than 0.

Figure 8.3: The four possible outcomes of calculating the Optimal-Achievable-Movement.

non-negligible corrective properties. Nachmias (1961) showed that it is not microsaccades alone that are influenced by the stimulus, but also drift. Therefore it is reasonable to expect that drift, too, can correct for fixation position in response to visual information. Based on previous reports of drifts alone being able to maintain a line of sight (e.g. Deubel & Elsner, 1986; Winterson & Robinson, 1975; Steinman et al., 1973), it can be assumed that the corrective power of microsaccades and drift

is at least equal, if not tipped in favour of drift.

8.4 Methods

8.4.1 Data

The eye movement data analysed for this experiment are the same as the data collected for Experiment One in Chapter 5. All the same data pre-processing steps apply, including data smoothing and microsaccade detection. This results in a total of 19 participants from Experiment One and 20 participants from Experiment Two. Of those 14 participated in both experiments, resulting in a total of 25 unique participants. To avoid sampling eye movements twice from the same participant, for the 14 who had participated in both experiment data from one was selected at random to be included in this analysis. Over 60 000 microsaccades were available for analysis.

8.4.2 Data Analysis

Microsaccades were defined as those movements selected as microsaccades by the binocular correlation method (ρ = .45 and ω = 65 ms). Drifts were determined to be all those eye movement samples not assigned to a microsaccade. The first and last sample in a movement trace were determined to represent the start and end point, accepting any potential overshoot, undershoot or error in how exact the determination of the last data sample is.

To counteract effects of the bias within the detection method three different versions were used for which different numbers of samples either side of a detected microsaccade were removed. The factor to determine this value is typically set to 2, but this leads to some underestimation of microsaccade size compared to a human observer (see Chapter 3). When the factor is set to 2, exactly half of the detected elevation in correlation is removed (a quarter either side). When the factor is set to a larger value fewer samples are removed as this factor is calculated by $\frac{\omega}{factor}$. Therefore two more liberal values were also used: 2.25 and 2.5.

Three different measures of how corrective a movement is were calculated:

1. Start-To-End-Error: The ratio between the distances to the centre from start to end position.

2. Movement-Towards-Median: The direction of the movement towards the centre of fixation, calculated as the angle of the line connecting the start and end position.

3. Optimal-Achievable-Movement: The component of the movement that follows the optimal movement.

Paired, Bonferroni-corrected t-tests were performed on the results of the 25 participants on the Start-To-End-Error and the Optimal-Achievable-Movement, after normality was established. As the Movement-Towards-Median is angular, circular statistics have to be used. Firstly it was established whether or not the data followed the von Mises distribution, which is the assumption about data distribution necessary to use parametric circular statistics. For this a Rayleigh test was used. Then a test on the mean direction of the samples relative to the reference direction towards the median was conducted.

Additionally the cumulative distributions for the Start-To-End-Error and the Optimal-Achievable-Movement are given. These plots allow as to compare how these measures change across their range, and if there are large differences in this behaviour between participants or microsaccades and drifts. The other tests compare only the central tendency of the distribution (mean or median, depending on the statistical test used), however, that does not allow for comparison of the shape of the distributions. To generate these cumulative distributions the distribution of all movements of all participants was first calculated, after the extreme outliers, the top and bottom 1% of data were excluded. Then this distribution was divided into 10 000 bins and each individual participant's data were sorted into these bins cumulatively. As these 10 000 bins still include some outliers, the graph limits represent the middle 80% of all data samples.

Heat maps of the two-dimensional distributions of the actual distances and angles of the movements compared to the optimal distances and angles are also given. In these plots a line of gradient 1 crossing though 0,0 would indicate the best possible angle or distance to move in, if only distance of direction was considered. The colour map chosen is a perceptual colourmap distributed by Kovesi (2015) (https://peterkovesi.com/projects/colourmaps/) under the name *CET-C2*.

8.5 Results

8.5.1 Start-End-Error

The Start-End-Errors of the 25 participants were first tested for normality using a Kolmogorov-Smirnov test, which showed that the data were not-normally distributed. As the data were right-skewed the data were transformed using a logarithm of base ten, yet normality was not achieved. Therefore a non-parametric Wilcoxon Signed Rank test was used to test for significant differences between the medians of the untransformed data. For the differences between microsaccades and drift with an end removal factor of 2 a significant difference (difference = 0.23) between the medians for drifts (Median = 1.53) and microsaccades (Median = 1.30) was found (z = -3.027, p = .002)(see Fig. 8.4). For the other two end removal factors this difference in means did not reach significance. The

results for the end removal factor of 2.5 show no significant difference (Difference = 0.03) between the medians of drifts (Median = 1.47) and microsaccades (Median = 1.50) (z = -0.740, p = .459).

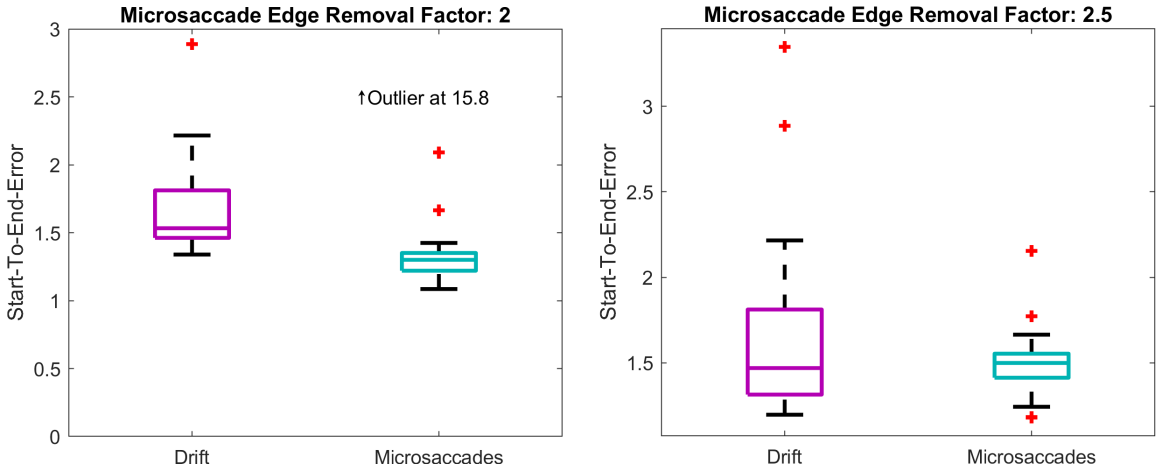


Figure 8.4: Box plots of drift and microsaccade Start-To-End-Errors. On the left data for an end removal factor of 2 are shown, while on the right data from an end removal factor of 2.5 are shown. Any value above one indicates that the movement was on average corrective, as the end position was closer to the median than the start position.

The cumulative probability plots of the Start-End-Error are given in Figure 8.5. The plots appear reasonably consistent across different edge removal factors and also show a relatively large amount of consistency between microsaccades (red) and drifts (blue).

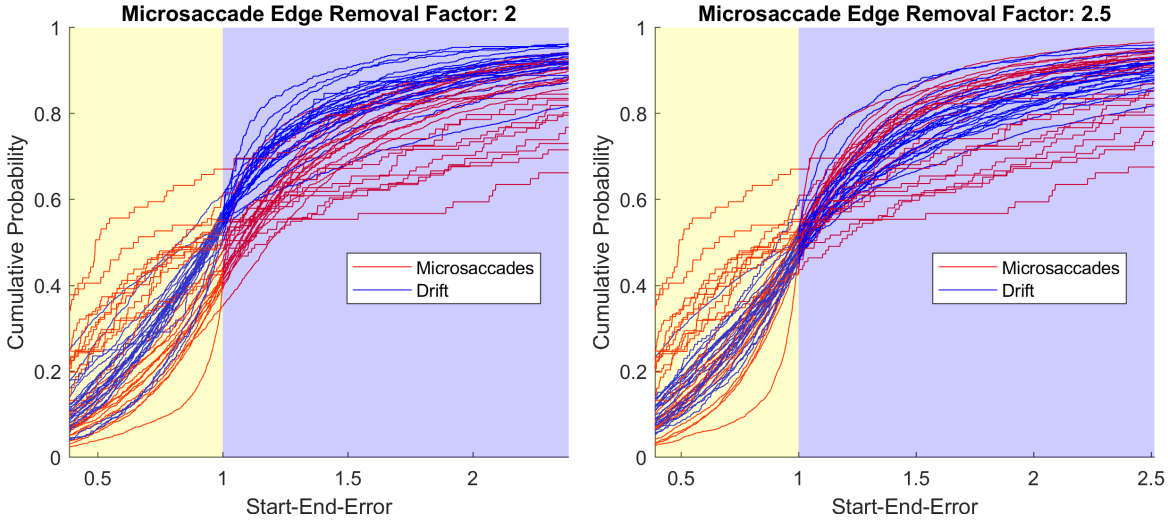


Figure 8.5: Cumulative probabilities of the the Start-End-Error. Each line represents one participant. The blue lines represent drift and the red lines represent microsaccades. The area shaded yellow represents an area for which the movement introduced error relative to the median of fixation. The area in blue contains movements that improved the distance to the target.

8.5.2 Movement-Towards-Median

Comparison of movement angles

The following results hold for all 3 levels of the edge removal factor. The Rayleigh test on the angles of movement for drift and microsaccades confirmed a von Mises distribution of the data. Testing if the mean direction of microsaccades or drift is significantly different from the direction towards the median at 1,0 was not significant for both microsaccades and drifts (see Fig 8.6).

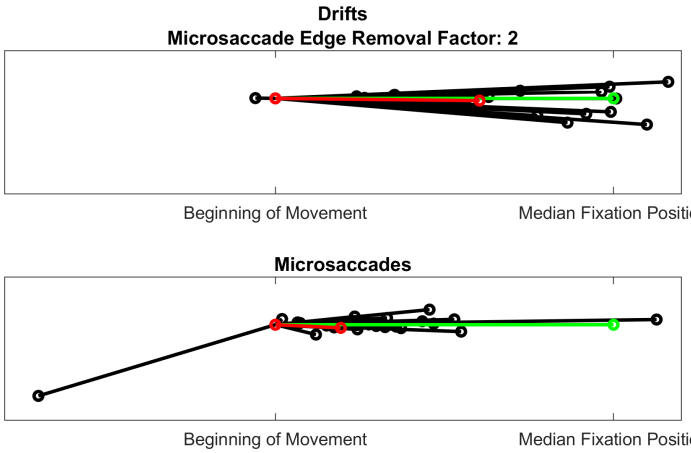
Comparison of Optimal-Achievable-Movements

The Optimal-Achievable-Movement of microsaccades and drift was first tested for normality. For data generated with an edge removal factor of 2 or 2.25 the normality criterion was not met. For data generated with an edge removal factor of 2.5 the normality criterion was met when tested using a Kolmogorov-Smirnov Test. For consistency all data were analysed using a non-parametric Wilcoxon-Signed Rank test. This test showed significant differences (Difference = 0.34) between the median of drifts (Median = 0.58) and microsaccades (Median = 0.24) (z = -2.785, p = .005) for an edge removal factor of 2. For both higher levels of the edge removal factor this test did not reach significance. With an edge removal factor of 2.5, the difference between the medians of drifts (Median = 0.41) and microsaccades (Median = 0.45) was 0.04 (z = -0.498, p = .619), which was not statistically significant.

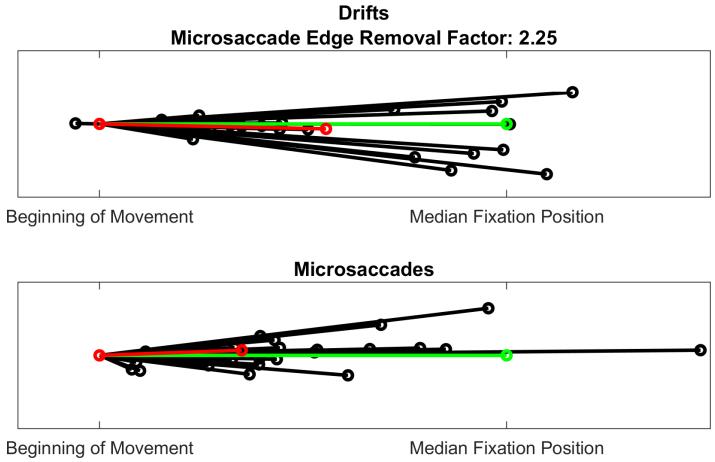
The cumulative probabilities for each participant's Optimal-Achievable-Movement are plotted in Figure 8.8. Two interesting features are visible in these plots, which also show reasonable consistency across the different edge removal factors. The first feature is the separation of the microsaccade (red) and drift (blue) lines, with the majority of blue drift lines rising earlier than the red microsaccade lines. The second feature is that the red lines form two clusters suggesting variation between participants. For some participants the red lines overlap with the bulk of the blue lines, while for some they appear separated.

Heat Maps

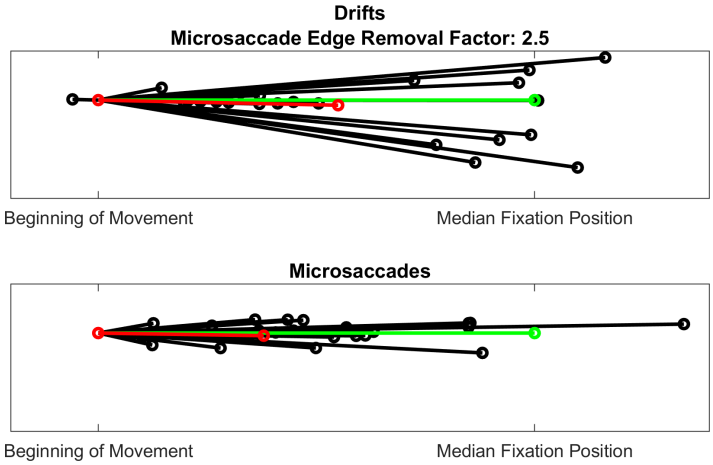
The first heat map (Fig. 8.9) shows the actual movement *angles* to the optimal movement *angles*. For microsaccades two bands at 270° and 90° can be observed. This is consistent with our knowledge about microsaccades, as these represent the two horizontal directions, along which microsaccades move preferentially. There is also a slight diagonal line, indicating some movements in a corrective direction. This microsaccade behaviour is also consistent with Nachmias (1959) who reported that microsaccades act in a corrective way only along some meridians and not others. For drifts the plot



(a) Plot of each participant's average microsaccade or drift movement relative to the movement towards the median of fixation for an edge removal factor of 2.



(b) Plot of each participant's average microsaccade or drift movement relative to the movement towards the median of fixation for an edge removal factor of 2.25.



(c) Plot of each participant's average microsaccade or drift movement relative to the movement towards the median of fixation for an edge removal factor of 2.5.

Figure 8.6: Movement-Toward-Median measure for all participants and edge removal factors. The participants' individual Movement-Toward-Median are shown in black, the mean of those is given in red and the optimal movement is shown in green.

looks very different, with a noticeable line falling along the optimal corrective diagonal.

The second heat map (Fig. 8.10) shows the actual movement *distances* compared to the optimal

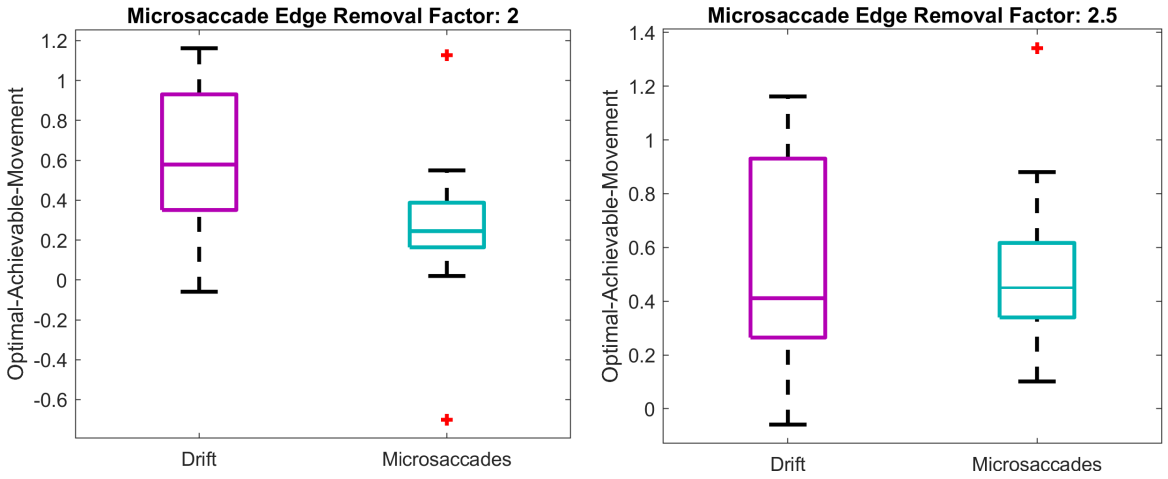


Figure 8.7: Box plot of the Optimal-Achievable-Movement for drift and microsaccades with different edge removal factors. On the left data for an end removal factor of 2 are shown, while on the right data from an end removal factor of 2.5 are shown.

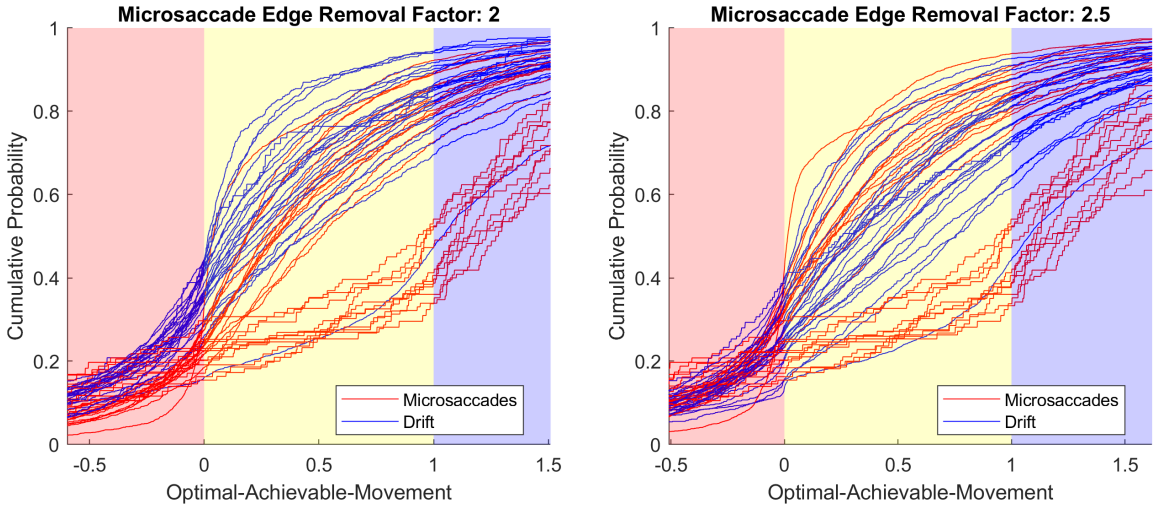
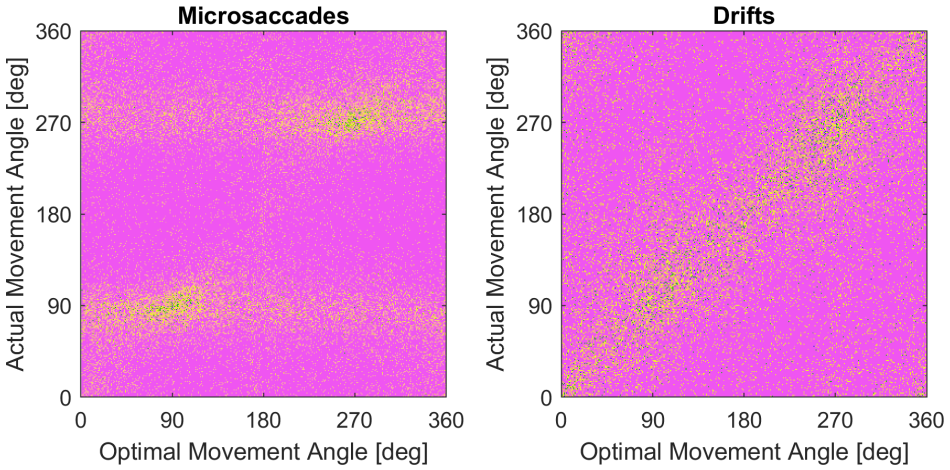


Figure 8.8: Cumulative probabilities of the the Optimal-Achievable-Movement. Each line represents one participant. The blue lines represent drift and the red lines represent microsaccades. The area shaded red represents movements for which the eyes moved away from the median of fixation. The yellow shading covers an area for which the eyes undershot the target. The area in blue contains movements for which the eyes overshot the target.

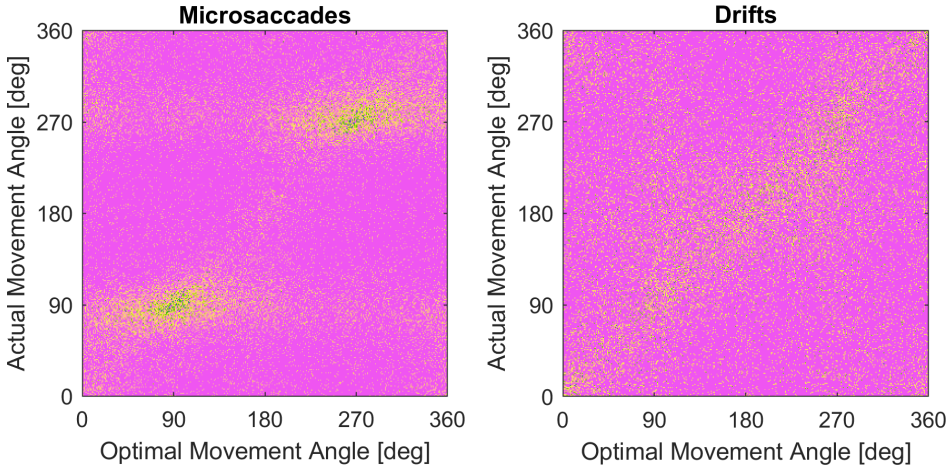
movement *distances*. In this map microsaccades and drifts appear more similar, with both being densely clustered in the bottom left corner representing the smaller actual and optimal movements. The drift heat map appears to show a characteristic tail towards the bottom right, indicating movements where the optimal distance was larger than the actual distance.

8.6 Discussion

The corrective power of microsaccades and drift was compared using three different metrics: the Start-End-Error, the angle of the Movement-Towards-Median and the Optimal-Achievable-Movement. In line with the hypothesis that both drift and microsaccades contribute to fixational stability it was found that, irrespective of how conservatively microsaccades were detected, the



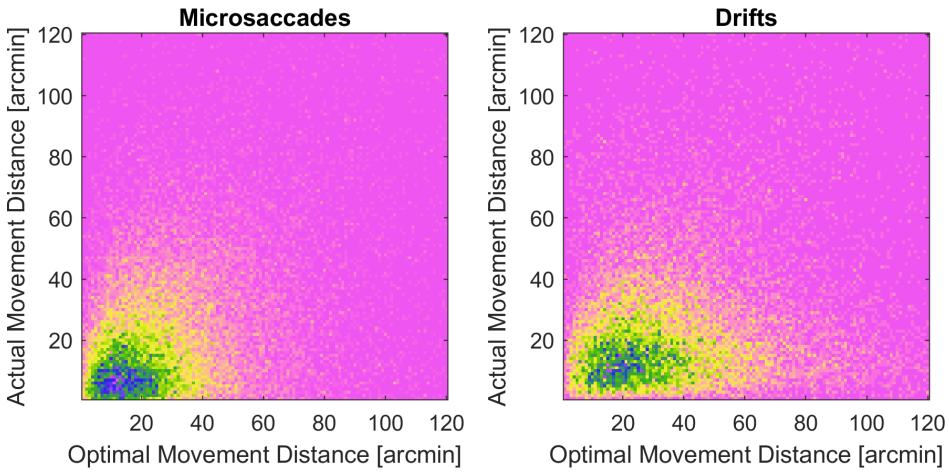
(a) An end removal factor of 2 was used to detect microsaccades in the data.



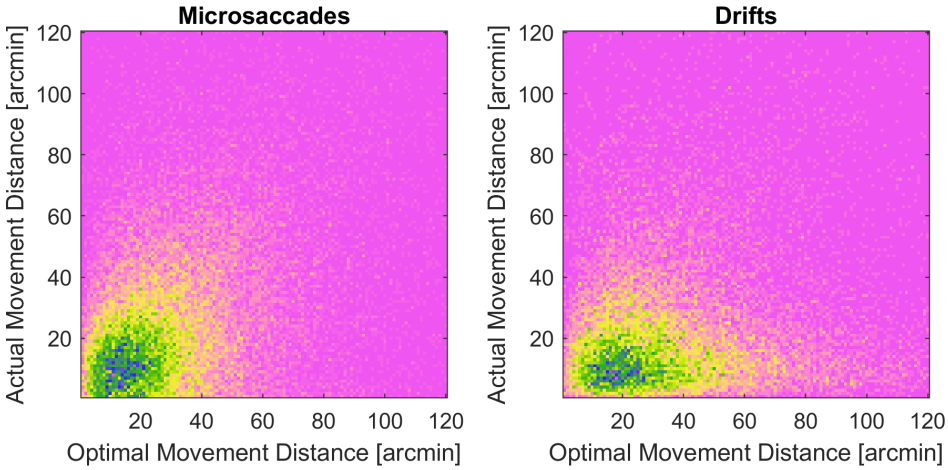
(b) An end removal factor of 2.5 was used to detect microsaccades in the data.

Figure 8.9: Heat maps of the distribution of actual and optimal movement directions for microsaccades (left) and drifts (right). A diagonal line though 0,0 with a gradient of 1 would represent the ideal movement.

direction of both drifts and microsaccades was, on average, not different from the movement towards the median. For both the Start-To-End-Error and the Optimal-Achievable-Movement the results of significance tests between microsaccades and drift changed depending on the edge removal factor. This suggests that correctly identifying microsaccades and drift in the data is important for these measures. Ultimately the results from the significance tests suggested that there was either no difference between the corrective power of microsaccades and drifts (for higher edge removal factors, i.e. more conservative removal of microsaccades) or that drifts were significantly more corrective (for lower edge removal factors). Which of these represents the true relationship in corrective power is hard to say, but leaning towards a more conservative interpretation, it still suggests that drifts and microsaccades both correct for fixational error. The heat maps of the actual compared to the optimal *angle* of movement suggest different roles for microsaccades and drift in correcting fixation position. While microsaccades appeared to fall and correct mainly along the horizontal meridian, drifts appeared to correct irrespective of angular orientation. This is consistent with findings by Nachmias (1959), who reported that microsaccades only correct along certain



(a) An end removal factor of 2 was used to detect microsaccades in the data.



(b) An end removal factor of 2.5 was used to detect microsaccades in the data.

Figure 8.10: Heat map of the distribution of actual and optimal movement distances for microsaccades (left) and drifts (right). A diagonal line though 0,0 with a gradient of 1 would represent the ideal movement.

meridians, while drifts correct position along others.

These findings suggest that microsaccades and drift both play important parts in maintaining a stable line of sight during fixation and that it is likely to be their combined nature that allows for stable fixation. The historical assumption that drift only introduces fixational error appears entirely at odds with these results, and in combination with previous work, should no longer be considered a useful hypothesis.

When evaluating conclusions drawn from these measures it is important to bear in mind that they only hold to the extent that the assumptions that were made about the data are true. One assumption is that the separation into microsaccades and drifts was accurate. While on visual inspection this appears to be true, it will not be true in 100% of cases: some small microsaccades may have been missed, while some drifts may have been falsely identified as microsaccades. On a smaller scale this also applies to the start and end samples of identified microsaccades. We cannot know for certain that the first sample labelled as either a microsaccade or a drift is in fact already part of that movement. This is a particularly important caveat, as for the purpose of this analysis

the first and last samples are assumed to characterise the motion that took place during that time. This in turn is the second assumption: that for the estimation of corrective power of a movement only its start and end point matter, not any of the movement that occurred in between. This is a large assumption to make for both drifts and microsaccades, as it is known that neither movement is linear in nature (e.g. Cherici et al., 2012). However, the above mentioned limitations have been limiting the study of how corrective microsaccades and drift are respectively for as long as there has been interest in the question. Some limitations will become less prominent with time, such as the error associated with microsaccade detection; while others will always be limitations, such as the assumption of linearity of movement. In this experiment we have tried to reduce the error based on microsaccade detection by varying how conservatively the automated method identified them, but other ways could be used, too, such as manual classification, or comparing a variety of different automated methods.

Future avenues for evaluating the exact interplay between microsaccades and drifts are to examine the temporal sequence in which microsaccades and drifts happen. There may also be interesting findings when comparing individual differences in these measures, as it is not clear how microsaccades and drifts interact in shorter time periods at an individual level, or why some participants showed differences in the cumulative probability plots for the Optimal-Achievable-Movement. Neither is it known if different stimuli, which change drift or microsaccade patterns, affect the interplay of these movements with regards to maintaining a line of sight, which in this analysis may be a limiting factor as data from two experiments with different, albeit internally counterbalanced, targets were used.

Chapter 9

Discussion

The uniting theme of this thesis is a desire to better understand fixational eye movements. For this three aspects of fixational eye movements were studied. Firstly, the way a stream of eye-movement data is segmented into periods of microsaccades and drifts/tremors was investigated by considering data capture and analysis, as well as developing two new detection methods for microsaccades. Secondly, the influence of stimulus features on fixational stability was investigated. Lastly, the contributions of microsaccades and drift to keeping the eyes on target were studied.

9.1 Improvements in microsaccade detection and data analysis

A large part of this thesis is focussed on improving the segmentation of eye movement traces into their microsaccade and drift/tremor components. As part of this, a review of microsaccade features over the last 70 years was reported in the Introduction, and aspects of those findings were used in Chapters 3 and 4 to develop new microsaccade detection methods. The binocular correlation method finds microsaccades based on raised correlation levels between the speeds in both eyes. A further contribution to improving microsaccade detection in the future is to build up a database of manually labelled datasets collected in different contexts. Manual labels do not represent the ground truth in the data, but currently they are the gold standard for the segmentation of eye movement traces. Providing access to more labelled eye tracking data will allow the field to rigorously train and test new methods, which will hopefully lead to more robust detection methods in the future. Another advantage of making this data accessible is that it provides information on the variability of eye tracking outputs between different eye trackers and experimental set ups.

9.2 Progress in understanding the interaction between the stimulus and fixational eye movements

Fixational eye movements represent an active part of the visual process and therefore merit exploring with regards to how they interact with the visual world we inhabit. It is known that, depending on size of the eye movement, fading of central or peripheral information can be prevented (Martinez-Conde et al., 2006; Clarke & Belcher, 1962). However, if this represents a desirable epiphenomenon of fixational eye movements or their primary purpose is not known. Additionally, any further interactions between fixational eye movements and the visual stimulus are poorly explored. There is some evidence that microsaccades enhance fine spatial detail (Rucci et al., 2007), but this needs further substantiation, as there is some conflicting information (Mostofi et al., 2016).

There is good reason to believe that fixational eye movements interact with the visual stimulus: microsaccades may have cortical origins (Martinez-Conde et al., 2013) and it has been shown that drift is biased by a moving background grating (Murphy et al., 1975). The higher up the visual stream a movement is initiated, the more complex the visual features it may be responding to, therefore it can only reasonably be expected that movements originating after the point where information from left and right eyes is combined to be able to respond to the visual stimulus. Also there is no known pathway directly from the retina to the eye muscles, making it impossible for an eye movement to compensate for any visual changes unique to one eye. It would be possible to test for this by showing a transfer effect of changes in fixational eye movements in one eye, which is exposed to the relevant stimulus, to the other eye, which is not directly exposed to it.

In Chapter 5 it was possible to show that target eccentricity influences fixational stability, with more central targets providing greater stability than more peripheral targets. It was also found that the orientation of a grating could influence fixational instability, with a higher root mean square (RMS) error found for movements along the bars of the grating, compared to perpendicular with them. Both of these findings suggest that visual feedback is used to stabilise the eye's position. As the same target presented closer to the fovea provides more information, due to the foveating structure of our visual system, this suggests that the amount of available visual information affects the stability of our eye movements. Similarly the effect of grating orientation suggests that it is not the centre-of-gravity of a stimulus that matters, but perhaps how reliably the centre can be estimated. This hypothesis is supported by the findings of Chapter 6, which showed that estimation of the centre of a stimulus and its unreferenced motion threshold are both good predictors of fixational stability. The results of Chapter 7 are also consistent with an explanation of fixational stability in terms of the ability to estimate the centre-of-gravity of the fixation stimulus, as there

appeared to be no significant difference between the different blur conditions. A difference would have been expected if the amount of flux on the retina was crucial in stabilising the eye, as that was the component most manipulated. However, all stimuli were similar in their spatial extents and had the same full width at half maximum (FWHM) which suggests that the estimability of their centres was approximately equal.

9.3 Keeping the eyes on target using microsaccades and drifts

This thesis has presented further evidence that the interaction between microsaccades and drift is not simply that microsaccades correct for drift. Instead the interaction between the two systems is more complex with both being able to correct for positional errors. Additionally, evidence of the importance of accurately defining microsaccades and drifts was presented. Changing detection thresholds can change which measures of corrective power reach significance.

9.4 Future avenues for research

Extensions on all three strands of research presented here - microsaccade detection, the interplay of microsaccades and drift and the interaction of fixational eye movement with the visual stimulus- are merited. In particular it would be beneficial to study the time course of fixation in more detail, as discerning the relative contributions of microsaccades and drift to stability over time can provide more information about the underlying neural pathways. To further establish the neural pathways supporting drift, which at this point are not known, it may be helpful to formally test for transfer effects in the drift component between the two eyes, as the presence of transfer would indicate that the drift movement signal originates from a structure beyond the optic chiasm where information from both eyes is combined.

The comparison between the two tracking systems in Chapter 2 has also highlighted the great potential of AOSLO eye tracking for fixational eye movement research. While the methods for data analysis are still in their infancy the potential payback through data at a higher spatial resolution with significantly reduced noise and a direct reference to the retina justifies the input required. Only by continuing to study fixational eye movements using this high resolution tracker will methods improve, and our understanding of fixational eye movement, too.

Future work on improving microsaccade detection, especially for the AOSLO data is highly desirable. Two immediate routes for this are the addition of an acceleration profile criterion, as well as a two-fold velocity threshold: one lower one to exclude data that are too slow to be part of a

microsaccade, and a second minimum peak velocity criterion. Other aspects of improving AOSLO microsaccade detection are about streamlining the eye movement extraction process within the lab, including automation of the exclusion of tracking failures, better handling of the flyback region and establishing the highest sampling rate that is robust to noise in the velocity trace.

Particular questions of interest in the general field of fixational eye movement research are: (i) how large is the interaction between fixational eye movements and the visual stimulus and (ii) what components of the eye movement trace are most influenced by the stimulus. Ultimately, the aim is to understand the visual triggers and neural pathways for the generation and control of fixational eye movements. An important aspect of this is to consider fixational eye movement an active part of vision which transforms the visual stimulus into a spatial and temporal signal for further processing.

References

Abadi, R. V. & Gowen, E. (2004). Characteristics of saccadic intrusions. *Vision Research*, *44*(23), 2675–2690. doi: 10.1016/j.visres.2004.05.009

Adelson, E. H. & Movshon, J. A. (1982). Phenomenal coherence of moving visual patterns. *Nature*, *300*(5892), 523–525. doi: 10.1038/300523a0

Adler, F. H. & Fliegelman, M. (1934). Influence of Fixation on the Visual Acuity. *Archives of Ophthalmology*, *12*(4), 475–483. doi: 10.1001/archopht.1934.00830170013002

Alfred Yarbus. (1967). *Eye movements and vision*. New York. doi: 10.1016/0028-3932(68)90012-2

Ammermüller, J. & Kolb, H. (1996). Functional architecture of the turtle retina. *Progress in Retinal and Eye Research*, *15*(2), 393–433. doi: 10.1016/1350-9462(96)00009-2

Armington, J. C. & Bloom, M. B. (1974). Relations between the amplitudes of spontaneous saccades and visual responses. *Journal of the Optical Society of America*, *64*(9), 1263–1271. doi: 10.1364/JOSA.64.001263

Atchison, D. A., Fisher, S. W., Pedersen, C. A. & Ridall, P. G. (2005). Noticeable, troublesome and objectionable limits of blur. *Vision Research*, *45*(15), 1967–1974. doi: 10.1016/j.visres.2005.01.022

Aungsakun, S., Phinyomark, A., Phukpattaranont, P. & Limsakul, C. (2011). Robust eye movement recognition using EOG signal for human-computer interface. *Communications in Computer and Information Science*, *180 CCIS*(PART 2), 714–723. doi: 10.1007/978-3-642-22191-0_63

Bachy, R. & Zaidi, Q. (2014). Troxler Fading, Eye Movements, and Retinal Ganglion Cell Properties. *i-Perception*, *5*(7), 611–612. doi: 10.1068/i0679sas

Bahill, A., Clark, M. R. & Stark, L. (1975). The main sequence, a tool for studying human eye movements. *Mathematical Biosciences*, *24*(3-4), 191–204. doi: 10.1016/0025-5564(75)90075-9

Bahill, A. & McDonald, J. D. (1983). Smooth pursuit eye movements in response to predictable target motions. *Vision Research*, *23*(12), 1573–1583. doi: 10.1016/0042-6989(83)90171-2

Bair, W. & O'Keefe, L. P. (1998). The influence of fixational eye movements on the response of neurons in area MT of the macaque. *Visual Neuroscience*, *15*, 779–786.

Barlow, H. B. (1952). Eye Movements during Fixation. *Journal of Physiology*, *116*(3), 290–306. doi: 10.1113/jphysiol.1952.sp004706

Barlow, H. B. (1963). Slippage of contact lenses and other artefacts in relation to fading and regeneration of supposedly stable retinal images. *Quarterly Journal of Experimental Psychology*, *15*(1), 36–51. doi: 10.1080/17470216308416550

Becker, W. & Fuchs, A. (1985). Prediction in the oculomotor system: smooth pursuit during transient disappearance of a visual target. *Experimental Brain Research*, *57*(3), 562–575. doi: 10.1007/BF00237843

Becker, W. & Jürgens, R. (1979). An analysis of the saccadic system by means of double step stimuli. *Vision Research*, *19*(9), 967–983. doi: 10.1016/0042-6989(79)90222-0

Beeler, G. W. (1967). Visual threshold changes resulting from spontaneous saccadic eye movements. *Vision Research*, *7*(9-10), 769–775. doi: 10.1016/0042-6989(67)90039-9

Behrens, F., MacKeben, M. & Schröder-Preikschat, W. (2010). An improved algorithm for automatic detection of saccades in eye movement data and for calculating saccade parameters. *Behavior Research Methods*, *42*(3), 701–708. doi: 10.3758/BRM.42.3.701

Bellet, M. E., Bellet, J., Nienborg, H., Hafed, Z. M. & Berens, P. (2019). Human-level saccade detection performance using deep neural networks. *Journal of Neurophysiology*, *121*(2), 646–661. doi: 10.1152/jn.00601.2018

Bengi, H. & Thomas, J. G. (1968). Three electronic methods for recording ocular tremor. *Medical & Biological Engineering*, *6*(2), 171–179. doi: 10.1007/BF02474271

Bentivoglio, A. R., Bressman, S. B., Cassetta, E., Carretta, D., Tonali, P. & Albanese, A. (1997). Analysis of blink rate patterns in normal subjects. *Movement Disorders*, *12*(6), 1028–1034. doi: 10.1002/mds.870120629

Berens, P. (2009). CircStat: A MATLAB Toolbox for Circular Statistics. *JournalofStatisticalSoftware*, *31*(10). doi: 10.1002/wics.10

Betta, E., Galfano, G. & Turatto, M. (2007). Microsaccadic response during inhibition of return in a target–target paradigm. *Vision Research*, *47*(3), 428–436. doi: 10.1016/j.visres.2006.09.010

Blakemore, C. & Cooper, G. F. (1970). Development of the Brain depends on the Visual Environment. *Nature*, *228*(5270), 477–478. doi: 10.1038/228477a0

Blanchard, T. C., Wilke, A. & Hayden, B. Y. (2014). Hot-hand bias in rhesus monkeys. *Journal of Experimental Psychology: Animal Learning and Cognition*, *40*(3), 280–286. doi: 10.1037/xan0000033

Bland, J. M. & Altman, D. G. (1995). Statistics notes: Calculating correlation coefficients with

repeated observations: Part 1–correlation within subjects. *BMJ*, *310*(6977), 446–446. doi: 10.1136/bmj.310.6977.446

Bolger, C., Bojanic, S., Sheahan, N. F., Coakley, D. & Malone, J. F. (1999). Dominant frequency content of ocular microtremor from normal subjects. *Vision Research*, *39*(11), 1911–1915. doi: 10.1016/S0042-6989(98)00322-8

Bowers, N. R., Boehm, A. E. & Roorda, A. (2018). The effects of tremor on the retinal image. *bioRxiv*(45), 39. doi: 10.1101/403964

Boyce, P. R. (1967). Monocular Fixation in Human Eye Movement. *Proceedings of the Royal Society B: Biological Sciences*, *167*(1008), 293–315. doi: 10.1098/rspb.1967.0028

Bradley, A. & Schor, C. (1988). The role of eye movements and masking in monocular rivalry. *Vision Research*, *28*(10), 1129–1137. doi: 10.1016/0042-6989(88)90139-3

Bridgeman, B. & Palca, J. (1980). The role of microsaccades in high acuity observational tasks. *Vision Research*, *20*(9), 813–817. doi: 10.1016/0042-6989(80)90013-9

Brisson, J., Mainville, M., Mailloux, D., Beaulieu, C., Serres, J. & Sirois, S. (2013). Pupil diameter measurement errors as a function of gaze direction in corneal reflection eyetrackers. *Behavior Research Methods*, *45*(4), 1322–1331. doi: 10.3758/s13428-013-0327-0

Cardinal, R. N. & Aitken, M. R. F. (2006). *ANOVA for the behavioural sciences researcher*. Erlbaum.

Casagrande, V. (1994). A third parallel visual pathway to primate area V1. *Trends in Neurosciences*, *17*(7), 305–310. doi: 10.1016/0166-2236(94)90065-5

Castet, E. & Crossland, M. (2012). Quantifying Eye Stability During a Fixation Task: A Review of Definitions and Methods. *Seeing and Perceiving*, *25*(5), 449–469. doi: 10.1163/187847611X620955

Cherici, C., Kuang, X., Poletti, M. & Rucci, M. (2012). Precision of sustained fixation in trained and untrained observers. *Journal of Vision*, *12*(6), 31–31. doi: 10.1167/12.6.31

Chung, S. T., Jarvis, S. H. & Cheung, S.-H. (2007). The effect of dioptric blur on reading performance. *Vision Research*, *47*(12), 1584–1594. doi: 10.1016/j.visres.2007.03.007

Clarke, F. J. J. & Belcher, S. J. (1962). On the localization of troxler's effect in the visual pathway. *Vision Research*, *2*, 53–68. doi: 10.1016/0042-6989(62)90063-9

Clowes, M. B. (1961). Some Factors in Brightness Discrimination with Constraint of Retinal Image Movement. *Optica Acta: International Journal of Optics*, *8*(1), 81–91. doi: 10.1080/713826365

Clowes, M. B. (1962). A Note on Colour Discrimination under Conditions of Retinal Image Constraint. *Optica Acta: International Journal of Optics*, *9*(1), 65–68. doi: 10.1080/713826405

Collewijn, H. & Kowler, E. (2008). The significance of microsaccades for vision and oculomotor control. *Journal of Vision*, *8*(14), 1–21. doi: 10.1167/8.14.20

Collewijn, H. & Van Der Mark, F. (1972). Ocular stability in variable visual feedback conditions in the rabbit. *Brain Research*, *36*(1), 47–57. doi: 10.1016/0006-8993(72)90765-2

Collewijn, H., Van der Steen, J., Ferman, L. & Jansen, T. C. (1985). Human ocular counterroll: assessment of static and dynamic properties from electromagnetic scleral coil recordings. *Experimental Brain Research*, *59*(1), 185–196. doi: 10.1007/BF00237678

Coren, S. & Hoenig, P. (1972). Effect of non-target stimuli. *Perceptual and Motor Skills*, *34*, 499–508.

Cornsweet, T. N. (1956). Determination of the Stimuli for Involuntary Drifts and Saccadic Eye Movements. *Journal of the Optical Society of America*, *46*(11), 987–988. doi: 10.1364/JOSA.46.000987

Cowey, A. & Rolls, E. (1974). Human cortical magnification factor and its relation to visual acuity. *Experimental Brain Research*, *21*(5), 447–454. doi: 10.1007/BF00237163

Crane, H. D. & Steele, C. M. (1985). Generation-V dual-Purkinje-image eyetracker. *Applied Optics*, *24*(4), 527. doi: 10.1364/AO.24.000527

Cui, J., Wilke, M., Logothetis, N. K., Leopold, D. A. & Liang, H. (2009). Visibility states modulate microsaccade rate and direction. *Vision Research*, *49*(2), 228–236. doi: 10.1016/j.visres.2008.10.015

Cunitz, R. J. & Steinman, R. M. (1969). Comparison of saccadic eye movements during fixation and reading. *Vision Research*, *9*, 683–693. doi: 10.1016/0042-6989(69)90125-4

Curcio, C. A., Allen, K. A., Sloan, K. R., Lerea, C. L., Hurley, J. B., Klock, I. B. & Milam, A. H. (1991). Distribution and morphology of human cone photoreceptors stained with anti-blue opsin. *Journal of Comparative Neurology*, *312*(4), 610–624. doi: 10.1002/cne.903120411

Curcio, C. A., Sloan, K., Packer, O., Hendrickson, A. & Kalina, R. (1987). Distribution of cones in human and monkey retina: individual variability and radial asymmetry. *Science*, *236*(4801), 579–582. doi: 10.1126/science.3576186

Curcio, C. A., Sloan, K. R., Kalina, R. E. & Hendrickson, A. E. (1990). Human photoreceptor topography. *The Journal of Comparative Neurology*, *292*(4), 497–523. doi: 10.1002/cne.902920402

Dacey, D. M. (1993). The mosaic of midget ganglion cells in the human retina. *The Journal of Neuroscience*, *13*(12), 5334–5355. doi: 10.1523/JNEUROSCI.13-12-05334.1993

Dacey, D. M. & Lee, B. B. (1994). The 'blue-on' opponent pathway in primate retina originates from a distinct bistratified ganglion cell type. *Nature*, *367*(6465), 731–735. doi: 10.1038/367731a0

Dacey, D. M., Peterson, B. B., Robinson, F. R. & Gamlin, P. D. (2003). Fireworks in the Primate Retina: In Vitro Photodynamics Reveals Diverse LGN-Projecting Ganglion Cell Types. *Neuron*,

37(1), 15–27. doi: 10.1016/S0896-6273(02)01143-1

De Valois, R. L. & De Valois, K. K. (1991). Vernier acuity with stationary moving Gabors. *Vision Research*, *31*(9), 1619–1626. doi: 10.1016/0042-6989(91)90138-U

de Weese Puckett, J. & Steinman, R. M. (1969). Tracking eye movements with and without saccadic correction. *Vision Research*, *9*(6), 695–703. doi: 10.1016/0042-6989(69)90126-6

Deaner, R. O. & Platt, M. L. (2003). Reflexive social attention in monkeys and humans. *Current Biology*, *13*, 1609–1613. doi: 10.1016/j.cub.2003.08.025

Déruaz, A., Goldschmidt, M., Whatham, A. R., Mermoud, C., Lorincz, E. N., Schnider, A. & Safran, A. B. (2006). A technique to train new oculomotor behavior in patients with central macular scotomas during reading related tasks using scanning laser ophthalmoscopy: immediate functional benefits and gains retention. *BMC Ophthalmology*, *6*(1), 35. doi: 10.1186/1471-2415-6-35

Desbordes, G. & Rucci, M. (2007). A model of the dynamics of retinal activity during natural visual fixation. *Visual Neuroscience*, *24*, 217–230. doi: 10.10170S0952523807070460

Deubel, H. & Bridgeman, B. (1995). Fourth Purkinje image signals reveal eye-lens deviations and retinal image distortions during saccades. *Vision Research*, *35*(4), 529–538. doi: 10.1016/0042-6989(94)00146-D

Deubel, H. & Elsner, T. (1986). Threshold perception and saccadic eye movements. *Biological Cybernetics*, *54*(6), 351–358. doi: 10.1007/BF00355540

Dice, L. R. (1945). Measures of the Amount of Ecologic Association Between Species. *Ecology*, *26*(3), 297–302. doi: 10.2307/1932409

Dimigen, O., Valsecchi, M., Sommer, W. & Kliegl, R. (2009). Human Microsaccade-Related Visual Brain Responses. *Journal of Neuroscience*, *29*(39), 12321–12331. doi: 10.1523/JNEUROSCI.0911-09.2009

Ditchburn, R. W. (1980). The function of small saccades. *Vision Research*, *20*, 271–272. doi: 10.1016/0042-6989(80)90112-1

Ditchburn, R. W. & Drysdale, A. E. (1977). The effect of retinal-image movements on vision I. Step-movements and pulse-movements. *Proceedings of the Royal Society of London, Series B*, *197*(1127), 131–144. doi: 10.1098/rspb.1977.0062

Ditchburn, R. W., Fender, D. H., Mayne, S. & Pritchard, R. M. (1956). A Stabilized Retinal Image of the Iris. *Proceedings of the Physical Society*, *69*, 1165–1166. doi: 10.1088/0370-1301/69/11/115

Ditchburn, R. W. & Ginsborg, B. L. (1952). Vision with a stabilized retinal image. *Nature*, *170*(4314), 36–37. doi: 10.1038/170036a0

Ditchburn, R. W. & Ginsborg, B. L. (1953). Involuntary eye movements during fixation. *The Journal of Physiology*, *119*, 1–17. doi: 10.1113/jphysiol.1952.sp004706

Donner, K. & Hemilä, S. (2007). Modelling the effect of microsaccades on retinal responses to stationary contrast patterns. *Vision Research*, *47*(9), 1166–1177. doi: 10.1016/j.visres.2006.11.024

Duchowski, A., Biele, C., Niedzielska, A., Krejtz, K., Kiefer, P., Giannopoulos, I., ... Schönenberg, M. (2017). An inverse-linear logistic model of the main sequence. *Journal of Eye Movement Research*, *10*(3), 1–19. doi: 10.16910/jemr.10.3.4

Dumoulin, S. O. & Wandell, B. A. (2008). Population receptive field estimates in human visual cortex. *NeuroImage*, *39*(2), 647–660. doi: 10.1016/j.neuroimage.2007.09.034

Eizenman, M., Frecker, R. & Hallett, P. (1984). Precise non-contacting measurement of eye movements using the corneal reflex. *Vision Research*, *24*(2), 167–174. doi: 10.1016/0042-6989(84)90103-2

Eizenman, M., Hallet, P. & Frecker, R. C. (1985). Power Spectra for Ocular Drift and Tremor. *Vision Research*, *25*(11), 1635–1640.

Engbert, R. (2006). Flick-Induced Flips in Perception. *Neuron*, *49*(2), 168–170. doi: 10.1016/j.neuron.2006.01.005

Engbert, R. & Kliegl, R. (2003). Microsaccades uncover the orientation of covert attention. *Vision Research*, *43*(9), 1035–1045. doi: 10.1016/S0042-6989(03)00084-1

Engbert, R. & Kliegl, R. (2004). Microsaccades Keep the Eyes' Balance During Fixation. *Psychological Science*, *15*(6), 431–436. doi: 10.1111/j.0956-7976.2004.00697.x

Engbert, R. & Mergenthaler, K. (2006). Microsaccades are triggered by low retinal image slip. *Proceedings of the National Academy of Sciences*, *103*(18), 7192–7197. doi: 10.1073/pnas.0509557103

Fabre-Thorpe, M., Richard, G. & Thorpe, S. J. (1998). Rapid categorization of natural images by rhesus monkeys. *NeuroReport*, *9*(2), 303–308. doi: 10.1097/00001756-199801260-00023

Fang, Y., Gill, C., Poletti, M. & Rucci, M. (2018). Monocular microsaccades: Do they really occur? *Journal of Vision*, *18*(3), 1–14. doi: https://doi.org/10.1167/18.3.18

Farnebäck, G. (2003). Two-Frame Motion Estimation Based on Polynomial Expansion. In *Lecture notes in computer science* (Vol. 2749, pp. 363–370). doi: 10.1007/3-540-45103-X_50

Field, G. D., Gauthier, J. L., Sher, A., Greschner, M., Machado, T. A., Jepson, L. H., ... Chichilnisky, E. J. (2010). Functional connectivity in the retina at the resolution of photoreceptors. *Nature*, *467*(7316), 673–677. doi: 10.1038/nature09424

Finlay, D. (1982). Motion Perception in the Peripheral Visual Field. *Perception*, *11*(4), 457–462. doi: 10.1068/p110457

Fried, M., Tsitsiashvili, E., Bonneh, Y. S., Sterkin, A., Wygnanski-Jaffe, T., Epstein, T. & Polat, U. (2014). ADHD subjects fail to suppress eye blinks and microsaccades while anticipating visual stimuli but recover with medication. *Vision Research*, *101*, 62–72. doi: 10.1016/j.visres.2014.05.004

Fuchs, A. F. & Robinson, D. A. (1966). A method for measuring horizontal and vertical eye movement chronically in the monkey. *Journal of Applied Physiology*, *21*(3), 1068–1070. doi: 10.1152/jappl.1966.21.3.1068

Gagl, B., Hawelka, S. & Hutzler, F. (2011). Systematic influence of gaze position on pupil size measurement: analysis and correction. *Behavior Research Methods*, *43*(4), 1171–1181. doi: 10.3758/s13428-011-0109-5

Galfano, G., Betta, E. & Turatto, M. (2004). Inhibition of return in microsaccades. *Experimental Brain Research*, *159*(3), 400–404. doi: 10.1007/s00221-004-2111-y

Galley, N. (1993). The evaluation of the electrooculogram as a psychophysiological measuring instrument in the driver study of driver behaviour. *Ergonomics*, *36*(9), 1063–1070. doi: 10.1080/00140139308967978

Gauthier, J. L., Field, G. D., Sher, A., Greschner, M., Shlens, J., Litke, A. M. & Chichilnisky, E. J. (2009). Receptive Fields in Primate Retina Are Coordinated to Sample Visual Space More Uniformly. *PLoS Biology*, *7*(4), e1000063. doi: 10.1371/journal.pbio.1000063

Gautier, J., Bedell, H. E., Siderov, J. & Waugh, S. J. (2016). Monocular microsaccades are visual-task related. *Journal of Vision*, *16*(3), 37. doi: 10.1167/16.3.37

Gaymard, B., Ploner, C. J., Rivaud, S., Vermersch, A. I. & Pierrot-Deseilligny, C. (1998). Cortical control of saccades. *Experimental Brain Research*, *123*(1-2), 159–163. doi: 10.1007/s002210050557

Gibson, J. J. (1958). Visually controlled locomotion and visual orientation in animals. *British Journal of Psychology*, *49*(3), 182–194. doi: 10.1111/j.2044-8295.1958.tb00656.x

Gilchrist, I. D., Brown, V. & Findlay, J. M. (1997). Saccades without eye movements. *Nature*, *390*(6656), 130–131. doi: 10.1038/36478

Gilchrist, I. D., Brown, V., Findlay, J. M. & Clarke, M. P. (1998). Using the eye movement system to control the head. *Proceedings of the Royal Society B: Biological Sciences*, *265*(1408), 1831–1836. doi: 10.1098/rspb.1998.0509

Gowen, E., Abadi, R. V., Poliakoff, E., Hansen, P. C. & Miall, R. C. (2007). Modulation of saccadic intrusions by exogenous and endogenous attention. *Brain Research*, *1141*(1), 154–167. doi:

10.1016/j.brainres.2007.01.047

Greschner, M., Bongard, M., Rujan, P. & Ammermüller, J. (2002). Retinal ganglion cell synchronization by fixational eye movements improves feature estimation. *Nature Neuroscience*, *5*(4), 341–347. doi: 10.1038/nn821

Haddad, G. M. & Steinman, R. M. (1973). The smallest voluntary saccade: Implications for fixation. *Vision Research*, *13*(6), 1075–1086. doi: 10.1016/0042-6989(73)90145-4

Hafed, Z. M. (2011). Mechanisms for generating and compensating for the smallest possible saccades. *European Journal of Neuroscience*, *33*(11), 2101–2113. doi: 10.1111/j.1460-9568.2011.07694.x

Hafed, Z. M. (2018). Superior Colliculus : A Vision for Orienting. *Current Biology*, *28*(18), R1111–R1113. doi: 10.1016/j.cub.2018.07.047

Hafed, Z. M. & Clark, J. J. (2002). Microsaccades as an overt measure of covert attention shifts. *Vision Research*, *42*(22), 2533–2545. doi: 10.1016/S0042-6989(02)00263-8

Hafed, Z. M., Goffart, L. & Krauzlis, R. J. (2009). A Neural Mechanism for Microsaccade Generation in the Primate Superior Colliculus. *Science*, *323*(5916), 940–943. doi: 10.1126/science.1166112

Hafed, Z. M. & Krauzlis, R. J. (2010). Microsaccadic Suppression of Visual Bursts in the Primate Superior Colliculus. *Journal of Neuroscience*, *30*(28), 9542–9547. doi: 10.1523/JNEUROSCI.1137-10.2010

Hafed, Z. M. & Krauzlis, R. J. (2012). Similarity of superior colliculus involvement in microsaccade and saccade generation. *Journal of Neurophysiology*, *107*(7), 1904–1916. doi: 10.1152/jn.01125.2011

Harris, C. M. & Wolpert, D. M. (2006). The Main Sequence of Saccades Optimizes Speed-accuracy Trade-off. *Biological Cybernetics*, *95*(1), 21–29. doi: 10.1007/s00422-006-0064-x

Hartmann, E., Lachenmayr, B. & Brettel, H. (1979). The peripheral critical flicker frequency. *Vision Research*, *19*(9), 1019–1023. doi: 10.1016/0042-6989(79)90227-X

Hecht, S., Shlaer, S. & Pirenne, M. H. (1942). Energy, Quanta, and Vision. *The Journal of General Physiology*, *25*(6), 819–840. doi: 10.1085/jgp.25.6.819

Hennig, M. H., Kerscher, N. J., Funke, K. & Wörgötter, F. (2002). Stochastic resonance in visual cortical neurons: Does the eye-tremor actually improve visual acuity? *Neurocomputing*, *44-46*, 115–120. doi: 10.1016/S0925-2312(02)00371-5

Hermens, F. & Walker, R. (2010). What determines the direction of microsaccades? *Journal of Eye Movement Research*, *3*(4), 1–20. doi: 10.16910/jemr.3.4.1

Hipp, J. F. & Siegel, M. (2013). Dissociating neuronal gamma-band activity from cranial and

ocular muscle activity in EEG. *Frontiers in Human Neuroscience*, *7*(July), 1–11. doi: 10.3389/fnhum.2013.00338

Hládek, u., Porr, B. & Brimijoin, W. O. (2018). Real-time estimation of horizontal gaze angle by saccade integration using in-ear electrooculography. *PLOS ONE*, *13*(1), e0190420. doi: 10.1371/journal.pone.0190420

Hofer, H., Carroll, J., Neitz, J., Neitz, M. & Williams, D. R. (2005). Organization of the Human Trichromatic Cone Mosaic. *Journal of Neuroscience*, *25*(42), 9669–9679. doi: 10.1523/JNEUROSCI.2414-05.2005

Hooge, I. T. C., Niehorster, D. C., Nyström, M., Andersson, R. & Hessels, R. S. (2018). Is human classification by experienced untrained observers a gold standard in fixation detection? *Behavior Research Methods*, *50*(5), 1864–1881. doi: 10.3758/s13428-017-0955-x

Horowitz, T. S., Fine, E. M., Fencsik, D. E., Yurgenson, S. & Wolfe, J. M. (2007). Fixational eye movements are not an index of covert attention. *Psychological Science*, *18*(4), 356–363. doi: 10.1111/j.1467-9280.2007.01903.x

Hubel, D. H. & Wiesel, T. N. (1970). The period of susceptibility to the physiological effects of unilateral eye closure in kittens. *The Journal of Physiology*, *206*(2), 419–436. doi: 10.1113/jphysiol.1970.sp009022

Jonas, J. B., Schneider, U. & Naumann, G. O. H. (1992). Count and density of human retinal photoreceptors. *Graefe's Archive for Clinical and Experimental Ophthalmology*, *230*(6), 505–510. doi: 10.1007/BF00181769

Kandel, E. R., Schwartz, J. H. & Jessell, T. M. (2000). *Principles of Neural Science* (4th ed.). McGraw-Hill Companies.

Karson, C. N., Burns, R. S., LeWitt, P. A., Foster, N. L. & Newman, R. P. (1984). Blink rates and disorders of movement. *Neurology*, *34*(5), 677–677. doi: 10.1212/WNL.34.5.677

Kitaoka, A. & Ashida, H. (2003). Phenomenal Characteristics of the Peripheral Drift Illusion. *Vision*, *15*(4), 261–262. doi: 10.24636/vision.15.4_261

Klein, R., Berry, G., Briand, K., D'Entremont, B. & Farmer, M. (1990). Letter identification declines with increasing retinal eccentricity at the same rate for normal and dyslexic readers. *Perception & Psychophysics*, *47*(6), 601–606. doi: 10.3758/BF03203112

Ko, H. K., Poletti, M. & Rucci, M. (2010). Microsaccades precisely relocate gaze in a high visual acuity task. *Nature Neuroscience*, *13*(12), 1549–1554. doi: 10.1038/nn.2663

Ko, H. K., Snodderly, D. M. & Poletti, M. (2016). Eye movements between saccades: Measuring ocular drift and tremor. *Vision Research*, *122*, 93–104. doi: 10.1016/j.visres.2016.03.006

Kolder, H. & Brecher, G. A. (1966). Fast Oscillations of the Corneoretinal Potential in Man. *Archives of Ophthalmology*, *75*(2), 232–237. doi: 10.1001/archopht.1966.00970050234017

Körding, K. P., Kayser, C., Betsch, B. Y. & König, P. (2001). Non-contact eye-tracking on cats. *Journal of Neuroscience Methods*, *110*(1-2), 103–111. doi: 10.1016/S0165-0270(01)00423-X

Kovesi, P. (2015). *Good colour maps: How to design them.*

Kowler, E. & Steinman, R. M. (1979). Miniature saccades: Eye movements that do not count. *Vision Research*, *19*(1), 105–108. doi: 10.1016/0042-6989(79)90129-9

Kowler, E. & Steinman, R. M. (1980). Small saccades serve no useful purpose: Reply to a letter by R. W. Ditchburn. *Vision Research*, *20*(3), 273–276. doi: 10.1016/0042-6989(80)90113-3

Krauskopf, J. (1960). Figural After-Effects with a Stabilized Retinal Image. *The American Journal of Psychology*, *73*(2), 294–297.

Krauskopf, J., Cornsweet, T. N. & Riggs, L. A. (1960). Analysis of Eye Movements during Monocular and Binocular Fixation*. *Journal of the Optical Society of America*, *50*(6), 572–578. doi: 10.1364/JOSA.50.000572

Krauzlis, R. J. (2013). Eye Movements. In *Fundamental neuroscience* (pp. 697–714). Elsevier. doi: 10.1016/B978-0-12-385870-2.00032-9

Krauzlis, R. J. & Miles, F. A. (1996). Decreases in the Latency of Smooth Pursuit and Saccadic Eye Movements Produced by the "Gap Paradigm" in the Monkey. *Vision Research*, *36*(13), 1973–1985. doi: 10.1016/0042-6989(95)00307-X

Laubrock, J., Engbert, R. & Kliegl, R. (2005). Microsaccade dynamics during covert attention. *Vision Research*, *45*(6), 721–730. doi: 10.1016/j.visres.2004.09.029

Laubrock, J., Engbert, R., Rolfs, M. & Kliegl, R. (2007). Microsaccades are an index of covert attention: Commentary on Horowitz, Fine, Fencsik, Yurgenson and Wolfe (2007). *Psychological Sciencecience*, *18*(4), 364–366. doi: 10.1111/j.1467-9280.2007.01904.x

Lee, B. B. (1996). Receptive field structure in the primate retina. *Vision Research*, *36*(5), 631–644. doi: 10.1016/0042-6989(95)00167-0

Levi, D. M., Klein, S. A. & Aitsebaomo, P. (1984). Detection and discrimination of the direction of motion in central and peripheral vision of normal and amblyopic observers. *Vision Research*, *24*(8), 789–800. doi: 10.1016/0042-6989(84)90150-0

Lishman, J. R. & Lee, D. N. (1973). The Autonomy of Visual Kinaesthesis. *Perception*, *2*(3), 287–294. doi: 10.1068/p020287

Liston, D. B., Krukowski, A. E. & Stone, L. S. (2013). Saccade detection during smooth tracking. *Displays*, *34*(2), 171–176. doi: 10.1016/j.displa.2012.10.002

Lueck, C. J., Zeki, S., Friston, K. J., Deiber, M.-P., Cope, P., Cunningham, V. J., ... Frackowiak, R. S. J. (1989). The colour centre in the cerebral cortex of man. *Nature*, *340*(6232), 386–389. doi: 10.1038/340386a0

Macas, M., Lhotska, L. & Novak, D. (2013). Hidden Markov Models for Analysis of Eye Movements of Dyslexic Children. *2013 18th International Conference on Digital Signal Processing (DSP)*, 1–5. doi: 10.1109/ICDSP.2013.6622783

Madelain, L. & Krauzlis, R. J. (2003). Effects of Learning on Smooth Pursuit During Transient Disappearance of a Visual Target. *Journal of Neurophysiology*, *90*(2), 972–982. doi: 10.1152/jn.00869.2002

Magoun, H. W., Atlas, D., Hare, W. K. & Ranson, S. W. (1936). The afferent path of the pupillary light reflex in the monkey. *Brain*, *59*(2), 234–249. doi: 10.1093/brain/59.2.234

Martinez-Conde, S. (2006). Fixational eye movements in normal and pathological vision. In *Progress in Brain Research* (Vol. 154, pp. 151–176). doi: 10.1016/S0079-6123(06)54008-7

Martinez-Conde, S. & Macknik, S. L. (2007). Windows on the mind. *Scientific American*, *297*(2), 56–63.

Martinez-Conde, S., Macknik, S. L. & Hubel, D. H. (2000). Microsaccadic eye movements and firing of single cells in the striate cortex of macaque monkeys. *Nature Neuroscience*, *3*(3), 251–258. doi: 10.1038/72961

Martinez-Conde, S., Macknik, S. L., Troncoso, X. G. & Dyar, T. A. (2006). Microsaccades Counteract Visual Fading during Fixation. *Neuron*, *49*(2), 297–305. doi: 10.1016/j.neuron.2005.11.033

Martinez-Conde, S., Otero-Millan, J. & Macknik, S. L. (2013). The impact of microsaccades on vision: towards a unified theory of saccadic function. *Nature Reviews Neuroscience*, *14*(2), 83–96. doi: 10.1038/nrn3405

Mazurowski, M. A., Habas, P. A., Zurada, J. M., Lo, J. Y., Baker, J. A. & Tourassi, G. D. (2008). Training neural network classifiers for medical decision making: The effects of imbalanced datasets on classification performance. *Neural Networks*, *21*(2-3), 427–436. doi: 10.1016/j.neunet.2007.12.031

McAlpine, D. & Araki, S. (1958). Minamata Disease an Unusual Neurological Disorder Caused by Contaminated Fish. *The Lancet*, *272*(7047), 629–631. doi: 10.1016/S0140-6736(58)90348-9

McCamy, M. B., Otero-Millan, J., Macknik, S. L., Yang, Y., Troncoso, X. G., Baer, S. M., ... Martinez-Conde, S. (2012). Microsaccadic Efficacy and Contribution to Foveal and Peripheral Vision. *Journal of Neuroscience*, *32*(27), 9194–9204. doi: 10.1523/JNEUROSCI.0515-12.2012

McInnis, H. (2014). *Microsaccades in Parkinson's Disease* (Unpublished master's thesis). Queen's

University, Canada.

Mergenthaler, K. & Engbert, R. (2007). Modeling the control of fixational eye movements with neurophysiological delays. *Physical Review Letters*, *98*(138104), 1–4. doi: 10.1103/PhysRevLett.98.138104

Merigan, W., Byrne, C. & Maunsell, J. (1991). Does primate motion perception depend on the magnocellular pathway? *The Journal of Neuroscience*, *11*(11), 3422–3429. doi: 10.1523/JNEUROSCI.11-11-03422.1991

Merigan, W., Katz, L. & Maunsell, J. (1991). The effects of parvocellular lateral geniculate lesions on the acuity and contrast sensitivity of macaque monkeys. *The Journal of Neuroscience*, *11*(4), 994–1001. doi: 10.1523/JNEUROSCI.11-04-00994.1991

Midena, E., Radin, P. P., Pilotto, E., Ghirlando, A., Convento, E. & Varano, M. (2004). Fixation pattern and macular sensitivity in eyes with subfoveal choroidal neovascularization secondary to age-related macular degeneration. A microperimetry study. *Seminars in Ophthalmology*, *19*(1-2), 55–61. doi: 10.1080/08820530490882896

Møller, F., Laursen, M. L. & Sjølie, A. K. (2006). The contribution of microsaccades and drifts in the maintenance of binocular steady fixation. *Graefe's Archive for Clinical and Experimental Ophthalmology*, *244*(4), 465–471. doi: 10.1007/s00417-004-0989-5

Møller, F., Laursen, M. L., Tygesen, J. & Sjølie, A. K. (2002). Binocular quantification and characterization of microsaccades. *Graefe's Archive for Clinical and Experimental Ophthalmology*, *240*(9), 765–770. doi: 10.1007/s00417-002-0519-2

Moshel, S., Zivotofsky, A. Z., Jin-Rong, L., Engbert, R., Kurths, J., Kliegl, R. & Havlin, S. (2008). Persistence and phase synchronisation properties of fixational eye movements. *European Physical Journal: Special Topics*, *161*(1), 207–223. doi: 10.1140/epjst/e2008-00762-3

Mostofi, N., Boi, M. & Rucci, M. (2016). Are the visual transients from microsaccades helpful? Measuring the influences of small saccades on contrast sensitivity. *Vision Research*, *118*, 60–69. doi: 10.1016/j.visres.2015.01.003

Munoz, D. P. & Wurtz, R. H. (1993). Fixation cells in monkey superior colliculus. I. Characteristics of cell discharge. *Journal of Neurophysiology*, *70*(2), 559–575. doi: 10.1152/jn.1993.70.2.559

Murakami, I. (2003). Illusory jitter in a static stimulus surrounded by a synchronously flickering pattern. *Vision Research*, *43*(9), 957–969. doi: 10.1016/S0042-6989(03)00070-1

Murakami, I., Kitaoka, A. & Ashida, H. (2006). A positive correlation between fixation instability and the strength of illusory motion in a static display. *Vision Research*, *46*(15), 2421–2431. doi: 10.1016/j.visres.2006.01.030

Murphy, B. J., Kowler, E. & Steinman, R. M. (1975). Slow oculomotor control in the presence of moving backgrounds. *Vision Research*, *15*(11), 1263–1268. doi: 10.1016/0042-6989(75)90172-8

Nachmias, J. (1959). Two-dimensional motion of the retinal image during monocular fixation. *Journal of the Optical Society of America*, *49*(9), 901–908. doi: 10.1364/JOSA.49.000901

Nachmias, J. (1961). Determiners of the drift of the eye during monocular fixation. *Journal of the Optical Society of America*, *51*(7), 761–766. doi: 10.1364/JOSA.51.000761

Neitz, J. & Neitz, M. (2011). The genetics of normal and defective color vision. *Vision Research*, *51*(7), 633–651. doi: 10.1016/j.visres.2010.12.002.The

Newsome, W. & Pare, E. (1988). A selective impairment of motion perception following lesions of the middle temporal visual area (MT). *The Journal of Neuroscience*, *8*(6), 2201–2211. doi: 10.1523/JNEUROSCI.08-06-02201.1988

Nyström, M., Andersson, R., Niehorster, D. C. & Hooge, I. (2017). Searching for monocular microsaccades – A red Hering of modern eye trackers? *Vision Research*, *140*, 44–54. doi: 10.1016/j.visres.2017.07.012

Nyström, M., Hansen, D. W., Andersson, R. & Hooge, I. (2016). Why have microsaccades become larger? Investigating eye deformations and detection algorithms. *Vision Research*, *118*, 17–24. doi: 10.1016/j.visres.2014.11.007

Nyström, M. & Holmqvist, K. (2010). An adaptive algorithm for fixation, saccade, and glissade detection in eyetracking data. *Behaviour Research Methods*, *42*(1), 188–204. doi: 10.3758/BRM.42.1.188

Olmedo-Payá, A., Martínez-Álvarez, A., Cuenca-Asensi, S., Ferrández, J. & Fernández, E. (2015). Modeling the role of fixational eye movements in real-world scenes. *Neurocomputing*, *151*(P1), 78–84. doi: 10.1016/j.neucom.2014.09.068

Osterberg, G. (1935). Topography of the layer of rods and cones in the human retina. *Acta Ophthalmologica*, *13*(6), 1–102.

Otero-Millan, J., Castro, J. L. A., Macknik, S. L. & Martinez-Conde, S. (2014). Unsupervised clustering method to detect microsaccades. *Journal of Vision*, *14*(18), 1–17. doi: 10.1167/14.2.18.doi

Otero-Millan, J., Macknik, S. L., Langston, R. E. & Martinez-Conde, S. (2013). An oculomotor continuum from exploration to fixation. *Proceedings of the National Academy of Sciences*, *110*(15), 6175–6180. doi: 10.1073/pnas.1222715110

Otero-Millan, J., Macknik, S. L. & Martinez-Conde, S. (2012). Microsaccades and Blinks Trigger Illusory Rotation in the "Rotating Snakes" Illusion. *Journal of Neuroscience*, *32*(17), 6043–6051.

doi: 10.1523/JNEUROSCI.5823-11.2012

Otero-Millan, J., Serra, A., Leigh, R. J., Troncoso, X. G., Macknik, S. L. & Martinez-Conde, S. (2011). Distinctive Features of Saccadic Intrusions and Microsaccades in Progressive Supranuclear Palsy. *Journal of Neuroscience*, *31*(12), 4379–4387. doi: 10.1523/JNEUROSCI.2600-10.2011

Otero-Millan, J., Troncoso, X. G., Macknik, S. L., Serrano-Pedraza, I. & Martinez-Conde, S. (2008). Saccades and microsaccades during visual fixation, exploration, and search: Foundations for a common saccadic generator. *Journal of Vision*, *8*(14), 21–21. doi: 10.1167/8.14.21

Pääkkönen, A. K. & Morgan, M. J. (2001). Linear mechanisms can produce motion sharpening. *Vision Research*, *41*(21), 2771–2777. doi: 10.1016/S0042-6989(01)00170-5

Pallikaris, A., Williams, D. R. & Hofer, H. (2003). The Reflectance of Single Cones in the Living Human Eye. *Investigative Opthalmology & Visual Science*, *44*(10), 4580. doi: 10.1167/iovs.03-0094

Panda-Jonas, S., Jonas, J. B. & Jakobczyk-Zmija, M. (1995). Retinal Photoreceptor Density Decreases with Age. *Ophthalmology*, *102*(12), 1853–1859. doi: 10.1016/S0161-6420(95)30784-1

Pastukhov, A. & Braun, J. (2010). Rare but precious: Microsaccades are highly informative about attentional allocation. *Vision Research*, *50*(12), 1173–1184. doi: 10.1016/j.visres.2010.04.007

Patrick, J. A., Roach, N. W. & McGraw, P. V. (2017). Motion-based super-resolution in the peripheral visual field. *Journal of Vision*, *17*(9), 1–10. doi: 10.1167/17.9.15

Pola, J. & Wyatt, H. J. (1980). Target position and velocity: The stimuli for smooth pursuit eye movements. *Vision Research*, *20*(6), 523–534. doi: 10.1016/0042-6989(80)90127-3

Poletti, M., Listorti, C. & Rucci, M. (2013). Microscopic eye movements compensate for non-homogeneous vision within the fovea. *Current Biology*, *23*(17), 1691–1695. doi: 10.1016/j.cub.2013.07.007

Poletti, M. & Rucci, M. (2008). Oculomotor synchronization of visual responses in modeled populations of retinal ganglion cells. *Journal of Vision*, *8*(14), 1–15. doi: 10.1167/8.14.4

Poletti, M. & Rucci, M. (2010). Eye movements under various conditions of image fading. *Journal of Vision*, *10*(3), 1–18. doi: 10.1167/10.3.6

Pritchard, R. M. (1961). Stabilized Images on the Retina. *Scientific American*, *204*(6), 72–79. doi: 10.1038/scientificamerican0661-72

Pritchard, R. M., Heron, W. & Hebb, D. O. (1960). Visual Perception Approached by the Method of Stabilized Images. *Canadian Journal of Psychology*, *14*(2), 67–77. doi: 10.1037/h0083168

Rashbass, C. (1961). The relationship between saccadic and smooth tracking eye movements. *The Journal of Physiology*, *159*(2), 326–338. doi: 10.1113/jphysiol.1961.sp006811

Ratliff, F. & Riggs, L. A. (1950). Involuntary motions of the eye during monocular fixation. *Journal of*

Experimental Psychology, *40*(6), 687–701. doi: 10.1037/h0057754

Rattle, J. & Foley-Fisher, J. (1968). A Relationship between Vernier Acuity and Intersaccadic Interval. *Optica Acta: International Journal of Optics*, *15*(6), 617–620. doi: 10.1080/713818126

Reichardt, W. (1961). Autocorrelation, a principle for evaluation of sensory information by the central nervous system. In W. A. Rosenblith (Ed.), *Principles of sensory communication* (pp. 303–317). New York: Wiley.

Remmel, R. S. (1984). An Inexpensive Eye Movement Monitor Using the Scleral Search Coil Technique. *IEEE Transactions on Biomedical Engineering*, *BME-31*(4), 388–390. doi: 10.1109/TBME.1984.325352

Riggs, L. A., Armington, J. C. & Ratliff, F. (1954). Motions of the retinal image during fixation. *Journal of the Optical Society of America*, *44*(4), 315–321. doi: 10.1364/JOSA.44.000315

Riggs, L. A. & Ratliff, F. (1951). Visual acuity and the normal tremor of the eyes. *Science*, *114*(2949), 17–18. doi: 10.1126/science.114.2949.17

Riggs, L. A., Ratliff, F., Cornsweet, J. C. & Cornsweet, T. N. (1953). The disappearance of steadily fixated visual test objects. *Journal of the Optical Society of America*, *43*(6), 495–501. doi: 10.1364/JOSA.43.000495

Robinson, D. A. (1965). The mechanics of human smooth pursuit eye movement. *The Journal of Physiology*, *180*(3), 569–591. doi: 10.1113/jphysiol.1965.sp007718

Rolfs, M. (2009). Microsaccades: Small steps on a long way. *Vision Research*, *49*(20), 2415–2441. doi: 10.1016/j.visres.2009.08.010

Rolfs, M., Kliegl, R. & Engbert, R. (2008). Toward a model of microsaccade generation: The case of microsaccadic inhibition. *Journal of Vision*, *8*(11), 1–23. doi: 10.1167/8.11.5

Rosser, G., Fletcher, A. G., Wilkinson, D. A., de Beyer, J. A., Yates, C. A., Armitage, J. P., ... Baker, R. E. (2013). Novel Methods for Analysing Bacterial Tracks Reveal Persistence in Rhodobacter sphaeroides. *PLoS Computational Biology*, *9*(10), e1003276. doi: 10.1371/journal.pcbi.1003276

Rovamo, J. & Raninen, A. (1984). Critical flicker frequency and M-scaling of stimulus size and retinal illuminance. *Vision Research*, *24*(10), 1127–1131. doi: 10.1016/0042-6989(84)90166-4

Rovamo, J. & Virsu, V. (1979). An estimation and application of the human cortical magnification factor. *Experimental Brain Research*, *37*(3), 495–510. doi: 10.1007/BF00236819

Rovamo, J., Virsu, V. & Näsänen, R. (1978). Cortical magnification factor predicts the photopic contrast sensitivity of peripheral vision. *Nature*, *271*(5640), 54–56. doi: 10.1038/271054a0

Rucci, M. & Desbordes, G. (2003). Contributions of fixational eye movements to the discrimination

of briefly presented stimuli. *Journal of Vision*, *3*(11), 852–864. doi: 10.1167/3.11.18

Rucci, M., Iovin, R., Poletti, M. & Santini, F. (2007). Miniature eye movements enhance fine spatial detail. *Nature*, *447*(7146), 852–855. doi: 10.1038/nature05866

Rucci, M. & Poletti, M. (2015). Control and Functions of Fixational Eye Movements. *Annual Review of Vision Science*, *1*(1), 499–518. doi: 10.1146/annurev-vision-082114-035742

Saito, T. & Rehmsmeier, M. (2015). The Precision-Recall Plot Is More Informative than the ROC Plot When Evaluating Binary Classifiers on Imbalanced Datasets. *PLOS ONE*, *10*(3), e0118432. doi: 10.1371/journal.pone.0118432

Satterfield, D. S. (1989). Prevalence and variation of astigmatism in a military population. *Journal of the American Optometric Association*, *60*(1), 14–8.

Schor, C. & Hallmark, W. (1978). Slow control of eye position in strabismic amblyopia. *Investigative Ophthalmology & Visual Science*, *17*(6), 577–581.

Schulz, E. (1984). Binocular micromovements in normal persons. *Graefe's Archive for Clinical and Experimental Ophthalmology*, *222*, 95–100. doi: 10.1007/BF02150640

Schütt, H. H., Harmeling, S., Macke, J. H. & Wichmann, F. A. (2016). Painfree and accurate Bayesian estimation of psychometric functions for (potentially) overdispersed data. *Vision Research*, *122*, 105–123. doi: 10.1016/j.visres.2016.02.002

Schweizer, G. (1857). Über das Sternschwanken. *Bulletin de la Societe imperiale des naturalistes de Moscou*, *3-4*(February), 440–457.

Shackel, B. (1967). Electro-Oculography. In P. H. Venables & I. Martin (Eds.), *A manual of psychophysiological methods* (pp. 299–334). North-Holland Publishing Complany - Amsterdam.

Sheehy, C. K., Yang, Q., Arathorn, D. W., Tiruveedhula, P., de Boer, J. F. & Roorda, A. (2012). High-speed, image-based eye tracking with a scanning laser ophthalmoscope. *Biomedical Optics Express*, *3*(10), 2611. doi: 10.1364/BOE.3.002611

Siegenthaler, E., Costela, F. M., Mccamy, M. B., Di Stasi, L. L., Otero-Millan, J., Sonderegger, A., … Martinez-Conde, S. (2014). Task difficulty in mental arithmetic affects microsaccadic rates and magnitudes. *European Journal of Neuroscience*, *39*(2), 287–294. doi: 10.1111/ejn.12395

Simon, J. & Wolf, J. D. (1963). Choice Reaction Time As A Function Of Angular Stimulus-Response Correspondence And Age. *Ergonomics*, *6*(1), 99–105. doi: 10.1080/00140136308930679

Skavenski, A. A. (1971). Extraretinal correction and memory for target position. *Vision Research*, *11*(7), 743–746. doi: 10.1016/0042-6989(71)90104-0

Snodderly, D. M. (1987). Effects of light and dark environments on macque and human fixation eye movements. *Vision Research*, *27*(3), 401–415. doi: 10.1016/0042-6989(87)90089-7

Song, H., Chui, T. Y. P., Zhong, Z., Elsner, A. E. & Burns, S. A. (2011). Variation of Cone Photoreceptor Packing Density with Retinal Eccentricity and Age. *Investigative Opthalmology & Visual Science*, *52*(10), 7376. doi: 10.1167/iovs.11-7199

Sorensen, T. (1948). A method of establishing groups of equal amplitude in plant sociology based on similarity of species contant. *Biologiske Skrifter*, *5*(4), 3–34.

Spauschus, A., Marsden, J., Halliday, D. M., Rosenberg, J. R. & Brown, P. (1999). The origin of ocular microtremor in man. *Experimental Brain Research*, *126*(4), 556–562. doi: 10.1007/s002210050764

St. Cyr, G. J. & Fender, D. H. (1969). The interplay of drifts and flicks in binocular fixation. *Vision Research*, *9*, 245–265. doi: 10.1016/0042-6989(69)90004-2

Steinman, R. M., Cunitz, R. J., Timberlake, G. T. & Herman, M. (1967). Voluntary control of microsaccades during maintained monocular fixation. *Science*, *155*(3769), 1577–1579. doi: 10.1126/science.155.3769.1577

Steinman, R. M., Haddad, G. M., Skavenski, A. A. & Wyman, D. (1973). Miniature Eye Movement. *Science*, *181*(4102), 810–819. doi: 10.1126/science.181.4102.810

Stevenson, S. B. & Roorda, A. (2005). Miniature eye movements measured simultaneously with ophthalmic imaging and a dual-Purkinje image eye tracker. *Journal of Vision*, *5*(8), 590–590. doi: 10.1167/5.8.590

Stevenson, S. B., Roorda, A. & Kumar, G. (2010). Eye tracking with the adaptive optics scanning laser ophthalmoscope. In *Proceedings of the 2010 symposium on eye-tracking research & applications - etra '10* (p. 195). New York, New York, USA: ACM Press. doi: 10.1145/1743666.1743714

Takeuchi, T., Morikawa, N., Matsumoto, H. & Shiraishi, Y. (1962). A pathological study of Minamata disease in Japan. *Acta Neuropathologica*, *2*(1), 40–57. doi: 10.1007/BF00685743

Taylor-King, J. P., van Loon, E. E., Rosser, G. & Chapman, S. J. (2015). From Birds to Bacteria: Generalised Velocity Jump Processes with Resting States. *Bulletin of Mathematical Biology*, *77*(7), 1213–1236. doi: 10.1007/s11538-015-0083-7

Thaler, L., Schütz, A. C., Goodale, M. A. & Gegenfurtner, K. R. (2013). What is the best fixation target? The effect of target shape on stability of fixational eye movements. *Vision Research*, *76*, 31–42. doi: 10.1016/j.visres.2012.10.012

Thier, P. & Ilg, U. J. (2005). The neural basis of smooth-pursuit eye movements. *Current Opinion in Neurobiology*, *15*(6), 645–652. doi: 10.1016/j.conb.2005.10.013

Troncoso, X. G., Macknik, S. L. & Martinez-Conde, S. (2008). Microsaccades counteract perceptual

filling-in. *Journal of Vision*, *8*(14), 1–9. doi: 10.1167/8.14.15

Troncoso, X. G., Macknik, S. L., Otero-Millan, J. & Martinez-Conde, S. (2008). Microsaccades drive illusory motion in the Enigma illusion. *Proceedings of the National Academy of Sciences*, *105*(41), 16033–16038. doi: 10.1073/pnas.0709389105

Troxler, D. (1804). Ueber das Verschwinden gegebner Gegenstrände innerhalb unseres Gesichtskreises. *Ophthalmologische Bibliothek*, *2*, 1–53.

Tse, P. U., Baumgartner, F. J. & Greenlee, M. W. (2010). Event-related functional MRI of cortical activity evoked by microsaccades, small visually-guided saccades, and eyeblinks in human visual cortex. *NeuroImage*, *49*(1), 805–816. doi: 10.1016/j.neuroimage.2009.07.052

Tse, P. U., Sheinberg, D. L. & Logothetis, N. K. (2002). Fixational eye movements are not affected by abrupt onsets that capture attention. *Vision Research*, *42*(13), 1663–1669. doi: 10.1016/S0042-6989(02)00076-7

Tynan, P. D. & Sekuler, R. (1982). Motion processing in peripheral vision: Reaction time and perceived velocity. *Vision Research*, *22*(1), 61–68. doi: 10.1016/0042-6989(82)90167-5

Ukwade, M. T. & Bedell, H. E. (1993). Stability of Oculomotor Fixation as a Function of Target Contrast and Blur. *Optometry and Vision Science*, *70*(2), 123–126.

Valsecchi, M., Betta, E. & Turatto, M. (2007). Visual oddballs induce prolonged microsaccadic inhibition. *Experimental Brain Research*, *177*(2), 196–208. doi: 10.1007/s00221-006-0665-6

Van Gisbergen, J. A. M. & Robinson, D. A. (1977). Control of Gaze by Brain Stem Neurons. In *Control of gaze by brain stem neurons* (pp. 301–308). Elsevier/North-Holland.

Van Gisbergen, J. A. M., Robinson, D. A. & Gielen, S. (1981). A quantitative analysis of generation of saccadic eye movements by burst neurons. *Journal of Neurophysiology*, *45*(3), 417–442. doi: 10.1152/jn.1981.45.3.417

Van Horn, M. R. & Cullen, K. E. (2012). Coding of Microsaccades in Three-Dimensional Space by Premotor Saccadic Neurons. *Journal of Neuroscience*, *32*(6), 1974–1980. doi: 10.1523/JNEUROSCI.5054-11.2012

Vikesdal, G. H. & Langaas, T. (2016). Optically induced refractive errors reduces fixation stability but saccade latency remains stable. *Journal of Eye Movement Research*, *9*(7), 1–8. doi: 10.16910/jemr.9.7.3

Visser, A. W. & Kiørboe, T. (2006). Plankton motility patterns and encounter rates. *Oecologia*, *148*(3), 538–546. doi: 10.1007/s00442-006-0385-4

Wandell, B. A. (1995). *Foundations of Vision*. Sinauer Associates.

Watson, A. B. (2014). A formula for human retinal ganglion cell receptive field density as a function

of visual field location. *Journal of Vision*, *14*(7), 15. doi: 10.1167/14.7.15

Westheimer, G. (1954). Mechanism of saccadic eye movements. *AMA Archives of Ophthalmology*, *52*(5), 710–724. doi: 10.1001/archopht.1954.00920050716006

White, A. L. & Rolfs, M. (2016). Oculomotor inhibition covaries with conscious detection. *Journal of Neurophysiology*, *116*(3), 1507–1521. doi: 10.1152/jn.00268.2016

Williams, L. J. & Lefton, L. A. (1981). Processing of Alphabetic Information Presented in the Fovea or the Periphery: Functional Visual Field and Cognitive Load. *Perception*, *10*(6), 645–650. doi: 10.1068/p100645

Winterson, B. J. & Collewijn, H. (1976). Microsaccades during finely guided visuomotor tasks. *Vision Research*, *16*(12), 1387–1390. doi: 10.1016/0042-6989(76)90156-5

Winterson, B. J. & Robinson, D. A. (1975). Fixation by the alert but solitary cat. *Vision Research*, *15*(12), 1349–1352. doi: 10.1016/0042-6989(75)90188-1

Wyatt, H. J. (1998). Detecting saccades with jerk. *Vision Research*, *38*(14), 2147–2153. doi: 10.1016/S0042-6989(97)00410-0

Yu, D., Legge, G. E., Wagoner, G. & Chung, S. T. (2018). Training peripheral vision to read: Boosting the speed of letter processing. *Vision Research*, *152*, 51–60. doi: 10.1016/j.visres.2017.06.005

Zuber, B. L. & Stark, L. (1965). Microsaccades and the Velocity-Amplitude Relationship for Saccadic Eye Movement. *Science*, *150*(3702), 1459–1460. doi: 10.1126/science.150.3702.1459

Zuber, B. L. & Stark, L. (1966). Saccadic Suppression: Elevation of visual threshold associated with saccadic eye movements. *Experimental Neurology*, *16*, 65–79. doi: 10.1016/0014-4886(66)90087-2

Chapter 10

Appendix

10.1 Table of Microsaccade Features

The following pages were formatted for A3 format, but are printed here in an A4 version. Please refer to the pdf version of this thesis to access the A3 formatted pages in full size.

Paper	Experiment	Recording Method	Number of Participants	Eyes - viewing	Eyes - recording	Recording frequency (Hz)	Direction of recording	Analysis Method	Fixation duration [sec]	Targets	Instruction	Min Distance [']	Average Distance [']	Max Distance [']	Min Speed [°/s]	Average Speed [°/s]	Max Speed [°/s]	Min Acceleration [°/s²]	Mean Acceleration [°/s²]	Max Acceleration [°/s²]	Min Duration [ms]	Average Duration [ms]	Max Duration [ms]	Minimum Frequency [1/s]	Average Frequency [1/s]	Maximum Frequency [1/s]	Main Sequence: Axes
Armington & Bloom, 1974	1	Contact Lens Mirror	3	M	M	N/A	X	criterion size and direction	600	vertically oriented stripes (.26-6.83cyc/°)	/	**1**	/	**12**	/	/	/	/	/	/	/	/	/	/	/	/	/
Barlow, 1952	1	Hg droplets on cornea	4	/	M	250	/	manual	180-300	point of light	fixate	/	/	/	/	/	/	/	/	/	/	40	/	0.20	/	/	/
Beeler, 1967	1	Contact Lens Mirror	2	M	M	/	/	first order differentiator and low-pass filter with a third order cutoff above 40 Hz	3	luminance targets / motion targets	report presence of stimulus since last response collection	/	/	30	/	/	/	/	/	/	/	/	/	/	/	/	/
Betta & Turatto, 2006	1	Eyelink II	12	B	M	500	B	Engbert & Kliegl	9	red or green disk	respond to stimuli appearing	/	/	/	/	/	/	/	/	/	/	/	/	**0.20**	/	**3.40**	/
Betta, Galfano, & Turatto, 2007	1	Eyelink II	26	B	M	500	B	Engbert & Kliegl	varied, ca 3sec	Central fixation dot and horizontal boxes	maintain gaze within imaginary central square	/	/	/	/	/	/	/	/	/	/	/	/	0.57	1.40	2.54	/
Boyce, 1967	1	Contact Lens Mirror	4	B/M	M	96	B	velocity filter	60	dotted cross	/	2	5	16	/	/	/	/	/	/	/	/	/	0	3	5	/
Bridgeman & Palca, 1980	1	photoelectric technique	7	/	/	/	X	< 15'arc	/	one stationary, one moving electrode	fixate tip of stationary electrode	/	/	/	/	/	/	/	/	/	/	/	/	0.51	/	1.60	/
Cherici, Kuang, Poletti, & Rucci, 2012	1	Dual Purkinje Image	14	M	R	1000	B	velocity >3°/s, amplitude >3', validated by humans	5	no marker	maintain accurate fixation	17†	40	67†	/	/	/	/	/	/	/	/	/	0.16†	1.07	2.14†	/
Cherici et al., 2012	2	Dual Purkinje Image	14	M	R	1000	B	velocity >3°/s, amplitude >3', validated by humans	5	marker	maintain accurate fixation	8†	20	31†	/	/	/	/	/	/	/	/	/	0.44†	1.32	2.29†	/
Cornsweet, 1956	1	Contact Lens Mirror	2	M	M	N/A	X	manual	45	vertical line circular background	/	**3**	/	**7**	/	/	/	/	/	/	/	/	/	0.40	0.95	1.56	/

Paper	Experiment	Recording Method	Number of Participants	Eyes - viewing	Eyes - recording	Recording frequency (Hz)	Direction of recording	Analysis Method	Fixation duration [sec]	Targets	Instruction	Min Distance [']	Average Distance [']	Max Distance [']	Min Speed [°/s]	Average Speed [°/s]	Max Speed [°/s]	Min Acceleration [°/s²]	Mean Acceleration [°/s²]	Max Acceleration [°/s²]	Min Duration [ms]	Average Duration [ms]	Max Duration [ms]	Minimum Frequency [1/s]	Average Frequency [1/s]	Maximum Frequency [1/s]	Main Sequence: Axes
Cunitz & Steinman, 1969	1	Contact Lens Optical Lever	2	/	/	500	X	microsaccade size limit of 11.6'	20	single letter / text	fixate / read	/	5.6 - 11.1	12	/	/	/	/	/	/	/	/	/	2.11†	/	2.7†	/
de Weese Puckett & Steinman, 1969	1	Contact Lens Optical Lever	2	/	R	200	X	manual	/	green point	fixate	/	/	/	/	/	/	/	/	/	/	/	/	1.32	1.78/1.59	2.56	/
de Weese Puckett & Steinman, 1969	2	Contact Lens Optical Lever	2	/	R	200	X	manual	/	green point	hold	/	/	/	/	/	/	/	/	/	/	/	/	0.18	0.9/.63	1.03	/
Deaner & Platt, 2003	1	Magnetic search coil technique	4	/	M	500	X	acceleration (8°/s for 3 samples onset & 5°/s for 1 sample offset)	.8-1.7	faces	N/A	/	52	/	/	/	/	/	/	/	/	/	/	/	/	/	/
Di Stasi et al., 2013 (45)	1	Eyelink 1000	12	B	B	500	B	Engbert & Kliegl	45	air traffic control task	free viewing / fixation	**4**	/	**60**	/	/	/	/	/	/	/	/	/	/	/	/	linear - linear
Dimigen, Valsecchi, Sommer, & Kliegl, 2009 (83)	1	IView-X Hi-Speed 1250, SMI	8	B	R	500	B	Engbert & Mergenthaler, 2006	10	black and white checkerboard with five fixation points	maintain perfect fixation	**6**	17	**60**	**20**	48.1 (peak)	**110**	/	/	/	/	10	/	/	0.62	/	linear - linear
Dimigen et al., 2009 (83)	2	IView-X Hi-Speed 1250, SMI	3	B	R	500	B	Engbert & Mergenthaler, 2006	10	.2° fixation point on face	maintain perfect fixation	**3**	16	**54**	**20**	43.9 (peak)	**110**	/	/	/	/	10	/	/	0.88	/	linear - linear
Dimigen et al., 2009 (83)	3	IView-X Hi-Speed 238, SMI	12	B	R	238	B	Engbert & Mergenthaler, 2006	50	.48° white point, intermittent coloured disks	minimise eye blinks and maintain fixation, count oddball colours	**2**	14	**60**	**3**	/	**65**	/	/	/	/	/	/	**0.20**	1.47	**6.50**	linear - linear
Ditchburn & Ginsborg, 1953	1	Contact Lens Mirror	2	B	B	N/A	B	Manual	/	Dots / cross	/	5	6.1/5.8	15	/	10	/	/	/	1000	/	/	/	0.20	.9-1.4	33.33	/

Paper	Experiment	Recording Method	Number of Participants	Eyes - viewing	Eyes - recording	Recording frequency (Hz)	Direction of recording	Analysis Method	Fixation duration [sec]	Targets	Instruction	Min Distance [']	Average Distance [']	Max Distance [']	Min Speed [°/s]	Average Speed [°/s]	Max Speed [°/s]	Min Acceleration [°/s²]	Mean Acceleration [°/s²]	Max Acceleration [°/s²]	Min Duration [ms]	Average Duration [ms]	Max Duration [ms]	Minimum Frequency [1/s]	Average Frequency [1/s]	Maximum Frequency [1/s]	Main Sequence: Axes
Ditchburn & Ginsborg, 1953	2	Contact Lens Mirror	1	B	B	N/A	B	manual	5	darkness	/	2	17	45	/	/	/	/	/	/	/	/	/	0.31	/	10.00	/
Engbert & Kliegl, 2004	1	Eyelink II	5	B	B	500	B	Engbert & Kliegl	3	black square (7.2')	fixate	/	/	/	/	/	/	/	/	/	/	/	/	0.80	/	1.90	/
Engbert & Kliegl, 2003	1	SMI Eyelink System	30	B	B	250	B	Engbert & Kliegl	3.5-4.5	cross - arrow cue -target	saccade to target / button press	/	32	/	/	/	/	/	/	/	/	/	/	0.13	1.27	4.00	log. - log.
Engbert & Kliegl, 2003	2	SMI Eyelink System	30	B	B	250	B	Engbert & Kliegl	3.5-4.5	cross - colour change -target	saccade to target / button press	/	/	/	/	/	/	/	/	/	/	/	/	**0.20**	/	**1.90**	log. - log.
Engbert & Kliegl, 2003	3	SMI Eyelink System	20	B	B	250	B	Engbert & Kliegl	3.5-4.5	cross - colour change / arrow	respond to offset of cue	/	/	/	/	/	/	/	/	/	/	/	/	**0.20**	/	**3.10**	log. - log.
Engbert & Mergenthaler, 2006	1	Eyelink II	29	B	B	500	B	Engbert & Kliegl	3	black square (7.2')	keep eyes on fixation target and not blink	**1**	/	60	**4**	/	**100**	/	/	/	/	/	/	/	1.13	/	log. - log.
Engbert & Mergenthaler, 2006	2	Eyelink II	17	B	B	500	B	Engbert & Kliegl	20	black square (7.2')	keep eyes on fixation target and not blink	/	/	60	/	/	/	/	/	/	/	/	/	/	1.21	/	log. - log.
Fried et al., 2014 (36)	1	Eyelink 1000	22	B	D	500	B	> 6msec; linear in 30° window; velocity >10°/s; amplitude >.1°	2	white fixation dot, grex boy with dark square	respond to target appearance	**6**	/	**192**	/	/	/	/	/	/	/	/	/	**0.40**	**2.25**	**5.20**	linear - linear
Gaarder, 1960	1	Contact Lens Mirror	1	/	/	N/A	B	manual	45	complex shapes	fixate on specific point of shape	1	/	30	/	/	/	/	/	/	/	/	/	/	/	/	/
Galfano, Betta, & Turatto, 2004	1	Eyelink II	13	B	B	500	B	Engbert & Kliegl	2.3	changing boxes	/	**4**	/	60	/	/	/	/	/	/	/	/	/	**0.30**	1.20	**2.40**	linear - linear
Haddad & Steinman, 1973	3	Contact Lens Optical Lever	/	/	/	12	B	computer	7	dots	make smallest voluntary saccade	3	11.4 / 10.6	13	/	/	/	/	/	/	/	/	/	/	0.04	/	/
Hafed & Clark, 2002	1	ISCAN	14	/	/	240	X	> .12° & < 1°, main sequence, velocity > 8°/s	/	pro cue task	/	7	/	60	8	/	**100**	/	/	/	/	/	/	/	/	/	log. - log.

Paper	Experiment	Recording Method	Number of Participants	Eyes - viewing	Eyes - recording	Recording frequency (Hz)	Direction of recording	Analysis Method	Fixation duration [sec]	Targets	Instruction	Min Distance [']	Average Distance [']	Max Distance [']	Min Speed [°/s]	Average Speed [°/s]	Max Speed [°/s]	Min Acceleration [°/s²]	Mean Acceleration [°/s²]	Max Acceleration [°/s²]	Min Duration [ms]	Average Duration [ms]	Max Duration [ms]	Minimum Frequency [1/s]	Average Frequency [1/s]	Maximum Frequency [1/s]	Main Sequence: Axes
Hafed & Clark, 2002	2	ISCAN	13	/	/	240	X	> .12° & < 1°, main sequence, velocity > 8°/s	/	anti cue task	/	7	/	60	8	/	**100**	/	/	/	/	/	/	/	/	/	log. - log.
Hipp & Siegel, 2013 (61)	1	EOG	24	B	B	1000	/	/	1.52	central cross, two moving peripheral bars	report nature of ambiguous stimulus	/	/	/	/	/	/	/	/	/	/	/	/	**0.10**	/	**2.20**	/
Ko, Poletti, & Rucci, 2010 (137)	1	Dual Purkinje Image	6	/	/	1000	B	velocity>3°/sec & larger than 1 min arc	17.5	threading a needle	threading a needle	/	19	**108**	/	/	/	/	/	/	/	/	/	**0.30**	**0.10**	**0.80**	/
Ko et al., 2010 (137)	2	Dual Purkinje Image	6	/	/	1000	B	velocity>3°/sec & larger than 1 min arc	17.5	fixating a needle	fixating a needle	/	20	**168**	/	/	/	/	/	/	/	/	/	**0.40**	**0.14**	**0.80**	/
Krauskopf, Cornsweet, & Riggs, 1960	1	Contact Lens Mirror	2	B	B	0.5	X	manual	300	/	/	**1**	1.55 - 3.96	**6**	/	/	/	/	/	/	/	/	/	/	/	/	/
Kuang, Poletti, Victor, & Rucci, 2012 (80)	1	Dual Purkinje Image	14	R	R	1000	B	speed >3°/s, amplitude >3' and <30'	10	greyscale pictures of natural scenes	memorise image	3	/	30	/	/	/	/	/	/	/	/	/	0.05	0.17	0.50	/
Laubrock, Kliegl, Rolfs, & Engbert, 2010 (35)	1	Eyelink II	20	/	/	500	B	Engbert & Mergenthaler	3-4.5	fixation cross and peripheral disk	manual / saccadic response to target	**1**	15	**60**	/	/	/	/	/	/	/	/	/	/	/	/	/
Laubrock, Engbert, & Kliegl, 2008	1	Eyelink II	16	B	B	500	B	Engbert & Kliegl	20.2-23.9	horizontally and vertically moving dots & ventral grey fixation dot	report motion direction	/	25	60	/	/	/	/	/	/	/	/	/	**0.40**	/	**1.50**	/
Laubrock et al., 2008	2	Eyelink II	23	B	B	500	B	Engbert & Kliegl	2.55	horizontally moving dots & central grey fixation dot	report motion direction	/	/	60	/	/	/	/	/	/	/	/	/	**0.10**	/	**1.40**	/
Laubrock, Engbert, & Kliegl, 2005	1	Eyelink II	32	B	B	500	B	Engbert & Kliegl	3.1-5.1	.03° disk and peripheral flash cues and brief Landolt ring target	/	3	22	90	/	/	/	/	/	/	/	/	/	**0.10**	/	**2.30**	/

Paper	Experiment	Recording Method	Number of Participants	Eyes - viewing	Eyes - recording	Recording frequency (Hz)	Direction of recording	Analysis Method	Fixation duration [sec]	Targets	Instruction	Min Distance [']	Average Distance [']	Max Distance [']	Min Speed [°/s]	Average Speed [°/s]	Max Speed [°/s]	Min Acceleration [°/s²]	Mean Acceleration [°/s²]	Max Acceleration [°/s²]	Min Duration [ms]	Average Duration [ms]	Max Duration [ms]	Minimum Frequency [1/s]	Average Frequency [1/s]	Maximum Frequency [1/s]	Main Sequence: Axes
Martinez-Conde, Macknik, Troncoso, & Dyar, 2006	1	Eyelink II	8	B	B	500	B	Martinez-Conde 2000	30	.05° red fixation dot, peripheral gabor target (9°)	fixate, button press when fading	**1**	**14**	**120**	**3**	/	**40**	/	/	/	/	/	/	**3.20**	/	**4.50**	log. - log. & linear - linear
Martinez-Conde et al., 2006	2	Eyelink II	6	B	B	500	B	Martinez-Conde 2000	30	.05° red fixation dot, peripheral gabor target (3°/6°)	fixate, button press when fading	/	/	/	/	/	/	/	/	/	/	/	/	/	/	/	log. - log. & linear - linear
Martinez-Conde et al., 2006	3	Eyelink II	7	B	B	500	B	Martinez-Conde 2000	30	.05° red fixation dot, peripheral gabor target	fixate, button press when fading	1	/	120	3	/	40	/	/	/	/	/	/	/	/	/	log. - log. & linear - linear
McCamy et al., 2012 (71)	1	Eyelink 1000	6	B	B	500	B	Engbert & Kliegl	30	.05° red spot and peripheral fading stimulus	fixate and report fading	**2**	/	**60**	**5**	/	**140**	/	/	/	/	20	/	**0.50**	1.07	**2.60**	linear - linear
McCamy, Otero-Millan, Di Stasi, Macknik, & Martinez-Conde, 2014 (44)	1	Eyelink II	8	B	B	500	B	Engbert & Kliegl	45	blank scene	free viewing / fixation	/	/	/	/	/	/	/	/	/	/	/	/	**0.13**	/	**0.25**	linear - linear
McCamy et al., 2014 (44)	2	Eyelink II	8	B	B	500	B	Engbert & Kliegl	45	natural scene	free viewing	**5**	/	**60**	/	/	/	/	/	/	/	/	/	**0.10**	/	**1.30**	linear - linear
McCamy et al., 2014 (44)	3	Eyelink II	8	B	B	500	B	Engbert & Kliegl	45	picture puzzle	find differences	**5**	/	**60**	/	/	/	/	/	/	/	/	/	**0.10**	/	**1.20**	linear - linear
McCamy et al., 2014 (44)	4	Eyelink II	8	B	B	500	B	Engbert & Kliegl	45	Where's Waldo	find Waldo	**5**	/	**60**	/	/	/	/	/	/	/	/	/	**0.10**	/	**1.20**	linear - linear

Paper	Experiment	Recording Method	Number of Participants	Eyes - viewing	Eyes - recording	Recording frequency (Hz)	Direction of recording	Analysis Method	Fixation duration [sec]	Targets	Instruction	Min Distance [']	Average Distance [']	Max Distance [']	Min Speed [°/s]	Average Speed [°/s]	Max Speed [°/s]	Min Acceleration [°/s²]	Mean Acceleration [°/s²]	Max Acceleration [°/s²]	Min Duration [ms]	Average Duration [ms]	Max Duration [ms]	Minimum Frequency [1/s]	Average Frequency [1/s]	Maximum Frequency [1/s]	Main Sequence: Axes
McCamy et al., 2013 (31)	1	Eyelink 1000	17	B	B	500	B	Enbert & Kliegl	30	circular target		**6**	/	**120**	/	/	/	/	/	/	/	/	/	**1.00**	/	**1.31**	linear - linear
Møller, Laursen, Tygesen, & Sjølie, 2002	1	SMI Eyelink System	10	B	B	250	B	Velocity > 5 °/s; acceleration > 2,500 °/s^2 ; overshoot	40	black cross on white (1.39°)	fixate on centre of cross	**6**	12.72 - 65.88	**150**	/	19 - 40	28 - 98	/	2322 - 6440	/	/	/	/	0.23†	0.61	0.93†	linear - linear
Møller, Laursen, & Sjølie, 2006	1	SMI Eyelink System	10	B	B	250	B	Velocity > 5 °/s; acceleration > 2,500 °/s^2 ; overshoot	40	black cross on white (1.39°)	fixate on centre of cross	14†	/	65†	5	/	/	2500	/	/	/	/	/	/	/	/	/
Nachmias, 1959	1	Contact Lens Optical Lever	2	M	M	N/A	B	manual	30	crosshairs (1.4')	/	/	/	/	/	/	/	/	/	/	/	/	/	2.14	/	/	
Nachmias, 1961	1	Contact Lens Optical Lever	2	M	M	N/A	B	manual	30	crosshairs (1.4')	maintain same passive attitude when target is present / not	1†	/	8†	/	/	/	/	/	/	/	/	/	/	/	/	
Otero-Millan et al., 2011 (67)	1	search coil/ Eyelink II	14	/	M/B	500	B	Engbert & Kliegl	10-120	.1° red spot / red cross	sustain steady fixation	/	28	/	**3**	39 (peak)	**300**	/	/	/	/	/	/	1.10	/	linear - linear	
Otero-Millan, Macknik, Langston, & Martinez-Conde, 2013 (45)	1	Eyelink 1000	10	B	B	500	B	Engbert & Kliegl	30	natural greyscale images / grey box / red fixation dot	free viewing / fixation	**5**	/	/	/	/	/	/	/	/	/	/	/	**1.30**	/	/	
Otero-Millan et al., 2013 (45)	2	Eyelink II	6	B	B	500	B	Engbert & Kliegl	30	larger natural greyscale images /red fixation dot	fixate / freely explore including head motion	**5**	/	/	/	/	/	/	/	/	/	/	/	**1.30**	/	/	
Otero-Millan, Troncoso, Macknik, Serrano-Pedraza, &	A	Eyelink II	8	B	B	500	B	Engbert & Kliegl	45	red cross (.75°)	fixate	**2**	25	**60**	**10**	/	42	/	/	/	**4**	13	**34**	/	0.80	/	linear - linear

Paper	Experiment	Recording Method	Number of Participants	Eyes - viewing	Eyes - recording	Recording frequency (Hz)	Direction of recording	Analysis Method	Fixation duration [sec]	Targets	Instruction	Min Distance [']	Average Distance [']	Max Distance [']	Min Speed [°/s]	Average Speed [°/s]	Max Speed [°/s]	Min Acceleration [°/s²]	Mean Acceleration [°/s²]	Max Acceleration [°/s²]	Min Duration [ms]	Average Duration [ms]	Max Duration [ms]	Minimum Frequency [1/s]	Average Frequency [1/s]	Maximum Frequency [1/s]	Main Sequence: Axes
Martinez-Conde, 2008																											
Otero-Millan et al., 2008	B	Eyelink II	8	B	B	500	B	Engbert & Kliegl	45	naturalistic images	fixate	**2**	26	**60**	**10**	/	44	/	/	/	**4**	13	**34**	/	0.80	/	linear - linear
Otero-Millan et al., 2008	C	Eyelink II	8	B	B	500	B	Engbert & Kliegl	45	Picture Puzzle	fixate	**2**	26	**60**	**10**	/	43	/	/	/	**4**	13	**34**	/	0.80	/	linear - linear
Otero-Millan et al., 2008	D	Eyelink II	8	B	B	500	B	Engbert & Kliegl	45	Where's Waldo	fixate	**2**	25	**60**	**10**	/	41	/	/	/	**4**	13	**34**	/	0.80	/	linear - linear
Otero-Millan, Macknik, & Martinez-Conde, 2012 (28)	1	Eyelink 1000	8	B	B	500	B	Enbert & Kliegl	30	central red fixation dot and peripheral rotating snake illusion	report transitions in motion	**3**	30	**153**	**15**	28 (peak)	**200**	/	/	/	4†	5	12†	0.48†	0.80	1.3†	linear - linear
Pastukhov & Braun, 2010 (63)	1	Eyelink 2000	5	B	B	1000	B	Engbert & Kliegl	4.82	fixation cross and peripheral targets	report letter identity or colour	**4**	/	**140**	/	/	/	/	/	/	/	/	/	**0.01**	/	**0.80**	log. - log.
Pastukhov & Braun, 2010 (63)	2	Eyelink 2000	5	B	B	1000	B	Engbert & Kliegl	4.32	fixation cross and peripheral targets	report letter identity	/	/	/	/	/	/	/	/	/	/	/	/	0.01	/	1.12	log. - log.
Pastukhov & Braun, 2010 (63)	3	Eyelink 2000	5	B	B	1000	B	Engbert & Kliegl	4.19	central targets	report letter identity or colour	/	/	/	/	/	/	/	/	/	/	/	/	**0.01**	.26/.12	2.24	log. - log.
Poletti & Rucci, 2010 (47)	1	Dual Purkinje Image	11	R	R	1000	B	velocity>3°/s, amplitude<30'	10	movie of natural scene greyscale image fading	/	**6**	19	**56**	/	/	/	/	/	/	/	/	/	0.50	1.20	2.10	/
Poletti & Rucci, 2010 (47)	2	Dual Purkinje Image	11	R	R	1000	B	velocity>3°/s, amplitude<30'	10	movie of natural scene greyscale image fading	/	**6**	20	**56**	/	/	/	/	/	/	/	/	/	/	1.30	/	/
Poletti & Rucci, 2010 (47)	3	Dual Purkinje Image	11	R	R	1000	B	velocity>3°/s, amplitude<30'	10	natural greyscale image under retinal stabilisation	/	**6**	21	**54**	/	/	/	/	/	/	/	/	/	/	1.10	/	/
Ratliff & Riggs, 1950	1	Contact Lens Mirror	5	R	R	N/A	B	manual	2-4	fixation point (3.45') / cross	fixate steadily	2	6	26	/	/	/	/	/	/	/	/	/	0.29	/	5.00	/

Paper	Experiment	Recording Method	Number of Participants	Eyes - viewing	Eyes - recording	Recording frequency (Hz)	Direction of recording	Analysis Method	Fixation duration [sec]	Targets	Instruction	Min Distance [']	Average Distance [']	Max Distance [']	Min Speed [°/s]	Average Speed [°/s]	Max Speed [°/s]	Min Acceleration [°/s²]	Mean Acceleration [°/s²]	Max Acceleration [°/s²]	Min Duration [ms]	Average Duration [ms]	Max Duration [ms]	Minimum Frequency [1/s]	Average Frequency [1/s]	Maximum Frequency [1/s]	Main Sequence: Axes
Rattle & Foley-Fisher, 1968	1	Scleral reflection / Contact Lens Optical Lever	9	R	L	N/A	X	manual	15	vernier targets 1° length	vernier task	2	/	/	/	/	/	/	/	/	/	/	/	**0.38**	/	**1.25**	/
Rolfs, Engbert, & Kliegl, 2004	1	Eyelink II	22	B	B	500	B	Engbert & Kliegl	2.6-3.6	central spot	respond to cues	/	/	60	/	/	/	/	/	/	/	/	/	**0.18**	/	**0.70**	/
Rolfs, Engbert, & Kliegl, 2005	1	Eyelink II	28	B	B	500	B	Engbert & Kliegl	2.1-3.1	fixation ring .8° outside, .1° inside	target colour judgement	/	/	/	/	/	/	/	/	/	/	/	/	0.40	0.80	1.40	/
Rolfs et al., 2005	2	Eyelink II	28	B	B	500	B	Engbert & Kliegl	2.1-3.1	fixation ring .8° outside, .1° inside	reply to target pitch	/	/	/	/	/	/	/	/	/	/	/	/	0.40	1.20	1.80	/
Rolfs et al., 2005	3	Eyelink II	25	B	B	500	B	Engbert & Kliegl	2.1-3.1	fixation ring .8° outside, .1° inside	cross of visual and auditory cues	/	/	/	/	/	/	/	/	/	/	/	/	0.20	1-1.2	**1.50**	/
Rolfs, Kliegl, & Engbert, 2008	1	Eyelink II	60	B	B	500	B	Engbert & Kliegl	1.1-3.1	fixation ring .8° outside, .1° inside	auditory or visual cue task	**6**	/	**18**	/	/	/	/	/	/	/	/	/	**0.30**	/	**2.00**	/
Rolfs, Kliegl, & Engbert, 2008	2	Eyelink II	27	B	B	500	B	Engbert & Kliegl	1.1-3.1	fixation ring .8° outside, .1° inside	auditory or visual cue task	**7**	/	**16**	/	/	/	/	/	/	/	/	/	**0.20**	/	**2.70**	/
Rolfs, Laubrock, & Kliegl, 2006	1	Eyelink II	31	B	B	500	B	Engbert & Kliegl	2.5	point	respond to cues	/	/	/	/	/	/	/	/	/	/	/	/	0.20	1.00	2.00	/
Rucci & Desbordes, 2003	1	Dual Purkinje Image	4	/	/	1000	B	velocity threshold: 10°/sec	2	bars with noise	reply to orientation of bar	18†	27	38†	/	/	/	/	/	/	/	/	/	0.95	1.50	2.25	/
Rucci & Desbordes, 2003	2	Dual Purkinje Image	4	/	/	1000	B	velocity threshold: 10°/sec	0.5	bars with noise	reply to orientation of bar	18†	27	40†	/	/	/	/	/	/	/	/	/	0.20	0.40	0.60	/
Sabrin & Kertesz, 1980	1.1	Dual Purkinje Image	2	B	B	120	B	<4minarc, shorter than 50msec	45	annulus, with different polarity to each eye	indicate rivalry	/	/	/	/	/	/	/	/	/	/	/	/	1.31	/	1.43	/
Sabrin & Kertesz, 1980	1.2	Dual Purkinje Image	2	B	B	120	B	<4minarc, shorter than 50msec	45	annulus, with different	indicate rivalry	/	/	/	/	/	/	/	/	/	/	/	/	1.95	/	2.26	/

Paper	Experiment	Recording Method	Number of Participants	Eyes - viewing	Eyes - recording	Recording frequency (Hz)	Direction of recording	Analysis Method	Fixation duration [sec]	Targets	Instruction	Min Distance [']	Average Distance [']	Max Distance [']	Min Speed [°/s]	Average Speed [°/s]	Max Speed [°/s]	Min Acceleration [°/s²]	Mean Acceleration [°/s²]	Max Acceleration [°/s²]	Min Duration [ms]	Average Duration [ms]	Max Duration [ms]	Minimum Frequency [1/s]	Average Frequency [1/s]	Maximum Frequency [1/s]	Main Sequence: Axes
										polarity to each eye																	
Sansbury, Skavenski, Haddad, & Steinman, 1973	1	Contact Lens Optical Lever	2	R	R	N/A	B	/	30	1.3° white disk	maintain fixation after target removed	8	/	9	/	/	/	/	/	/	/	/	/	2.10	/	2.50	/
Sansbury et al., 1973	2,3,4	Contact Lens Optical Lever	2	R	R	N/A	B	/	30	4 disks	maintain fixation after target removed	10	/	24	/	/	/	/	/	/	/	/	/	1.40	/	2.40	/
Sansbury et al., 1973	5,6	Contact Lens Optical Lever	2	R	R	N/A	B	/	30	two disks	maintain fixation after target removed	16	/	21	/	/	/	/	/	/	/	/	/	1.90	/	2.50	/
Sansbury et al., 1973	7	Contact Lens Optical Lever	2	R	R	N/A	B	/	30	darkness	maintain fixation after target removed	32	/	40	/	/	/	/	/	/	/	/	/	1.80	/	2.00	/
Schor & Hallmark, 1978	1	infrared eye movement detector	1	M	M	/	X	/	40	points	fixate alternately	/	8	/	/	/	/	/	/	/	/	/	/	0.60	/	/	
Schulz, 1984	1	Contact Lens Mirror	6	B	B	200	B	/	10.25	snellen target	/	3	/	50	8	/	35	/	/	/	16	/	25	1.00	/	3.00	linear - linear
Siegenthaler et al., 2014 (51)	1	Eyelink 1000	11	B	B	500	B	Engbert & Kliegl	180	black dot	control task	**6**	27	**120**	**10**	/	**170**	/	/	/	/	/	/	1.35	/		linear - linear
Siegenthaler et al., 2014 (51)	2	Eyelink 1000	11	B	B	500	B	Engbert & Kliegl	180	black dot	easy arithmetic	**6**	34	**120**	**10**	/	**170**	/	/	/	/	/	/	1.53	/		linear - linear
Siegenthaler et al., 2014 (51)	3	Eyelink 1000	11	B	B	500	B	Engbert & Kliegl	180	black dot	difficult arithmetic	**6**	42	**120**	**10**	/	**170**	/	/	/	/	/	/	1.13	/		linear - linear
Simon, Schulz, Rassow, & Haase, 1984	1	Contact Lens Mirror	/	B	B	2000	B	/	10.24	snellen target	/	5	/	32	/	/	**35**	/	/	/	/	/	/	2.10	/	/	

Paper	Experiment	Recording Method	Number of Participants	Eyes - viewing	Eyes - recording	Recording frequency (Hz)	Direction of recording	Analysis Method	Fixation duration [sec]	Targets	Instruction	Min Distance [']	Average Distance [']	Max Distance [']	Min Speed [°/s]	Average Speed [°/s]	Max Speed [°/s]	Min Acceleration [°/s²]	Mean Acceleration [°/s²]	Max Acceleration [°/s²]	Min Duration [ms]	Average Duration [ms]	Max Duration [ms]	Minimum Frequency [1/s]	Average Frequency [1/s]	Maximum Frequency [1/s]	Main Sequence: Axes
Snodderly, 1987	1 (in light)	Dual Purkinje Image	2	B	R	200	B	/	>1.4	spot dimming	report when spot disappears	/	5 - 10.11	18	/	/	/	/	/	/	/	/	0.13	/	1.66	/
Snodderly, 1987	2 (in dark)	Dual Purkinje Image	2	B	R	200	B	/	>1.4	spot dimming	report when spot disappears	/	8 - 11.8	20	/	/	/	/	/	/	/	/	0.15	/	0.61	/
Steinman, 1965	1&2	Contact Lens Mirror	2	R	R	N/A	B	/	30	concentric targets: different sizes & luminances	/	/	/	/	/	/	/	/	/	/	/	/	**1.25**	/	**2.15**	/
Steinman & Cunitz, 1968	1	Contact Lens Optical Lever	2	/	M	/	B	/	10 / 45	disk of scotopic tunsten light, 5.4'	maintain fixation	5†	23 - 39	82†	/	/	/	/	/	/	/	/	/	/	/	/
Steinman, Cunitz, Timberlake, & Herman, 1967	1	Contact Lens Optical Lever	2	/	/	/	B	/	9.8	white light	fixate	/	8	/	/	/	/	/	/	/	/	/	/	0.86	/	1.47	/
Steinman et al., 1967	2	Contact Lens Optical Lever	2	/	/	/	B	/	9.8	white light	hold	/	/	/	/	/	/	/	/	/	/	/	/	0.33	/	0.57	/
Steinman, Skavenski, & Sansbury, 1969	1	Contact Lens Optical Lever	2	/	/	/	B	/	/	white light	fixate	2	/	10	/	/	/	/	/	/	/	/	/	1.13	/	2.15	/
Steinman et al., 1969	2	Contact Lens Optical Lever	2	/	/	/	B	/	/	white light	hold	2	/	10	/	/	/	/	/	/	/	/	/	0.10	/	0.35	/
Thaler, Schütz, Goodale, & Gegenfurtner, 2013 (45)	1&2	Eyelink II	12	B	M	250	B	Engbert & Kliegl	17	range of fixation targets	keep gaze directed at centre as stable as possible	**2**	11	**60**	/	/	/	/	/	/	/	/	/	**1.65**	**/**	**1.80**	/
Troncoso, Macknik, & Martinez-Conde, 2008	1	Eyelink II	6	B	B	500	B	Engbert & Kliegl	/	small spot	fixate, report on visibility of artificial scotoma	**2**	25	180	/	41 (peak)	**100**	/	/	/	**2**	13	**101**	**0.20**	0.70	**2.00**	log. - log.
Tse, Baumgartner,	2	Limbus tracker	8	/	R	1000	B	zero crossing in velocity space between 10 and	445	black fixation point on	maintain fixation	**0**	/	**83**	**6**	/	**50**	/	/	/	/	/	/	/	/	/	log. - log

Paper	Experiment	Recording Method	Number of Participants	Eyes - viewing	Eyes - recording	Recording frequency (Hz)	Direction of recording	Analysis Method	Fixation duration [sec]	Targets	Instruction	Min Distance [']	Average Distance [']	Max Distance [']	Min Speed [°/s]	Average Speed [°/s]	Max Speed [°/s]	Min Acceleration [°/s²]	Mean Acceleration [°/s²]	Max Acceleration [°/s²]	Min Duration [ms]	Average Duration [ms]	Max Duration [ms]	Minimum Frequency [1/s]	Average Frequency [1/s]	Maximum Frequency [1/s]	Main Sequence: Axes
& Greenlee, 2010 (31)								100ms and not in top 5% of distance		checkerboard image																	
Turatto, Valsecchi, Tamè, & Betta, 2007	1	Eyelink II	25	B	B	500	B	Engbert & Kliegl	1.5	green or red diamond array	visual search	/	/	/	/	/	/	/	/	/	/	/	/	**0.10**	/	**1.10**	/
Valsecchi & Turatto, 2009	1	Eyelink II	22	B	B	500	B	Engbert & Kliegl	38	white fixation point (.5°)	count rare auditory signal	/	/	/	/	/	/	/	/	/	/	/	/	**0.25**	/	**1.40**	/
Valsecchi & Turatto, 2009	2	Eyelink II	22	B	B	500	B	Engbert & Kliegl	12	green or red circles (2°)	count rare auditory or visual signal	/	/	/	/	/	/	/	/	/	/	/	/	**0.10**	/	**3.00**	/
Valsecchi & Turatto, 2009	3	Eyelink II	12	B	B	500	B	Engbert & Kliegl	12	green or red circles (2°)	count rare auditory or visual signal	/	/	/	/	/	/	/	/	/	/	/	/	**0.05**	/	**2.80**	/
Valsecchi & Turatto, 2007	1	Eyelink II	15	B	B	500	B	Engbert & Kliegl	10.98	white circle (.5°) on green or red circles (2°)	respond to oddball	/	/	/	/	/	/	/	/	/	/	/	/	**0.10**	/	**2.75**	/
Valsecchi & Turatto, 2007	2	Eyelink II	6	B	B	500	B	Engbert & Kliegl	10.98	white circle (.5°) on blue or red circles (2°)	respond to oddball	/	/	/	/	/	/	/	/	/	/	/	/	**0.10**	/	**2.60**	/
Valsecchi, Betta, & Turatto, 2007	1	Eyelink II	17	B	B	500	B	Engbert & Kliegl	10	white fixation, peripheral coloured disks	maintain gaze	**2**	/	90	**3**	/	**290**	/	/	/	/	/	/	0.73	1.544 - 1.797	**3.10**	linear - linear
Valsecchi et al., 2007	2	Eyelink II	20	B	B	500	B	Engbert & Kliegl	20	white fixation, central coloured disks	maintain gaze	**2**	/	90	**3**	/	**290**	/	/	/	/	/	/	0.25	1.251 - 1.269	**2.90**	linear - linear
Winterson & Collewijn, 1976	1	Search coil	7	/	/	66.67	B	/	N/A	rifle / needle	fixate	**1**	7	**20**	/	/	/	/	/	/	/	/	/	1.27	2.04	2.58	/
Winterson & Collewijn, 1976	1	Search coil	7	/	/	66.67	B	/	N/A	rifle, target	shoot	**1**	7	**30**	/	/	/	/	/	/	/	/	/	0.83	1.19	1.57	/

Paper	Experiment	Recording Method	Number of Participants	Eyes - viewing	Eyes - recording	Recording frequency (Hz)	Direction of recording	Analysis Method	Fixation duration [sec]	Targets	Instruction	Min Distance [']	Average Distance [']	Max Distance [']	Min Speed [°/s]	Average Speed [°/s]	Max Speed [°/s]	Min Acceleration [°/s²]	Mean Acceleration [°/s²]	Max Acceleration [°/s²]	Min Duration [ms]	Average Duration [ms]	Max Duration [ms]	Minimum Frequency [1/s]	Average Frequency [1/s]	Maximum Frequency [1/s]	Main Sequence: Axes
Winterson & Collewijn, 1976	1	Search coil	7	/	/	66.67	B	/	N/A	needle and thread	thread	**1**	7	**60**	/	/	/	/	/	/	/	/	/	0.08	1.25	1.78	/
Winterson & Collewijn, 1976	1	Search coil	7	/	/	66.67	B	/	N/A	rifle / needle	suppress	/	7	/	/	/	/	/	/	/	/	/	/	0.09	0.51	0.87	/
Yuval-Greenberg, Tomer, Keren, Nelken, & Deouell, 2008	2	Eyelink II	3	B	B	500	B	Engbert & Kliegl	2-3	images of common objects with bars masking them, either shuffled or normal appearance	respond to rare target	/	/	100	/	/	**200**	/	/	/	/	/	/	**0.10**	/	**9.00**	/
Yuval-Greenberg, Merriam, & Heeger, 2014	1	Eyelink 1000	8	/	/	1000	B	Engbert & Mergenthaler	2.6	8 grating patches around centre of screen	discriminate orientation	**5**	/	**60**	**10**	/	**100**	/	/	/	/	/	/	/	/	/	log. - log.
Yuval-Greenberg et al., 2014	2	Eyelink 1000	8	/	/	1000	B	Engbert & Mergenthaler	2.6	8 grating patches around centre of vision	discriminate orientation	**6**	/	**186**	/	/	/	/	/	/	/	/	/	/	/	/	log. - log.
Zuber & Stark, 1965	1	Limbus tracker	1	L	L	/	B	/	/	grid	/	**2**	/	**13**	**3**	/	**14**	/	/	/	/	/	/	/	/	/	log. - log. & linear - linear

Notes: Articles listed here that were published after the review by Rolfs (2009) were retrieved on the 8th October 2018. Behind the authors' names and publication date the number of citations at retrieval from Scopus is given.

References for Appendix

Armington, J. C., & Bloom, M. B. (1974). Relations between the amplitudes of spontaneous saccades and visual responses. *Journal of the Optical Society of America*, *64*(9), 1263–1271. http://doi.org/10.1364/JOSA.64.001263

Barlow, H. B. (1952). Eye Movements during Fixation. *Journal of Physiology*, *116*(3), 290–306. http://doi.org/10.1113/jphysiol.1952.sp004706

Beeler, G. W. (1967). Visual threshold changes resulting from spontaneous saccadic eye movements. *Vision Research*, *7*(9–10), 769–775. http://doi.org/10.1016/0042-6989(67)90039-9

Betta, E., Galfano, G., & Turatto, M. (2007). Microsaccadic response during inhibition of return in a target–target paradigm. *Vision Research*, *47*(3), 428–436. http://doi.org/10.1016/j.visres.2006.09.010

Betta, E., & Turatto, M. (2006). Are you ready? I can tell by looking at your microsaccades. *NeuroReport*, *17*(10), 1001–1004. http://doi.org/10.1097/01.wnr.0000223392.82198.6d

Boyce, P. R. (1967). Monocular Fixation in Human Eye Movement. *Proceedings of the Royal Society B: Biological Sciences*, *167*(1008), 293–315. http://doi.org/10.1098/rspb.1967.0028

Bridgeman, B., & Palca, J. (1980). The role of microsaccades in high acuity observational tasks. *Vision Research*, *20*(9), 813–817. http://doi.org/10.1016/0042-6989(80)90013-9

Cherici, C., Kuang, X., Poletti, M., & Rucci, M. (2012). Precision of sustained fixation in trained and untrained observers. *Journal of Vision*, *12*(6), 31–31. http://doi.org/10.1167/12.6.31

Cornsweet, T. N. (1956). Determination of the Stimuli for Involuntary Drifts and Saccadic Eye Movements. *Journal of the Optical Society of America*, *46*(11), 987–988. http://doi.org/10.1364/JOSA.46.000987

Cunitz, R. J., & Steinman, R. M. (1969). Comparison of saccadic eye movements during fixation and reading. *Vision Research*, *9*, 683–693. http://doi.org/10.1016/0042-6989(69)90125-4

de Weese Puckett, J., & Steinman, R. M. (1969). Tracking eye movements with and without saccadic correction. *Vision Research*, *9*(6), 695–703. http://doi.org/10.1016/0042-

6989(69)90126-6

Deaner, R. O., & Platt, M. L. (2003). Reflexive social attention in monkeys and humans. *Current Biology*, *13*, 1609–1613. http://doi.org/10.1016/j.cub.2003.08.025

Di Stasi, L. L., Mccamy, M. B., Catena, A., Macknik, S. L., Cañas, J. J., & Martinez-Conde, S. (2013). Microsaccade and drift dynamics reflect mental fatigue. *European Journal of Neuroscience*, *38*(3), 2389–2398. http://doi.org/10.1111/ejn.12248

Dimigen, O., Valsecchi, M., Sommer, W., & Kliegl, R. (2009). Human Microsaccade-Related Visual Brain Responses. *Journal of Neuroscience*, *29*(39), 12321–12331. http://doi.org/10.1523/JNEUROSCI.0911-09.2009

Ditchburn, R. W., & Ginsborg, B. L. (1953). Involuntary eye movements during fixation. *The Journal of Physiology*, *119*, 1–17. http://doi.org/10.1113/jphysiol.1952.sp004706

Engbert, R., & Kliegl, R. (2003). Microsaccades uncover the orientation of covert attention. *Vision Research*, *43*(9), 1035–1045. http://doi.org/10.1016/S0042-6989(03)00084-1

Engbert, R., & Kliegl, R. (2004). Microsaccades Keep the Eyes' Balance During Fixation. *Psychological Science*, *15*(6), 431–436. http://doi.org/10.1111/j.0956-7976.2004.00697.x

Engbert, R., & Mergenthaler, K. (2006). Microsaccades are triggered by low retinal image slip. *Proceedings of the National Academy of Sciences*, *103*(18), 7192–7197. http://doi.org/10.1073/pnas.0509557103

Fried, M., Tsitsiashvili, E., Bonneh, Y. S., Sterkin, A., Wygnanski-Jaffe, T., Epstein, T., & Polat, U. (2014). ADHD subjects fail to suppress eye blinks and microsaccades while anticipating visual stimuli but recover with medication. *Vision Research*, *101*, 62–72. http://doi.org/10.1016/j.visres.2014.05.004

Gaarder, K. (1960). Relating a component of physiological nystagmus to visual display. *Science*, *132*(3425), 471*472. http://doi.org/10.1126/science.132.3425.471

Galfano, G., Betta, E., & Turatto, M. (2004). Inhibition of return in microsaccades. *Experimental Brain Research*, *159*(3), 400–404. http://doi.org/10.1007/s00221-004-2111-y

Haddad, G. M., & Steinman, R. M. (1973). The smallest voluntary saccade: Implications for fixation. *Vision Research*, *13*(6), 1075–1086. http://doi.org/10.1016/0042-6989(73)90145-4

Hafed, Z. M., & Clark, J. J. (2002). Microsaccades as an overt measure of covert attention shifts. *Vision Research*, *42*(22), 2533–2545. http://doi.org/10.1016/S0042-6989(02)00263-8

Hipp, J. F., & Siegel, M. (2013). Dissociating neuronal gamma-band activity from cranial and ocular muscle activity in EEG. *Frontiers in Human Neuroscience*, *7*(July), 1–11. http://doi.org/10.3389/fnhum.2013.00338

Ko, H. K., Poletti, M., & Rucci, M. (2010). Microsaccades precisely relocate gaze in a high visual acuity task. *Nature Neuroscience*, *13*(12), 1549–1554. http://doi.org/10.1038/nn.2663

Krauskopf, J., Cornsweet, T. N., & Riggs, L. A. (1960). Analysis of eye movements during monocular and binocular fixation. *Journal of the Optical Society of America*, *50*(6).

Kuang, X., Poletti, M., Victor, J. D., & Rucci, M. (2012). Temporal encoding of spatial information during active visual fixation. *Current Biology*, *22*(6), 510–514. http://doi.org/10.1016/j.cub.2012.01.050

Laubrock, J., Engbert, R., & Kliegl, R. (2005). Microsaccade dynamics during covert attention. *Vision Research*, *45*(6), 721–730. http://doi.org/10.1016/j.visres.2004.09.029

Laubrock, J., Engbert, R., & Kliegl, R. (2008). Fixational eye movements predict the perceived direction of ambiguous apparent motion. *Journal of Vision*, *8*(14), 1–17. http://doi.org/10.1167/8.14.13

Laubrock, J., Kliegl, R., Rolfs, M., & Engbert, R. (2010). When do microsaccades follow spatial attention? *Attention, Perception, & Psychophysics*, *72*(3), 683–694. http://doi.org/10.3758/APP.72.3.683

Martinez-Conde, S., Macknik, S. L., Troncoso, X. G., & Dyar, T. A. (2006). Microsaccades counteract visual fading during fixation. *Neuron*, *49*(2), 297–305. http://doi.org/10.1016/j.neuron.2005.11.033

McCamy, M. B., Otero-Millan, J., Di Stasi, L. L., Macknik, S. L., & Martinez-Conde, S. (2014). Highly Informative Natural Scene Regions Increase Microsaccade Production during Visual Scanning. *Journal of Neuroscience*, *34*(8), 2956–2966. http://doi.org/10.1523/JNEUROSCI.4448-13.2014

McCamy, M. B., Otero-Millan, J., Macknik, S. L., Yang, Y., Troncoso, X. G., Baer, S. M., …

Martinez-Conde, S. (2012). Microsaccadic Efficacy and Contribution to Foveal and Peripheral Vision. *Journal of Neuroscience*, *32*(27), 9194–9204. http://doi.org/10.1523/JNEUROSCI.0515-12.2012

McCamy, Michael B., Collins, N., Otero-Millan, J., Al-Kalbani, M., Macknik, S. L., Coakley, D., … Martinez-Conde, S. (2013). Simultaneous recordings of ocular microtremor and microsaccades with a piezoelectric sensor and a video-oculography system. *PeerJ*, *1*, e14. http://doi.org/10.7717/peerj.14

Møller, F., Laursen, M. L., & Sjølie, A. K. (2006). The contribution of microsaccades and drifts in the maintenance of binocular steady fixation. *Graefe's Archive for Clinical and Experimental Ophthalmology*, *244*(4), 465–471. http://doi.org/10.1007/s00417-004-0989-5

Møller, F., Laursen, M. L., Tygesen, J., & Sjølie, A. K. (2002). Binocular quantification and characterization of microsaccades. *Graefe's Archive for Clinical and Experimental Ophthalmology*, *240*(9), 765–770. http://doi.org/10.1007/s00417-002-0519-2

Nachmias, J. (1959). Two-dimensional motion of the retinal image during monocular fixation. *Journal of the Optical Society of America*, *49*(9), 901–908. http://doi.org/10.1364/JOSA.49.000901

Nachmias, J. (1961). Determiners of the drift of the eye during monocular fixation. *Journal of the Optical Society of America*, *51*(7), 761–766. http://doi.org/10.1364/JOSA.51.000761

Otero-Millan, J., Macknik, S. L., Langston, R. E., & Martinez-Conde, S. (2013). An oculomotor continuum from exploration to fixation. *Proceedings of the National Academy of Sciences*, *110*(15), 6175–6180. http://doi.org/10.1073/pnas.1222715110

Otero-Millan, J., Macknik, S. L., & Martinez-Conde, S. (2012). Microsaccades and Blinks Trigger Illusory Rotation in the "Rotating Snakes" Illusion. *Journal of Neuroscience*, *32*(17), 6043–6051. http://doi.org/10.1523/JNEUROSCI.5823-11.2012

Otero-Millan, J., Serra, A., Leigh, R. J., Troncoso, X. G., Macknik, S. L., & Martinez-Conde, S. (2011). Distinctive Features of Saccadic Intrusions and Microsaccades in Progressive Supranuclear Palsy. *Journal of Neuroscience*, *31*(12), 4379–4387. http://doi.org/10.1523/JNEUROSCI.2600-10.2011

Otero-Millan, Jorge, Troncoso, X. G., Macknik, S. L., Serrano-Pedraza, I., & Martinez-Conde, S. (2008). Saccades and microsaccades during visual fixation, exploration, and search: Foundations for a common saccadic generator. *Journal of Vision*, *8*(14), 21–21. http://doi.org/10.1167/8.14.21

Pastukhov, A., & Braun, J. (2010). Rare but precious: Microsaccades are highly informative about attentional allocation. *Vision Research*, *50*(12), 1173–1184. http://doi.org/10.1016/j.visres.2010.04.007

Poletti, M., & Rucci, M. (2010). Eye movements under various conditions of image fading. *Journal of Vision*, *10*(3), 1–18. http://doi.org/10.1167/10.3.6

Ratliff, F., & Riggs, L. A. (1950). Involuntary motions of the eye during monocular fixation. *Journal of Experimental Psychology*, *40*(6), 687–701. http://doi.org/10.1037/h0057754

Rattle, J. D., & Foley-Fisher, J. A. (1968). A Relationship between Vernier Acuity and Intersaccadic Interval. *Optica Acta: International Journal of Optics*, *15*(6), 617–620. http://doi.org/10.1080/713818126

Rolfs, M., Engbert, R., & Kliegl, R. (2004). Microsaccade orientation supports attentional enhancement opposite a peripheral cue: Commentary on Tse, Sheinberg, and Logothetis (2003). *Psychological Science*, *15*(10), 705–707. http://doi.org/10.1111/j.0956-7976.2004.00744.x

Rolfs, M., Engbert, R., & Kliegl, R. (2005). Crossmodal coupling of oculomotor control and spatial attention in vision and audition. *Experimental Brain Research*, *166*, 427–439. http://doi.org/10.1007/s00221-005-2382-y

Rolfs, M., Kliegl, R., & Engbert, R. (2008). Toward a model of microsaccade generation: The case of microsaccadic inhibition. *Journal of Vision*, *8*(11), 1–23. http://doi.org/10.1167/8.11.5

Rolfs, M., Laubrock, J., & Kliegl, R. (2006). Shortening and prolongation of saccade latencies following microsaccades. *Experimental Brain Research*, *169*(3), 369–376. http://doi.org/10.1007/s00221-005-0148-1

Rucci, M., & Desbordes, G. (2003). Contributions of fixational eye movements to the discrimination of briefly presented stimuli. *Journal of Vision*, *3*(11), 852–864.

http://doi.org/10.1167/3.11.18

Sabrin, H. W., & Kertesz, A. E. (1980). Microsaccadic eye movements and binocular rivalry. *Perception & Psychophysics*, *28*(2), 150–154. http://doi.org/10.3758/BF03204341

Sansbury, R. V., Skavenski, A. A., Haddad, G. M., & Steinman, R. M. (1973). Normal fixation of eccentric targets. *Journal of the Optical Society of America*, *63*(5), 612–614. http://doi.org/10.1364/JOSA.63.000612

Schor, C., & Hallmark, W. (1978). Slow control of eye position in strabismic amblyopia. *Investigative Ophthalmology & Visual Science*, *17*(6), 577–581.

Schulz, E. (1984). Binocular micromovements in normal persons. *Graefe's Archive for Clinical and Experimental Ophthalmology*, *222*, 95–100. http://doi.org/10.1007/BF02150640

Siegenthaler, E., Costela, F. M., Mccamy, M. B., Di Stasi, L. L., Otero-Millan, J., Sonderegger, A., … Martinez-Conde, S. (2014). Task difficulty in mental arithmetic affects microsaccadic rates and magnitudes. *European Journal of Neuroscience*, *39*(2), 287–294. http://doi.org/10.1111/ejn.12395

Simon, F., Schulz, E., Rassow, B., & Haase, W. (1984). Binocular micromovement recording of human eyes: - methods. *Graefe's Archive for Clinical and Experimental Ophthalmology*, *221*(6), 293–298. http://doi.org/10.1007/BF02134127

Snodderly, D. M. (1987). Effects of light and dark environments on macque and human fixation eye movements. *Vision Research*, *27*(3), 401–415. http://doi.org/10.1016/0042-6989(87)90089-7

Steinman, R. M. (1965). Effect of Target Size, Luminance, and Color on Monocular Fixation. *Journal of the Optical Society of America*, *55*(9), 1158–1165. http://doi.org/10.1364/JOSA.55.001158

Steinman, R. M., & Cunitz, R. J. (1968). Fixation of targets near the absolute foveal threshold. *Vision Research*, *8*, 277–286. http://doi.org/10.1016/0042-6989(68)90015-1

Steinman, R. M., Cunitz, R. J., Timberlake, G. T., & Herman, M. (1967). Voluntary control of microsaccades during maintained monocular fixation. *Science*, *155*(3769), 1577–1579. http://doi.org/10.1126/science.155.3769.1577

Steinman, R. M., Skavenski, A. A., & Sansbury, R. V. (1969). Effect of lens accommodation on holding the eye in place without saccades. *Vision Research*, *9*(5), 629–631. http://doi.org/10.1016/0042-6989(69)90026-1

Thaler, L., Schütz, A. C., Goodale, M. A., & Gegenfurtner, K. R. (2013). What is the best fixation target? The effect of target shape on stability of fixational eye movements. *Vision Research*, *76*, 31–42. http://doi.org/10.1016/j.visres.2012.10.012

Troncoso, X. G., Macknik, S. L., & Martinez-Conde, S. (2008). Microsaccades counteract perceptual filling-in. *Journal of Vision*, *8*(14), 1–9. http://doi.org/10.1167/8.14.15

Tse, P. U., Baumgartner, F. J., & Greenlee, M. W. (2010). Event-related functional MRI of cortical activity evoked by microsaccades, small visually-guided saccades, and eyeblinks in human visual cortex. *NeuroImage*, *49*(1), 805–816. http://doi.org/10.1016/j.neuroimage.2009.07.052

Turatto, M., Valsecchi, M., Tamè, L., & Betta, E. (2007). Microsaccades distinguish between global and local visual processing. *NeuroReport*, *18*(10), 1015–1018. http://doi.org/10.1097/WNR.0b013e32815b615b

Valsecchi, M., Betta, E., & Turatto, M. (2007). Visual oddballs induce prolonged microsaccadic inhibition. *Experimental Brain Research*, *177*(2), 196–208. http://doi.org/10.1007/s00221-006-0665-6

Valsecchi, M., & Turatto, M. (2007). Microsaccadic Response to Visual Events That Are Invisible to the Superior Colliculus. *Behavioral Neuroscience*, *121*(4), 786–793. http://doi.org/10.1037/0735-7044.121.4.786

Valsecchi, M., & Turatto, M. (2009). Microsaccadic responses in a bimodal oddball task. *Psychological Research*, *73*(1), 23–33. http://doi.org/10.1007/s00426-008-0142-x

Winterson, B. J., & Collewijn, H. (1976). Microsaccades during finely guided visuomotor tasks. *Vision Research*, *16*(12), 1387–1390. http://doi.org/10.1016/0042-6989(76)90156-5

Yuval-Greenberg, S., Merriam, E. P., & Heeger, D. J. (2014). Spontaneous Microsaccades Reflect Shifts in Covert Attention. *Journal of Neuroscience*, *34*(41), 13693–13700. http://doi.org/10.1523/JNEUROSCI.0582-14.2014

Yuval-Greenberg, Shlomit, Tomer, O., Keren, A. S., Nelken, I., & Deouell, L. Y. (2008). Transient

Induced Gamma-Band Response in EEG as a Manifestation of Miniature Saccades. *Neuron*, *58*(3), 429–441. http://doi.org/10.1016/j.neuron.2008.03.027

Zuber, B. L., & Stark, L. (1965). Microsaccades and the Velocity-Amplitude Relationship for Saccadic Eye Movement. *Science*, *150*(3702), 1459–1460. http://doi.org/10.1126/science.150.3702.1459